universität wien

MASTERARBEIT / MASTER'S THESIS

Titel der Masterarbeit / Title of the Master's Thesis

„Comparative application of two microclimate simulation tools to analyze the interaction between climate and urban structure“

verfasst von / submitted by

Shyama Asen, BSc

angestrebter akademischer Grad / in partial fulfilment of the requirements for the degree of

Master of Science (MSc)

Wien, 2020 / Vienna 2020

Studienkennzahl lt. Studienblatt / degree programme code as it appears on the student record sheet:	A 066 856
Studienrichtung lt. Studienblatt / degree programme as it appears on the student record sheet:	Kartographie und Geoinformation
Betreut von / Supervisor:	Ass.-Prof. Mag. Dr. Andreas Riedl

Acknowledgment

The following master thesis was developed in cooperation with the AIT, Austrian Institute of Technology.

Many thanks to the whole unit of Digital Resilient Cities at the AIT, but especially to my supervisor Dr. Wolfgang Loibl, MSc, without whom my master thesis would not have been possible.

A big thank you goes to DI Dr.techn Milena Vuckovic, DI Romana Stollnberger and DI Dr. Tanja Tötzer, who answered me every question and helped me with every problem.

I would also like to express my special thanks to my supervisor, Ass.-Prof. Mag. Dr. Andreas Riedl, for the motivating conversations and for the constant support during the creation of the work.

Furthermore, I would like to thank everyone who accompanied and supported me during my studies. Above all my grandfather, who always takes the time to answer every question, no matter how small, and supports me in my decisions.

Besides that, I want to thank my family, who lovingly accompanies and motivates me on every path of life. Thanks to all friends and fellow students who have contributed a lot to this degree.

Above all I would like to thank my partner in life, David, who always believes in me and gave me the needed motivation. Also, I would like to thank my proofreaders Katy, Lily and Mike.

Abstract

More than 50% of the world's population lives in cities. This number is constantly rising and leading to a densification of urban areas. Together with progressive climate change, this has a strong impact on the urban microclimate, for example in form of urban heat islands. The analysis of the microclimate is one of the first steps taken in the early design phase of urban planning. One way to improve the microclimate in urban areas is the vegetation (trees, green buildings), the material used (buildings and ground) and the height and shape of the buildings. Computer based numerical microclimate simulation software is the tool to analyze and predict the microclimate. Two important microclimate simulation tools are ENVI-met and the open source plug-in for Rhino 3D/Grasshopper, the Ladybug Tools. In this thesis these two tools are compared to show their advantages and limitations. The work is divided into two parts. The first part was a sensitivity analysis where each tool was tested for how it reacts to changes in building materials, different seasons and the addition of vegetation, like trees, facade and roof greening, and how these changes affect the microclimate. The second part was a case study where a real area was modeled and then the simulated results of both tools were compared with the data measured on site. The results show that ENVI-met can, depending on the handling and input data, produce accurate data but it has problems whit simulating the vegetation. MRT, air temperature and surface temperature were examined and compared to the literature and different results were found. The biggest limitation of the Ladybug Tools is, they are not able to include evapotranspiration in their simulations. Therefore, the results do not sufficiently deal with the characteristics of vegetation. Apart from that the Ladybug Tools offer a lot of advantages, especially regarding their usability. In general, both programs create correct results, if certain parameters are considered and applied correctly. Further studies should deal with the integration of evapotranspiration in the Ladybug Tools (Grasshopper).

Kurzfassung

Mehr als 50% der Weltbevölkerung lebt in Städten. Dieses stetige Wachstum der Städte führt zu einer zunehmenden Verdichtung der urbanen Gebiete. Zusammen mit dem fortschreitenden Klimawandel wirkt sich dies stark auf das urbane Mikroklima aus, zum Beispiel in Form von städtischen Wärmeinseln. Die Analyse des Mikroklimas ist einer der ersten Schritte in der frühen Planungsphase der Stadtplanung. Eine Möglichkeit zur Verbesserung des Mikroklimas in städtischen Gebieten ist die Vegetation (Bäume, Gebäudebegrünungen), das verwendete Material (von Gebäude und Boden) und die Höhe und Form der Gebäude. Computergestützte numerische mikroklima Simulationssoftware ist ein Werkzeug zur Analyse und Vorhersage des Mikroklimas. Zwei sehr wichtige Mikroklima-Simulationsprogramme sind ENVI-met und das Open-Source-Plug-in für Rhino 3D/Grasshopper, die Ladybug Tools. In der vorliegenden Masterarbeit werden diese beiden Programme verglichen, um ihre Vorteile und Grenzen aufzuzeigen. Die Arbeit ist in zwei Abschnitte unterteilt. Der erste Teil ist eine Sensitivitätsanalyse, bei der jede Software getestet wurde, wie sie auf Veränderungen der Baumaterialien, verschiedene Jahreszeiten und das Hinzufügen von Vegetation, in Form von Bäumen oder Fassaden- und Dachbegrünungen, reagiert und wie sich diese Veränderungen auf das Mikroklima auswirken. Der zweite Teil ist eine Fallstudie, bei der ein reales Gebiet modelliert wurde und dann die simulierten Ergebnisse beider Programme mit den vor Ort gemessenen Daten verglichen wurden. Die Ergebnisse zeigen, dass ENVI-met, abhängig von der Handhabung und den Eingabedaten, genaue Daten produzieren kann, aber es Schwierigkeiten bei der Simulation der Vegetation gibt. MRT, Lufttemperatur und Oberflächentemperatur wurden untersucht und mit der Literatur verglichen, wobei fehlerhafte Ergebnisse aufgedeckt werden konnten. Die größte Einschränkung der Ladybug Tools ist, dass sie nicht in der Lage sind, die Evapotranspiration in ihre Simulation einzubeziehen, daher gehen die Ergebnisse nicht ausreichend auf die Eigenschaften der Vegetation ein. Abgesehen davon bieten die Ladybug Tools eine Menge Vorteile, insbesondere hinsichtlich deren Anwendbarkeit. Grundsätzlich erstellen beide Programme korrekte Ergebnisse, wenn bestimmte Parameter beachtet und richtig angewendet werden. Zukünftige Studien sollten sich mit der Integration der Evapotranspiration in die Ladybug Tools (Grasshopper) beschäftigen.

Contents

List of Figures

List of Tables

List of Abbreviations

AIT	Austrian Institute of Technology
API	Application Programming Interface
BC	Basecase
CAD	Computer-Aided Design
CFD	Computational Fluid Dynamics
DEM	Digital Elevation Model
DMI	Default Moderate Insulation
FG	Facade Greening
FGRG	Facade and Roof Greening
GH	Grasshopper
IDE	Integrated Development Environment
LT	Ladybug Tools
MRT	Mean Radiant Temperature
PET	Physiological Equivalent Temperature
RG	Roof Greening
SDK	Software Development Kit
TMY	Typical Meteorological Year
UHI	Urban Heat Island
UTCI	Universal Thermal Climate Index
VPL	Visual Programming Language

1. Introduction

Climate change is one of the greatest global challenges facing the world today (Betsill & Bulkeley, 2003). Cities in particular have to deal with climate change. Urban areas are significant sources of greenhouse gas emissions and are vulnerable to the effects of climate change. More than half of the world's population lives in cities, and studies show that this number is rising (Bai et al., 2018). This urbanization leads to growth and densification of cities. This in turn leads to a change in the urban microclimate in the form of e.g. heat island effects. These developments can already be observed under current climate conditions and are likely to intensify under future climate conditions (Loibl et al., 2019). This is exactly why a prediction of the thermal effects of the respective urban design elements based on preliminary designs has become very significant, both for buildings and cities. However, such urban scale models are often very time and resource consuming and therefore not necessarily useful for the early design process. In intelligent urban design processes, representative maps showing the effects of different urban design elements, such as buildings, but also greening measures, on the direct environment (e.g. the street canyon) are of great importance. Such numerical simulation models have become an integral part of architectural and urban planning design processes in recent years. They provide a large part of the decision support at an early stage of the design phase (Elwy et al., 2018b). These tools must be tested and compared with field measurements to ensure that they provide correct results.

Urban planners and architects are working on building cities in a more sustainable and climate-friendly way in order to counter rising temperatures. The AIT, Austrian Institute of Technology, is working on several research projects dealing with sustainable urban planning and smart cities. One project examines microclimate changes, triggered by urban densification, assuming building height increase to height zoning limits, where Meidling, Vienna, serves as a study area representing an already urbanized district. A second project examines microclimate changes, triggered by adding new property developments, some of them with high-rise buildings, where Linz serves as a study area to demonstrate these effects. To better cope with such socioeconomic and climatic change in urban environments in the future, adaptation measures will be tested reducing the climate impact as well as urban fabric impact: (a) extension of urban green in streets, facades, rooftop areas; (b) improved layout of open spaces, streetscapes; (c) building extension design. This shall be carried out through comprehensive microclimate simulations considering 3D city models reflecting the different densification and open space scenarios and different building designs (Loibl et al., 2019).

Currently two tools are applied at the AIT to model urban microclimate considering the physical principles to model urban atmosphere dynamics: ENVI-met and the Ladybug Tools.

ENVI-met is one of the most widely used microclimate simulation tools (Tsoka, Tsikaloudaki, et al., 2018). It is an integrated three-dimensional non-hydrostatic model, initially developed to model surface plant interactions, currently more often used to simulate microclimate dynamics in built urban environments (Bruse & Fleer, 1998). The model input are 3D arrays, describing building, vegetation and soil properties. Severe disadvantages of ENVI-met are the black box concept allowing no changes or extensions in the program code and the long calculation time: typical simulations of microclimate dynamics of a day for a few 100x100 grid cells take about a week, finally providing hourly results (Loibl et al., 2019).
The Ladybug plug-in of the Rhino3D / Grasshopper environment experiences growing interest among users interested in urban microclimate simulation. The Ladybug Tools collection inherit the physical principles and functionalities of underlying simulation engines (e.g. Radiance, EnergyPlus, OpenFoam) (Roudsari et al., 2013). Input and output are interlinked between these engines and a visual scripting interface allows for comprehensive simulation and analysis. The source code is open, which allows to extend the tool by linking it to other simulation software (Peronato et al., 2017). The plug-in makes use of standard 2,5D ESRI shapefiles containing building layout and vegetation property information with fine resolution. As a big advantage the calculations are carried out much faster: 24 hour simulations take only a few hours calculation time (Loibl et al., 2019).

1.1. State of the Art

A large number of research teams are working on the problems of growing cities, their effects on the microclimate in view of the advancing climate change and what measures can be taken to deal with this (Robitu et al., 2006; Shashua-Bar et al., 2010). In order to investigate the microclimate, numerical simulation tools are used in addition to remote sensing methods. These can show the interactions of the various elements, such as buildings, vegetation, etc. and their influence on the microclimate (Toparlar et al., 2017).
There are some studies that compare different microclimate simulation tools with each other and with measured data (Elwy et al., 2018a; Mohammad & Balint, 2019; Naboni et al., 2018; Naboni et al., 2017; Wang et al., 2015). However, the studies are mainly concerned with air temperature or MRT and the influence of vegetation (trees or green buildings).
Some studies have been found that deal with the material of the buildings, primarily the albedo of the material. However, a lot of studies are primarily concerned with interior comfort and not with the influence of the various materials on the urban microclimate. There are many studies dealing with ENVI-met, but there are relatively few studies on the Ladybug Tools.

1.2. Problem Definition

While working with ENVI-met at the AIT, there were unexpected results. Especially regarding the impact of the materials used in the buildings and the impact of green infrastructure on the surrounding environment. This thesis tests both, ENVI-met and the Ladybug Tools,

in terms of input and output data and their results compared to real measurements.
During the process of creating different microclimate scenarios with ENVI-met at the AIT there were several inconsistencies:

- Performance of the different wall materials, especially at night
- The effect of vegetation on the microclimate especially at night using the MRT
- The relationship of the effect of vegetation and wall materials on the microclimate
- The computing time

A wide range of literature has been found to support the use of ENVI-met, but only a few papers to document its setup and calibration (Skelhorn et al., 2014). The results expected from experience and literature can be better achieved with the help of the Ladybug Tools. However, working with Ladybug Tools has one major limitation: It does not include the evapotranspiration of vegetation.

1.3. Aim and Related Research Questions

The following work deals with the application of different microclimate software in order to integrate the gained knowledge into the work with urban agglomerations and their impact on the environment as an overall goal. This thesis distinguishes several objectives, whose comprehensive subject areas, although they are not a direct subject of the work, must always be included and considered.

The ultimate goal is to find measures that make cities more climate-friendly, cool cities, counter UHIs and make cities livable. Sustainable urban planning deals, among other things, with the influence of urban densification on the microclimate and its effects on people and the environment.
The next goal is to highlight the problem of increasing urban densification and its effects and to create knowledge by forecasting the future and showing the effects of countermeasures. Such comparisons and visualizations can be created with microclimate software.
The aim of the thesis is to compare and evaluate two microclimate tools and to apply them in a way that, according to the literature, correct results are created.

This leeds to the following research questions:

- Which are the most appropriate models to show the impact of urban densification on microclimate conditions on different scales?
- What limitations do ENVI-met and the Ladybug Tools have simulating the microclimate?
- Can we always trust available tools?

- What effect have different greening measurements (e.g. green buildings, trees) on the microclimate in the Ladybug Tools as well as in ENVI-met?
- What effects do different building materials have on the microclimate in the Ladybug Tools as well as in ENVI-met?
- How does the input (weather) data effect the simulation result?

1.4. Structure of the Thesis

After the introduction and location of the research topic, selected subject areas are explained in more detail in order to understand and interpret the results and finally to answer the research question. Chapter 2 deals with the microclimate and explains the development of this research topic so far. Chapter 3 discusses various aspects of building physics and goes into more detail about important physical parameters of various building materials. Chapter 4 presents different types of building greening and their effects on the microclimate. Chapter 5 focuses on the two microclimate simulation tools to be investigated (ENVI-met and Ladybug Tools).
The methodology discusses the data used and the individual methods applied. The practical work is divided into a sensitivity analysis and a case study. In the sensitivity analysis the respective microclimate simulation tools are tested on the basis of different parameters. In the case study, the simulation results of the two programs are compared with data measured directly on site. The individual work steps, from the beginning of the analysis to the visualization, are explained in detail.
Great attention is paid to the results and the subsequent discussion with appropriate literature. Here again, a distinction is made between sensitivity analysis and case study. The results of one specific hour for the whole analyse area are visualized in microclimate maps. The daily performance on a specific point is shown in diagrams. Heat maps were used to give a overview of the daily microclimate performance at every location, for the simulation software as well as the measured data. The statistic indices of the comparison of the two simulation tools and the real measurements are listed in tables.
The master thesis ends with a conclusion in which important outcomes are pointed out again and the research questions are answered in this chapter as well. Last but not least, further studies and work steps are mentioned in the chapter outlook.

2. Urban Microclimate

There are two main approaches in urban microclimate research: observational and simulation approaches. The observational approach usually consists of measurement techniques from the field or remote sensing data. With the development of computer power, however, the application of numerical simulations increased. The main advantage of these is that parameters can be easily changed and their effects or the difference between these scenarios can be simulated and analysed. CFD (Computational Fluid Dynamics) tools in particular offer many advantages, as they are able to include flows such as wind speed in the simulation. With computer simulation tools the urban climate can be studied on several scales (Toparlar et al., 2017). In microclimate simulation tools the urban climate is analyzed from the microscale level to the indoor level.

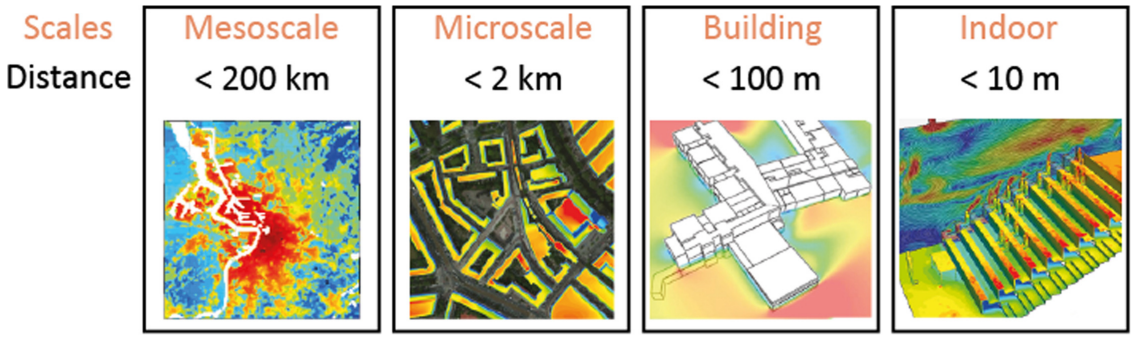

Figure 2.1. Different spatial scales in the climate modeling (Toparlar et al., 2017, P. 1615)

The analysis of the microclimate is one of the first steps that architects or urban planners take in the early design phase. This involves documenting the physical elements of the site (e.g. buildings, street canyons and vegetation), but also the environmental factors (e.g. weather data) that influence the area. The analysis of the microclimate is essential for decision making and the development of strategies that respond to the climate (Awino, 2019; Elwy et al., 2018b).

2.1. Development of Urban Climate Research

Luke Howard, who is considered a pioneer in urban climate studies, was the first to recognize that urban areas have an effect on their local climate in the study "the climate of London" in 1883 and can be identified as the starting point (Howard, 1883). According to Vysoudil (2015), there has been a strong development in urban climate research since the middle of the 20th century, due to the development of measurement techniques, statistical/mathematical

methods, but also to the gradual development of spatial technologies as GIS methods. Many studies investigating urban climate use remote sensing and GIS methods for the analysis and monitoring of UHIs (Aniello et al., 1995; Bornstein, 1968; Nakata-Osaki et al., 2018; Nichol, 2005; Roth et al., 1989).

Since the middle of the 20th century there have been several stages of development in urban climate research:

- 1960s: Measurement of urban microclimate process variables, employment of statistical methods to test hypotheses, moving towards an energy budget approach and explanations;
- 1970s: application of computer techniques in modeling, a more rigorous definition of the urban "surface", urban scales and observing urban effects;
- 1980s: adoption of common urban forms for modeling and measurement, the use scaled-physical models, measurement of fluxes in different cities;
- 1990s: establishing relationships between urban forms and their climatic effects, urban field projects examined by research teams; and
- since 2000s: development of realistic urban microclimate models and employment of new techniques for the analysis of urban microclimate, increased links between modeling and measurement programs.

(Toparlar et al., 2017; Vysoudil, 2015).

2.2. Urban Heat Islands (UHI)

Urban heat islands are the most widely investigated urban climate phenomenas. As mentioned before, a lot of research has been done in this direction, especially since the 1960s. The term "Urban Heat Island" was also mentioned in the Bornstein (1968) study. In this study, an instrumented helicopter was used to measure the temperature field at various heights over a period of more than two years at different locations in New York City. The results show that the temperature in urban areas is higher than in rural areas (Bornstein, 1968).

Many sources, among others the Canadian climatologist Oke (1995), name the following as the most important factors causing UHIs:

- The absence of trees and other vegetation and the associated minimization of shading and evapotranspiration
- The waste heat from traffic, industry and building cooling
- Cities have a larger surface area compared to rural areas, which can store more heat

- Densely built-up areas with narrow street canyons reduce wind speed and prevent the heat from rising into the clear sky
- Buildings made of material with high heat input and the roughness of urban areas

(Filho et al., 2017; Oke, 1995).

The UHI effect has not only a spatial extension (urban - rural), but also a temporal one. This shows a diurnal pattern with the highest intensity at night, indicating a delayed cooling of cities (Awino, 2019). This statement, however, is especially true for cities in temperate climates during the summer. UHIs can occur all year round in all climate regions, day or night (Filho et al., 2017; Oke, 1995).

2.3. Mean Radiant Temperature (MRT)

According to Li (2016) the mean radiant temperature (MRT) is defined as "the uniform temperature of an imaginary enclosure (or environment) in which the radiant heat transfer from the human body is equal to the radiant heat transfer in the actual nonuniform enclosure (or environment)". It is composed of short- and long-wave radiation fluxes, which can be direct, diffuse or reflected, to which a human body is exposed (Rakha et al., 2005).

The MRT differs from the air temperature: The mean radiant temperature is a measure of the radiant heat loss and gain in the environment and the air temperature is a measure of the average air temperature in the environment. Despite a cold winter's day, if the human body is exposed to the sun, it can feel the radiation heat gain from the sun (Li, 2016). In the open air the MRT depends on the temperature of the sky, the ground, the vegetation and the surrounding houses. For this reason it is not easy to predict reliably (Rakha et al., 2005).

In contrast to air temperature the MRT also takes into account the surrounding surface temperatures and thus has greater significance for thermal comfort. Therefore it is used very frequently. It is one of the comfort indicators, along with PET, for example (Li, 2016).

The MRT can be measured by certain instruments as Black Globe Thermometer, Two Sphere Radiometer or constant air temperature sensors and another method is to calculate the MRT. There are several variants to calculate e.g. from the temperature of the surrounding surfaces. The problem with the method of calculation is that it can lead to inaccurate results, depending on the variant chosen. (Godbole, 2018).

3. Building Physics

In order to better understand the analyses and results of the master thesis, it is important to first deal with the building physics of the materials used. There are important physical parameters that are decisive for materials in terms of their thermal performance.

According to the Institute for Building Construction and Technology at the Technical University of Vienna (2014), three objectives are pursued with structural thermal insulation:

- Protection of the users of the buildings against extreme climatic influences (heat, cold, solar radiation, etc.) and thus the creation of a comfortable, health-compatible indoor climate
- Energy savings through more economical operation of heating and air conditioning systems
- Protection of the building itself (e.g. protection against moisture)

The distinction is made between thermal insulation in summer, which deals with excessive temperature or solar radiation, and thermal insulation in winter, which must ensure that a pleasant living climate is maintained (Bölcskey & Bruckner, 2014).

Heat as a physical term is the content of kinetic energy of the molecules of a substance. It is directly related to temperature and increases with its increase. Bodies with different temperatures that are in contact with each other strive for a common compensation temperature. During heat transfer, a specific heat flow q flows from areas of higher heat to areas of lower temperature. Three types of heat transfer can be distinguished:

- Convection (carrying of heat by particle flows in gases and liquids)
- Thermal radiation (transfer of heat by radiation through surfaces of solid bodies)
- Heat conduction (heat exchange of adjacent particles in solid, liquid and gaseous bodies)

Only heat radiation, as electromagnetic wave movement, is not bound to material, but heat conduction and convection are. The heat flow is influenced by the thermal properties of the building materials. Depending on the storage capacity of a building material, a component can resist short-term temperature fluctuations (Bölcskey & Bruckner, 2014).

Black surfaces absorb, white surfaces reflect electromagnetic radiation (Bölcskey & Bruckner, 2014). This is the basis of the albedo effect, which also influences the (micro)climate to a great extent. This is why a dark asphalt is much warmer than a light concrete. The reflected radiation is not available to the body (Li, 2016).

In the following some physical parameters which describe the thermal performance of building materials are mentioned.

3.1. Density ρ

The density influences numerous technical properties of the material. Density indicates the amount of mass contained in the selected volume unit. The more mass is contained in the selected volume unit, the denser the material is (Bölcskey & Bruckner, 2014).

$$Density \quad = \quad mass \quad of \quad the \quad body \quad / \quad volumen \quad of \quad the \quad body \tag{3.1}$$

$$\rho = m/V \tag{3.2}$$

The density is usually given in g/cm^3 or kg/m^3.

3.2. Thermal Conductivity λ

For a given component thickness and temperature difference, the heat flux density is determined exclusively by the thermal conductivity coefficient of the building material. The coefficient of thermal conductivity indicates the amount of heat that flows through 1m^2 of a 1m thick component at a temperature difference of 1 K per second (Bölcskey & Bruckner, 2014).

There is a difference between the surface temperature and the room air temperature 3.1, which is due to the transfer of heat between the solid material and the air, which takes place within a thin layer of air directly on the wall surface. The heat flux density in the inside or outside transition zone is

$$q = \alpha * (\vartheta - \vartheta) \tag{3.3}$$

The heat transfer coefficient α depends mainly on the wind speed and the surface condition (roughness) of the component. The same applies to the outside (Bölcskey & Bruckner, 2014).

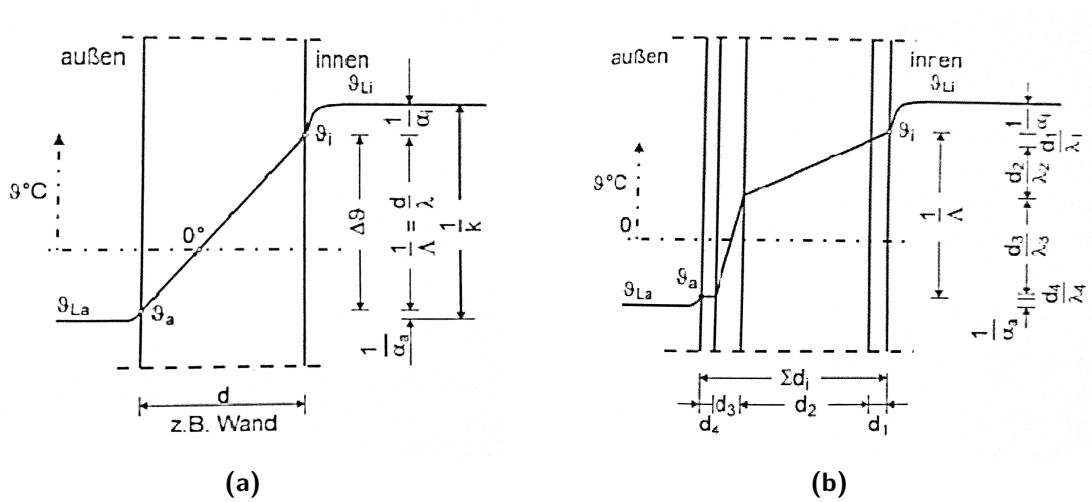

Figure 3.1. Heat transfer in a stationary state through a single-layer component (a) through a multilayer component (b) (Bölcskey & Bruckner, 2014, P. 101f)

Unit sizes have been introduced to assess the insulation capacity. The heat flux density in relation to the temperature difference is called the heat transmission coefficient and its reciprocal value, the heat transmission resistance. The heat transmission resistance $1/\Lambda$ serves to assess the thermal insulation and increases with increasing layer thickness and decreasing coefficient of thermal conductivity. In the case of a component with several layers, this is made up of the partial resistances of the individual layers (Bölcskey & Bruckner, 2014).

Materials with a low density have a lower coefficient of thermal conductivity. Metals are good heat conductors and foamed polymers as well as fibrous materials are very poor, which makes them good thermal insulation materials. The thermal conductivity coefficient is influenced by the structure, porosity, density, moisture content and temperature. If the density is small, a high porosity prevails, resulting in a low coefficient of thermal conductivity (good thermal insulation/bad heat conductor). With a high bulk density it is exactly the opposite. Crystalline structures of the building material have a high thermal conductivity (metals), while amorphous structures have a low thermal conductivity (Bölcskey & Bruckner, 2014).

3.3. Specific Heat Capacity c

The heat storage capacity is determined by the specific heat and the density. The specific heat capacity is the amount of heat that a body with a mass of 1 kg absorbs when heated by 1 K. It can be used to determine the heat content of bodies at certain temperatures, but also temperature changes. It is only very slightly dependent on temperature; as humidity increases, specific heat rises according to the moisture content (Bölcskey & Bruckner, 2014).

$$c = heat\ quantity\ /\ mass\ *\ temperature\ increase \tag{3.4}$$

The Specific heat unit is kJ/kgK or J/kgK.

The Tables 3.1 and 3.2 show three physical parameters (density, thermal conductivity and specific heat capacity) for selected building materials from different sources.

Material	**Density [kg/m³]**	**Thermal Conductivity [W/mK]**	**Specific Heat [J/kgK]**
Concrete	2400	2.04	1500
Lightweight Concrete	1700	0.8	150
Full Brick	1800	0.8	840
Perforated Brick	1200	0.52	840
Glass	2500	1.16	840
Steel	7850	58	500
Fibres	100	0.04	840
Foamed Polymers	25	0.04	1380

Table 3.1. Thermal properties of the building materials according to TU Vienna (Bölcskey & Bruckner, 2014)

Material	**Density [kg/m³]**	**Thermal Conductivity [W/mK]**	**Specific Heat [J/kgK]**
Concrete	2400	2	950
Lightweight Concrete	1800	1.3	1000
Full Brick	2000	0.96	840
Perforated Brick	1400	0.58	1000
Glass	2500	0.76	840
Steel	7850	50	470
Fibres	115	0.045	1300
Foamed Polymers	20	0.04	1500

Table 3.2. Thermal properties of the building materials according to Ubakus ("Ubakus", n.d.)

4. Green Buildings

Green buildings can help to improve the urban microclimate. Due to the reduced summer heating of the building facade and the evaporation capacity of plants and substrate, green areas achieve a noticeable cooling effect and act as "near-natural air conditioning systems" (Kraus et al., 2019). Especially for the necessary cooling at night, it is crucial that the temperature increase in urban areas can be significantly reduced by greening.
Due to the increasing urbanization and the lack of space in the urban area, in addition to the planting of vegetation, especially building greenery plays an important role. The oldest example of building greenery are probably the Hanging Gardens of Babylon dating back to 500 BC. According to Besir and Cuce (2018) also the Roman and Greek empires have used this type of greenery to create cooler conditions. Since the beginning of the 1980s, green facades have been studied in a scientific context and are considered to play a key role in ecological urban development (Besir & Cuce, 2018).

The most common forms of greening buildings are green facades and green roofs.

4.1. Vertical Greenery Systems

There are many different types of green walls. Each type of greening has advantages and disadvantages and the decision for a type of greening depends on the respective wall (Kraus et al., 2019). Besir and Cuce (2018) have shown the different types of vertical greening in Figure 4.1. There are two different systems into which they can be separated - green facades and living walls. With the **green facade** the vegetation grows over the building envelope naturally. In the case of the **living wall**, many systems are attached to the wall (e.g. trays, vessels) in which the plants grow (Besir & Cuce, 2018).

The green wall can be further divided into two main groups. In **traditional green facades** the plants use the envelope as supporter material and the growing media remains on the ground (see Figure 4.2). This was often the case before vertical greening systems were intentionally installed on buildings (Besir & Cuce, 2018).
The **continuous guides** are based on double skin scaffolding along the entire surface and have an air cavity between the wall and a vertical support structure. The **modular trellis** is the same system, except that here the plant does not grow from the ground, but from flower pots with soil from which the vegetation grows (see Figure 4.2) (Besir & Cuce, 2018).

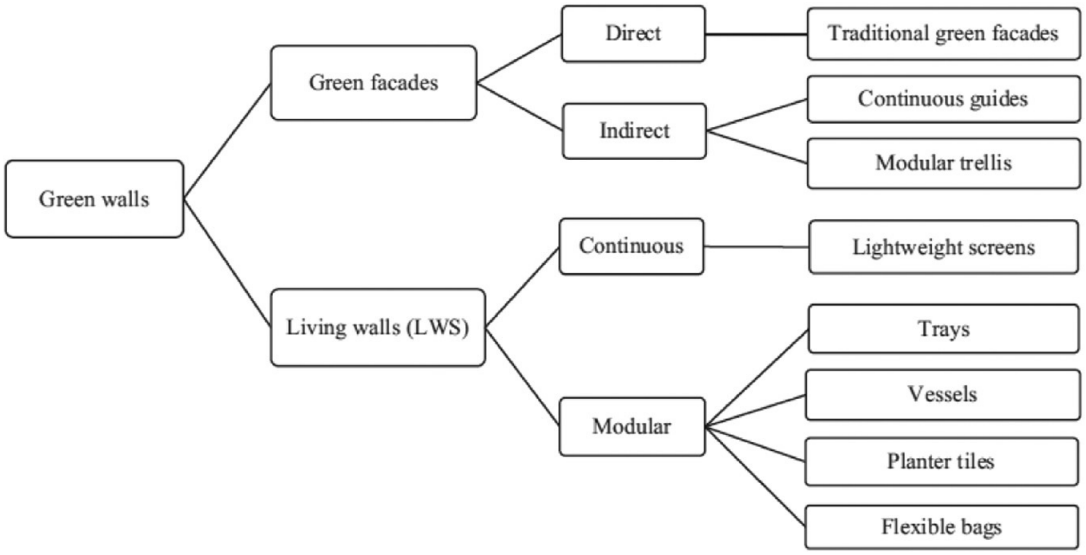

Figure 4.1. Classification of green walls according to their construction characteristic (Besir & Cuce, 2018, P. 919)

The living walls are divided into **continuous** and **modular**, where both systems are similar and only the growing media is different (see Figure 4.2).
Due to the use of a geotextile membrane, a growth medium is not required in **continuous** living walls. This material can be used instead of soil. The plants grow by irrigation with hydroponic techniques.
The system, in which the plants can grow in **modular** living walls, can consist of trays, vessels, planting tiles and flexible bags (Besir & Cuce, 2018).

The applicability of the plants changes according to the system used. Depending on the system, the efficiency also varies.

4.2. Green Roof

There are basically three types of green roofs. **Intensive** green roofs, **extensive** green roofs and their mixed form. According to Hong et al. (2019), **intensive** green roofs, are used as a park or garden. Elements of garden design such as trees, grass, pavilions, pools, etc. can be integrated, combining the functions of green space ecology and recreation (Hong et al., 2019). **Extensive** green roofs are not like a typical "roof garden" and planted with low and resistance vegetation like moss and grass (Besir & Cuce, 2018). In contrast to intensive construction methods, these cost-effective constructions are easier to maintain and, due to the lighter load, suitable for more buildings (Hong et al., 2019). Due to the active use and the heavier construction of the intensive roof greening, the demands on the building statics increase. Important differences between the different types of green roofs are listed in Table 4.1 (Besir & Cuce, 2018). **Semi intensive** roofs are a mixture of the two, with substrate

thicknesses greater than those of extensive roofs. A wider range of plants can also be used and simple recreational facilities can be accommodated on them (Hong et al., 2019).

The structure of green roofs varies depending on the type, but in principle, green roofs consist of the layers shown in Figure 4.4 (Besir & Cuce, 2018).
In addition to these, other components such as irrigation systems are sometimes required. It is important to adjust the plants to the climatic conditions, as this can save irrigation and maintenance costs (Besir & Cuce, 2018).

	Extensive	**Semi intensive**	**Intensive**
Maintenance	Low	Periodically	High
Irrigation	No	Periodically	Regularly
Plant communities	Moss-Sedum-Herbs and Grasses	Grass- Herbs and Shrubs	Lawn or Perennials, Shrubs and Trees
Cost	Low	Middle	High
Weight	60–150 kg/m2	120–200 kg/m2	180–500 kg/m2
Use	Ecological protection layer	Designed green roof	Park like garden
System build-up height	60–200 mm	120–250 mm	150–400 mm

Table 4.1. Differnt types of green roofs (Besir & Cuce, 2018, P. 918)

4.3. Advantages of Green Buildings

Besir and Cuce (2018) have published a review paper in which they compare several studies on green buildings. According to the results, there is an advantage of green buildings in relation to energy savings of buildings. These are achieved through thermal insulation, evapotranspiration and shading (Besir & Cuce, 2018).

The additional layers (substrate, vegetation) on green buildings provide a stronger insulation of the buildings. According to studies, the difference is greater the thicker these layers are. Especially the vegetation layer contributes a large part. For vertical greening systems, also the air gap has a significant influence on the cooling amount. As with insulation materials, thin layers of substrate with porous air pockets can achieve a better insulation performance (Besir & Cuce, 2018).

In a comparison by Lazzarin et al. (2005), a roof without greenery was compared with a green roof. The results show that in summer, when the ground is almost dry, the green roof reduces the heat flow to the space below by about 60 % compared to a traditional non-green roof covering with an insulating layer. This can be attributed to the higher solar reflection

and absorption of the vegetation. However, evapotranspiration is very limited in this case. When the ground of the green roof is in a humid state, evapotranspiration has an additionally effect and the green roof functions as a passive cooler. In winter, evapotranspiration is mainly driven by the air vapor pressure deficit. The not negligible weight generates a heat flow from the roof, which is 40 % higher than the corresponding heat flow of a highly solar-absorbing and insulated roof covering (Lazzarin et al., 2005).

Shading effect is another advantage of green spaces Systems for energy saving, as the vegetation contributes to the absorption of solar radiation. Above all, the density of the vegetation and the degree of coverage influence the shading performance on the building facade (Besir & Cuce, 2018).
As mentioned by Besir and Cuce (2018), previous work in the research field shows that the shading effects of the vegetation reduce the temperature of exterior and interior walls. Above all, the surface temperature of the facade can be lowered by several degrees, depending on the study (Besir & Cuce, 2018). Yin et al. (2017) have investigated direct facade greening on hot summer days and the results show that this effect is particularly pronounced around midday and decreases significantly at night. This suggests that shading contributes to a large extent to the reduction of the surface temperature.

Perini et al. (2011) investigated different vertical greening systems with respect to energy savings and wind speed. The results show that direct greening system and the living wall system based on planter boxes are the most effective wind barriers. A reduction of the wind velocity within one meter of a facade leads to an adjustment of the exterior surface resistance to the interior surface resistance. This in turn influences the total thermal resistance of the wall, which can lead to energy savings (Perini et al., 2011).

A comparison of the energy consumption between a building without greening and one with roof greening and one with facade greening was shown by Feng and Hewage (2014). The results show a slight reduction in energy consumption for heating in the winter months with regard to the greened buildings. With regard to cooling capacity, a significant reduction can be seen in the summer months (June, July, August) with regard to green buildings. Especially buildings with vertical greenery show the greatest difference in energy consumption (Feng & Hewage, 2014).

Direct Facade Greenery

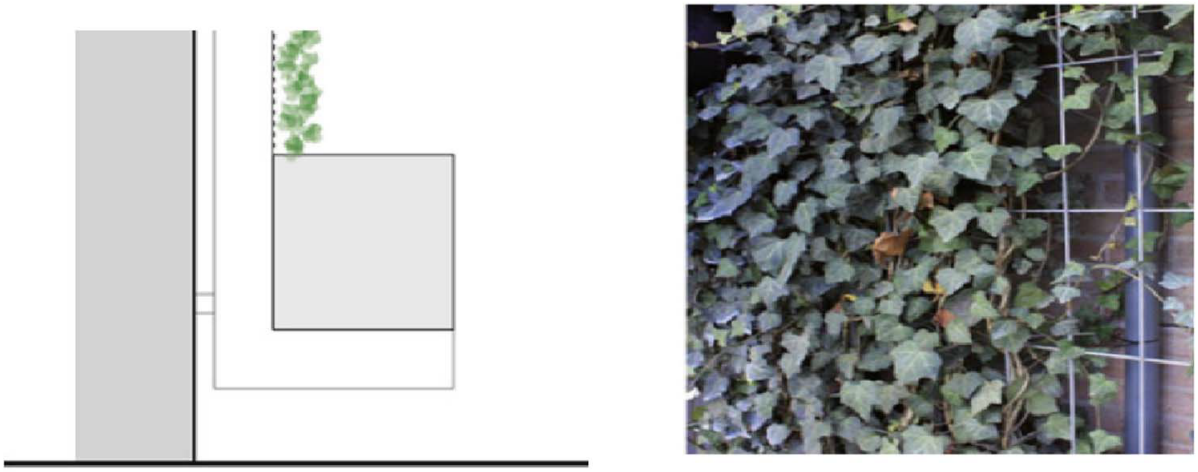

Indirect Facade Greenery

Living Wall (planter boxes)

Figure 4.2. Different types of vertical greening (Besir & Cuce, 2018, P. 919)

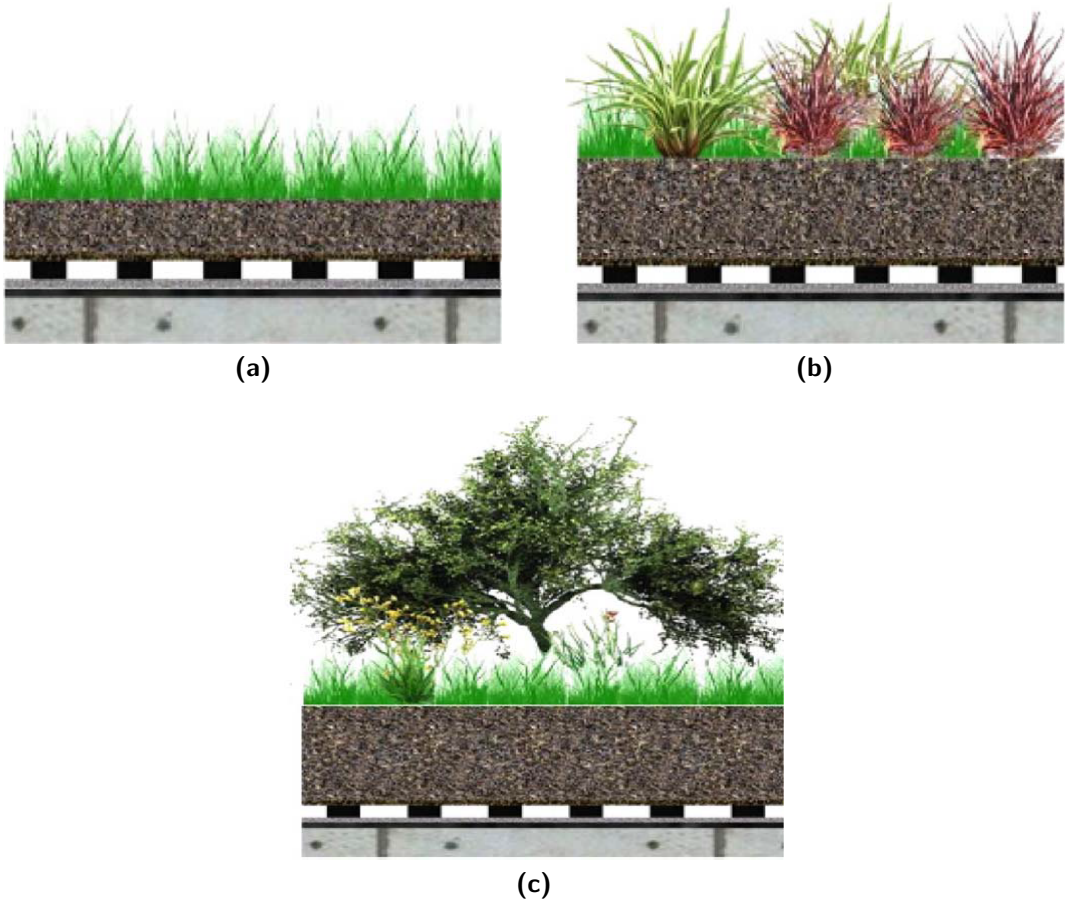

Figure 4.3. Different types of green roofs: Extensive (a) Semi intensive (b) Intensive (c) (Besir & Cuce, 2018, P. 918)

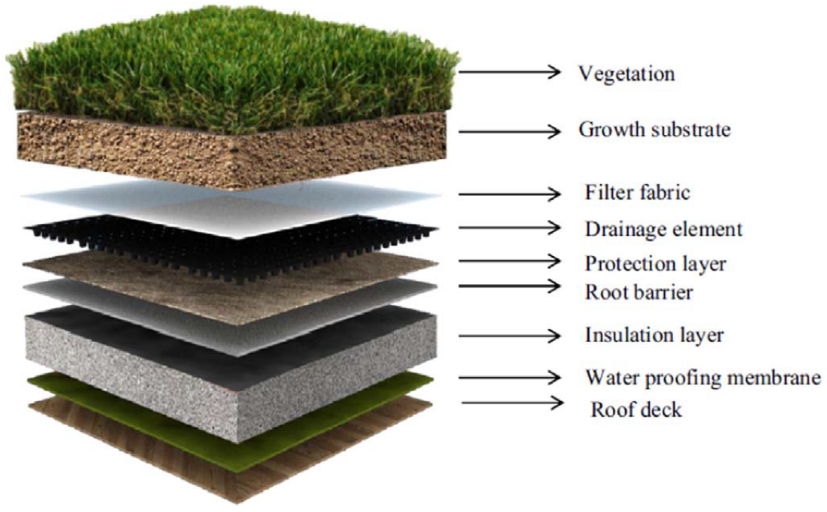

Figure 4.4. Construction of green roofs (Besir & Cuce, 2018, P. 917)

5. Software

5.1. Microclimate Software

There are several tools that can be used for computer based microclimate simulations. In the following, available programs are briefly introduced, but only the two that are used in this thesis (ENVI-met and the Ladybug Tools) are discussed in more detail. ENVI-met is one of the most widely used software when it comes to microclimate simulation (Tsoka, Tsikaloudaki, et al., 2018). It has been used to simulate the microclimate since the early 2000s. The Ladybug Tools have a different approach than ENVI-met, are younger, very compatibility oriented and are an open source plug-in for Grasshopper. The team and community behind Grasshopper plug-ins is constantly growing and developing new features. For these reasons the two programs were selected for use in this master thesis.

5.1.1. The SOLWEIG-model

SOLWEIG, short for Solar Long Wave Environmental Irradiance Geometry model, was released in 2010 by a research team of the University of Gothenburg. This model simulates spatial variations of mean radiation temperature and 3D fluxes of long and short wave radiation. SOLWEIG works with high-resolution urban DEMs in ESRI-ACIIGRID-format and a few meteorological parameters as input (Lindberg et al., 2008).

5.1.2. RayMan

RayMan was developed by the University of Freiburg and deals with the effects of weather, climate and air quality on the human organism. It simulates the effects of clouds and solid obstacles on short- and long-wave radiation fluxes and it calculates solid angle fractions of urban structures. RayMan calculates short and long wavelength radiation fluxes as well as the MRT. The final result of this model is the calculated average radiation component temperature, which is required for humans in the energy balance model (Matzarakis et al., 2000).

5.1.3. ANSYS

ANSYS was founded in 1970 and is one of the leading engineering simulation tools. According to the ANSYS (n.d.) website the software is "used to predict how product designs will behave in real-world environments." It includes CFD, thermal and dynamics. Due to the CFD, wind simulations can be performed with ANSYS (Albdour & Baranyai, 2019; ANSYS, n.d.).

5.1.4. Autodesk CFD

Autodesk CFD software provides fluid dynamic and thermal simulation tools that can help in decision making. Autodesk CFD software supports direct data exchange with most CAD software tools (Albdour & Baranyai, 2019).

5.1.5. CitySim Pro

CitySim Pro is basically a freeware tool, but the import and export functions only work with registration. Built on the CitySim-Solver and developed at the Solar Energy and Building Physics Laboratory of the EPFL (École polytechnique fédérale de Lausanne), CitySim Pro is a graphical user interface that supports the simulation and optimization of sustainable planning of urban settlements. CitySim is relatively fast and requires little input data (Albdour & Baranyai, 2019).

5.1.6. Tas Engineering

According to the website of "TAS Engineering" (n.d.), Tas is a dynamic building simulation package. It is modular, with special tools that serve a specific purpose and facilitate a methodical work flow. The 3D Modeller is responsible for building models and for the simulation and execution of daylight analyses. The building simulator is used to add openings, internal reinforcements, constructions and to perform a dynamic simulation. Systems is a powerful HVAC modeler for calculating energy consumption based on the requirements predicted by the building simulator ("TAS Engineering", n.d.).

5.1.7. Meteodyn

Meteodyn was founded in 2003 and deals with micro-meteorology. The software was developed for the simulation of wind and solar radiation for all types of terrain. Meteodyn is also a CFD-based tool (Meteodyn, n.d.).

5.1.8. ENVI-met

"ENVI-met is a software that can simulate climates in urban environments and assess the effects of atmosphere, vegetation, architecture and materials" ("ENVI-met", n.d.).

ENVI-met, founded in 1994 by Michael Bruse, is a microclimate software with an holistic approach. According to the ENVI-met website, different approaches have been integrated into one model so that all elements can interact with each other as in the real world (ENVI-met, n.d.-c).

The model consists of 2 horizontal dimensions (x and y) and a vertical dimension (z), in which the interacting elements are placed (buildings, plants, etc.). To act as a numerical model, this 3D model consists of grid cells. The smaller the voxel, the more accurate the

result. However, with high resolution comes an enormous increase in computing time. The resolution of a grid cell is typically between 0.5 and 10 m. The temporal resolution is in time steps of 1 to 5 seconds (ENVI-met, n.d.-b, n.d.-d).

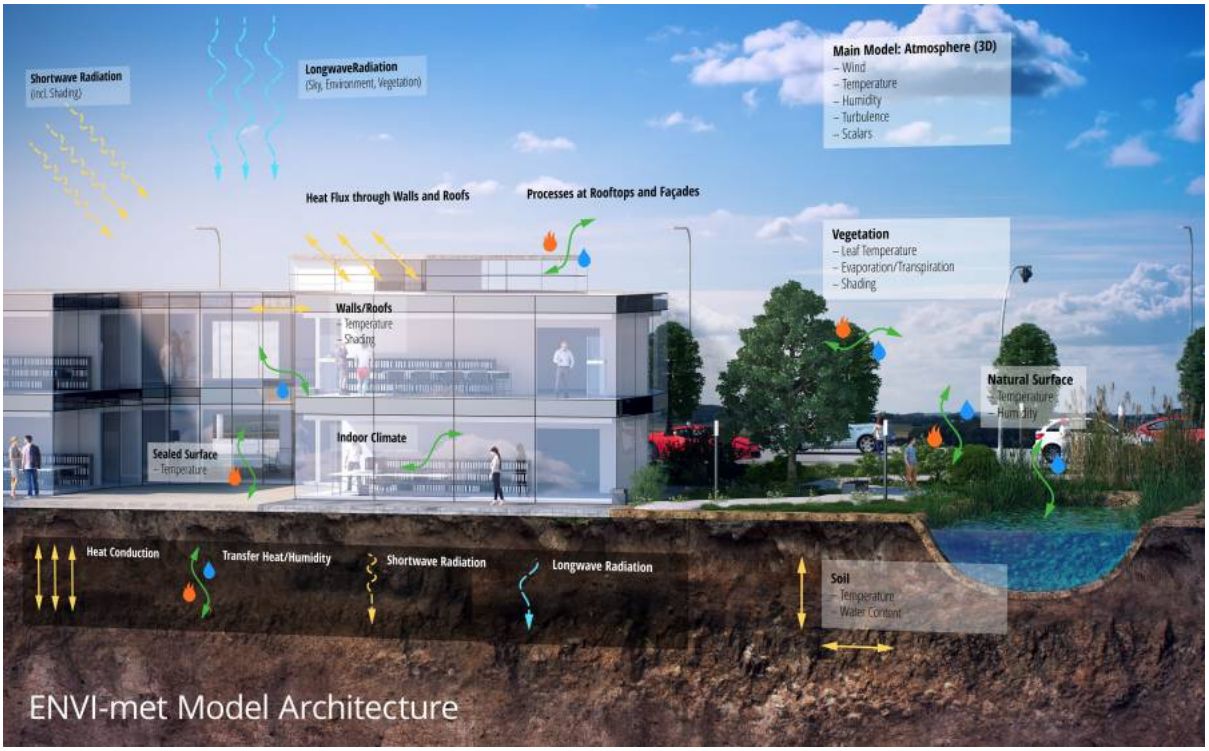

Figure 5.1. ENVI-met Model Architecture (ENVI-met, n.d.-d)

The model calculation in ENVI-met contains the following points according to their website:

- Short- and long-wave radiation fluxes in terms of shading, reflection and back reflection of building systems and vegetation
- Transpiration, evaporation and perceptible heat flow from vegetation into the air including the complete simulation of all plant physical parameters (e.g. photosynthesis rate)
- Dynamic surface temperature and wall temperature calculation for each facade and roof element, which carries up to 3 material layers and 7 calculation points in the wall/roof.
- Water and heat exchange within the soil system, including water absorption by plants
- 3D representation of the vegetation including dynamic water balance modeling of the individual species

- Dispersion of gases and particles. The model supports particles (including sedimentation and deposition on leaves and surfaces), inert gases and reactive gases of the NO-NO2 ozone reaction cycle.
- Calculation of bio meteorological indices like mean radiation temperature, PMV/PPD, PET or UTCI via BioMet (ENVI-met, n.d.-d).

In ENVI-met the results are divided into several outputs. The first output is the Atmospheric model, where the air temperature and humidity are calculated, but ENVI-met also includes a 3D Computational Fluid Dynamics (CFD) model to calculate the wind field. In the soil model you can find the calculation of the surface and soil temperature. The Buildings model includes the temperature of the outer or inner wall, the temperature inside a building or the temperature in front of the buildings facade (ENVI-met, n.d.-d).

Since a large part of the master thesis investigates the interaction of buildings and their environment, an overview of the wall structure in ENVI-met is given. The wall or roof constructions which can be assigned to the building geometry always consist of three material layers which are described in the later mentioned Database Manager. The results of the wall and roof constructions are divided into seven prognostic calculation nodes. Node 1 describes the temperature of the outermost layer and node 7 the temperature of the innermost layer (ENVI-met, n.d.-d).

Basically the ENVI-met software consists of four features:

- Spaces
- ENVIGuide
- EnviMET
- Leonardo

Spaces

With Spaces, the user can create the geometry of the simulation, i.e. the model space. This input file required for the simulation is saved in .INX format. The creation of the model space includes the modeling but also the allocation of the respective material of the elements like buildings, vegetation or surfaces. For the assignment of the different materials the ENVI-met database is used. In this database all materials are exactly defined and stored. The user can use the materials predefined by ENVI-met, or create or modify them himself (ENVI-met, n.d.-g). Spaces works both 2D and 3D. In order to create the geometry data (e.g. buildings) they have to be digitized from a satellite image. Since the winter release 2018/2019 there is also another possibility. The new feature is called "Monde" and it allows to import, modify and export vector based data e.g. shape files as INX files. Also the geometry data does not have to be drawn by the user, but can be imported from the OpenStreetMap (ENVI-met,

n.d.-e).
When working with spaces there are some important points to consider, such as how to keep enough distance between the buildings and the model boundary, which are explained in the ENVI-met tutorials on the website (www.envi-met.com) or in the documentation (ENVI-met, n.d.-d).
In Albero, similar to the material database, you can either create plants yourself or modify existing ones in ENVI-met (ENVI-met, n.d.-a).

ENVIGuide

The simulation settings are defined in ENVIGuide. The start date and time as well as the time span of the simulation are set here. The previously defined INX file is also selected. There are three different levels to define the weather data:

- Basic
- Intermediate
- Advanced

In Basic only the minimum and maximum temperature and the wind direction and strength can be set. In the higher levels, there is a wide range of parameters that can be configured. With the help of Full Forcing an external weather file can be used. The finished file is saved in the .SIMX format and used as input file for the simulation (ENVI-met, n.d.-f).

ENVIMET

The actual simulation runs in ENVIMET. To start the simulation, the previously defined SIMX file must be loaded. The finished simulation files can be post-processed in BioMet to calculate different human thermal comfort indices (ENVI-met, n.d.-f). Depending on the power of the computer and the size or detail of the model, the simulation can take several weeks (ENVI-met, n.d.-d).

Leonardo

In Leonardo the result data (in EDX/EDT format) can be analyzed and visualized in 2D and 3D maps. Maps can only be created for a single hour, but in the diagrams single data points (voxels) can be displayed over a longer period of time (ENVI-met, n.d.-d).

The NetCDF tool was also introduced with the winter release 2018/2019. This tool enables the conversion of EDX data into NetCDF data, which is compatible with other software, unlike EDX data (ENVI-met, n.d.-f).

To learn how to use ENVI-met it is recommended to work through the video tutorials on the ENVI-met website and visit the ENVI-met forum (“ENVI-met”, n.d.).

5.1.9. Ladybug Tools

When talking about the Ladybug Tools, it must be first refered to visual programming languages (VPLs), such as Grasshopper or Dynamo (Davidson, n.d.; “Dynamo”, n.d.). Since this work was done with Grasshopper, Dynamo is not discussed here.

Grasshopper and Rhino 3D

According to Davidson (n.d.), Grasshopper is "for designers who are exploring new shapes using generative algorithms. Grasshopper is a graphical algorithm editor tightly integrated with Rhino's 3-D modeling tools. Unlike RhinoScript, Grasshopper requires no knowledge of programming or scripting, but still allows designers to build form generators from the simple to the awe-inspiring." Since Rhino 6 Grasshopper is included in Rhino. This makes Grasshopper appear as VPL plug-in for use with Rhino 3D (Davidson, n.d.).
Rhinoceros 3D (also Rhino) is a commercial, CAD based 3D modeler software developed in 1980 by Robert McNeel and Associates (McNeel-and-Associates, n.d.).

Ladybug and Honeybee

The Ladybug Tools were originally developed by Mostapha Sadeghipour Roudasri in 2012. At first only Ladybug was released as a plug-in for Grasshopper and around one year later in 2014 Honeybee was released as a Grasshopper plug-in. After that Chris Mackey joined and helped to improve Ladybug. Both now act as co-founders of the Ladybug Tools LLC (“Ladybug Tools”, n.d.)

Ladybug and Honeybee are two open source plug-ins for Grasshopper/Rhino developed to help research and assess environmental performance.

Ladybug imports standard EnergyPlus weather files (.EPW) into Grasshopper and offers a variety of interactive 2D and 3D graphics. It supports the evaluation and decision making of initial design phases through solar radiation studies, view analysis, sunshine hour modeling and more (see Figure 5.2). Integration in the visual programming environment allows for flexible working and immediate feedback on changes (Roudsari et al., 2013).

Honeybee, on the other hand, deals with daylight and thermodynamic models, which are usually most relevant in the later design phases. To achieve this, it combines Grasshopper's visual programming environment with four simulation engines (EnergyPlus, Radiance, Daysim and OpenStudio), which evaluate the energy consumption, comfort and daylighting of buildings (see Figure 5.3) (Roudsari et al., 2013). It also serves as an object-oriented application programming interface (API) for these engines. As it is a free and open source development, users can adapt the tool to their needs and contribute to the source code (Roudsari et al., 2013).

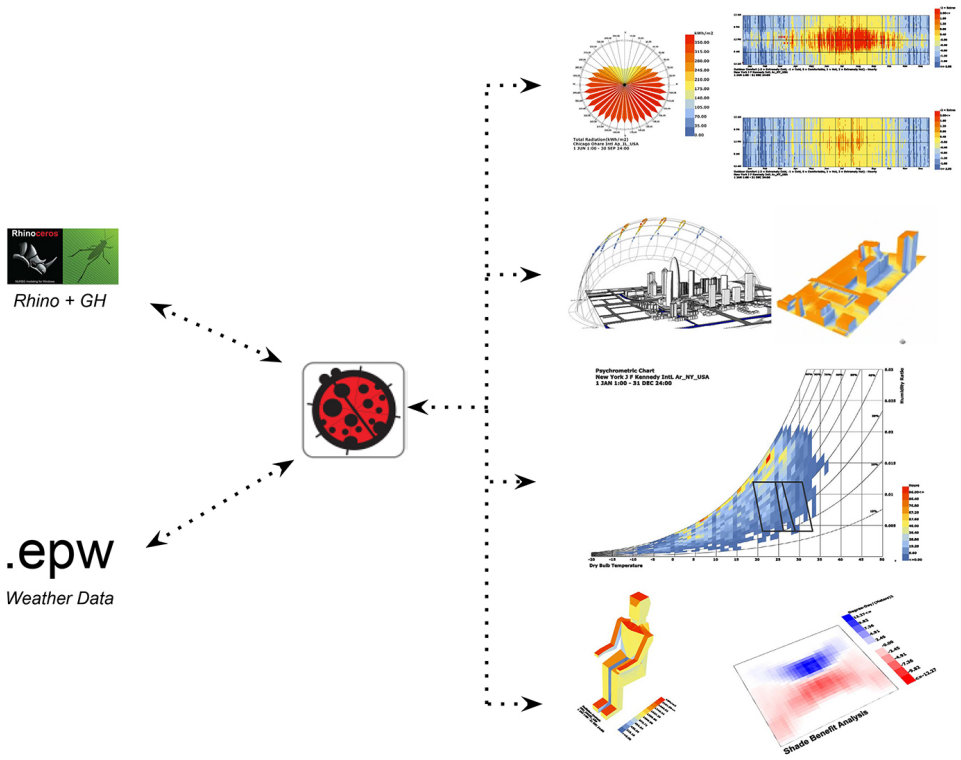

Figure 5.2. Ladybug workflow (Wintour, 2016)

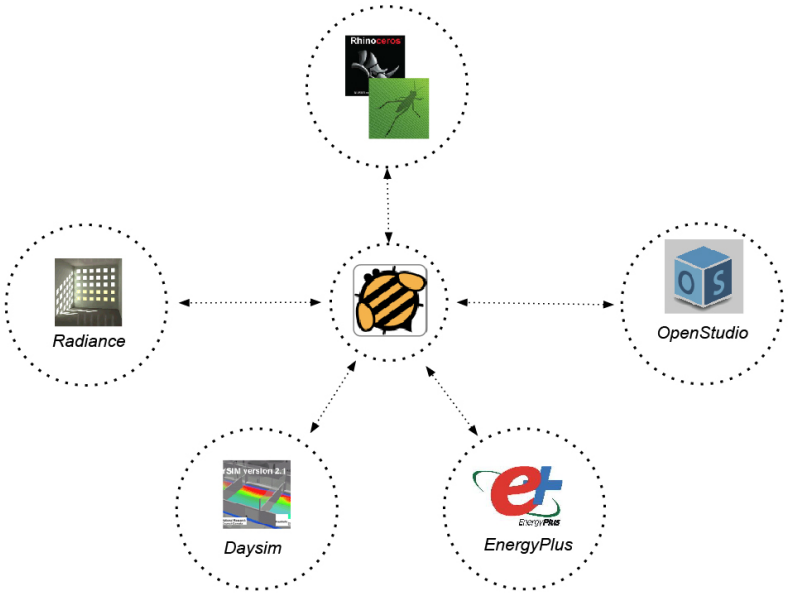

Figure 5.3. Tools Honeybee is using (Wintour, 2016)

As handled in many other programs, not many inputs are needed for the execution. Many values are set as default, but experienced users can also overwrite the default inputs, to generate a more accurate output and therefore more accurate results (e.g. adding wall thickness/material, etc.) (Mackey & Roudsari, 2017) and (Roudsari et al., 2013).
The properties of the default material are obtained from EnergyPlus. For the microclimate analysis in Honeybee the path to the respective weather file is required, as well as the geometry. If needed, context geometries and other shading objects can be added (Roudsari et al., 2013).
With Honeybee the results of the analyses can be displayed as a map. There are different possibilities to explore and visualize the results in Honeybee (Roudsari et al., 2013).

Mosthapha and Chris discussed in Mackey and Roudsari (2017) the expression "tool vs toolkit", which serves as a sort of guiding principle for the creation of the software. It underlines the importance of VPLs, as Grasshopper is one, in software integration, because the software functions as "components" literally turn them into a toolbox (Mackey & Roudsari, 2017).

It also discusses how to stay within defined boundaries and not cover everything. "Do One Thing and Do It Well". In the case of the Ladybug Tools this is analysis related to climate/weather data. So it is pointed out that for the analysis of the result data, "better" programs are available and should be used (Mackey & Roudsari, 2017).

This also includes the exchange between other programs/tools. Care should be taken to offer import and export data in different formats to ensure an exchange of different tools. The use of standardized open formats helps to ensure this data transfer. In the Ladybug Tools data can be exported as EXCEL files using another plug-in. The Ladybug Tools are modularized as this ensures a higher degree of customization and possible integration with other tools (Mackey & Roudsari, 2017).

As mentioned above, not much needs to be adjusted to achieve a result, but since so much can be interfered with the process if you have the necessary knowledge, a lot can be adjusted and modified. Therefore the plug-in is basically suitable for all users. Due to the structure of the Ladybug Tools, the program is not only a black box, but the processes can be traced and it is possible to intervene (Mackey & Roudsari, 2017).

To learn how to use the Ladybug Tools it is recommended to work through the YouTube tutorials and visit the Ladybug Tools forum as well as Hydra. Hydra is a platform to share scripts and example files from Grasshopper (Chris et al., 2015).

EnergyPlus

EnergyPlus is not a direct microclimate simulation program, it is a building energy simulation program. It can model the energy consumption for heating, cooling, ventilation, lighting etc.

in buildings. Due to its features it can be well integrated into the microclimate simulation (Crawley et al., 2000).

OpenFoam

OpenFOAM is an open source CFD software, which is mainly developed by OpenCFD Ltd. since 2004. It can be used to solve complex fluid flows involving chemical reactions, turbulence, heat transfer, acoustics, solid mechanics and electromagnetics (OpenCFD-Limited, n.d.).

Open Studio

OpenStudio is a collection of software tools to support energy modeling of entire buildings with EnergyPlus and advanced daylight analysis with Radiance. OpenStudio is an open source project and includes graphical user interfaces together with a Software Development Kit (SDK) (Alliance-for-Sustainable-Energy-LLC, n.d.).

5.1.10. Ladybug Tools vs. ENVI-met

Parameter	Ladybug Tools	ENVI-Met
Computing Expenses	Medium	High
Includes Evapotranspiration	No	Yes
Open Source	Yes	No
Compatibility	Very High	Moderate
Accurracy	Very High	High
User Interface	Friendly	Friendly
Operating System	Windows, Mac and Linux	Windows
Visualization and Graphics	High	High
	Output Parameters	
MRT	Yes	Yes
Air Temperature	Yes	Yes
PET	No	Yes
UTCI	Yes	Yes
Relative Humidity	No	Yes
Wind Speed	Yes	Yes
Wind Direction	Yes	Yes
Solar Radiation	Yes	Yes
Surface Temperature	Yes	Yes
Sky View Factor	Yes	Yes
	Elements to Investigate	
Materials and Albedo	Yes	Yes
Green Buildings	Yes	Yes
Buildings Height	Yes	Yes
Building Shape	Yes	Yes
Waterbody	No	Yes
Vegetation	Limited	Yes

Table 5.1. Comparison of ENVI-Met and the Ladybug Tools (Albdour & Baranyai, 2019)

5.2. GIS Software

5.2.1. Arc GIS

ArcGIS was invented in 1999 and belongs to ESRI Inc. (Environmental Systems Research Institute) which is an in Redland, CA, US based supplier of geographic information system (GIS) software, founded by Jack and Laura Dangermond in 1969. ArcGIS is the global market leader in GIS software (Esri, n.d.-a).

According to Esri (n.d.-b), "ArcGIS offers a unique set of capabilities for applying location-based analytics to your business practices. Gain greater insights using contextual tools to visualize and analyze your data. Collaborate with others and share your insights via maps, apps, and reports" (Esri, n.d.-b).

The main functions of ArcGIS are:

- Spatial Analytics
- Imagery and Remote Sensing
- Mapping and Visualization
- Real-Time GIS
- 3D GIS
- Data Collection and Management (Esri, n.d.-b).

For the sake of completeness, it should be mentioned that all steps ArcGIS was used for in this thesis are also feasible with QGIS. So if ArcGIS is not available or an open source project is to be done, all steps can also be implemented with QGIS.

5.3. Python

Python is an easy to learn and powerful object-oriented programming language with a huge amount of users in a lot of different fields (Waldmann, 2019). It was founded by Guido van Rossum in 1991.

The Anaconda distribution is a free and open-source distribution for scientific computing. Spyder is a powerful scientific environment written in Python. It features a combination of advanced editing, analysis, debugging and profiling functionality of a comprehensive development tool with the data exploration, interactive execution, deep inspection and visualization capabilities of a scientific package. An advantage of Spyder is, that many popular packages, as NumPy, Pandas or Matplotlib are integrated, but nevertheless it can always be extended via plug-ins. It is integrated in the Anaconda distribution and comes with the Python(x,y) and WinPython distributions for Windows (Waldmann, 2019) (PythonSoftwareFoundation, n.d.).

6. Methods

The method chosen in this thesis to answer the research question is, besides the literature research, the experiment. The experiment is a basic scientific procedure and investigates causal relationships in a controlled environment by manipulating an experimental variable in a repeatable manner and measuring the effect of the manipulation (Balzert, 2008). Experiments can be performed in the field (field experiments) or in the laboratory (laboratory experiment). In the field, it is a natural situation and the experiment is subject to disturbance factors. In the laboratory it is a completely controlled situation. Characteristics of the experiment are the measurability of the results, it must be repeatable and verifiable (Balzert, 2008).

Besides the literature review, two methods had been chosen to answer the research question:

- Sensitivity analysis
- Case study

Sensitivity analysis is a laboratory experiment. The experiment takes place in a controlled environment. A variable (building material) is manipulated in a repeatable way and its effect on the system is measured (Balzert, 2008).
The case study is a field experiment, as the experiment is exposed to disturbance sources and is not fully controllable. The focus is less on the causal relationship than on the final alignment. The question is to find the variable (software, parameters) that is most similar to the real world or which means (software) should be used to achieve certain goals (plausible results) (Balzert, 2008).

Sensitivity analysis and case study both bring measurable results. For example, the difference in temperature in the same pixel, at the same time, but a different building material. Both experiments are also repeatable and therefore verifiable. The case study is conditionally repeatable, because it is a field experiment and the prevailing factors are not always the same.

At first the sensitivity analysis doesn't compare the two microclimate tools with each other, rather than it evaluates the microclimate tools by itselfs. In each experiment only one parameter changes, while all the others remain the same. The different results can be compared and analyzed in which dimension the model acts, like how sensitive it is, as well as how close these are to the, according to literature, expected results.
These sensitivity analysis will take place with ENVI-met, on the one hand, and the Ladybug Tools in Grasshopper on the other hand. As mentioned before, the analysis is separated for

each software and the main focus is not to compare the results of both softwares, it is to compare te results from each software on its on.

The case study takes place to compare the two simulation tools with each other, as well as with real measured data. The study area is a real existing area in which every marked point has been measured. In both simulations, the same area was rebuilt and the same points are marked as receptors to get the results always from the same place/pixel. With this method, the results from the measurement of the real world, as well as both simulation tools, can be compared with each other. The results show how much both tools differ from each other and how close each tool is to the real measured data.

6.1. Data

The primary data which were used in this thesis, are weather data, on the one hand, and geometry data on the other hand.

6.1.1. Weather Data

The weather data used in this thesis are from EnergyPlus, where a file is available for virtually every major city in the world. According to EnergyPlus they provide weather files in EnergyPlus weather format for more than 2100 locations on their website. The USA is most densely populated, followed by Canada, but there are also more than 1000 locations in 100 other countries of the world. The weather data is organized by region and country of the World Meteorological Organization (Crawley et al., 2000).

The file format .epw stands for Energy Plus weather file, which is a simple ascii file containing the hourly or sub-hourly weather data for this location. The epw data format was developed by Energy Plus to create a generalized weather data format. All the data are in SI units (U.S.DepartmentofEnergy, 2019).

After downloading, the folder comes with three files:

- DDY
- EPW
- STAT

The Design Day data (DDY) is not directly needed for the simulation. It is a collection of the climate design data, that are needed for the sizing in EnergyPlus. The EnergyPlus Weather file is the actual weather file, which is used as the input weather file for the simulation. In the statistics file (STAT), the statistics used by the weather file are displayed (U.S.DepartmentofEnergy, 2019).

The weather file used for the simulation is a typical weather data set. A typical weather data set contains one year of hourly data, i.e. 8760 hours per data set, which are synthesized to represent long-term statistical trends and patterns in weather data for a longer recording period (Crawley, 1998). An EPW file represents the TMY (typical meteorological year) of this exact location. This set consists of 12 months, covering a period of about 23 years (1952-1975, available data varies by location) to represent typical months. For this data set, individual months are selected rather than whole years. The TMY months have been calculated on the basis of a monthly composite weighting of solar radiation, dry temperature, dew point and wind speed compared to the long-term distribution of these values. The resulting TMY data files each contain months from a number of different years, which is the most representative of a typical year at that location (Crawley, 1998).

6.1.2. Geometry Data

The geometry data required for the Ladybug Tool in Grasshopper comes from the City of Vienna. The City of Vienna provides a lot of open source data on their website (www.data.gv.at). They also provide 3D-models of the buildings in Vienna, but this data was not used in this thesis, because the structure of the buildings is very detailed. This is generally very good, however, experiments have shown that the computing time is extended by a lot, but the results are not strongly influenced. To overcome this problem, only the foot prints (outline) of the buildings was taken and visualized in Grasshopper. Based on the footprints, the buildings can be extruded in Grasshopper. The vegetation, e.g. trees, was taken from the data set "Baumkataster", in which every tree in the city is localized as a point. These point data were modeled in Grasshopper as tree crowns. Soil data, such as asphalt or grass, were digitized in a GIS from a satellite image.

On one hand, the same data were used for ENVI-met as for the Ladybug Tools (case study), and on the other hand the data was created in ENVI-met itself (sensitivity analysis).

6.2. Software

6.2.1. Microclimate Software

All microclimate analyses were carried out with ENVI-met or with the Ladybug Tools in Grasshopper/Rhino.

ENVI-met

The ENVI-met (www.envi-met.com) version 4.4 Winter Release 2018/2019, the ENVI-met version 4.4.3 Summer 2019 and the ENVI-met version 4.4.4 Winter 2019/2020 were used for this thesis.

Ladybug Tools

Rhinoceros 3D (www.rhino3d.com) version 6, which includes Grasshopper, was used for the thesis. The following plug-ins were used:

- Ladybug 0.0.67 and Honeybee 0.0.64 (https://www.food4rhino.com/app/ladybug-tools)
- GhShp 0.1 (https://www.food4rhino.com/app/ghshp)
- TTToolbox 1.9 (https://www.food4rhino.com/app/tt-toolbox)
- item selector -> Human + Tree Frog (https://www.food4rhino.com/app/human)

6.2.2. Arc GIS

The version used for the work on this thesis is ArcGIS 10.4.

ArcGIS was used to create georeferenced footprints, as a basis for the 3D data of the model areas used in the Ladybug Tools and ENVI-met.

6.2.3. IRT Cronista

The Grayess IRT cronista® is a professional thermographic analysis and reporting tool for researchers that provides: accurate detailed analysis, including sequence analysis (different types of ROIs and statistics), quickly made eye-catching reports in Microsoft Word plus, it has integrated communication for real-time image acquisition, analysis and process control (Vardasca et al., 2014).

The Grayess IRT cronista software was used to set the emissivity and to export the data as CSV files.

6.2.4. Python

In this thesis, Python version 3.6 and the Anaconda distribution are used to post-process the data of the case study and to calculate the statistics. The open source software Spyder is used as IDE (integrated development environment), but Jupyter Notebook was also used to visualize the diagrams and figures.

The main libraries involved in this thesis were:

- Numpy for calculations and statistics
- Pandas to handle the CSV files
- Matplotlib for plots and visualizations

6.3. Sensitivity Analysis

A fictitious model area was created for the sensitivity analysis. The focus of the sensitivity analysis is on different wall materials and on the interaction between the buildings and their surroundings, as well as the vegetation and its surroundings. The fictitious model therefore includes buildings in different shapes and vegetation such as trees (see Figure 6.1).

Since only one parameter, for example the wall material or the vegetation, was changed in each of the tests, the differences in the models are easy to see. According to literature, each selected material performs in a different way (see chapter 3 Building Physics), therefore the results of the different models show how sensitively the tool works.

6.3.1. Wall Material

ENVI-met

The model area was created with SPACES (see chapter 5.1.8). No satellite image was used as a template due to it being a fictitious test area. Nevertheless, a place on earth had to be specified and Linz was chosen.

The Table 6.1 shows the input model parameters of the analysis of the different wall materials.

Location	Linz
Latitude	48.31
Longitude	14.30
Model Dimensions	40,40,25 (x,y,z)
Grid cell size [m]	2,2,2 (x,y,z)
Surface/Soil	Loamy soil
Vegetation	4x Tree 10m very dense, leafless base
	1x Cylindric, medium trunk, dense, small (5m)

Table 6.1. Model area parameter

For each analysis the settings of the created area were static, only the wall materials were modified. Therefore a few materials have been picked to be analyzed:

- Glass (clear float)
- Passive wall (good insulation)
- Concrete (hollow block)
- Concrete (heavy)
- No insulation (corresponds to brick)

- Default moderate insulation

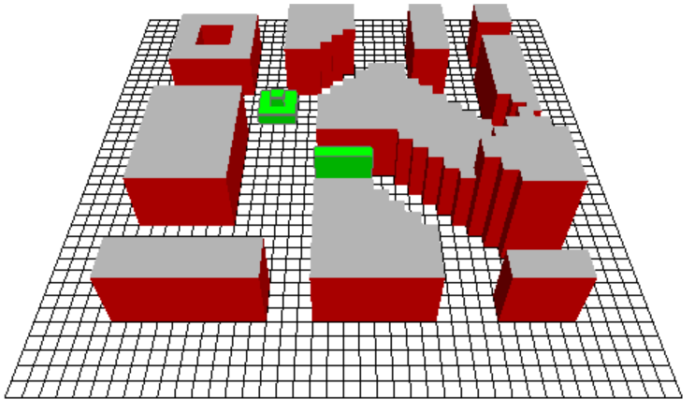

Figure 6.1. Fictitious model area 3D (wall material brick) in ENVI-met

All chosen materials are default from the ENVI-met database manager. Table 6.2 and Figure 6.2 show the physical parameters and the wall structure of the different materials according to the ENVI-met database.

Parameter	Glass	Concrete (Heavy)	Concrete	No Insulation
Thickness of Layers m	0.01, 0.01, 0.01	0.1, 0.1, 0.1	0.1, 0.1, 0.1	0.02, 0.38, 0.01
Absorption Frac	0.5	0.7	0.7	0.42
Transmission Frac	0.9	0.0	0.0	0.13
Reflection Frac	0.05	0.3	0.3	0.45
Emissivity Frac	0.9	0.9	0.9	0.9
Specific Heat J/(kg*K)	750	840	840	829.84003
Thermal Conductivity W/(m*K)	1.05	1.3	0.86	0.84
Density kg/m^3	2500	2000	930	1856

Table 6.2. Glass, concrete (heavy), concrete (hollow block) and no-insulation (brick) wall material parameters

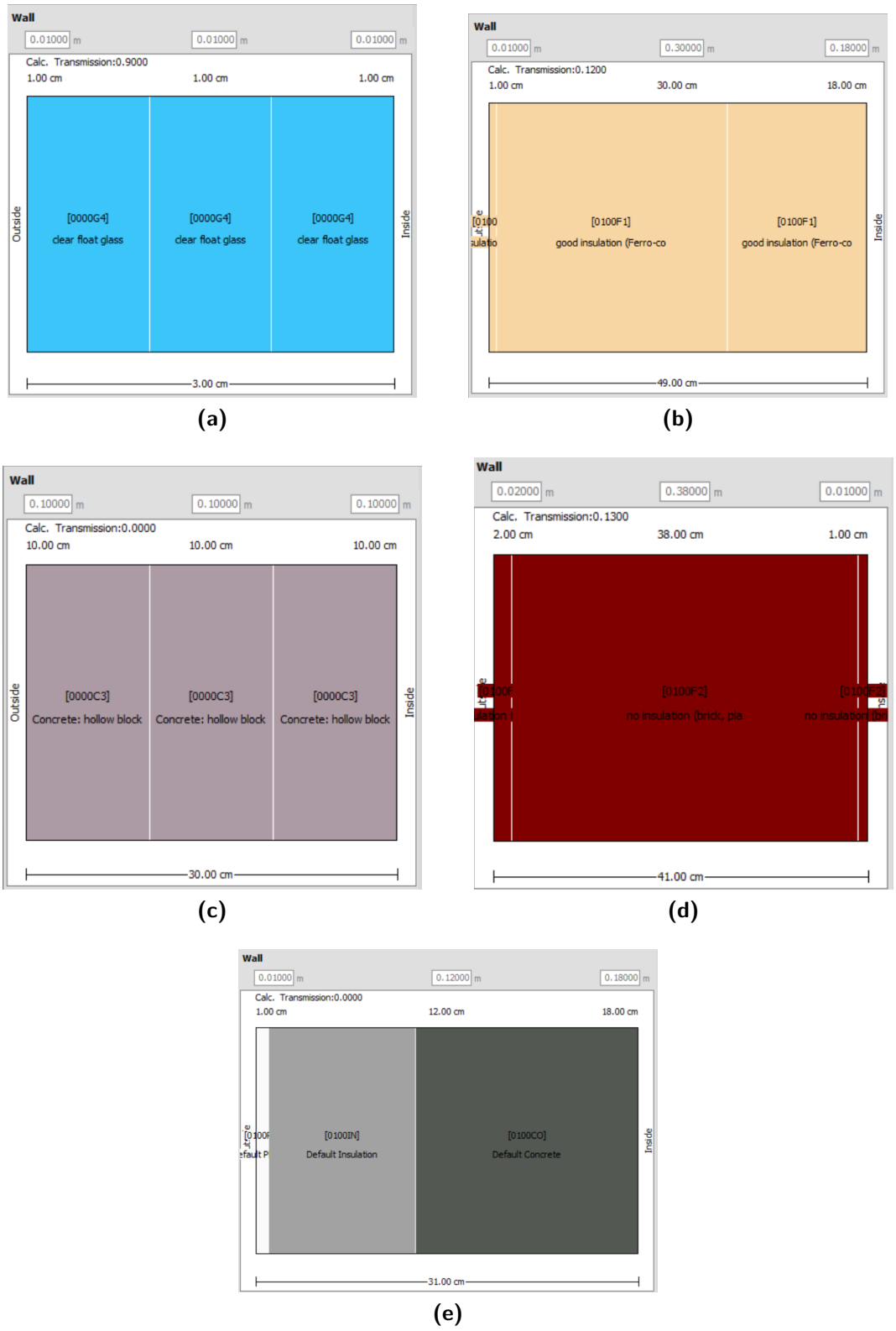

Figure 6.2. Construction of the different wall materials glass (a), passive-wall (b), concrete (c), no-insulation (d), moderate-insulation (e)

Since the default-moderate-insulation and the passive-wall consists of several different materials, these are shown separately in the Table 6.3 and Table 6.4. According to the ENVI-met Library the passive-wall consists of plaster, ferro-concrete and good-insulation (see Figure 6.2). Since there is no good-insulation material, it was assumed that the insulation is also the default-insulation material as in the DMI wall. The no-insulation wall consists of 38 cm brick and 3 cm plaster.

Parameter	Default Plaster	Default Insulation	Default Concrete
Thickness of Layers [m]	0.01	0.12	0.18
Absorption [Frac]	0.5	0.5	0.5
Transmission [Frac]	0.0	0.0	0.0
Reflection [Frac]	0.5	0.5	0.5
Emissivity [Frac]	0.9	0.9	0.9
Specific Heat [J/(kg*K)]	850	1500	850
Thermal Conductivity [W/(m*K)]	0.6	0.07	1.6
Density [kg/m^3]	1500	1274.64001	2220

Table 6.3. Default-moderate-insulation wall parameters

Parameter	Default Plaster	Default Insulation	Ferro-Concrete
Thickness of Layers [m]	0.01	0.30	0.18
Absorption [Frac]	0.5	0.5	0.5
Transmission [Frac]	0.0	0.0	0.0
Reflection [Frac]	0.5	0.5	0.5
Emissivity [Frac]	0.9	0.9	0.9
Specific Heat [J/(kg*K)]	850	1500	1000
Thermal Conductivity [W/(m*K)]	0.6	0.07	2.3
Density [kg/m^3]	1500	1274.64001	2520

Table 6.4. Passive-wall parameters

Receptors are placed at certain points of interest, such as near the wall or under the tree, to obtain a time series for a specific location for the entire simulation time.
A typical summer day (23.7.) was chosen for the simulation. The EPW file from Linz works as input weather file.

The visualization of the ENVI-met output took place in Leonardo (see section 5.1.8). From there the final maps were exported as PNG files.
Using the NetCDF converter tool provided by ENVI-met, the finished result files were converted from EDX (which can only be opened in Leonardo) to NetCDF. With the help of a Python script (see appendix D.4), difference maps were created from this data to represent the day/night temperature or the mean temperature for the whole day. This script can also be used to compare different scenarios (e.g. greening) or create difference maps of various

materials.
When creating the microclimate maps, attention was paid to ensure that the maps to be compared have the same legend.

Simulations with the same approach were also carried out for a typical winter day (23.1.).

Ladybug Tools

For the Ladybug Tools, the area was rebuilt from ENVI-met in a GIS and then imported to the Grasshopper canvas with the *Shapefile Import component*. As already in (chapter Data 6.1) described, the footprints of the buildings were extruded in Grasshopper (see Figure 6.3).

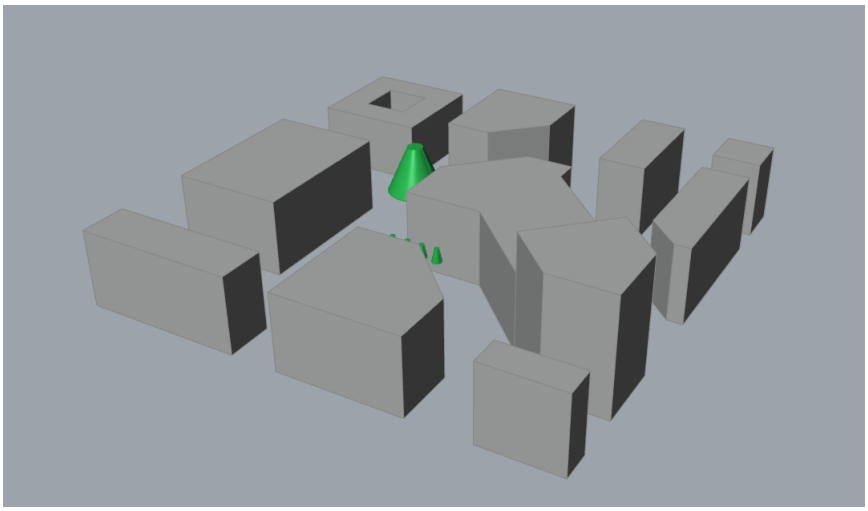

Figure 6.3. 2D geometry from ArcGIS extruded to 3D geometry in Rhino 3D/Grasshopper

The Table 6.5 shows the model parameters of the analysis of the different wall materials.

Location	Linz
Grid cell size [m]	2
Soil surface type	Asphalt as asphalt
Vegetation [m]	shape: truncated cone
	radius at the bottom: 2 and 7
	radius at the top: 1 and 2
	height: 6 and 2
	treetop height (z-unit): 2 and 5

Table 6.5. Model area parameters in the Ladybug Tools

The same wall materials as in ENVI-met were used, except only one kind of concrete wall was analyzed. Heavy weight concrete is the more typical concrete wall. Therefore the hollow concrete wall was excluded in the Ladybug Tools.

Used materials in the Ladybug Tools are:

- Brick corresponds to no-insulation
- Concrete (heavy)
- Passive wall (good insulation)
- Moderate Insulation
- Glass

Table 6.6 shows the different physical parameters of the wall material used in the Ladybug Tools. The EnergyPlus default materials were used for the concrete, brick and glass facade.

Parameter	Concrete	Brick
Thickness of Layers [m]	3 * 0.1016	3 * 0.1016
Thermal Absorption [Frac]	0.9	0.9
Solar Absorption [Frac]	0.85	0.7
Visible Absorption [Frac]	0.85	0.7
Specific Heat [J/(kg*K)	836.8	790
Thermal Conductivity [W/(m*K)	1.311	0.89
Density [kg/m^3]	2240	1920

Table 6.6. Parameters of concrete wall and brick wall

Glass was created with different parameters than the other materials. Therefore an extra table was created (see Table 6.7).

Parameter	Glass
U-Value [W/(m^2*K)]	3
Thickness of Layers [m]	0.003, 0.13, 0.003
Solar Transmittance [Frac]	0.837
Solar Reflectance [Frac]	0.075
Visible Transmittance [Frac]	0.898
Visible Reflectance [Frac]	0.081
Conductivity [W/(m*K)]	0.9
Emissiviy [Frac]	0.84

Table 6.7. Parameters of the glass material in the Ladybug Tools

The parameters of the default-moderate-insulation and the passive-wall are the same as defined in ENVI-met(see Table 6.3 and 6.4).

The materials of the wall and the roof were set with materials from the EP Construction Library (brick, concrete, glass) or a new EP construction was created based on the

ENVI-met values (passive-wall, moderate-insulation). With the *HoneybeeSet EP Zone Construction* component the wall material was modified. With the *HoneybeeCreate EP Ground* component, the soil material was set to asphalt. As in ENVI-met a typical summer day (23.7.) and a typical winter day (23.1.) was chosen for the simulations. The input weather data is the EnergyPlus weather file from Linz.

After the geometry data, the materials and the weather file are set, there are three main steps:

- Viewfactor analysis
- Analysis in OpenStudio
- Microclimate map

The input for the *IndoorViewFactor* component are the modified buildings, the soil surface and the vertical polygon. The grid size is 2m, because the same raster defined as in ENVI-met should be produced. After that part the geometry and weather data were analyzed in EnergyPlus (*exportToOpenStudio* component) and then the microclimate map was created (see appendix B(1)).

The results of the microclimate map from the Ladybug Tools, can be visualized by the *VisualizeMicroclimate* component in Grasshopper. The output of this component was "baked" to Rhino 3D and then exported as a PNG file.
For the difference maps, the microclimate result file was read by the *readMicroclimateMtx* component and then converted into an actual data tree. The data tree was split into 24 hours and the hours needed were selected. The average item across the tree for each hour and each grid ID was calculated. The same happened to an other map or an other selected time period and the outputs of the both were subtracted. The result can be visualized with the *reColorMesh* component. For the whole script see appendix B(3).
As in ENVI-met when creating the microclimate maps, attention was paid to ensure that the maps to be compared have the same legend.

6.3.2. Climate Adaption Measures

ENVI-met

The parameters of the model area and the input weather data are nearly the same as described in the chapter Wall Material (see chapter 6.3.1). The only difference is, there are no trees in this model area. Two wall materials were selected to simulate climate adaptation strategies in the form of facade and roof greening. The selected materials are no-insulation and concrete, which correspond to the parameters in the Table 6.2.

The basecase is a simulation of the area without greening. Exactly this model was taken and a green roof was added as the first scenario and a green facade as the second. As a third

scenario, it was tested how the temperature changes when a green roof and a green facade are added to the buildings.

The "green + sandy loam substrate" greening system is default from the ENVI-met greening library. This system was used for the roof and the facade greening. The greening system consists of a substrate layer and the greening itself (see Figure 6.4).

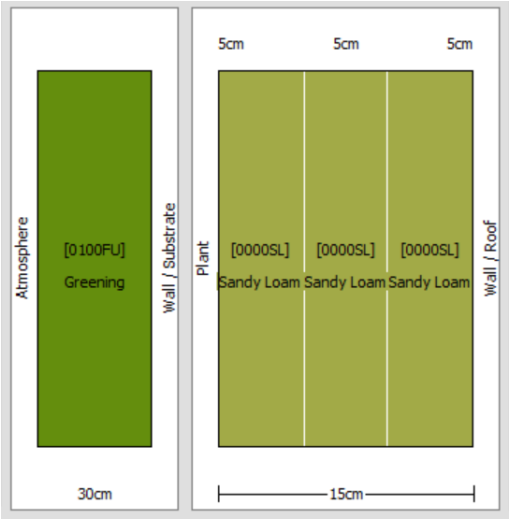

Figure 6.4. Construction of the "green + sandy loam substrate" greening material from the ENVI-met database

Ladybug Tools

As in ENVI-met, the parameters of the model area and the input weather data are the same as described in the chapter Wall Material (chapter 6.3.1) except:

- The experiment was only testet with concrete and brick. The parameters of the materials correspond to the parameters in the Table (6.6).
- There are no trees in the model area.

As in ENVI-met, the basecase (without greening) was tested, as well as only with roof greening, only with facade greening and with roof and facade greening . The entire workflow can be read in the Grasshopper script in the appendix B(1).

To create a roof or facade greening in Grasshopper, the "RoofVegetation material" has to be added to the canvas (“Bigladder Software”, n.d.). The material was modified to fit the ENVI-met substrate settings (Figure 6.4). The wall materials were set with the same components as in chapter Wall Materials 6.3.1, the greening material is added on top of the roof or wall material (for the parameters see Figure 6.5 and 6.6).

Modified grass

```
                    Material:RoofVegetation,
              GreenRoof,                      !- Name
            0.6,                          !- Height of Plants {m}
          1,                            !- Leaf Area Index {dimensionless}
          0.5,                        !- Leaf Reflectivity {dimensionless}
                0.95,                       !- Leaf Emissivity
          180,                        !- Minimum Stomatal Resistance {s/m}
                Green Roof Soil,            !- Soil Layer Name
                   MediumRough,               !- Roughness
                0.15,                        !- Thickness {m}
          0.35,                       !- Conductivity of Dry Soil {W/m-K}
             500,                       !- Density of Dry Soil {kg/m3}
        3000,                       !- Specific Heat of Dry Soil {J/kg-K}
                0.5,                        !- Thermal Absorptance
                 0.7,                       !- Solar Absorptance
                0.75,                       !- Visible Absorptance
      0.6,                        !- Saturation Volumetric Moisture Content of
                                   the Soil Layer
      0.4,                       !- Residual Volumetric Moisture Content of the
                                    Soil Layer
      0.4,                        !- Initial Volumetric Moisture Content of the
                                    Soil Layer
        Advanced;                  !- Moisture Diffusion Calculation Method
```

Figure 6.5. Characteristics of the modified "GreenRoof" material for the green building simulation in the Ladybug Tools

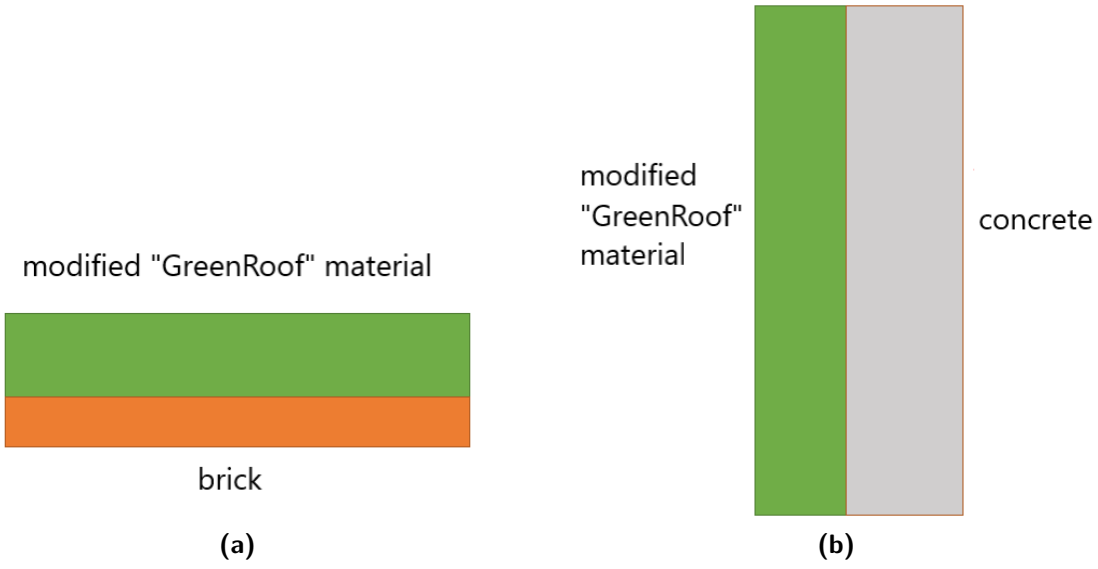

Figure 6.6. Construction of the roof greening (a) and the facade greening (b) in the Ladybug Tools

6.3.3. Vegetation

The model area and settings were created in ENVI-met as described in Bruse (2000) (see Figure 6.7).

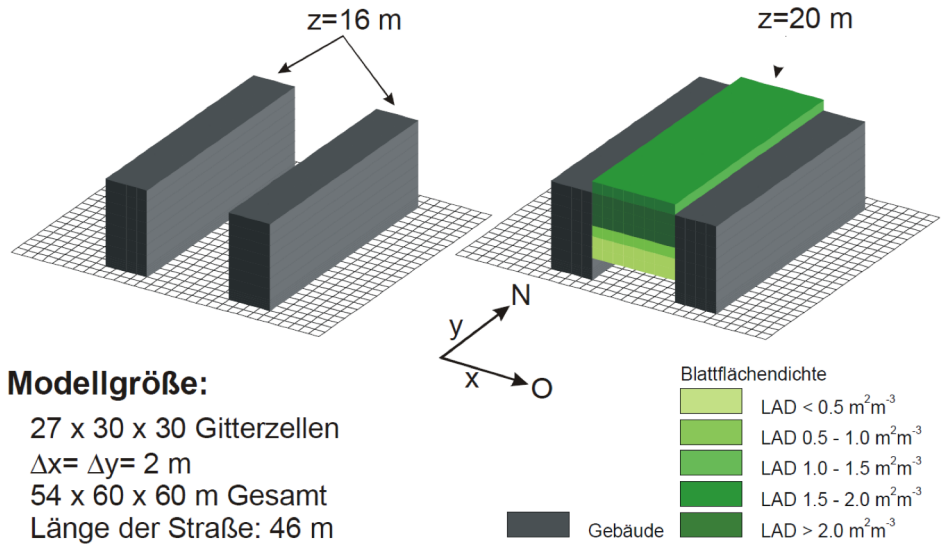

Figure 6.7. 3D view of the model area (Bruse, 2000)

Since the paper did not specify the material of the buildings, the material chosen was default-moderate-insulation (for the parameters see Table 6.3) (Bruse, 2000).

One scenario consists of two building blocks only and in the other scenario vegetation was added between the two building blocks (see Figure 6.7). In both areas receptors were placed in the middle of the street canyon.

6.4. Case Study

6.4.1. Location

The aim of the case study is to compare ENVI-met and the Ladybug Tools with the measured data as well as the two microclimate tools to each other to explore their limitations.

As the results from the sensitivity analysis show, there is a mismatch in the interaction between different wall materials and the surrounding environment. Also the results between vegetation and non-vegetation were different than expected according to literature.
Therefore, the following locations 6.8 were picked to fit the parameters of interest.

Some of the locations were chosen to compare them to themselves and some locations primarily to compare them with the ENVI-met and Ladybug results.

The study area is located in the 21. district, Floridsdorf, in Vienna. The area includes the buildings of the AIT, Austrian Institute of Technology. This area was chosen because it is close to the measure equipment and additionally, every needed parameter could be found at the territory (e.g. glass wall, passive house, greening).

Number	Name	Annotation
1	Asphalt sun	Parkinglot 65
2	Asphalt shadow	Parkinglot 62
3	Gravel sun	-
4	Grass sun	-
5	Grass shadow	under tree
6	Facade east	GG 4
7	Facade north	GG 4
8	Facade west	GG 4
9	Facade south	GG 4
10	Asphalt south	Parkinglot 16
11	Glass facade	SW, GG4
12	Tree	BK 202
13	Grass under tree	BK 202
14	Tree crown	BK 202
15	Tree asphalt	sun/shade
16	Facade	GG 6
17	Energy Base sign	GG 6
18	Terrace concrete	GG 6
19	Terrace wood	GG 6
20	Terrace greening	vertical
21	Terrace greening	horizontal

Table 6.8. Locations case study

6.4.2. Thermal Camera

The thermal camera model used for the measurements was the Handy Thermo TVS 200EX Avio. According to the Avio (n.d.) website, it is a handy-type thermography which supports various applications from research and development to facility maintenance and survey/diagnosis of buildings and concrete structures. In Table 6.9, some specifications of the camera are listed (Avio, n.d.).
The measurements took place from 19.8.2019 15:00 to 20.08.2019 17:00 every hour. The last measurement on 19.08.2019 took place at 21:00 and the first one on 20.08.2019 again at 07:00. This means that from 22:00 till 07:00 no measurements were taken. First the thermal camera has to be calibrated (holding it on a surface with known emissivity and setting this

Camera	Handy Thermo TVS 200EX avio
Temperature range	-20 to 500 °C
Accuracy	2°C
Detector	UFPA, 320(H) x 240(V) VOx microbolometer
Spectral range	8 to 14 µm
Spatial resolution /IFOV	1.68 mrad
Field of View FOV	30.6°(H) x 23.1°(V) (with standard 14mm lens)
Frame time	1/60 seconds

Table 6.9. Specifications Thermal Camera

value). For the following images it must not pay attention to this, because the adjustment of the emissivity can be done afterwards. Every hour a picture was taken in the same order from each location with the thermal camera. After each hourly round of photographing the locations, the images were immediately transferred to the laptop and explicitly named to avoid errors (see post processing 6.4.2).

Post-processing with Python

The first step during post-processing is to name all thermal cam pictures in a consistent way. For example 20082019170001, 20 stands for the day, 08 for the month (August), 2019 for the year, 17 for the hours (equals 5 pm), 00 for the minutes und 01 for the location, in our example "asphalt sun".

Unfortunately, the emissivity had to be adapted manually for each picture in the Thermal Camera software IRT cronista. The following table (6.10) shows which values for the emissivity were set for each location. The emissivity depends on the wavelength of the thermal camera. As mentioned in Table 6.9 the wavelength of the used Camera is from from 8 to 14 µm. Therefore the following values are set:

Material	Emissivity
Asphalt	0.9
Grass	0.99
Tree	0.95
Dry grassland	0.88
Wood	0.93
Stone	0.95
Concrete	0.9
Glass	0.9

Table 6.10. Emissivity of the materials in the case study

After that step, every picture of every location and each hour was exported as a CSV file. The result is a folder with hourly files for each location. One CSV file contains every value

for each pixel for that specific hour at that location.

The aim of this post-processing of the measured thermal cam data is to have one CSV file with an hourly value for each location. To reach this aim and to automate this process a Python script was written (see appendix D.1).

The script imports every CSV file from each location folder. The mean, min, max and median was calculated for each file. The min and max was calculated to evaluate if the value for each pixel scatters a lot. The reason for a wide scattering could be pixels on the edge which belongs to another material. To eliminate these, the edge pixels were cut off.

The newly calculated values were exported in a CSV file with the same filename and "_edited" added. To these CSV the column "DTime" (date and time), "Date" and "Time" were added and filled with the date and time from the CSV filename. All CSV files with "edited" in the filename were merged to one location file. At some locations, there were errors during the measurement - these missing values were interpolated (see appendix D.2). The final output from this script is a CSV file named "Location_xx" for each of the 21 locations. Every file includes the dtime (date and time), date, time, mean, min, max and median value.

The visualization of the diagrams was made with the matplotlib library in Python as well as with Microsoft Excel. The output CSV files from ENVI-met, the Ladybug Tools and the measured data were merged into one CSV file for each location. The final diagrams shown in chapter 7.2 were created with this file.

6.4.3. ENVI-met

Monde is a new feature in ENVI-met that simplifies the creation of geometry data (see 5.1.8). For the creation of the 3D model of the study area, instead of using only spaces, as in the sensitivity analysis, (see chapter 6.3) to digitize the model, shape files were converted to an INX file in Monde.

After creating a new project, the shape files created in chapter (6.4.4) were imported into Monde and appear there georeferenced. The shape files have to be assigned to features like buildings, soil, vegetation etc. It also must be set that the buildings height is taken from the attribute "height". A subarea, i.e. a section of the area must be defined, which contains all features that want to be exported (see Figure 6.8). Before the section can be converted into an INX file, certain parameters must be set, such as model size, grid size, building material, ground cover material, etc. After that the area can be converted into an INX file and this format can be opened in Spaces. In Spaces, there was still a little bit to post-process. For example, since no building materials were defined in the shape file "Buildings", all buildings in Monde were the same material (concrete), which had to be redefined in Spaces based on the real world (see Figure 6.9). The trees were also defined in Spaces.

Figure 6.8. Defined georeferenced subarea (GG, light yellow) including shapefiles of buildings (grey), grass (green), soil (yellow) and asphalt (black) before conversion to INX in Monde

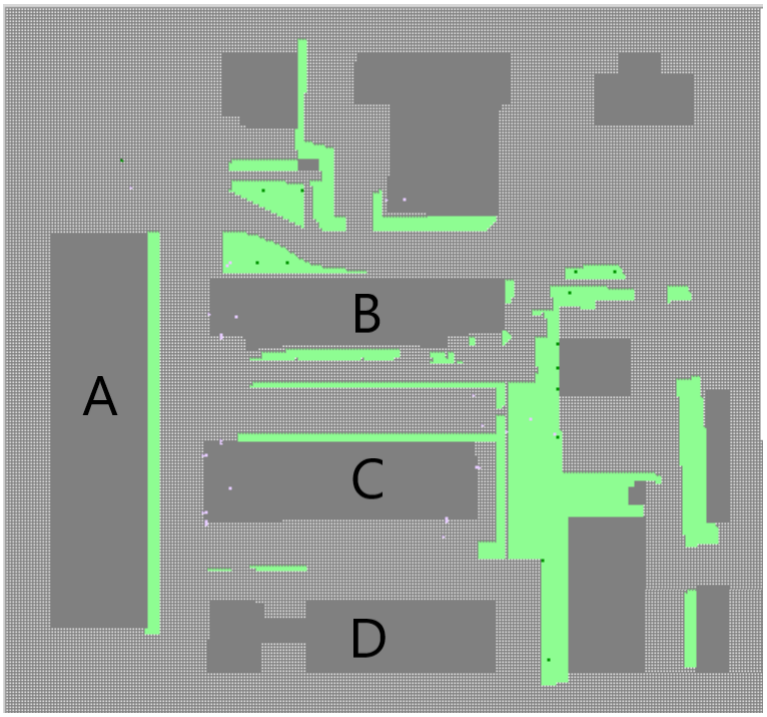

Figure 6.9. Model area case study in ENVI-met (INX-format) with receptor positions (violet) (see Table 6.12), greening (green), buildings (dark grey), asphalt (light grey) - A: steel (one layer), B: passive wall - good insulation and greening (green + sandy loam substrat), C: passive wall - good insulation, D: default-moderate-insulation, all others: concrete (heavy)

These different building materials used for the model area are default from the ENVI-met database manager and shown in Figure 6.9.

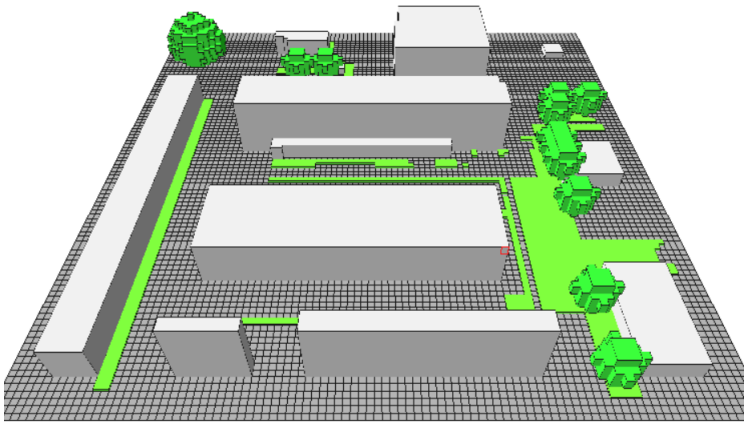

Figure 6.10. 3D model area of case study in ENVI-met

The Table 6.11 shows the model parameters of the case study.

Location	Giefinggasse 6, 2110 Wien, Austria
Latitude	48.27
Longitude	16.43
Model Dimensions	97,99,20 (x,y,z)
Grid cell size [m]	2,2,3 (x,y,z)
Surface/Soil	Asphalt Road
	Sandy Soil
Vegetation	Grass 25cm aver, dense
	Spherical, medium trunk, dense, medium (15m)
	Spherical, medium trunk, dense, large (25m)

Table 6.11. Model Area Parameter

On each location, point receptors were placed to get the values from always the exact same voxel (see Table 6.12). When selecting the voxels, it must be considered that the location points are on different levels. The Receptors were set while post-processing the IDX file in Spaces.

Number	Name	Pixel Location (x,y)
1	Asphalt sun	65, 42
2	Asphalt shadow	67, 38
3	Gravel sun	71, 39
4	Grass sun	73, 38
5	Grass shadow	79, 35
6	Facade east	67, 29, 5
7	Facade north	25, 35, 5
8	Facade west	22, 32, 5
9	Facade south	63, 21, 5
10	Asphalt south	61, 19
11	Glass facade	22, 22, 5
12	Tree	25, 64, 6
13	Grass under tree	25, 64
14	Tree crown	25, 64, 7
15	Tree asphalt	10, 76
16	Facade	24, 53, 5
17	Energy Base sign	24, 53, 5
18	Roof concrete	30, 54, 11
19	Terrace wood	-
20	Roof greening	28, 54, 11
21	Roof greening vertical	28, 54, 11

Table 6.12. Receptor locations case study in ENVI-met

Regarding the weather file, the date which corresponds to the real world measurements is set. The EnergyPlus weather file of Vienna serves as the input weather file. The start date of the simulation is 18.08.2019, the start time is 15:00 and the simulation duration is 50 hours. The start time of the simulation starts 24 hours before the actual measurement, so the model has enough spin-up time. Experiments have shown that the values vary greatly depending on the spin-up time and whether the model heats up (see 7.1.4).

The simulation takes about four to five days on a laptop with four CPU's and 16 GB RAM.

Post-processing with Python

Different ENVI-met outputs (MRT, AirtTemp,...) can be stored as XLS or CSV per point for a certain time period. These XLS or CSV files can be created from the outputs of the air data, but also from the building or ground surface temperature. With this data, diagrams can then be created about the temperature course, for example. The used output is opened in Leonardo and the respective voxel is selected. It is important that the height of the point is also taken into account and therefore the same voxel is used for each location. The next step is to save the required data (Air temperature, MRT,...) and the required time period

for each voxel as XLS file. A consistent file name is required for the Python script that modifies the files as needed for the analysis. The Python script basically consists of three steps:

- Change XLS to CSV
- Delete columns and rows not needed
- Add date and time column
- Merge all parameters (MRT, Surface Temperature,...) to one file
- Save as new file

The final CSV file consists in the date, the time and the values of the individual parameters for each location.

6.4.4. Ladybug Tools

The model area was preprocessed in ArcGIS (see Figure 6.11).

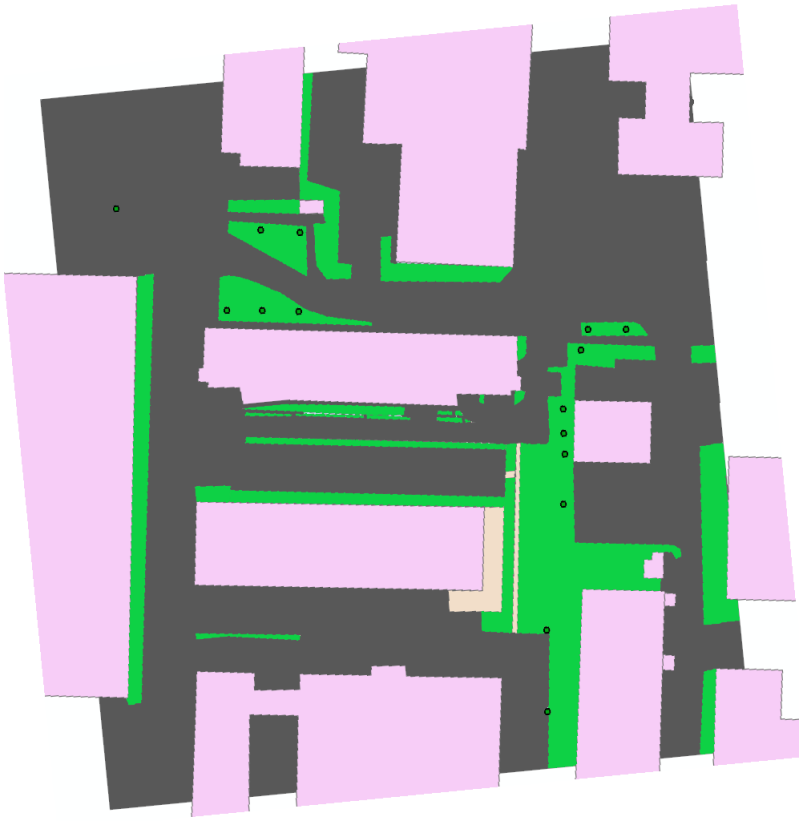

Figure 6.11. Constructed geometry in ArcGIS - buildings (pink), asphalt (grey), grass (green), soil (ocher), trees (green dots)

The following input data from the city of Vienna (www.data.gv.at) were used:

- "Mehrzweckkarte" as shapefile for the buildings' footprints and the height information of the buildings
- "Baumkataster" as shapefile for the tree position

To create the shape files for the ground cover polygons, a satellite image was used and digitized in ArcGIS. Three different types of ground cover were distinguished:

- Grass
- Soil/Gravel
- Asphalt

The final shape files used as an input for the 3D Model were:

- Trees
- Grass
- Soil/Gravel
- Asphalt
- Buildings

The in GIS prepared study area was imported to the Grasshopper canvas. Here the buildings were extruded based on their "height" attribute. Based on the centered points of the tree locations, the tree crown has been modeled as shown in Table 6.13. The Surface polygons have been extruded all by 1 meter and the z-axis was put to -1, so that the upper surface is at the same level as the bottom of the buildings. Because a lot of the buildings have different wall materials, the buildings "brep" has to be split up based on their material (see Figure 6.12). Each of the building groups are assigned with the respective material. The same happened with the different soil surface materials (see appendix B(2)).

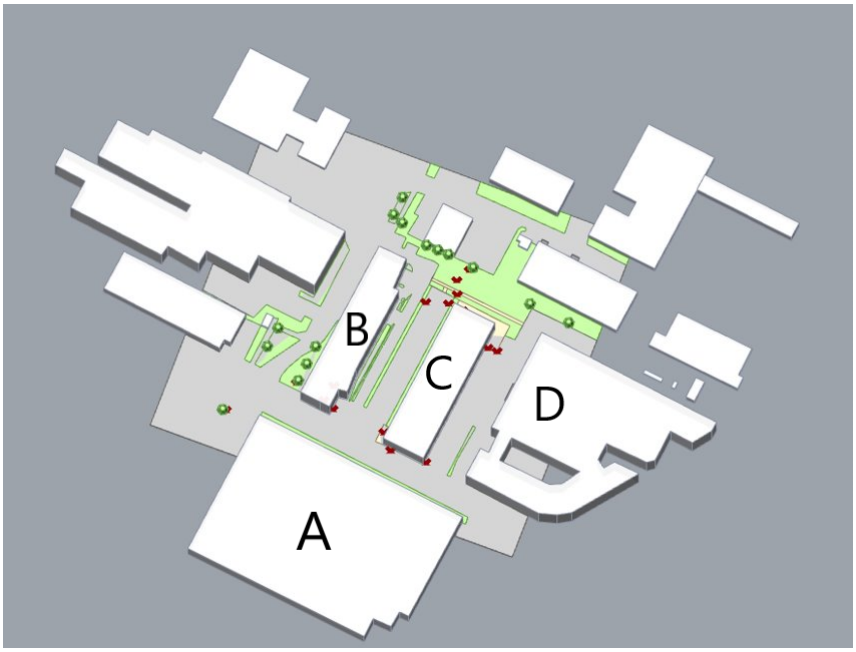

Figure 6.12. Model area case study in Grasshopper with receptor points (red) greening (green), soil (ocher), buildings (white), asphalt (light grey) - A: steel (one layer), B: passive-wall and green roof, C: passive-wall, D: default-moderate-insulation, all others: concrete (heavy)

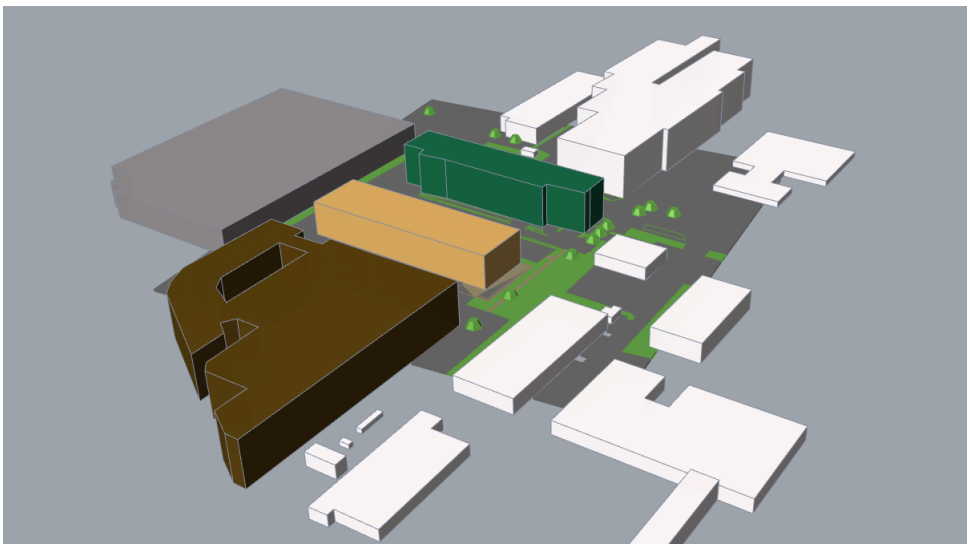

Figure 6.13. 3D model area of the case study in Grasshopper - steel (grey), passive-wall with green roof (green), passive-wall (ocher), default-moderate-insulation (brown), concrete (white)

The Table 6.13 shows the model parameters used for the case study.

Location	Floridsdorf
Grid cell size [m]	2
Soil surface type	Asphalt as asphalt
	Moist soil as Grass
	Dry Sand as Soil/Gravel
Vegetation [m]	shape: truncated pyramid
	radius at the bottom: 4
	radius at the top: 3
	height: 3
	treetop height (z-unit): 10

Table 6.13. Model Area Parameter

The EPW file of Vienna serves as input weather file. The start date of the simulation is 19.08.2019, the start time is 01:00 and the simulation duration is 48 hours.

The workflow of the analysis is basically the same as the one already mentioned in the chapter Sensitivity Analysis 6.3. For the whole script see appendix B(2).

The UTCI and the MRT are calculated in the same way as in the chapter Sensitivity Analysis 6.3. For the calculation of the surface temperature, the surface to be calculated (e.g. grass or asphalt) was divided into 2m raster in a GIS system. This surface was imported as SHP file into Grasshopper and converted into an EnergyPlus surface. After the analysis the surface outdoor temperature will be visualized with the component "ColorSurfaces". The result values will be exported as CSV files with the TTTool Box plug-in (see appendix B(2)).

The View Factor calculation for the two meter grid takes about six hours, the analysis in Energyplus about five hours and the microclimate map about four hours. The whole simulation takes about one to two days on a laptop with four CPU's and 16 GB RAM.

Post-processing with Python

For the preparation of the data, the required results of the microclimate analysis were exported as CSV file with TTToolBox. Before that, the required period was already selected in Grasshopper (see appendix B(2)). In Python unneeded columns were deleted, a time and date column was added and all parameters (MRT, Surface Temperature, ...) were merged into one file. This procedure was performed for all locations.

6.4.5. Statistics

Two statistical indices were selected, R^2 (coefficient of determination) and RMSE (root mean square error).

R^2 is a measure of the quality of linear regression and cannot become less than 0 and not

greater than 1, where the value 1 describes the situation where all data pairs lie on a straight line and thus a perfect fit is present (Pflieger, 2014).

Formula for calculating the R^2:

$$R^2 = \frac{\sum_{i=1}^{n}(\hat{y}_i - \bar{y})^2}{\sum_{i=1}^{n}(y_i - \bar{y})^2} = \frac{\text{explained variation}}{\text{total variation}} \tag{6.1}$$

or

$$R^2 = 1 - \frac{\sum_{i=1}^{n} e_i^2}{\sum_{i=1}^{n}(y_i - \bar{y})^2} = 1 - \frac{\text{unexplained variation}}{\text{total variation}} \tag{6.2}$$

- n = the number of observations
- y_i = single observation
- $\hat{y}_i$ = predicted value
- e_i = deviation between observed and model predicted value (error or residual)

(Pflieger, 2014).

If a regression has an R^2 close to 0, it means that the independent variables chosen are not well suited to predict the dependent variable. This is also called a poor model fit. Since R^2 is a unit value, it can also be expressed as a percentage (Pflieger, 2014).

The RMSE indicates how close a regression line is to a series of points. The RMSE is calculated from the square root of the average forecast error. The smaller the mean square error is, the closer it is to the line of best fit (Glen, n.d.).

$$RMSE = \sqrt{(f - o)^2} \tag{6.3}$$

- f = expected values
- o = observed values (Glen, n.d.).

The night hours (22:00 till 06:00) had not been included in the statistics, only the measured hours served as an input. The statistics have been calculated in Python (see appendix D.3).

7. Results and Discussion

In the following chapter, the previously prepared results, as described in the chapter Methods, are shown and discussed with the literature.
First of all, the sensitivity analysis in which the microclimate simulation tools themselves are compared is presented. Then, the results of the case study are shown, in which the microclimate simulation programs ENVI-met and the Ladybug Tools are compared with real measured data.

7.1. Sensitivity Analysis

7.1.1. Wall Material Summer

The choice of the building material has an impact on the microclimate. The effect of buildings is considered as one of the main reasons for the UHI effect. The thermal masses of the buildings increase the thermal capacity, which effects the temperature of the city. The building materials absorb the heat during the day and re-emit it to the surrounding environment after sunset. Therefore, higher surface temperatures of the buildings increase the ambient temperature. The temperature performance of a material is mostly determined by its thermal balance (Priyadarsini et al., 2008). With the right material choice in the right place, the temperature can be lowered. For example, highly reflective materials can reduce the surface temperature and cooling energy demand of a building during hot periods (Chokhachian et al., 2017). For this reason, different common building materials and their effects were tested in ENVI-met and the Ladybug Tools. In particular, the behavior at 22:00 was investigated because, as already mentioned, the UHI effect occurs most strongly in the evening or at night.

ENVI-met

Figure 7.1 shows the MRT results of the different building materials produced in ENVI-met at a height of 1.4 meters at 22:00.
Table 7.1 lists the air temperature and the MRT of the different materials during the day and in the evening.

The glass wall emits the most heat to the environment and the moderate-insulation (DMI) wall the least at 22:00. The difference between the two materials is about 3.2°C (MRT). At 13:00 the concrete wall emits the most heat and the glass wall the least. The difference is about 6.3°C (MRT).

		Glass	DMI	Concrete	Concrete H	No Insulation	Passive
MRT (°C)	13:00	52.88	58.51	59.16	55.3	58.3	56.16
	22:00	19.11	15.91	18.78	18.52	18.75	16.36
Air temperature (°C)	13:00	32.96	27.25	33.4	33.0	32.72	27.05
	22:00	29.03	23.59	29.05	29.00	29.05	23.62

Table 7.1. MRT and air temperature of the different wall materials at 13:00 and 22:00

Figure 7.4 shows the values of a specific point (voxel) on the microclimate map. Since it is intended to show how the temperature of the different materials changes over time, the voxel chosen is near the building facade and at pedestrian level.
In Table 7.1 and Figure 7.4 it can be seen that the MRT performs in an opposite way to the air temperature. During the night the air temperature is higher than the MRT and during the day it is exactly the opposite. It can also be seen that the different wall materials have a very similar course over the hours on the air temperature and the MRT.
Air temperature and air temperature in front of the facade perform very similarly. In both cases it is clearly visible that the passive-wall and DMI have a greater cooling effect on the surrounding temperature than the other materials.

The physical properties of the individual materials in the ENVI-met library are basically the same as found in the literature. Many different kinds of concrete exist. However the lightweight concrete in ENVI-met seems to insulate a bit more than found in the literature (see chapter 3 and 6.3). DMI represents a medium insulated wall and should therefore be less insulated than the passive-wall. Also, according to the thermal properties of DMI and passive-wall designed in ENVI-met, DMI should be less insulated than the passive-wall. A highly insulated wall does not absorb as much radiation during the day and can therefore not emit, as much radiation at night (Oke et al., 1991). This may lead to the assumption: the higher the insulation properties of the wall, the lower the emitted radiation and therefore MRT. Looking at the results, the MRT and the surface temperature is the lowest in the DMI scenario and not in the passive-wall scenario, which does not seem right under that assumption.

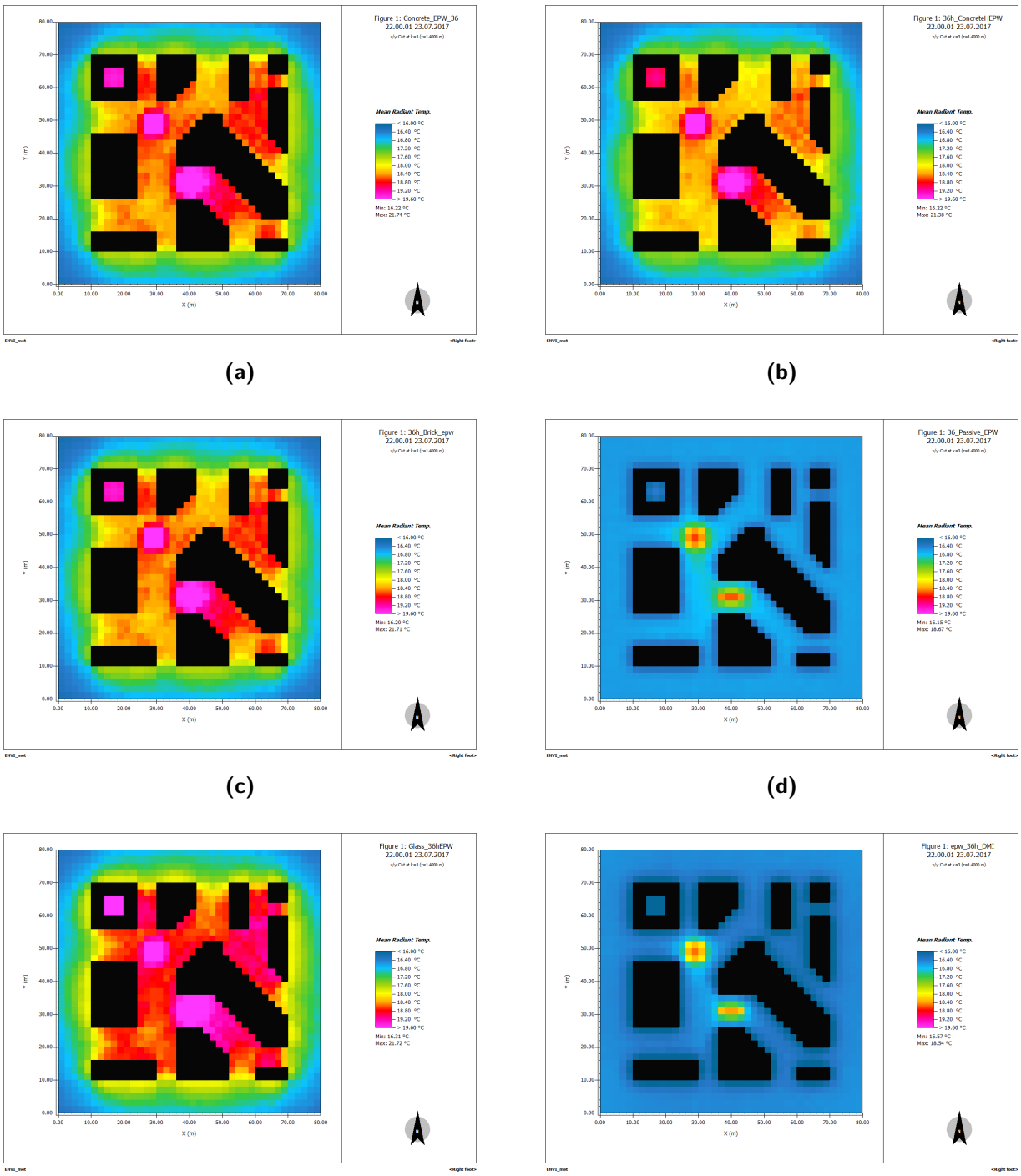

Figure 7.1. MRT (°C) of the different wall materials at 1.4 m height at 22:00 - concrete (a), hollow concrete (b), no-insulation (c), passive-wall (d), glass (e), moderate-insulation (f)

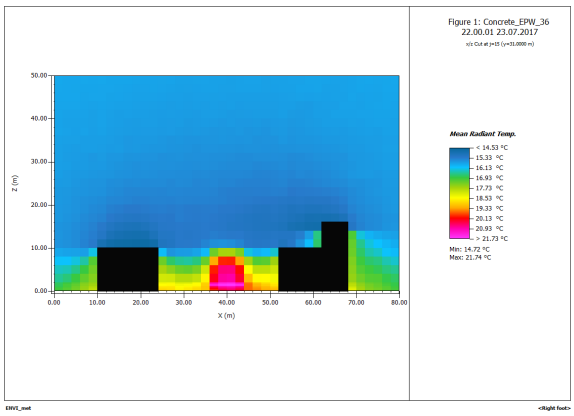

(a)

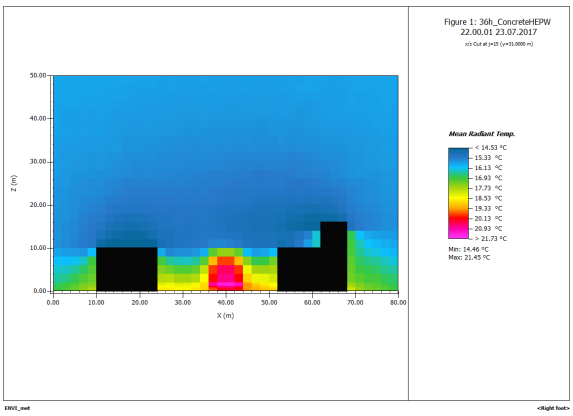

(b)

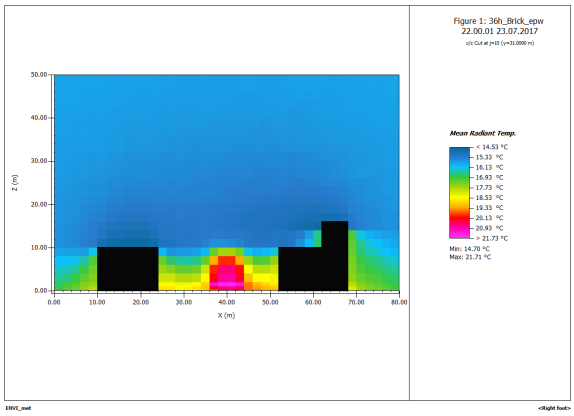

(c)

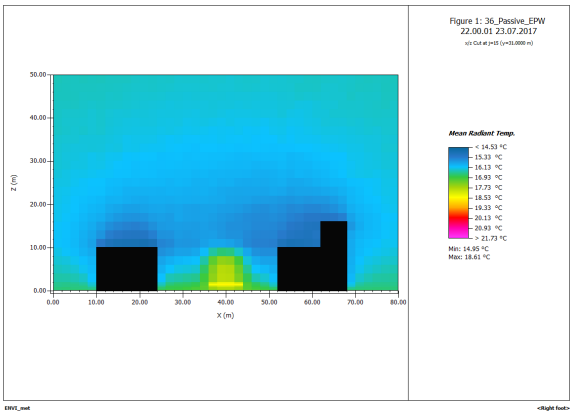

(d)

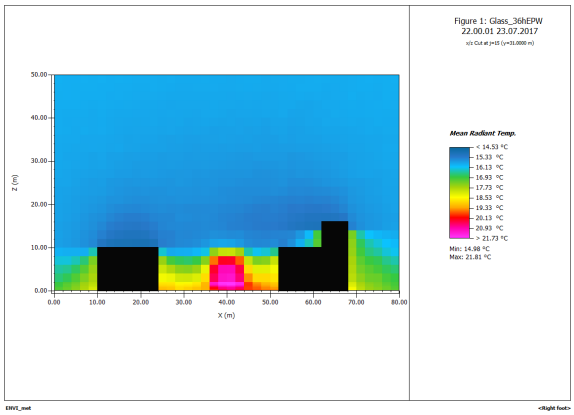

(e)

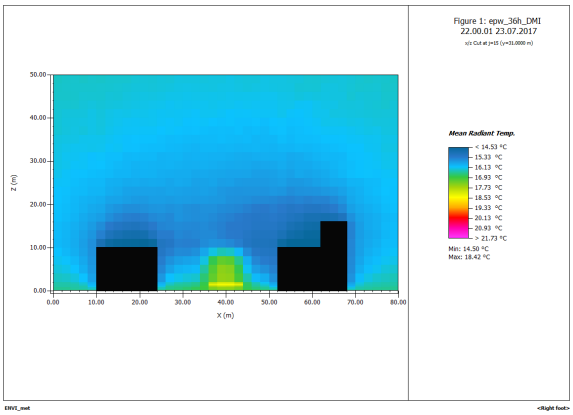

(f)

Figure 7.2. MRT (°C) of the different wall materials at 22:00 (x/z cut, y = 31m) - concrete (a), hollow concrete (b), no-insulation (c), passive-wall (d), glass (e), moderate-insulation (f)

Looking at the results of the horizontal section at 1.4 m (Figure 7.1), two points become obvious. There is a relatively small temperature difference between the DMI and the passive-wall scenario and a relatively large temperature difference between DMI and the passive-wall compared to all other materials. In every microclimate map, the trees appear as heat islands. However, a difference in the height of the temperature near the vegetation is visible depending on the chosen material. The cooler materials also have cooler trees compared to the other materials, which seems to be right, for the MRT takes the radiations from all surfaces into account. The radiation depends on the material and therefore differs with the different material. In the vertical section (Figure 7.2), which goes right through the vegetation, exactly the same can be observed. This view shows that the heat accumulates under the tree crown, resulting in higher temperatures.

A higher MRT with vegetation than without vegetation during the night can be true according to Perini et al. (2018) and Perini et al. (2017). The lower MRT under trees during day is mainly because of the shading effect. The tree crown limits the incoming solar radiation. According to Perini et al. (2018) "during night the vegetation works the other way around". According to Chokhachian et al. (2017) the MRT is mostly affected by material properties of built environment. Also, with the assumption that the MRT with vegetation is higher during the night, based on the previous statements, the MRT should be more visible at the building's facade than under the tree, which is not the case in these simulations.
On the other side, there are studies like Salata et al. (2015) where the results show the MRT was the lowest in the configuration with greening, also during the night. Also in Tan et al. (2013), the MRT at the measure points located at the park show lower MRT values at night compared to the measure points located near buildings. Vegetation can make an important contribution to human thermal comfort, even if the effect on the air temperature is not that high. It does not only contribute to comfort by creating shade, but also by reducing long-wave emissions from the surfaces and by limiting the amount of solar radiation reflected from them (Shashua-Bar et al., 2011).

Surface Temperature The various materials perform mainly as already mentioned in Figure 7.3. Glass is the hottest material in the early evening, due to the heat of the whole day and one of the coolest in the early morning hours. Although depending on the literature and on the specific glass, the peak hours differ a bit and glass could be already cooler at 22:00, than shown in the ENVI-met results (Bölcskey & Bruckner, 2014). The highly insulated materials, DMI and passive-wall, do not absorb as much heat during the day and do therefore not emit as much heat at night. Concrete and brick behave relatively similar at night, but concrete is always a little warmer, especially during the day. Concrete has much greater temperature fluctuations than no-insulation (brick). It can be seen again that DMI is cooler than the passive-wall at 22:00, which, as already mentioned seems like a doubtful result. Looking at the course over the day, the course of the DMI and passive-wall is different than expected. After the model has settled, it appears that the insulation is rated more strongly (leading to less increase in temperature) than on the first day of the simulation. This does not apply to the air temperature in front of the building.

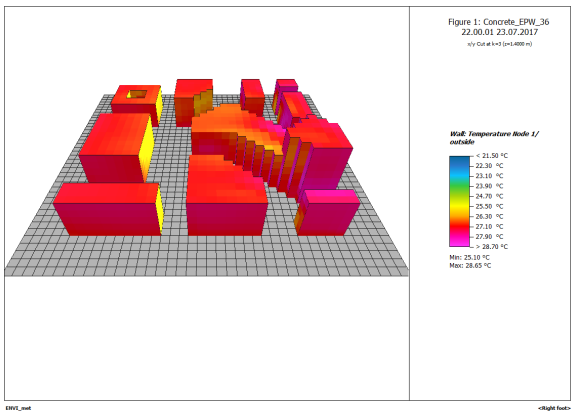

(a)

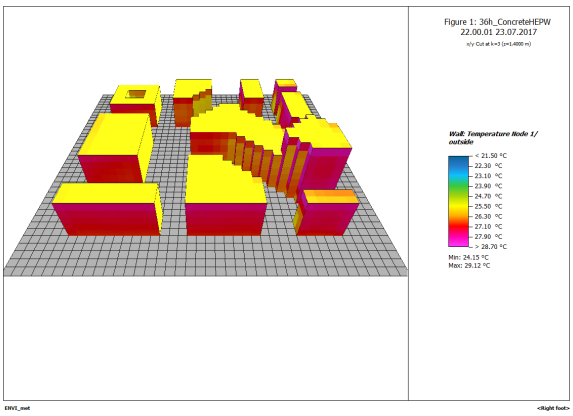

(b)

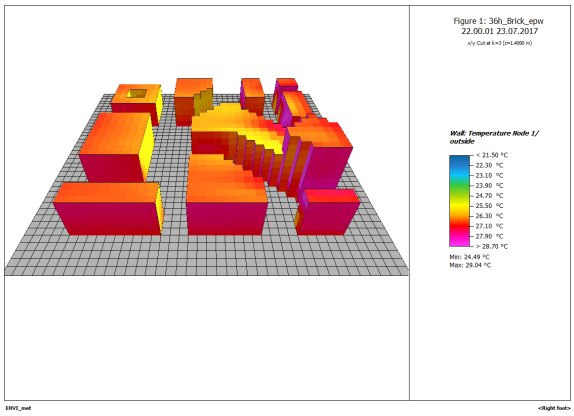

(c)

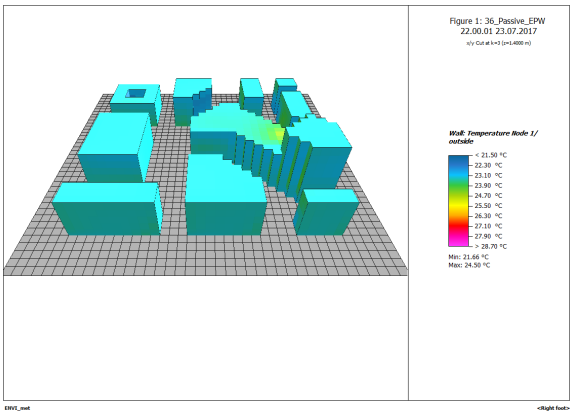

(d)

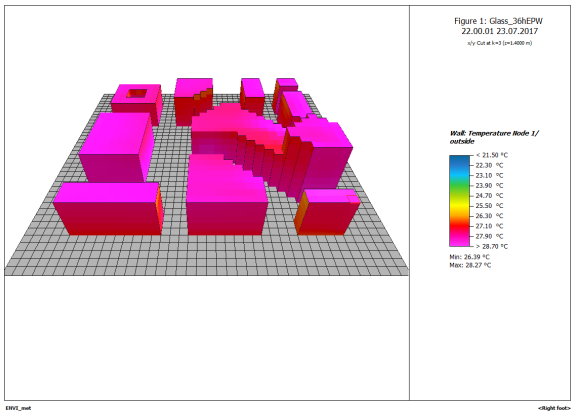

(e)

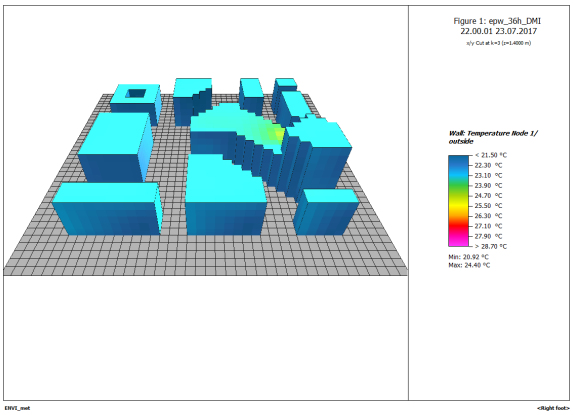

(f)

Figure 7.3. Outside wall temperature (°C) of the different wall materials at 22:00 - concrete (a), hollow concrete (b), no-insulation (c), passive-wall (d), glass (e), moderate-insulation (f)

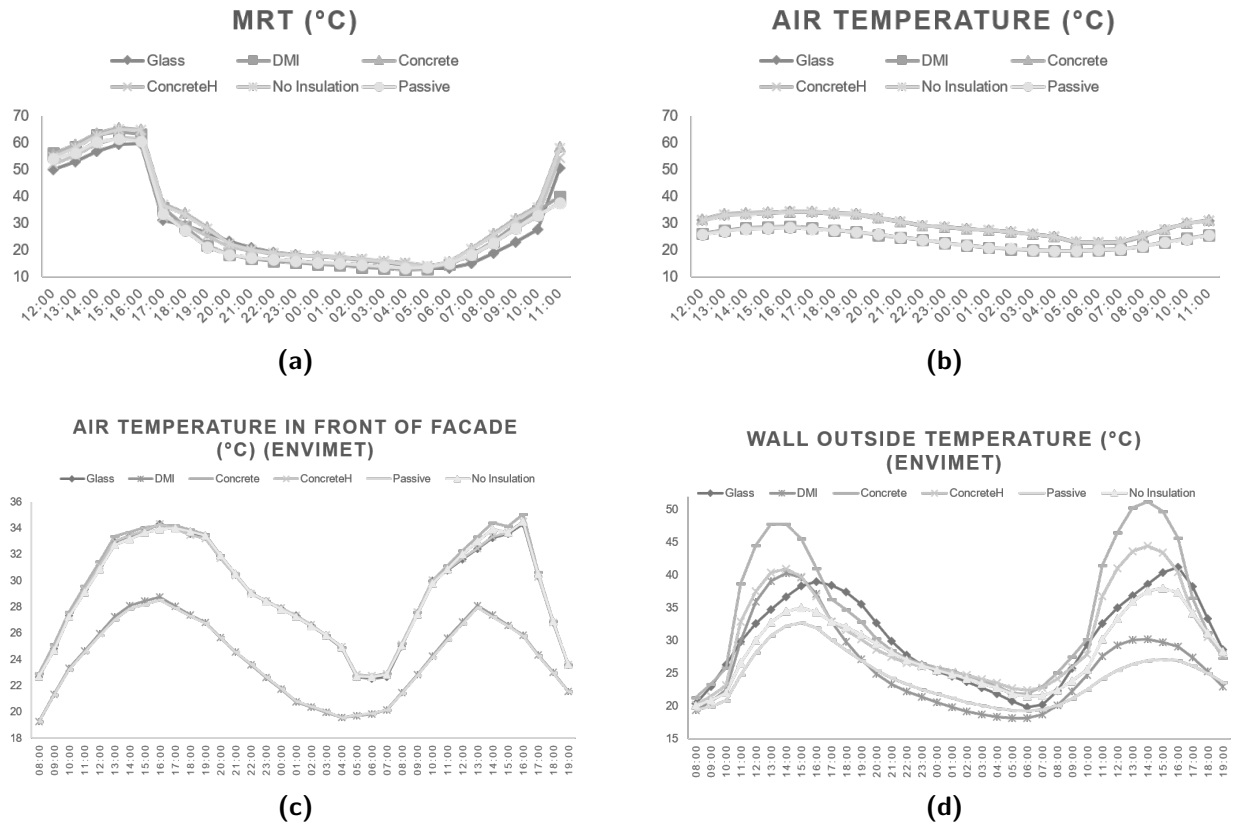

Figure 7.4. Performance of the different materials throughout the day - MRT (°C) (a), air temperature (°C) (b), air temperature in front of facade (c) and outside wall surface temperature (°C) (d) simulated in ENVI-met

As already mentioned, literature was found which states that MRT with vegetation should be cooler (Salata et al., 2015). According to Perini et al. (2018), it is also possible that vegetation as trees increase the MRT at night. However, even in this case the radiation from the walls should be more visible at night than the radiation from the trees, so it appears to be a doubtful result. This point is discussed in more detail in chapter 7.1.4.

In the ENVI-met documentation you can find the note that the model needs initialization time and the simulation should be started at night or in the morning, which was done (ENVI-met, n.d.-b).

According to Salata et al. (2016) the spin-up time of the simulation should be two days. Other studies like Skelhorn et al. (2014) and Jänicke et al. (2015) achived a higher agreement of the measured and the simulated data due to increasing spin-up time. Since the simulation in ENVI-met heats up with increasing spin-up time, it is possible that the walls may also heat up more and thus emit more. Figure 7.5 (b) shows the result after a spin-up time of two days. It is clearly visible that the buildings emit more and approach the tem-

perature under the trees. Therefore another trial was tried in which the spin-up time was extended to seven days (Figure 7.5 (c)).
After the model had a seven-day spin-up time, the trees no longer appear as extreme as before as heat islands and the temperatures of the buildings and the trees are becoming increasingly similar. However, the vegetation still appears warmer than the buildings.

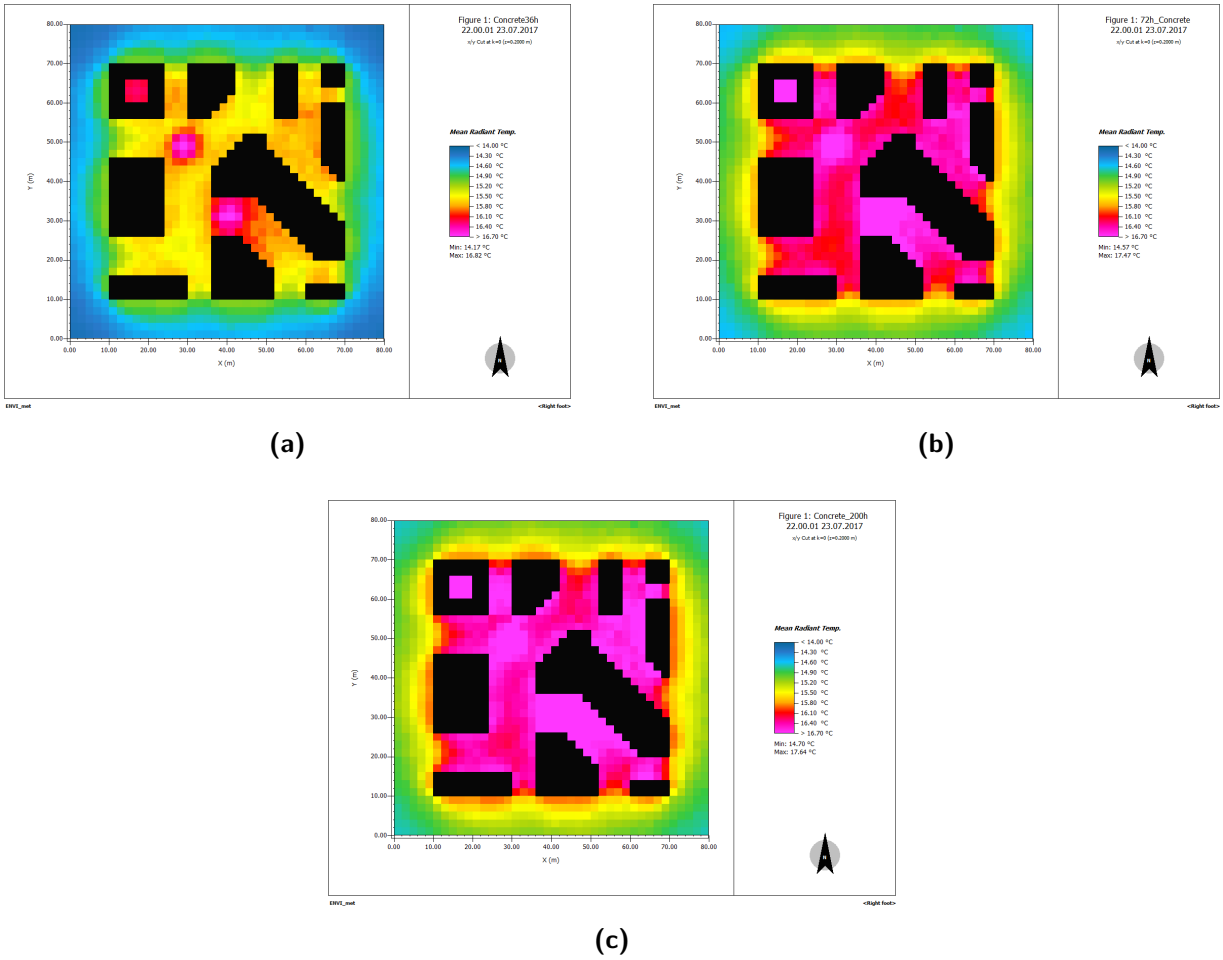

Figure 7.5. Result after half a day spin-up time (a), result after two days spin-up time (b), result after seven days spin-up time (c)

NetCDF As mentioned in chapter Wall material - ENVI-met (6.3.1), difference maps were created using a Python script and the NetCDF converter tool. However, the finished maps looked incorrect. On closer inspection and comparison of the NetCDF files with the EDX files, it was noticed that the conversion from EDX files to NetCDF files was not correct. The EDX files of a certain time in Leonardo did not correspond to the NetCDF files of the same hour. There was a mix-up of the hours after conversion and also some files were corrupted afterwards. The table with the comparison of the EDX files and the NetCDF data can be found in appendix C.

Ladybug Tools

The different materials in the Ladybug Tools perform similar to the simulations in ENVI-met. However, the glass wall behaves completely different (see Figure 7.6 and 7.7). The reason why the glass wall does not act similar to the one in ENVI-met could be the difference of the default parameters in the two simulation tools. Passive wall and DMI were created with the same physical parameters in ENVI-met and in the Ladybug Tools. As in ENVI-met the DMI scenario simulates lower values than the passive-wall, which leads to the assumption that the default moderate-insulation wall is better insulated than the passive-wall.

There are different kinds of brick lengths described in literature. In ENVI-met the no-insulation wall has a 38 cm thick brick layer, which is thicker compared to the brick layer used in the Ladybug Tools (30cm). However, brick and concrete wall have very similar physical parameters as in ENVI-met and therefore act similarly in both tools. The facade materials in the Ladybug Tools at 22:00 perform mainly as expected.

The influence of the trees is not visible at 22:00, because in Grasshopper trees, are seen as shading elements and have no evapotranspiration (see chapter 5 Software). At 22:00 the concrete facade emits the most and the glass facade the least (Figure 7.6 and 7.7). During the 24-hour period, the DMI facade emits the most and the glass facade the least (Figure 7.8).

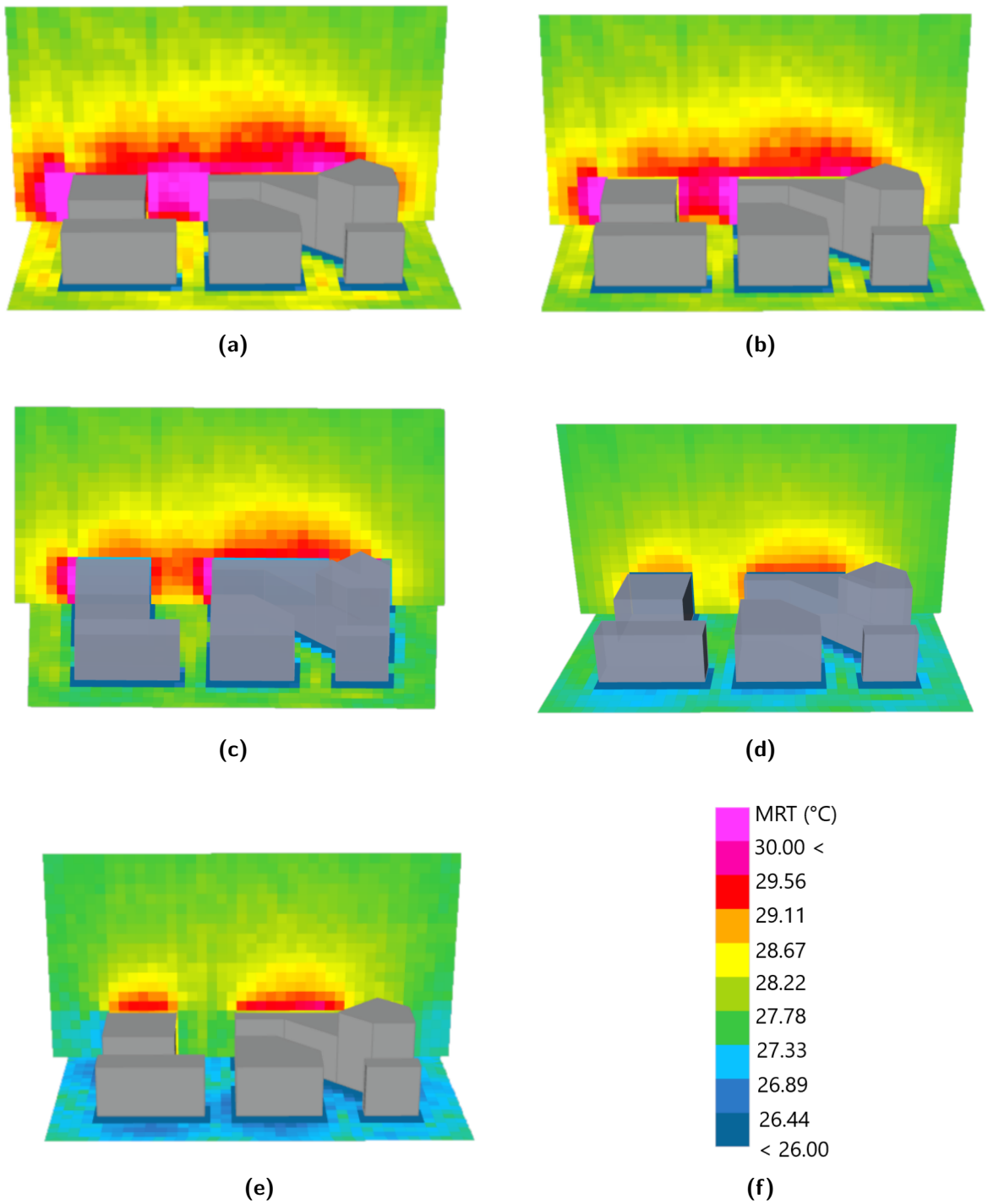

Figure 7.6. MRT (°C) of the different wall materials at 22:00 (vertical section) - concrete (a), brick (b), passive-wall (c), moderate-insulation (d), glass (e)

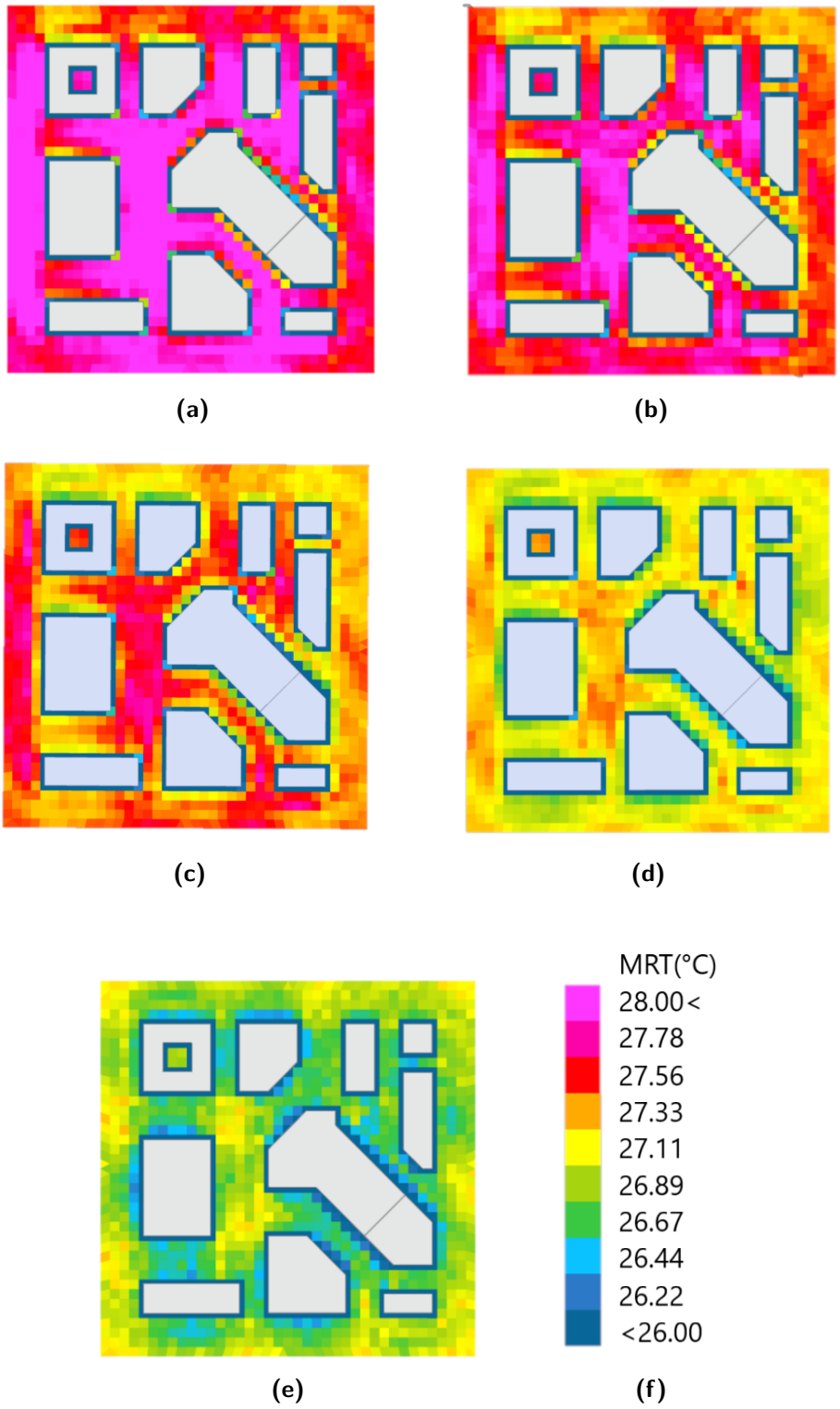

Figure 7.7. MRT (°C) of the different wall materials at 22:00 (horizontal section) - concrete (a), brick (b), passive-wall (c), moderate-insulation (d), glass (e)

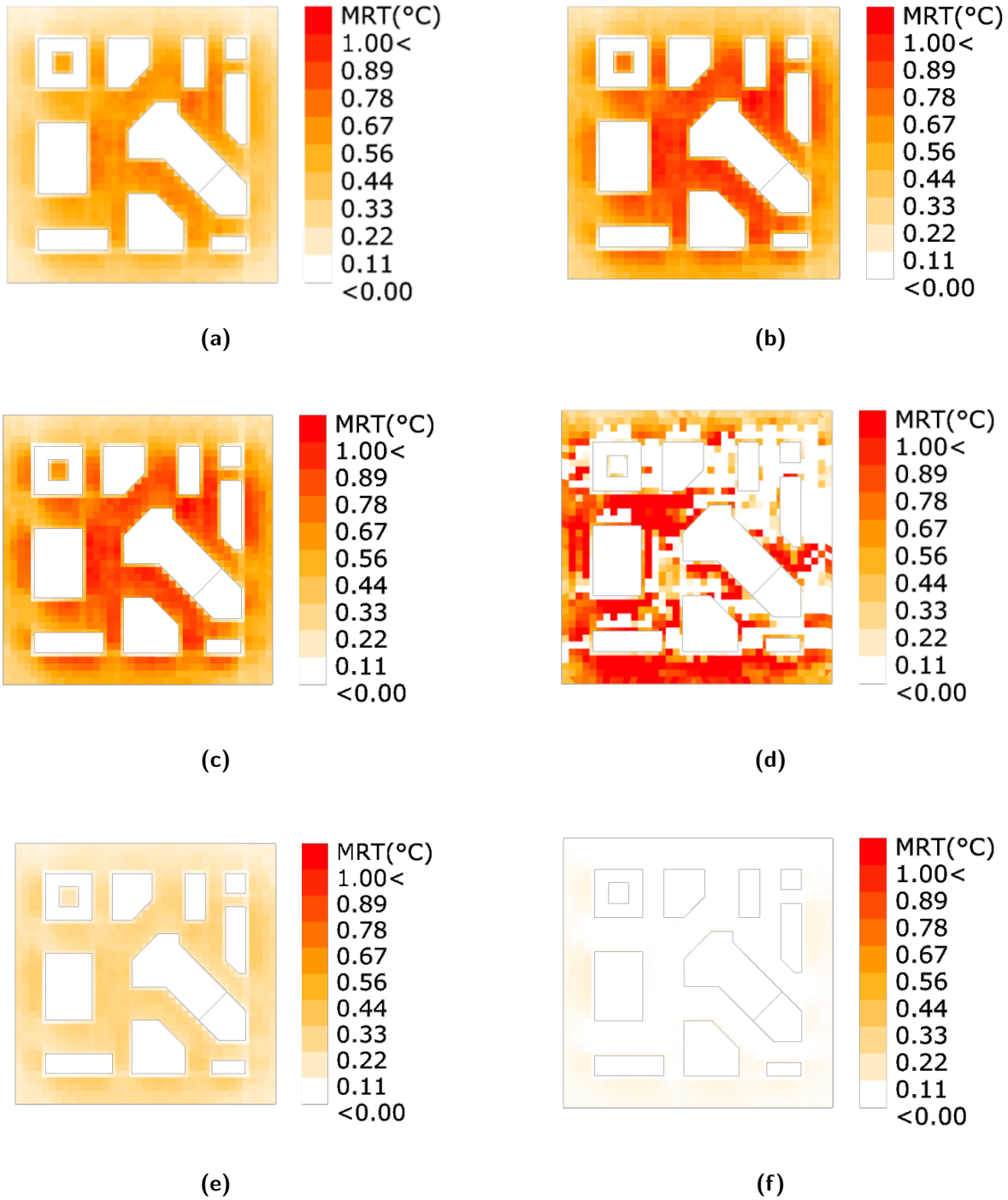

Figure 7.8. Difference maps of the daily average of the different wall materials in MRT (°C) DMI - concrete wall (a), DMI - brick wall (b), DMI - passive wall (c), DMI - glass wall (d), concrete wall - brick wall (e), brick wall - passive wall (f)

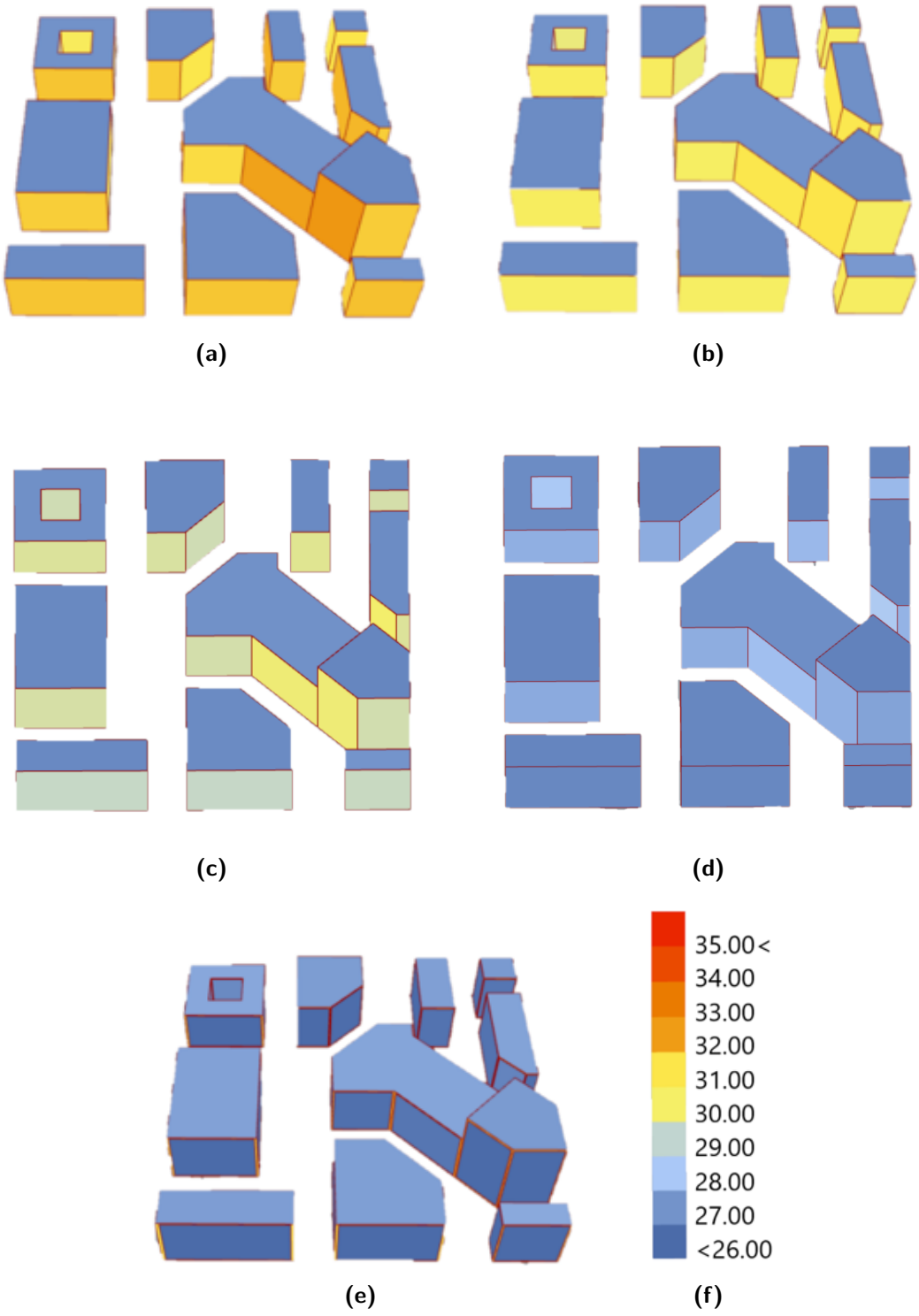

Figure 7.9. Outside surface temperature (°C) of the different wall materials at 22:00 - concrete (a), brick (b), passive-wall (c), moderate-insulation (d), glass (e)

Ladybug Tools vs. ENVI-met

	ENVI-met		Ladybug Tools	
	MRT	Surface temperature	MRT	Surface temperature
Glass facade				
Concrete facade				
No Insulation facade				
Passive facade				
DMI facade				
Concrete hollow facade				

Table 7.2. Performance of the simulated temperature for the different wall materials at 22:00 in ENVI-met and the Ladybug Tools during summer

All tested materials act the same on a typical summer day in ENVI-met and the Ladybug Tools, only the performance of the glass facade differs (see Table 7.2). In both simulation programs, the DMI facade insulates more than the passive-wall, although the passive-wall should be better insulated than a medium insulation. Since the same result is achieved not only in ENVI-met but also in the Ladybug Tools, it is most likely due to the composition of the wall.

7.1.2. Wall Material Winter

ENVI-met

The warmest scenario on a cold day in winter at 22:00 appears with the concrete (hollow) wall followed by the glass wall. The coolest scenario is, as during the summer, again with the DMI wall. Unlike in summer, the passive-wall is no longer the second coolest but the no-insulation wall is. The no-insulation and the passive facade have a relatively equal effect on the microclimate. The difference of the MRT under the tree and near the facade is even higher in the cooler scenarios (see Figure 7.10). In the vertical section (Figure 7.11) it can be seen that the MRT is only in layers close to the ground higher under the tree, than without the tree and disappears with height.

Figure 7.10. MRT (°C) of the different wall materials at 1.4 m height at 22:00 - concrete (a), hollow concrete (b), no-insulation (c), passive-wall (d), glass (e), moderate-insulation (f)

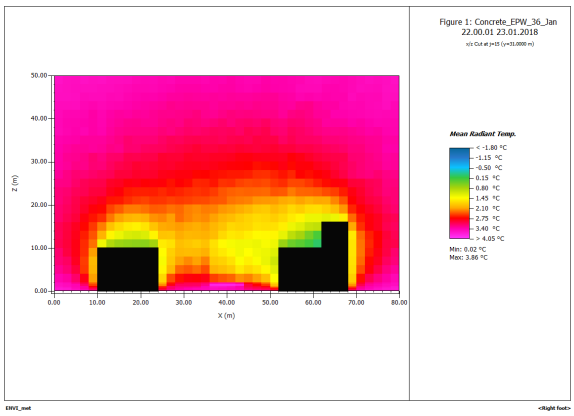

(a)

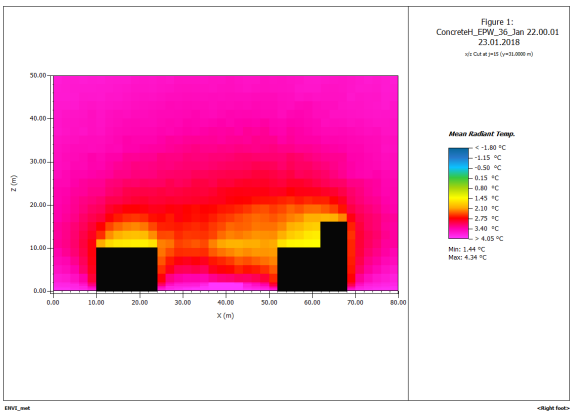

(b)

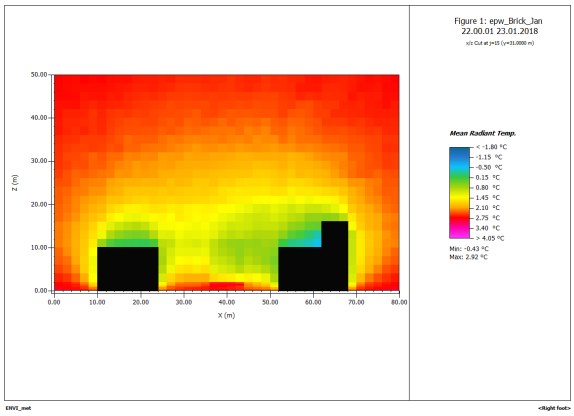

(c)

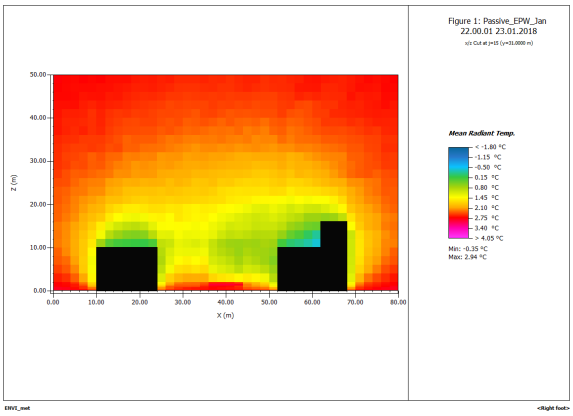

(d)

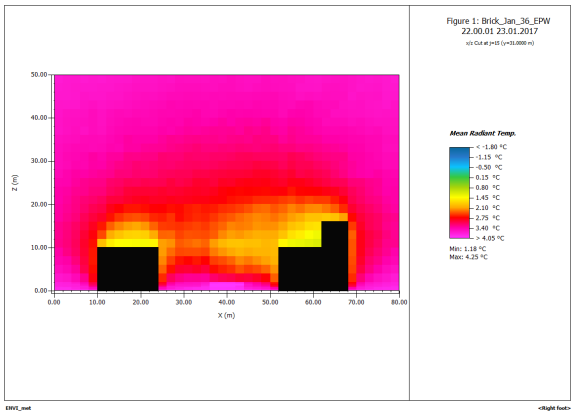

(e)

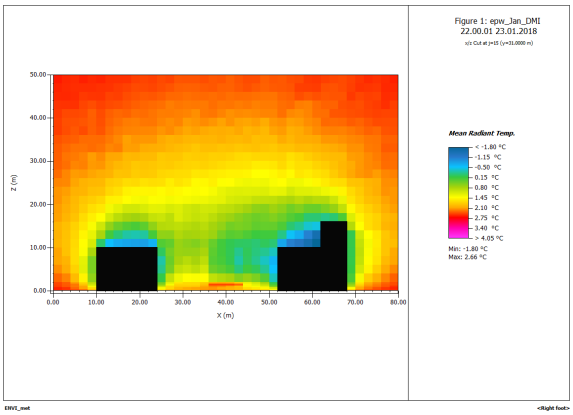

(f)

Figure 7.11. MRT (°C) of the different wall materials at 22:00 (x/z cut, y = 31m) - concrete (a), hollow concrete (b), no-insulation (c), passive-wall (d), glass (e), moderate-insulation (f)

Ladybug Tools

Just like in Summer, the scenario with the glass wall is the coolest, followed by the DMI facade. The warmest scenario is concrete, followed by the passive-wall and the brick wall (see Figure 7.16. Basically, it can be said that the different materials have very similar effects on the microclimate in winter and the respective MRTs do not show any major differences.

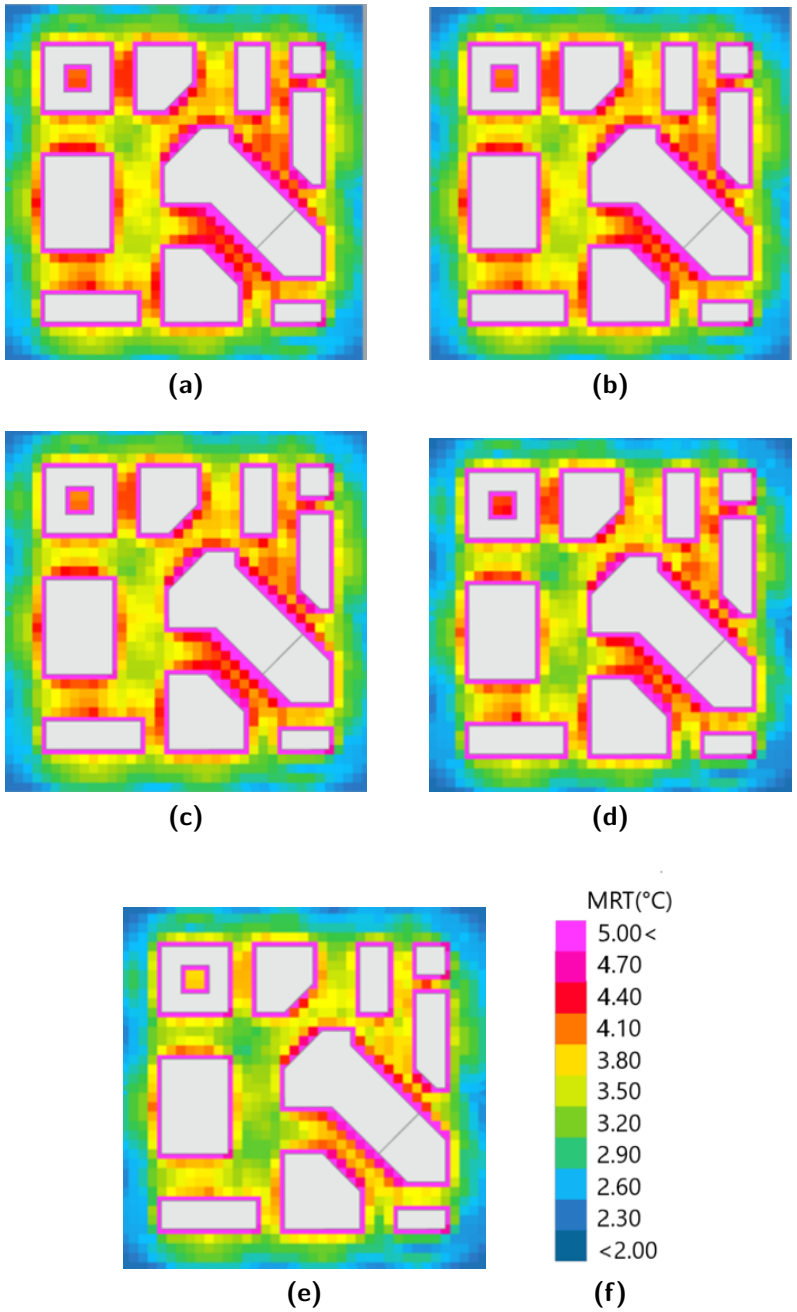

Figure 7.12. MRT (°C) of the different wall materials at 1.4 m height at 22:00 - concrete (a), brick (b), passive-wall (c), glass (d), moderate-insulation (e)

Ladybug Tools vs. ENVI-met

	ENVI-met		Ladybug Tools	
	MRT	Surface temperature	MRT	Surface temperature
Concrete hollow facade				
Glass facade				
Concrete facade				
Passive facade				
No Insulation facade				
DMI facade				

Table 7.3. Performance of the simulated temperature for the different wall materials at 22:00 in ENVI-met and the Ladybug Tools during winter

As in summer, if the different performance of the glass facade is excluded, all tested materials act the same at a typical winter's day in ENVI-met and the Ladybug Tools (see Table 7.3).

7.1.3. Climate Adaptation Measures

This chapter shows the effect of different greening scenarios on the microclimate in an ENVI-met and a Ladybug Tools simulation.

ENVI-met

Figure 7.13 shows the MRT of the four different scenarios: Basecase (BC), roof greening (RG), facade greening (FG) and roof and facade greening (FGRG). It can be seen that the BC has a lower MRT as the FG and the FGRG scenario. It is already known that the MRT can react like this during the night with regard to vegetation (see chapter 7.1.1 and 7.1.4), but with this assumption, the green roof should also be warmer than the BC. If the cooling in green roof is mainly due to the additional insulation, the same should be true for both green roof and FGRG and not BC and RG. Also Jänicke et al. (2015) research shows that the facade greening in ENVI-met has a higher MRT as the bare facade. According to Berardi (2016) studies, the roof greening has a huge influence on the roof's microclimate and with greening, the MRT is lower during the night than without greening. Therefore, the achieved results seem to be not correct. Solcerova et al. (2016) mentioned that extensive roofs do not really have an impact on cooling the microclimate. Also, the selected plants species have an extreme influence on the impact on the microclimate (Solcerova et al., 2016).

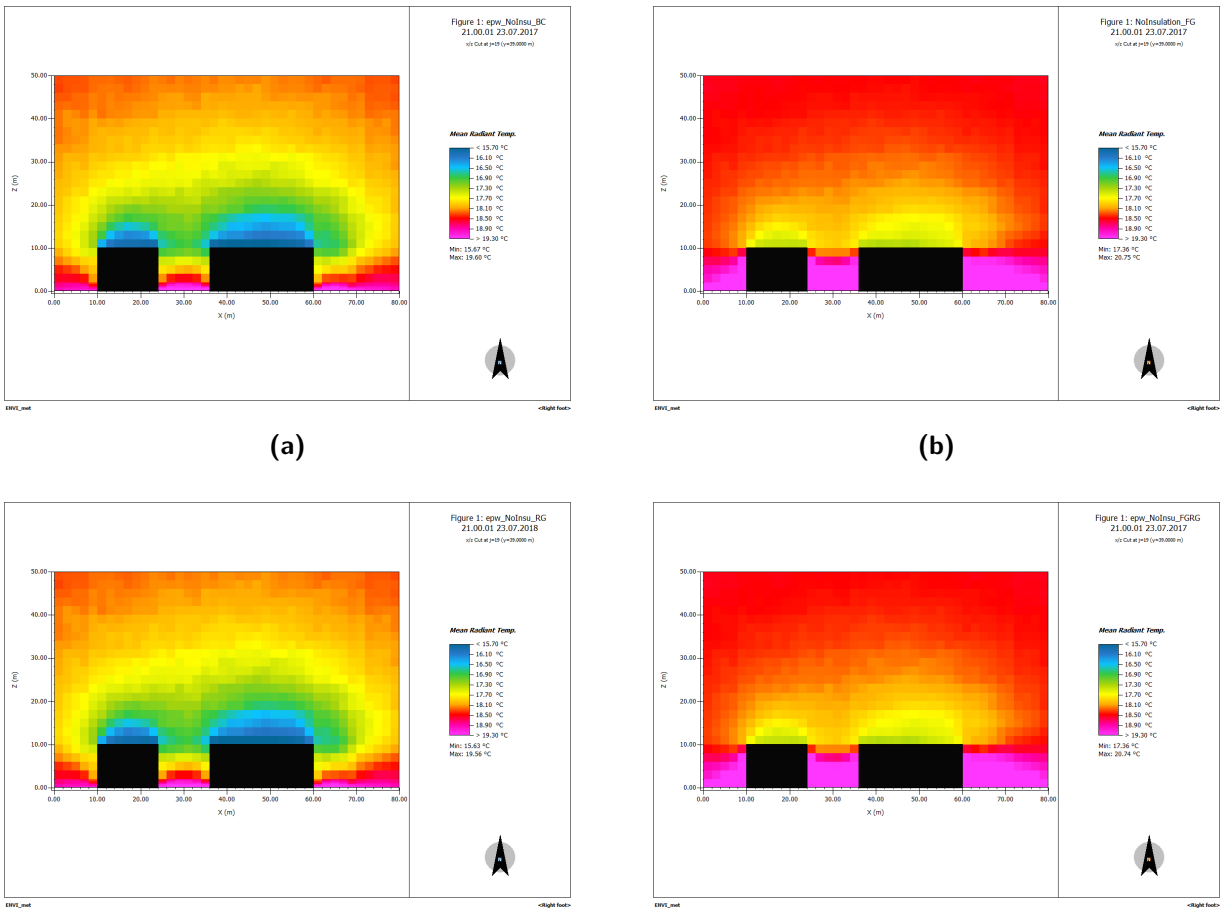

(a) **(b)**

(c) **(d)**

Figure 7.13. MRT (°C) of the different scenarios (x/z cut = 39m) at 21:00 - Basecase (a), facade greening (b), roof greening (c), facade and roof greening (d)

The air temperature created with the same input data shows that with green facades and green roofs the coolest scenario prevails and with BC the warmest 7.14.

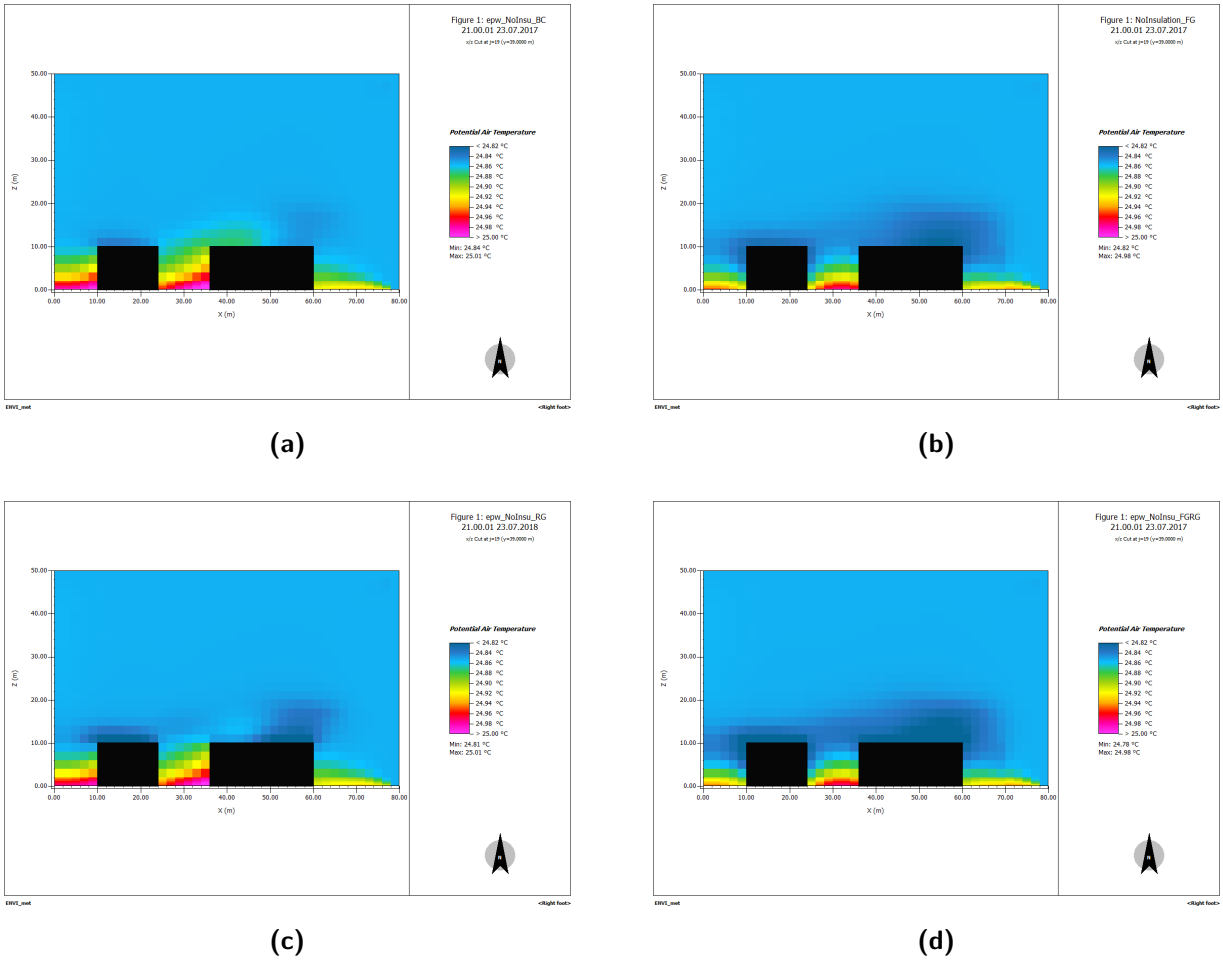

Figure 7.14. Air temperature (°C) of the different scenarios (x/z cut = 39m) at 21:00 - Basecase (a), facade greening (b), roof greening (c), facade and roof greening (d)

Looking at the horizontal section (Figure 7.15) the MRT results with the greened facade are around 1°C warmer, which seems right according to the assumption (see chapter 7.1.1 and 7.1.4) that MRT is higher during the night close to vegetation. Jänicke et al. (2015) measured the MRT at a greened and a bare facade and simulated the same with different microclimate models. The observed MRT in front of the building at the bare site is, except for one time in the morning, always higher than the greened site (Jänicke et al., 2015). According to these results, the simulation of the facade greening in ENVI-met creates a doubtful result. It is correct that there is less influence of the roof greening on a height of 0.2 m, so BC and RG look very similar. In the study of Berardi (2016) the MRT had also no impact on the pedestrian level, but as already mentioned, huge differences on the roof top.

The basecase material of these results is no-insulation, but the same study was taken with concrete as well. If the material of the wall or roof construction is changed to concrete (see Figure 6.2), this has, as already shown in the chapter Wall Material 7.1.1, an affect on the surrounding microclimate but the effects of the greening are the same as with no-insulation.

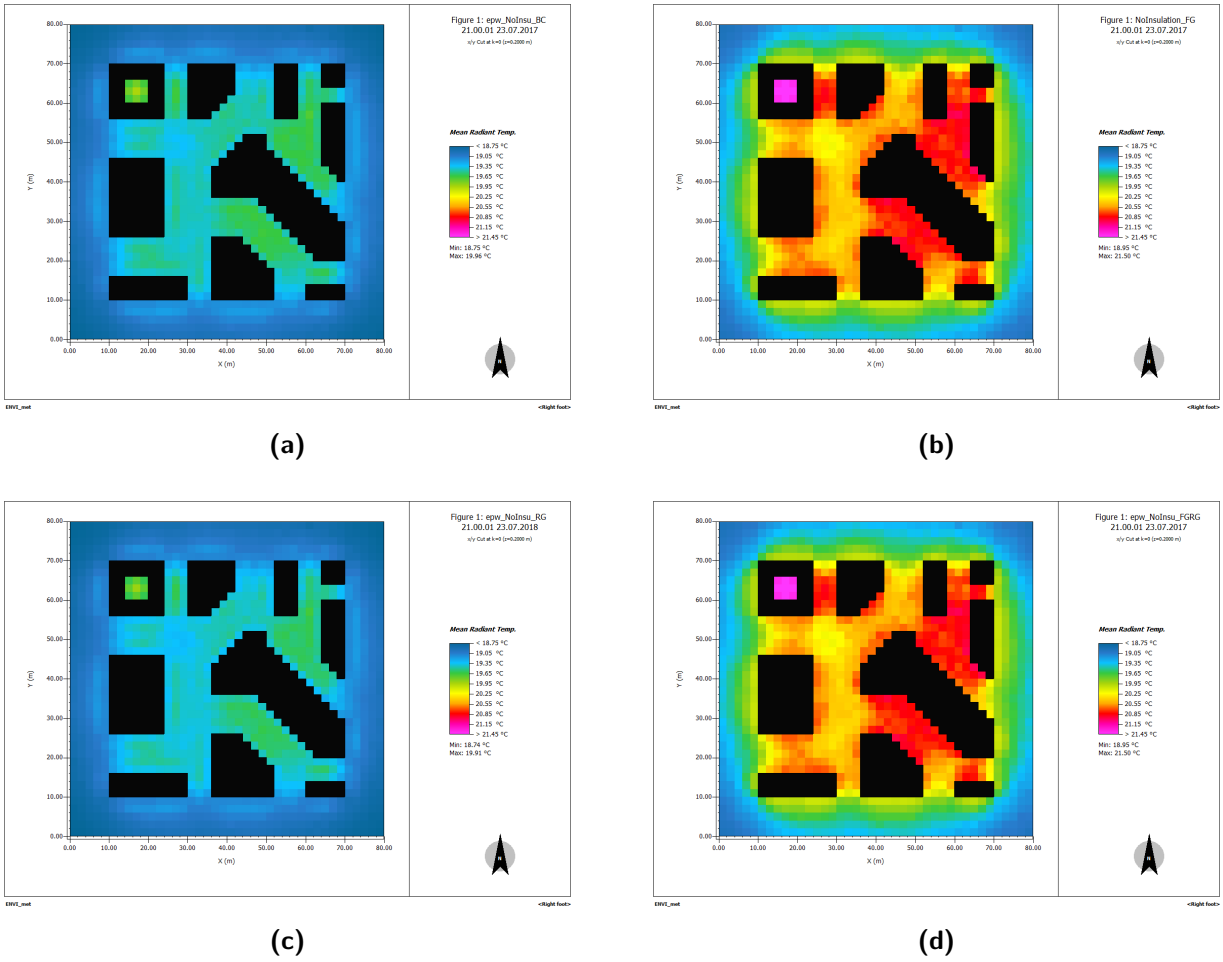

Figure 7.15. MRT (°C) of the different scenarios (x/z cut = 39m) at 21:00 - Basecase (a), facade greening (b), roof greening (c), facade and roof greening (d)

Because of the doubtful MRT results during the night, the surface temperature of the outside was examined more closely. Therefore, two points, one on the facade and one on the roof, were chosen to compare the different scenarios for a longer period of time. The diagrams 7.16 show the comparison between the basecase (no-insulation) and the different building greening scenarios.

As input for the diagrams 7.16 (a,b) a point on the facade was chosen, which is at a height of 1.6 m (relevant height for an average person) and is located in a densely built-up area, i.e. a building is located opposite and next to it.

The diagram outside surface temperature 7.16 (a) shows that the basecase and the green roof scenario are very similar. From 7:00 to 17:00 the wall temperature is cooler in the green roof scenario and the basecase is cooler at night. The facade greening scenario and the facade and roof greening scenario are also very similar. In the scenario with both types of greening, the wall temperature is 0.04 °C to 0.11 °C cooler than in the scenario with only the facade greening. BC and RG both have no facade greening, which at this height leads to a very similar course of both scenarios, so the result seems to be correct. The same applies to FG and FGRG. Since both scenarios have a facade greening, both have a similar course at this height. Considering the outside surface temperature, there is a cooling of the facade due to the greening. This can be achieved, as described in chapter 4 Green Buildings, by e.g. shading, insulation due to the additional layer or evapotranspiration of the plants.

As input for the diagrams 7.16 (c) and 7.16 (d), a roof voxel was chosen. The same observation as for the outside surface temperature applies to the air temperature in front of the facade. The same can be observed as before seen at the facade voxel, just vice versa. BC and FG have a similar performance as well as RG and FGRG (Figure 7.16 (c)). The air temperatur in front of the roof does not differ much in the four scenarios, only RG und FGRG are up to 1°C cooler between 02:00 and 06:00. This means the most cooling is between these hours (Figure 7.16 (d)). The inside building temperature is always the same and does not depend on the chosen voxel. It has the highest values with the BC and the coolest with the FGRG (Figure 7.16 (e)).

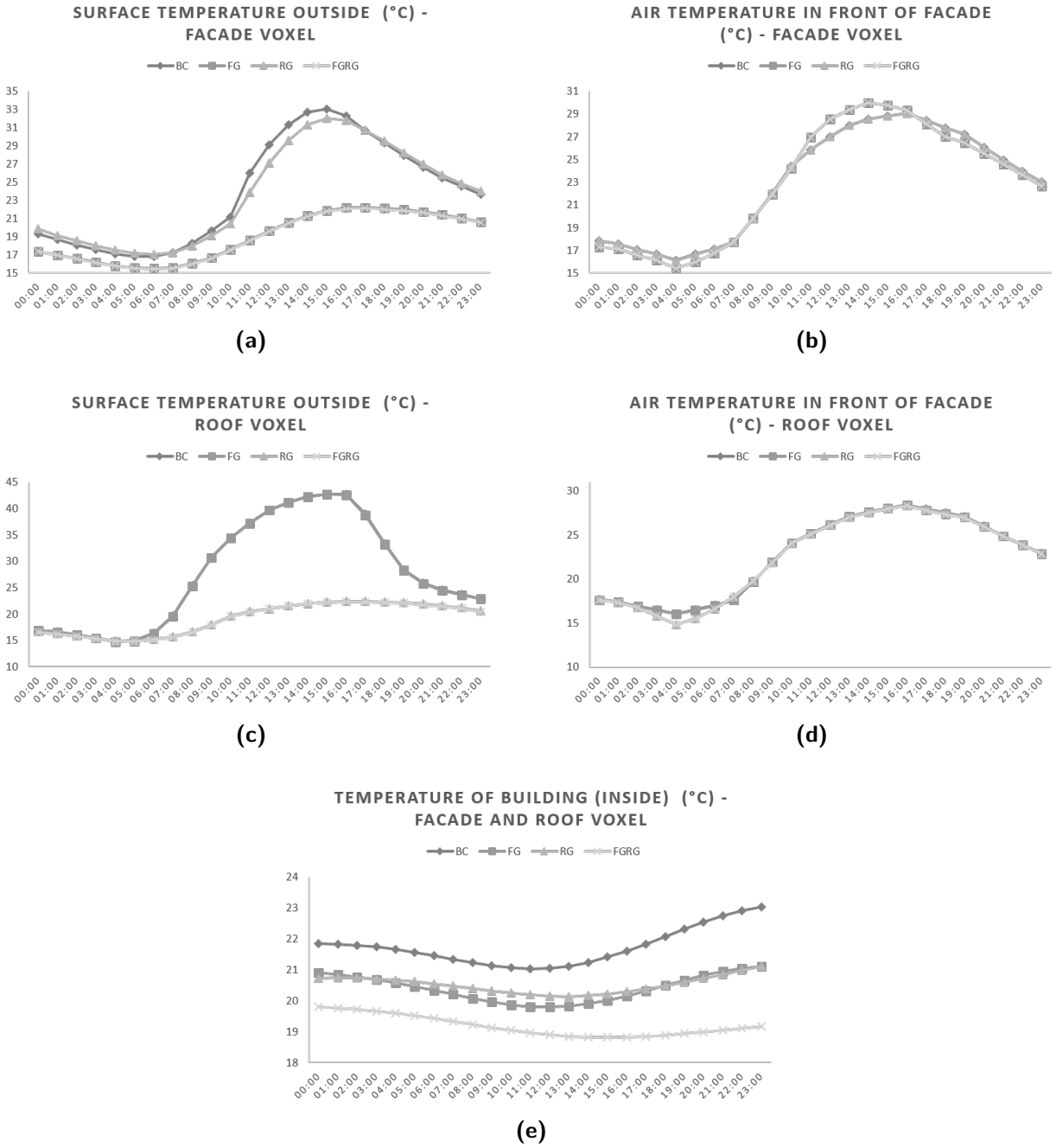

Figure 7.16. Comparison of the different greening scenarios - outside surface temperature (facade voxel) (a), air temperature in front of facade (facade voxel) (b), outside surface temperature (roof voxel) (c), air temperature in front of facade (roof voxel) (d), building inside temperature (same for facade and roof voxel)(e)

Ladybug Tools

The basecase (without greening), buildings with facade or roof greening and buildings with facade and roof greening were simulated with the Ladybug Tools.

Figure 7.17 shows the basecase and the three different scenarios in the 24 hour average for brick. Here, it can be clearly seen that green buildings in particular provide significant cooling between 2-4°C.

At 21:00, the cooling of the greening can be seen very clearly (Figure 7.18). The difference between the fully greened scenario and the basecase is 4 - 6 °C. Since evapotranspiration is not included in the Ladybug Tools, cooling is mainly caused by the additional layer of the wall and roof construction (see chapter Green Buildings 4).

If the material of the wall or roof construction is changed to concrete (see Figure 7.19), this has, as already shown in the chapter Wall Material 7.1.1, mainly an effect on the basecase, but the scenarios with greening remain relatively similar to the simulations with brick.

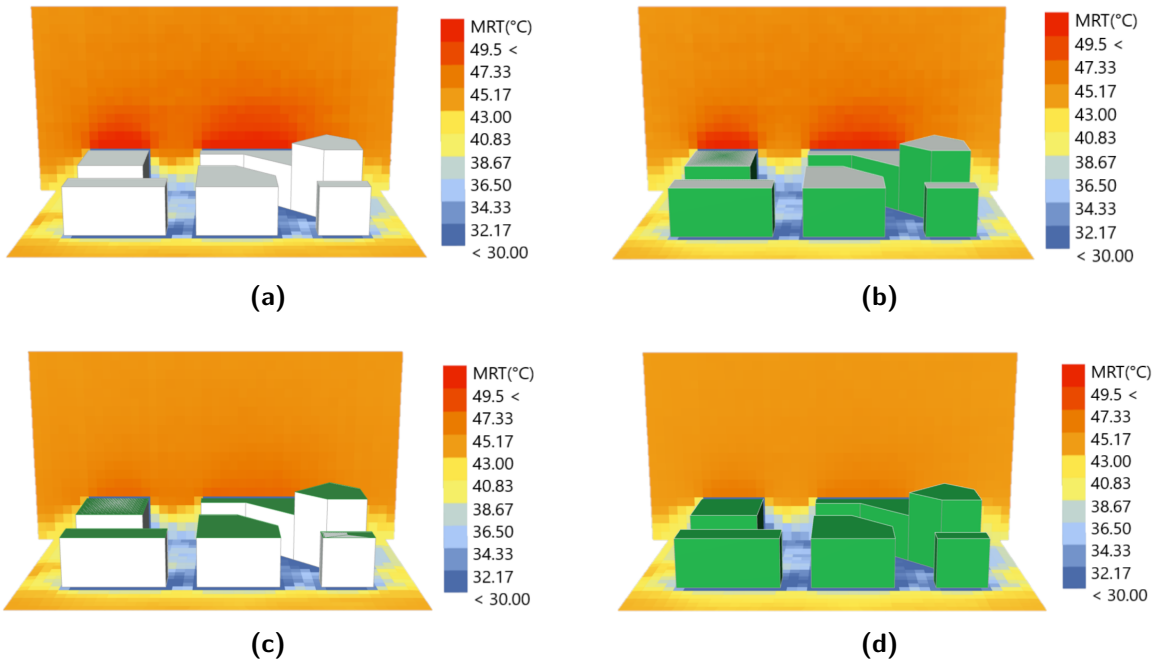

Figure 7.17. MRT (°C) of the different scenarios averaged over 24 hours - basecase (brick wall) (a), facade greening (b), roof greening (c), facade and roof greening (d)

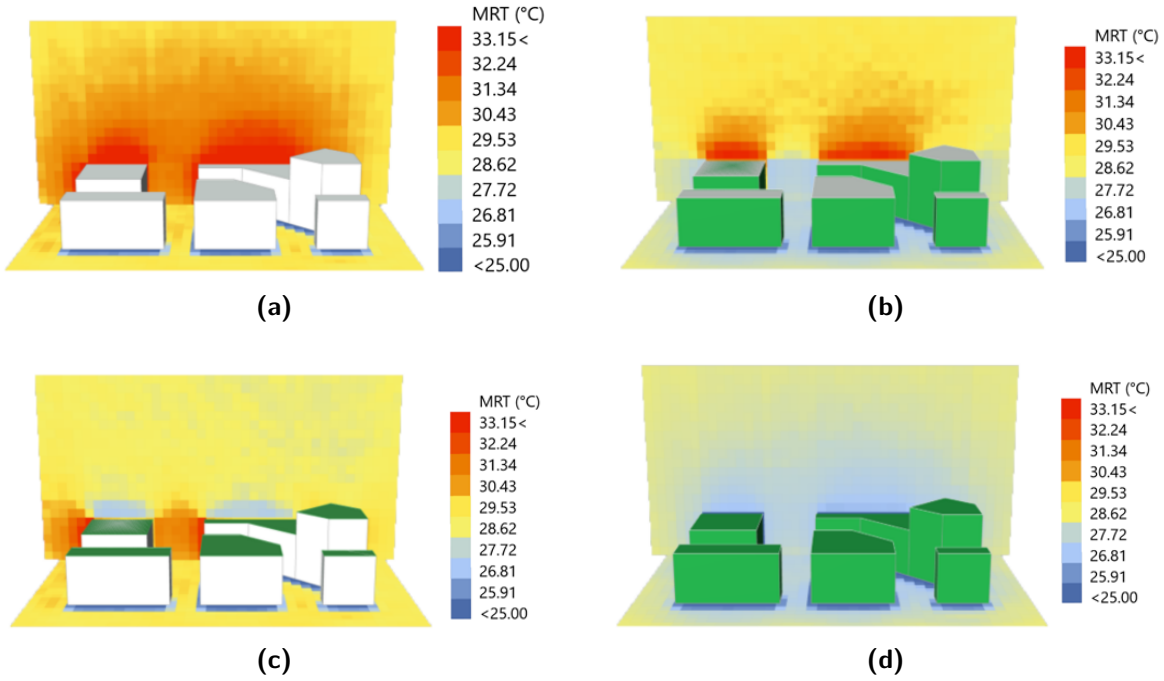

Figure 7.18. MRT (°C) of the different scenarios at 21:00 - basecase (brick wall) (a), facade greening (b), roof greening (c) and facade, roof greening (d)

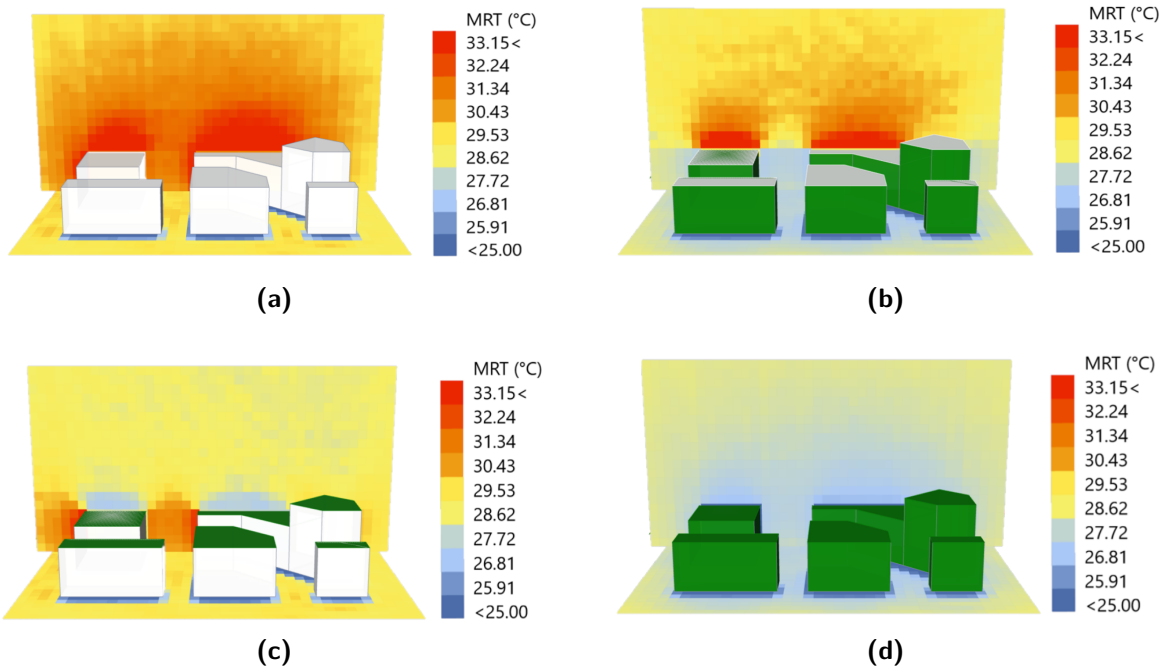

Figure 7.19. MRT (°C) of the different scenarios at 21:00 - basecase (concrete wall) (a), facade greening (b), roof greening (c), facade and roof greening (d)

Ladybug Tools vs. ENVI-met

			BC	FG	RG	FGRG
ENVI-met	MRT	Facade	cold	warm	cold	warm
	21:00	Roof	cold	warm	cold	warm
	Air Temperature	Facade	warm	cold	warm	cold
	21:00	Roof	warm	cold	cold	cold
Ladybug	MRT	Facade	warm	cold	warm	cold
Tools	21:00	Roof	warm	warm	cold	cold
	MRT	Facade	warm	cold	warm	cold
	average over 24h	Roof	warm	warm	cold	cold

Table 7.4. Performance of different greening scenarios divided each into facades and roof level - Basecase (BC), facade greening (FG), roof greening (RG) and facade and roof greening (FGRG) in ENVI-met and the Ladybug Tools

The Table 7.4 summarizes how a simulation of different greening scenarios affects the microclimate in ENVI-met and the Ladybug Tools. At 21:00 the MRT in ENVI-met behaves differently than in the Ladybug Tools and as indicated in the literature. The air temperature behaves like in the Ladybug Tools. Only the roof area on the facade greening scenario appears different, but it is possible that the facade greening also has an influence on the roof level.

7.1.4. Vegetation

Since the sensitivity analysis did not produce a satisfactory result regarding vegetation, the simulation shown in Bruse (2000, 2003) was reproduced in ENVI-met because it shows a correct result according to literature.
Figure 7.20 shows the results achieved in Bruse (2000, 2003) and Figure 7.21 shows the results from the vegetation analysis (chapter 6.3.3).

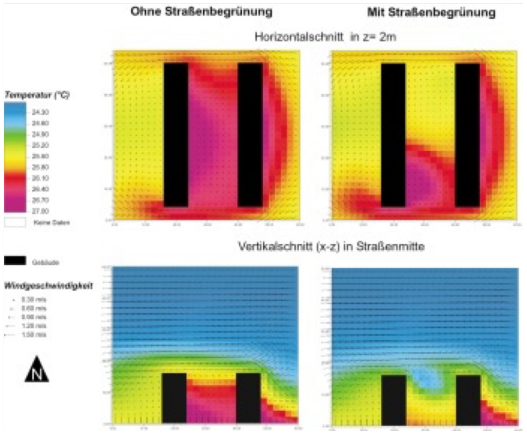

Figure 7.20. Air temperature during the day (11:00) from Bruse (2003)

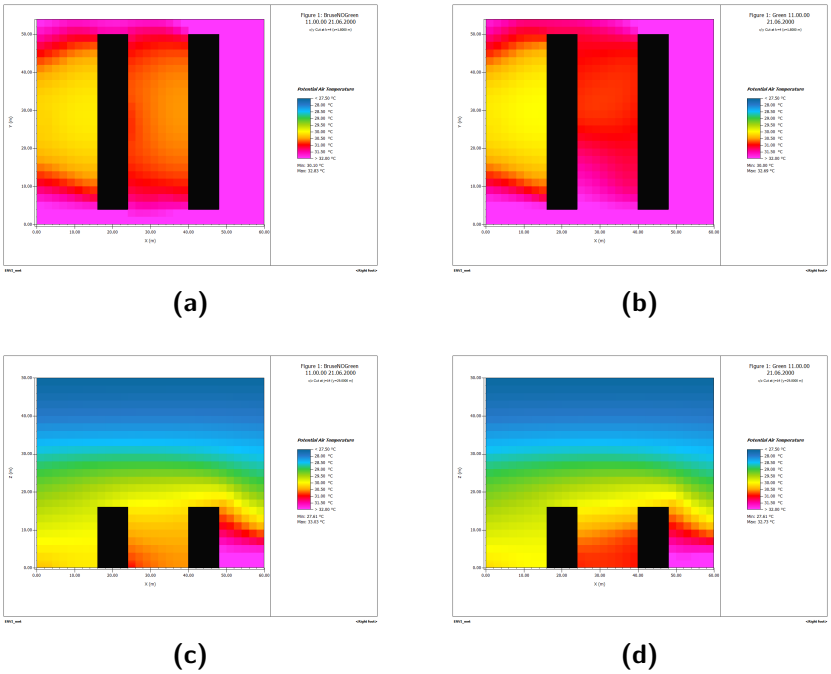

Figure 7.21. Air temperature during the day (11:00) horizontal section - without greening (a) and with greening (b), Air temperature during the day (11:00) vertical section - without greening (c) and with greening (d) simulated in ENVI-met

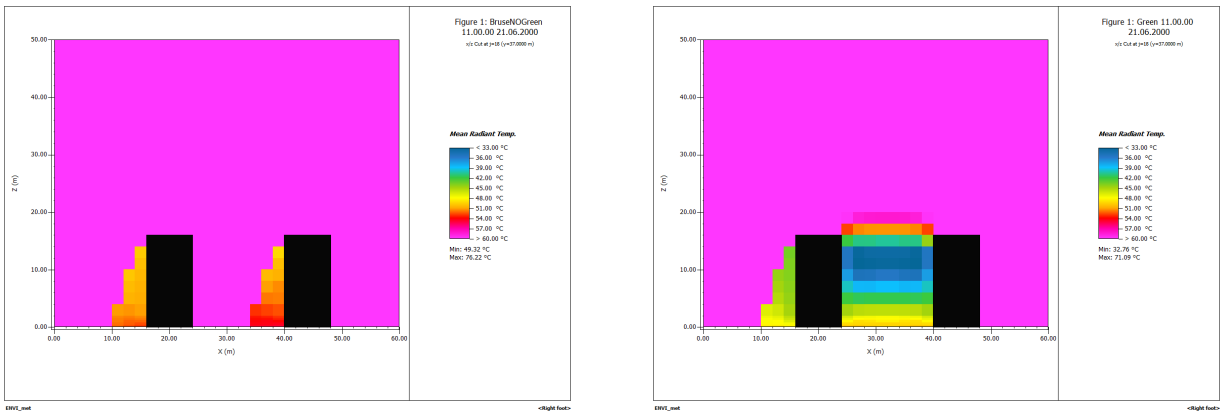

(a) **(b)**

Figure 7.22. MRT during the day (11:00) - without greening (a) and with greening (b)

The result, produced in the chapter Vegetation (6.3.3), is a reproduction of the simulation created by Bruse (2000, 2003). The Figures 7.21 show the air temperature at 11:00. The air temperature is warmer with vegetation and cooler without. In the example of Bruse (2000, 2003), it is exactly the opposite result (Figure 7.20). Based on the position of the sun and by requesting by e-mail, it can be said that the results shown in Bruse (2003) show 11:00 as in the simulation.

According to literature, the result obtained by Bruse (2003) is correct, the air temperature should be cooler in the case of greening than in the case without greening (Salata et al., 2015; Shashua-Bar et al., 2010). In the study of Perini et al. (2018), the same result as in Bruse (2000, 2003) has been achieved while simulating with ENVI-met. In Roth and Lim (2017), different scenarios for UHI mitigation have been simulated with ENVI-met. There again, the scenario without trees was slightly warmer during the day than with trees (Roth & Lim, 2017).

No paper was found that shows a higher air temperature in the vegetated scenario and a lower air temperature in the non-vegetated scenario. Since many other studies show the same results as Bruse (2000, 2003), the experiment was repeated to exclude random errors, but the same doubtful results were achieved again. The air temperature from the wall material tests (6.3.1) was also checked during the day. Again there is no clear difference between vegetation and non-vegetation. However, in these tests only single standing trees and not a street canyon full of trees like in this experiment was used, so this effect may not be clearly visible here. Perhaps the version used in the studies of Bruse (2000, 2003), Perini et al. (2018) and Roth and Lim (2017) also plays an important role, otherwise no explanation for the result achieved here could be found. The results show only a very slightly higher air temperature with vegetation, but according to Bruse (2003), it should show a significantly lower temperature. Thus, the results differ clearly.

In Bruse (2000), a difference map of the night temperature was found (Figure 7.25). Looking at the two results during the night hours, very similar values are obtained. The night air temperature with greening is cooler in both results than the one without greening.

Figure 7.27 shows the relationship between MRT and air temperature in ENVI-met. As already mentioned in the chapter 7.1.1 Wall Material, the MRT in ENVI-met acts exactly opposite to the air temperature. During the day, the MRT in the greened scenario is cooler and at night warmer than in the non-greened case. According to Perini et al. (2018), these results correspond to the real values.

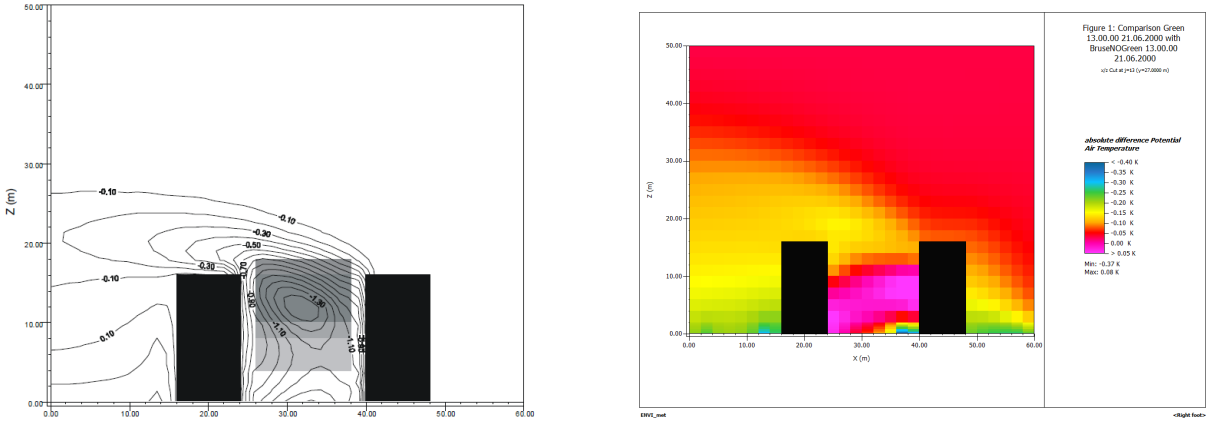

(a) **(b)**

Figure 7.23. Air temperature difference map during the day (13:00) - Bruse (2000) (a) and simulated in ENVI-met (b)

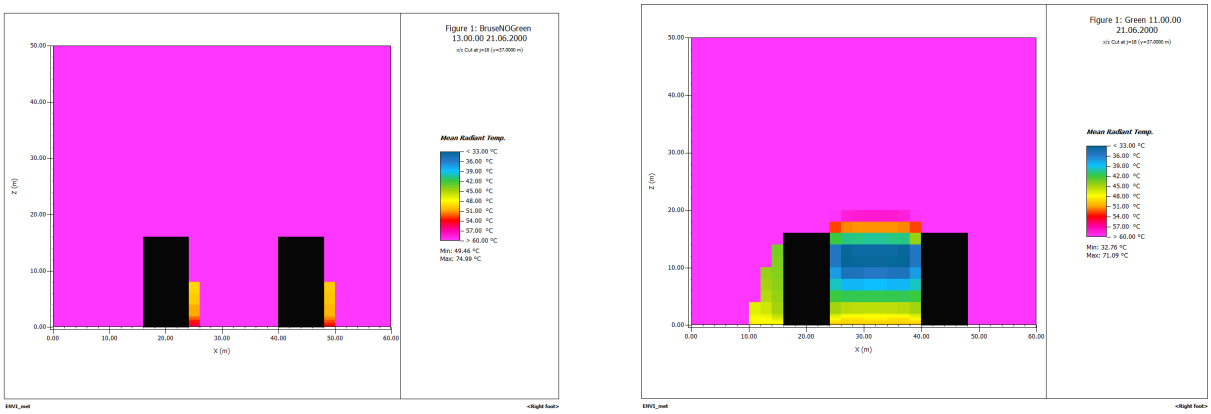

(a) **(b)**

Figure 7.24. MRT during the day (13:00) - without greening (a) and with greening (b)

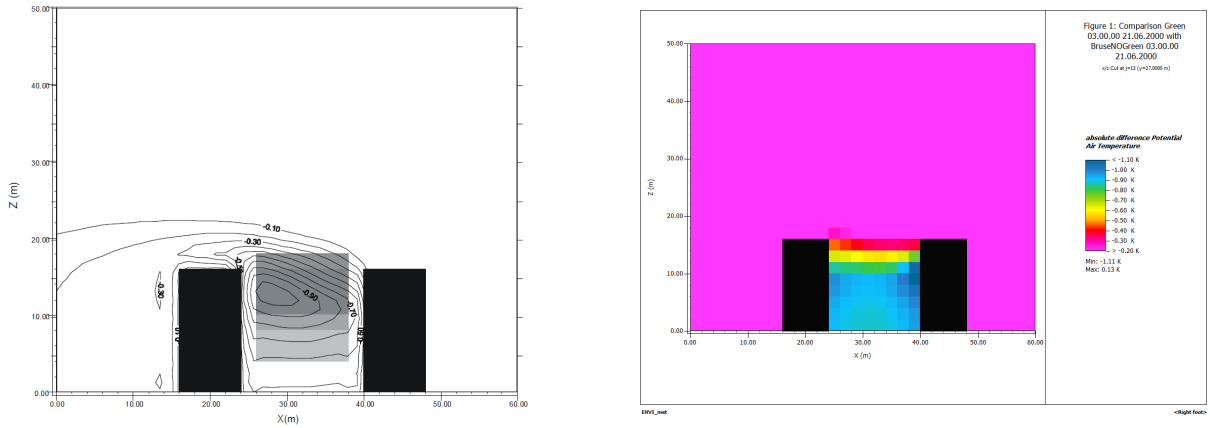

(a) **(b)**

Figure 7.25. Air temperature difference map during the night (03:00) - Bruse (2000) (a) and simulated (b)

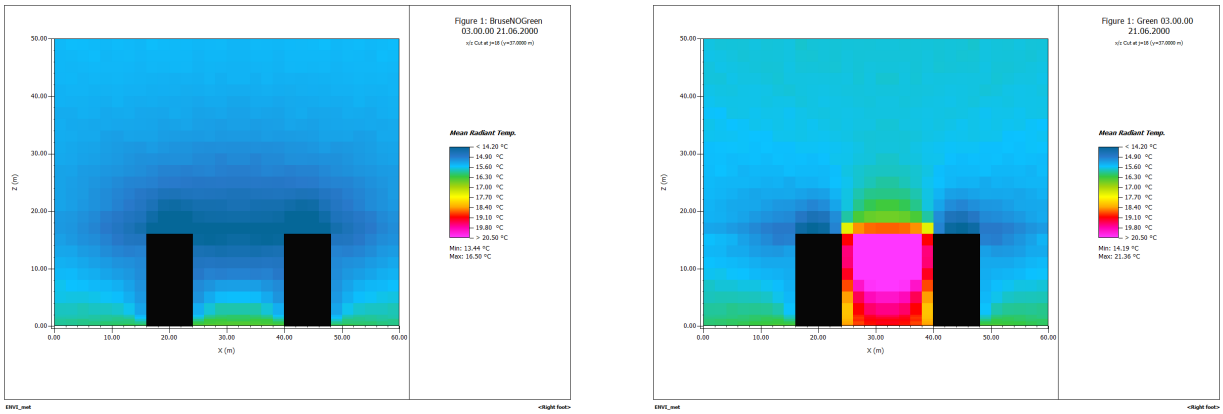

(a) **(b)**

Figure 7.26. MRT during the night (03:00) - without greening (a) and with greening (b)

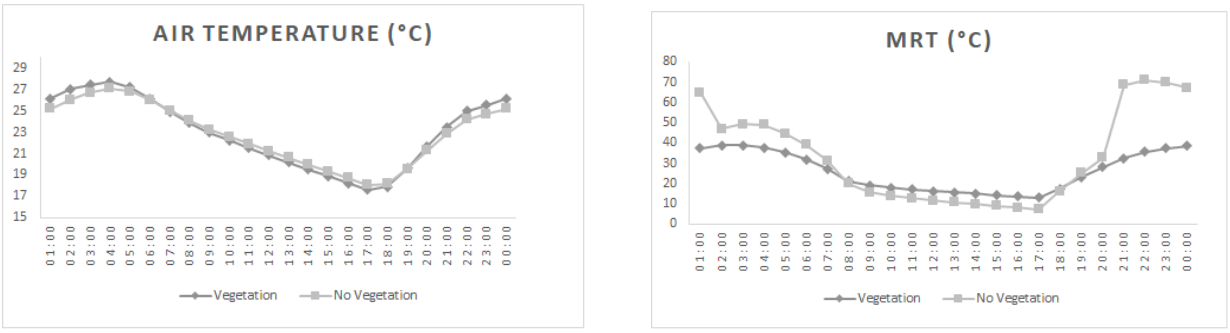

(a) (b)

Figure 7.27. Performance of the temperature with and without vegetation during the day simulated in ENVI-met - Air Temperature(°C) (a) and MRT (°C) (b)

	Day		Night	
	NO Green	Green	NO Green	Green
Air Temperature	colder	warmer	warmer	colder
MRT	warmer	colder	colder	warmer
PET	warmer	colder	colder	warmer

Table 7.5. Performance of the simulated temperature with and without greening compared to each other

The Table 7.5 summarizes how the temperature performs in the two scenarios. The air temperature during the day is cooler in the non-greened building canyon than in the greened one. At night, however, the opposite is true. The result of the simulation of Bruse (2003) shows the air temperature at 11:00 and thus a cooling of the vegetation during the day. When reconstructing this simulation, the same result could not be achieved. Looking at the results of the MRT, the vegetation cools down the building canyon during the day and warms it up during the night, as already seen in chapter 7.1.1. The PET, which is calculated from the MRT, performs very similar to the latter.

7.2. Case Study

7.2.1. Measured Data

The following diagrams show the performance of different measured surfaces. Due to the results of the sensitivity analysis, attention was paid to include locations of different building materials, vegetation and roof greening.

Figure 7.28 (a) shows the measured surface temperature of grass and asphalt, one in the sun and one in the shade. The asphalt ground surface is warmer than the grass-covered area at almost all times. Only at 8:00 a breakaway occurs and grass sun is 4.3°C warmer than asphalt sun. Similarly, areas facing the sun are warmer than those in the shade at almost every hour. The reason why they are not warmer every hour can be that the thermal camera was always taken at the same location and depending on the time of the day, it was sometimes more or less in the sun or in the shade. Especially in the afternoon or evening, the radiation of the heat stored in the sunny asphalt is clearly visible, although in the morning the temperature differences are quite small at 2°C.

Figure 7.28 (b) again shows asphalt and grass but also gravel. All three soil surfaces were measured in a sunny location. Except for the previously mentioned exceptions of grass sun, gravel is relatively in the middle of grass and asphalt, but mainly closer to grass.

Figure 7.28 (c) shows different heights and types of vegetation. Since, as described in chapter 7.1, it appears in ENVI-met as if heat accumulates under the vegetation during the night, the temperature of the tree crown and the temperature under the tree were measured (tree). Grass under tree and grass sun was also used as a reference. As already mentioned, grass sun is almost always hotter than the grass in the shade. However, in the evening hours (from 18:00 or 19:00) the temperature of the tree crown and the tree and the grass under the tree is higher. This could be, as already mentioned, because the IR-camera always measured the same spot, but the point of the grass sun might have been in the shade from that time on. Nevertheless, it can be seen that grass sun has higher fluctuations, which could indicate that under vegetation the heat is harder to get through but also that it is accumulated and can therefore be released more slowly. Unfortunately there are not enough values at night to evaluate this more precisely. Because it is the surface temperature, no exact statements can be made about the MRT in this case.

Figure 7.28 (d) shows different types of roof materials. Concrete, wood and roof greening were measured to relate to the results of the climate adaptation measures described in chapter 7.1. It shows that green roof always has the lowest temperature compared to wood and concrete, except at 11:00 concrete is 1.2 °C cooler than the green roof, which can again be attributed to the fact that at this time an area was more or less in the shade or in the sun. Wood often has a warmer surface than concrete, but it can be clearly seen that as soon as the sun is gone, the wood also cools down quickly and as soon as the sun comes back in the morning, it heats up quickly. Concrete, on the other hand, has a strong radiation of

the heat stored during the day from 18:00 onward and is therefore significantly warmer at night. During the day, however, concrete takes longer to heat up again. The temperature difference between the surface of a concrete roof and a green roof in the evening (21:00) is 6.4°C and during the day (14:00) is 4.4°C.

Figure 7.28 (e) shows the same wall material, but in different orientations. In the morning, the east facade is the warmest, as it is exposed to the sun. At noon the south facade is the warmest and in the evening the west facade. The north facade is at no hour the coldest or the warmest surface, which is correct.

Figure 7.28 (f) shows different buildings and materials. Since chapter 7.1.1 was about building materials and their performance, it was tried to create a reference with these measurements. The orientation of the three materials is always south. It is clearly visible that glass heats up fast, but as soon as the sun is gone, it cools down again quickly. The GG4 is the newest building in the test area and meets the best energy standards, which is why it has the lowest surface temperature. In chapter 7.1.1 ENVI-met calculates at 22:00 moderate-insulation as the coolest, then comes the glass wall and then the passive-wall facade. Since in ENVI-met moderate-insulation facade has better insulating properties than the passive-wall, the relation of GG 4 to GG 6 would fit quite well. The results calculated in the Ladybug Tools show glass as the coolest material at 22:00, followed by moderate-insulation and passive-wall. For moderate-insulation and passive-wall the same properties were defined in Grasshopper as in ENVI-met, so they perform the same. Glass therefore performs differently from the simulations results made in the sensitivity analysis.

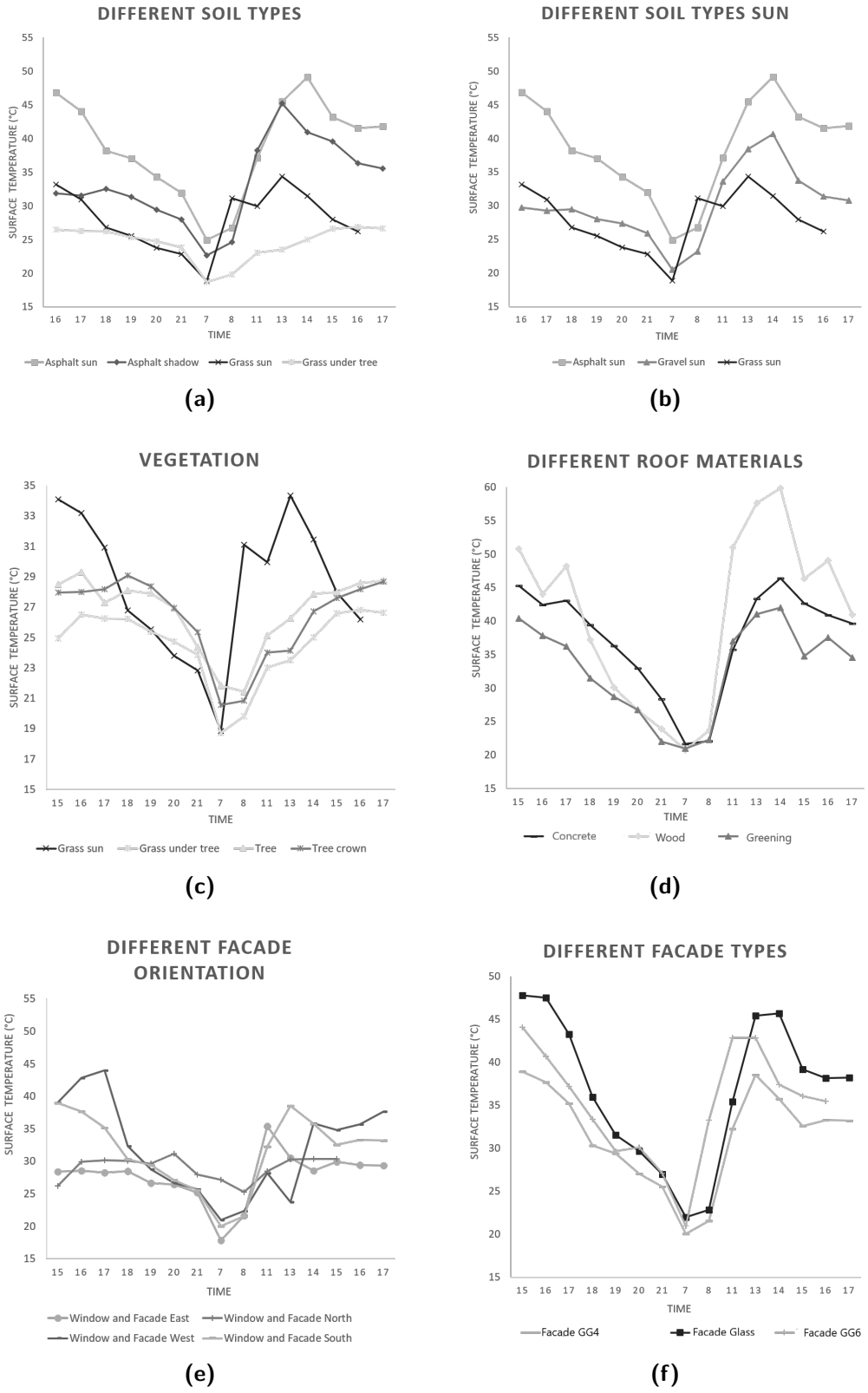

Figure 7.28. Performance of the measured surface temperature (°C) of asphalt and grass in shadow/sun (a), different soil types in the sun (b), different tree heights (c), different roof materials (d), different facade orientation (e), different facade types (f)

7.2.2. Comparison of the Surface Temperature

The diagrams in Figure 7.30, 7.31, 7.32 and the heat map (Figure 7.29) show the curve of the surfaces calculated in ENVI-met and the Ladybug Tools, as well as the surfaces measured with the thermal imaging camera, over the entire measurement period.

Asphalt sun (Figure 7.32 (a)) and asphalt south (Figure 7.32 (b)) both represent a measuring point on asphalt, which is largely unshaded and exposed to the sun. The results simulated in ENVI-met during the day are significantly lower than the measured values (up to approx. 15°C). In the evening, but especially in the morning hours, the difference of 4°C is significantly less. The values simulated in the Ladybug Tools are, significantly higher than the values measured in ENVI-met, especially during the day. In the afternoon or evening the values are similar to the measured ones or fall below them. The results from ENVI-met with a R^2 of 0.9 have a higher correlation than the results calculated in the Ladybug Tools with a R^2 of 0.73. The values from ENVI-met and from the Ladybug Tools are very similar over the simulation time, but ENVI-met is always cooler than the Ladybug Tools. The difference is greatest during the day and adjusts during the night. The R^2 between the two tools is with 0.86 a relatively good correlation.
Asphalt south basically shows a very similar trend as asphalt sun.

Asphalt shadow (Figure 7.32 (c)) and asphalt under tree (Figure 7.32 (d)) both represent a measuring point on the asphalt that are in a shaded area. Asphalt shadow is shaded by a building and tree asphalt is mainly shaded by a tree. It can be clearly seen that the tree asphalt lets the sun through, unlike the building, and that the asphalt surface is generally warmer. At night the temperature curve of ENVI-met and Ladybug Tools is very similar. With sunrise, the surface temperature in the Ladybug Tools increases extremely and the difference between Ladybug Tools and ENVI-met is about 15°C. According to the measurements of the surface temperature, the extreme temperature rise as seen in Ladybug Tools is more similar to the measured temperature rise than to the results in ENVI-met. The R^2 is relatively similar with 0.71 (ENVI-met) and 0.7 (Ladybug Tools), but the RMSE in Ladybug Tools is lower with 3.6 than in ENVI-met (6.4).

It can be seen that ENVI-met always simulates the facade temperature cooler than the Ladybug Tools. At night, these differ more than the asphalt temperature described above. The peak of the east facing facade (Figure 7.30 (a)) is 11:00 at the measured temperature in the morning. For LT, this is slightly earlier at 8:00 and 9:00 respectively, but for ENVI-met it is 15:00. Not only the temperature differs very much at the east facing facade, but also the course is very different for all three, which can be clearly seen from the values of R^2 and RMSE (Table 7.6). The north-facing facade (Figure 7.30 (b)) is the coolest of the four facade orientations both in the measurements and in the simulations. In all cases, the peak is visible at 15:00 (if the measured outliers are ignored at 19:00), which makes sense, since facade north is never directly illuminated by the sun and the maximum temperature of the day is reached during this period. The two simulated results appear to be relatively similar (R^2 0.96 and RMSE of 2.5), but they differ from the measured values. Apart from a few ex-

ceptions in the measured values, the curves of ENVI-met, Ladybug Tools and the measured results are relatively similar on the west-facing facade (Figure 7.30 (c)). The peak can be seen at 16:00 and 17:00 on all of them. On the second day of measurement for ENVI-met and Ladybug Tools at 14:00, facade west represents the warmest of the four orientations, which is perhaps explained by the fact that the facades are not 100% aligned with the corresponding cardinal directions. The peak of the surface temperature at facade south (Figure 7.30 (d)) is 14:00 and the temperature curves are realistically similar to each other. However, it is clearly visible that the measured values decrease and increase much more strongly than the simulated values, resulting in a higher temperature fluctuation.

The glass facade south, facade south and facade energy base south each represent facades with a different building material. Glass facade south (Figure 7.30 (e)) has the hottest values compared to the other two. It is noticeable that for the first time on all facade surfaces, the temperature simulations during the day with ENVI-met are higher than the values from Ladybug Tools and therefore better match the measured values. The course between ENVI-met and Ladybug Tools is very different, with different maximum and minimum times. The course, as well as the maximum and minimum times of the energy base facade (Figure 7.30 (f)) are relatively similar for the measured and simulated ones. The highest value for all south exposed facades is at 13:00 and 14:00. Facade south is slightly warmer (around 0.25°C during the day and up to 1.5°C at night) than facade energy base south in most hours.

Roof concrete and roof green describes an unshaded point on the roof. It is clearly visible that roof concrete (Figure 7.31 (a)) has higher values than roof green (Figure 7.31 (b)). The measured values are in both cases much higher than the simulated values and seem to be lower at night. So the fluctuations are much larger than simulated. The course of roof concrete is relatively different in the simulated and the measured values, but a significantly higher correlation can be found with ENVI-met (R^2 0.61) than with LT (R^2 0.22). For roof green the course is more similar (LT R^2 0.7) and the temperatures in ENVI-met and LT are very similar in the evening and at night. The high temperature differences with roof green may be due to the fact that this green roof is extensive, but an intensive one was simulated. The differences between the roof types can be very variable (see chapter 4 Green Buildings).

Grass shadow (Figure 7.31 (c)) and grass under tree (Figure 7.31 (d)) represent both measuring points on grass under a tree. Both perform very different. Grass shadow shows that the measured values are below the simulated values. The course is similar but there are extreme temperature differences, especially Ladybug Tools is up to 20 °C warmer. Ladybug Tools does not include evapotranspiration cooling in the calculation, which could possibly indicate the difference. However, ENVI-met is also up to 10°C warmer than the measured values in some cases. With grass under tree, the two simulated results are very different, especially in the evening and at night. The measured values have many outliers, which could explain the extremely bad correlation to the simulated values. However, the measured values are more similar to the Ladybug Tools than to ENVI-met in terms of course and temperature differences. The shading at this point comes not only from a tree but also from a building,

unlike grass shadow. This explains the slightly stronger correlation of the Ladybug Tools, but not the bad correlation of ENVI-met.

Gravel (Figure 7.31 (e)) and grass sun (Figure 7.31 (f)) are measuring points without shading. Both show a very similar course despite the outliers in the Ladybug Tools and the measured values. ENVI-met shows very similar curves at both measuring points and acts in the same temperature range. The Ladybug Tools however show significantly cooler values at gravel than at grass sun. The temperature range of the measured values at grass sun corresponds very poorly with the values from the Ladybug Tools and is significantly lower. ENVI-met, however, has a good agreement.

	E/M		**LT/M**		**E/LT**	
	RMSE	**R^2**	**RMSE**	**R^2**	**RMSE**	**R^2**
Asphalt sun	9.757	0.903	5.054	0.731	12.556	0.858
Asphalt shadow	6.411	0.711	3.625	0.701	6.917	0.551
Gravel	4.315	0.639	4.525	0.762	7.200	0.621
Grass sun	2.201	0.740	8.523	0.788	8.934	0.648
Grass shadow	5.019	0.639	11.747	0.443	7.039	0.817
Facade east	2.617	0.641	4.392	0.020	4.589	0.002
Facade north	4.385	0.474	2.030	0.453	2.848	0.961
Facade west	6.161	0.774	4.261	0.767	3.494	0.948
Facade south	4.737	0.910	3.221	0.896	3.185	0.852
Asphalt south	9.696	0.748	7.333	0.506	13.882	0.857
Glass facade south	6.910	0.871	9.935	0.796	4.662	0.685
Grass under tree	4.437	0.026	2.810	0.156	3.186	0.457
Asphalt under tree	6.350	0.677	6.898	0.526	9.369	0.902
Facade Energy Base south	7.784	0.872	5.745	0.892	3.031	0.913
Roof concrete	16.029	0.612	16.580	0.216	1.843	0.746
Roof green	9.196	0.621	6.244	0.703	4.592	0.267

Table 7.6. R^2 and RMSE for the surface temperature of Ladybug Tools (LT), ENVI-met (E) and Field measurements (M)

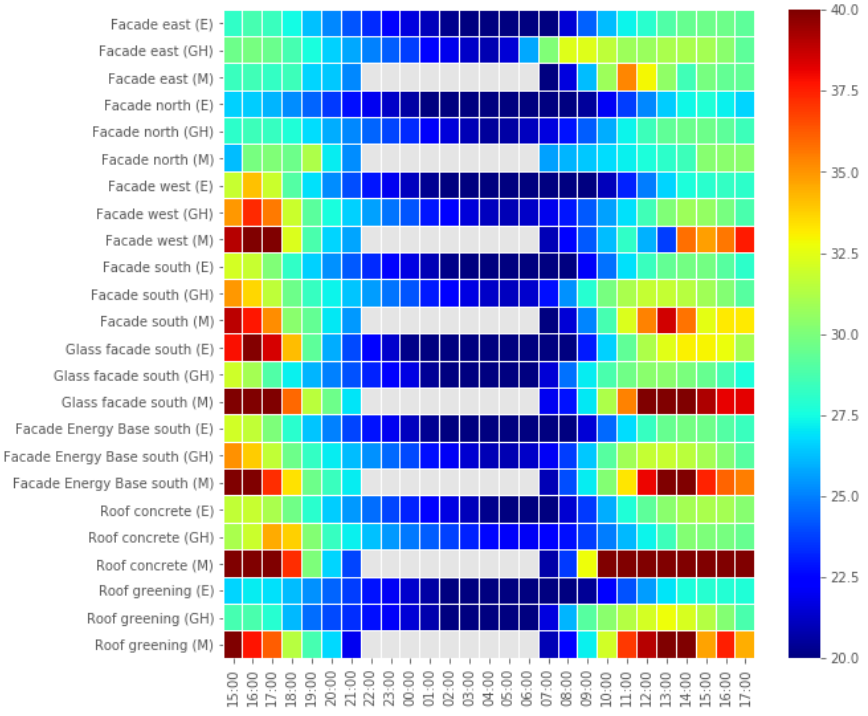

(a)

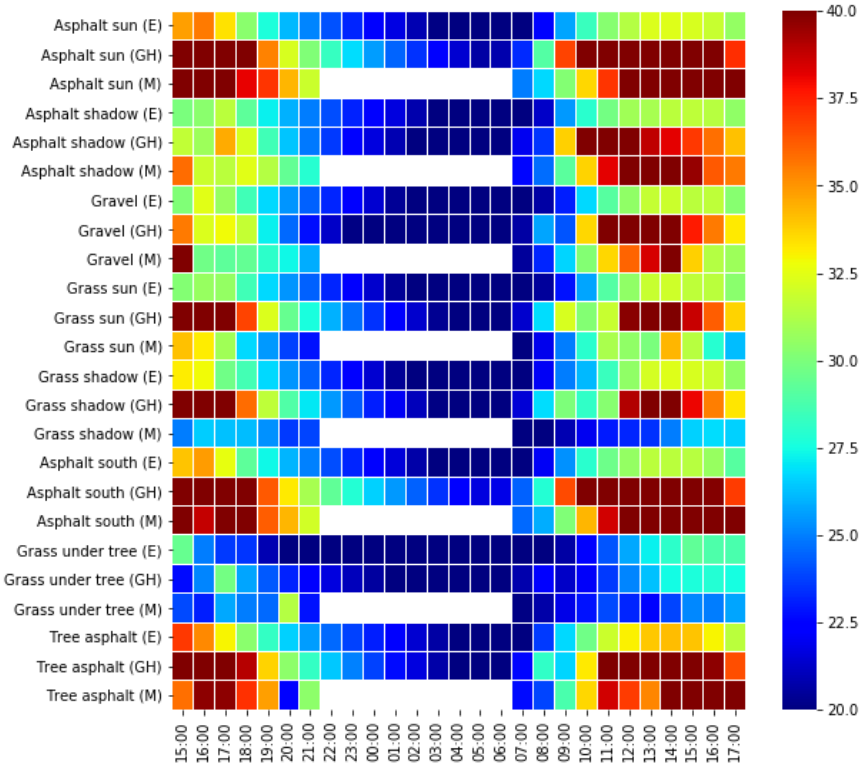

(b)

Figure 7.29. Comparison of the measured (M), the ENVI-met (E) and the Ladybug Tools (GH) surface temperature (°C) of the buildings (a) and of all other surfaces (b)

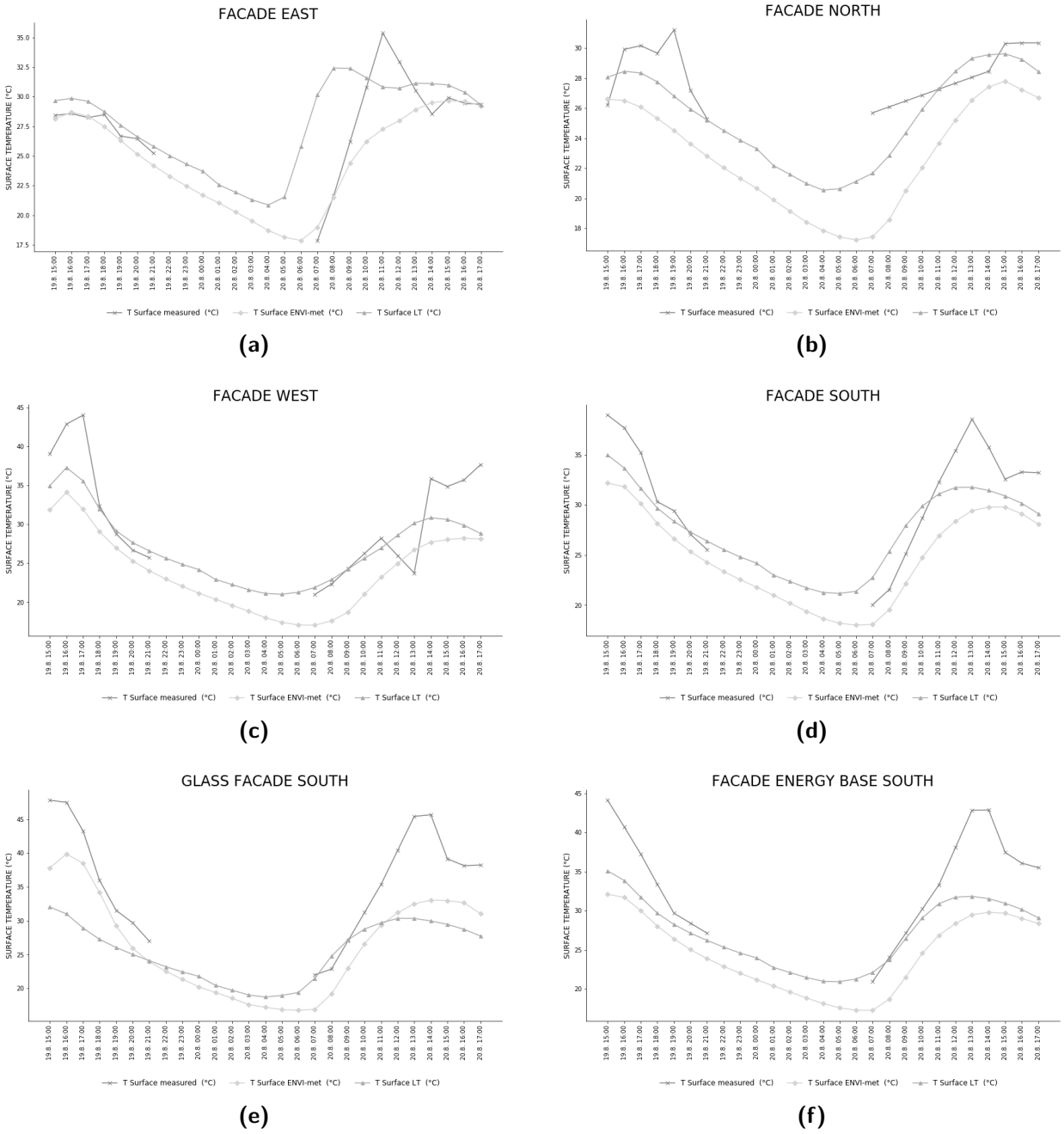

Figure 7.30. Comparison of the measured, the ENVI-met and the Ladybug Tools surface temperature (°C) of the different locations

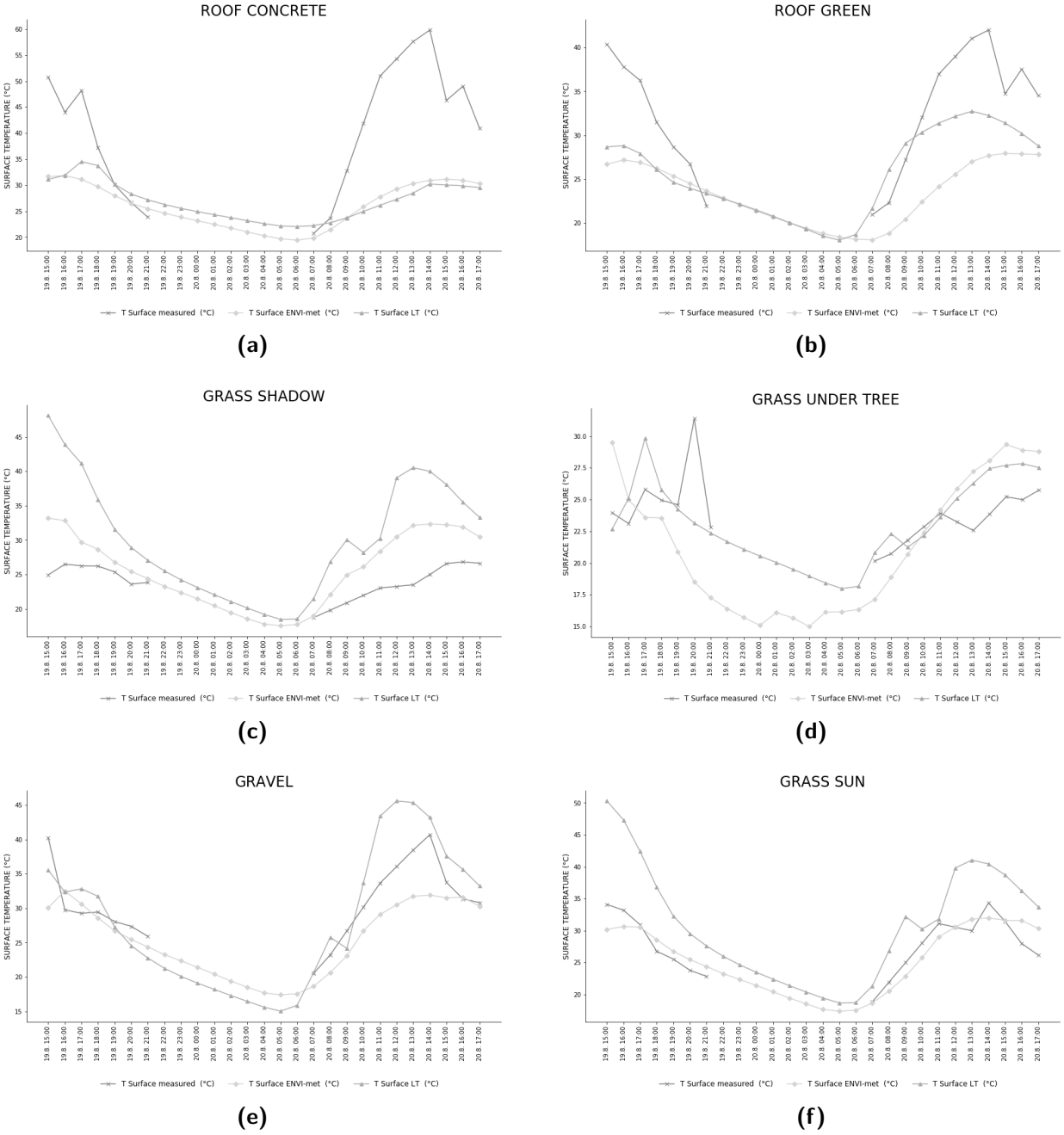

Figure 7.31. Comparison of the measured, the ENVI-met and the Ladybug Tools surface temperature (°C) of the different locations

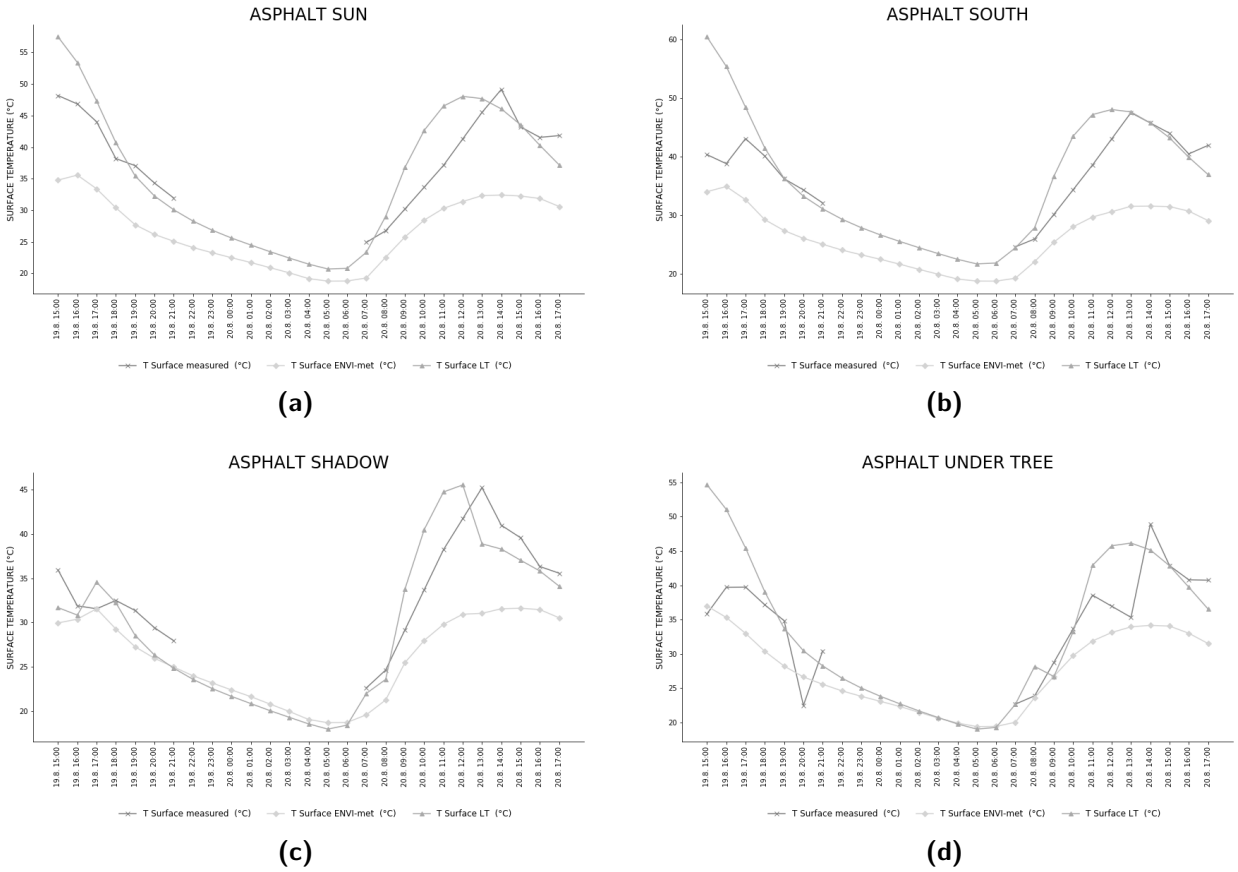

Figure 7.32. Comparison of the measured, the ENVI-met and the Ladybug Tools surface temperature (°C) of the different locations

7.2.3. Comparison of the Mean Radiant Temperature

The following diagrams (Figure 7.33) compare the MRT from the two microclimate simulation tools and the values from the IR-measurements. It was decided not to calculate the MRT from the IR -measurements, as the results would have been too inaccurate with the existing variables. However, the simulated MRTs were nevertheless compared with the measured values, because the performance of the simulated MRTs in relation to the measured values needed to be investigated. For this comparison, R^2 and RMSE were calculated from the results of the microclimate simulation and the IR-measurements (Table 7.7), in order to show the correlation and errors.

The course of the MRT is very similar at most sites, but, with a few exceptions, the results from the Ladybug Tools always have higher values than ENVI-met. It is noticeable that the values from the Ladybug Tools during the day are usually only slightly above the one from ENVI-met, but at night there are large temperature differences (sometimes 20°C), especially on the facades of buildings. During the day, the unshaded measuring points on the asphalt have a higher MRT and at night the values of the shaded measuring points are slightly higher (see Figure 7.33).
All individual diagrams of the respective measurement site can be found in appendix A.1.

	E/M		**LT/M**		**E/LT**	
	RMSE	**R^2**	**RMSE**	**R^2**	**RMSE**	**R^2**
Asphalt sun	11.739	0.312	10.494	0.398	7.241	0.922
Asphalt shadow	9.354	0.243	7.981	0.315	8.940	0.540
Gravel	11.268	0.210	11.770	0.310	9.630	0.523
Grass sun	9.069	0.536	14.537	0.651	12.599	0.310
Grass shadow	15.823	0.000	23.698	0.015	10.857	0.763
Facade east	8.014	0.227	11.605	0.267	11.217	0.832
Facade north	9.531	0.076	4.909	0.218	10.318	0.279
Facade west	12.682	0.310	10.585	0.152	12.644	0.614
Facade south	11.751	0.312	12.368	0.453	10.809	0.952
Asphalt south	13.799	0.078	10.467	0.150	7.565	0.959
Glass facade south	12.756	0.284	9.989	0.368	10.713	0.958
Tree 202	6.832	0.333	12.839	0.388	7.838	0.738
Grass under tree	14.047	0.004	11.726	0.003	8.062	0.581
Tree crown	9.022	0.129	13.862	0.258	6.559	0.862
Asphalt under tree	13.042	0.208	14.495	0.201	5.885	0.953
Facade Energy Base south	12.704	0.329	9.400	0.560	11.190	0.857
Roof concrete	12.729	0.500	12.710	0.624	15.822	0.900
Roof green	11.901	0.479	27.637	0.543	22.004	0.944

Table 7.7. R^2 and RMSE for the MRT temperature of Ladybug Tools (LT), ENVI-met (E) and the surface temperature of the field measurements (M)

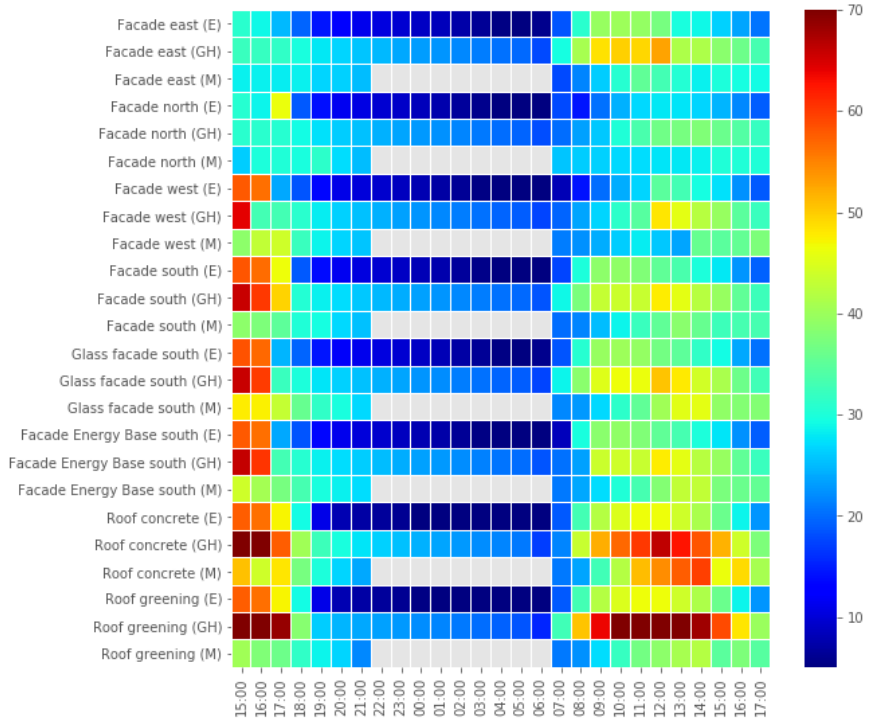

(a)

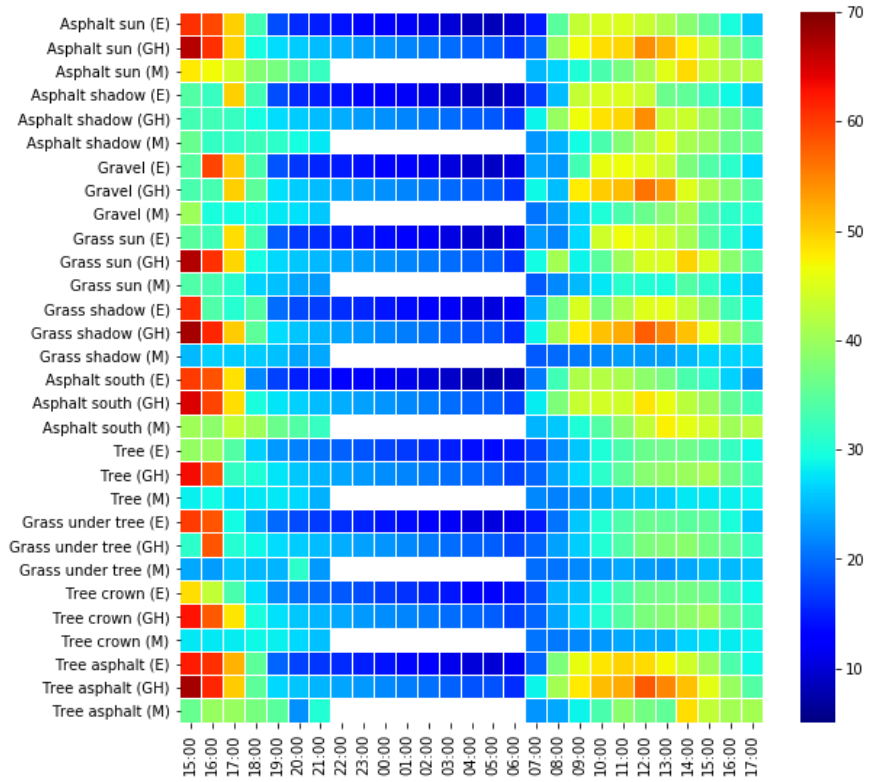

(b)

Figure 7.33. Comparison of the ENVI-met (E) and the Ladybug Tools (GH) mean radiant temperature (°C) and the values from the IR - measurements (M), of the buildings (a) and of all other surfaces (b)

Shaded measuring points on grass at night also have higher values than sunny measuring points on grass. During the day, the situation is exactly the opposite. However, with the Ladybug Tools there is a difference, if the shade is caused by a tree and not by a building, as with grass shadow or asphalt under tree (by tree) and with grass under tree and asphalt shadow (tree and/or building). The values during the day are higher at the shaded measuring point (see Figure 7.33). This may be because in the Ladybug Tools, trees work as shading elements and the shadow moves with the sun (Figure 7.34). But since the measuring point is always the same, it is not in the shade during a certain period of time.

It is noticeable that in ENVI-met, the MRT of the south facade and the glass facade (warmest facades) is lower than the MRT of the measurement points with shading by trees. In the Ladybug Tools, the two facades are sometimes cooler during the day, but from 18:00 onward the facade is always warmer than the measurement points in the shade of trees.

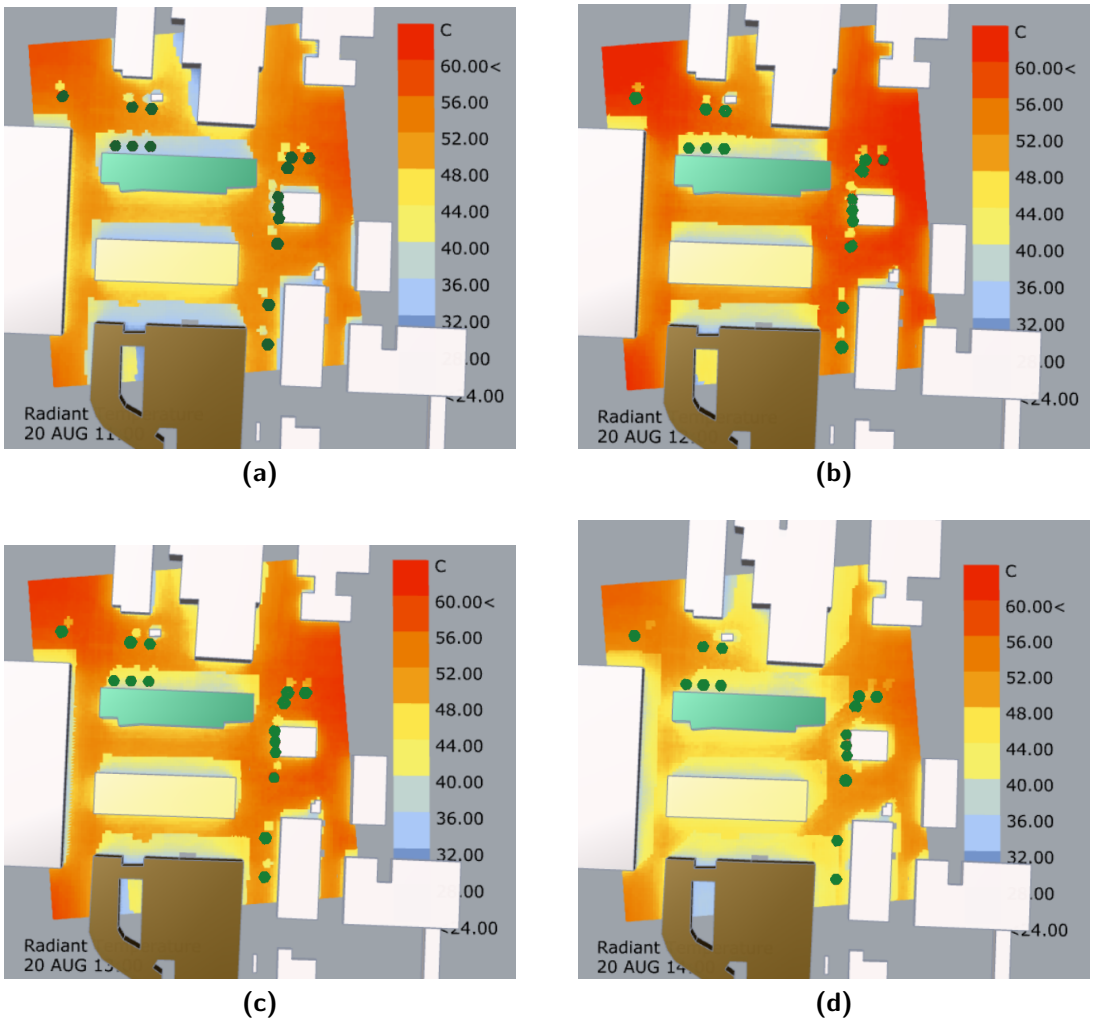

Figure 7.34. Hourly change of the shadow in the Ladybug Tools at 11:00 (a), 12:00 (b), 13:00 (c), 14:00 (d)

7.2.4. Air Temperature and UTCI

The air temperature was also simulated and compared with the measured values to see how they behave. Air Temperature could not be displayed in the Ladybug Tools, because after the calculation, there was always only one value for the whole simulated area. It seems to be a bug in the simulation. Instead of the air temperature, the UTCI was calculated and displayed in the Ladybug Tools.

MRT and air temperature in ENVI-met act the same way as already seen in chapter 7.1. MRT is significantly warmer during the day and significantly cooler at night than the air temperature (Figure 7.35 (a, b)).

It is interesting to see that at almost all locations the Ladybug Tools MRT values of the hours 18:00 - 07:00 are very similar to the ENVI-met air temperature values (Figure 7.35 (a) and (b)). At some measurement locations the air temperature in ENVI-met has very similar values and performs similar to the surface temperature in ENVI-met (Figure 7.35 (c)).
All other diagrams are shown in appendix A.2.

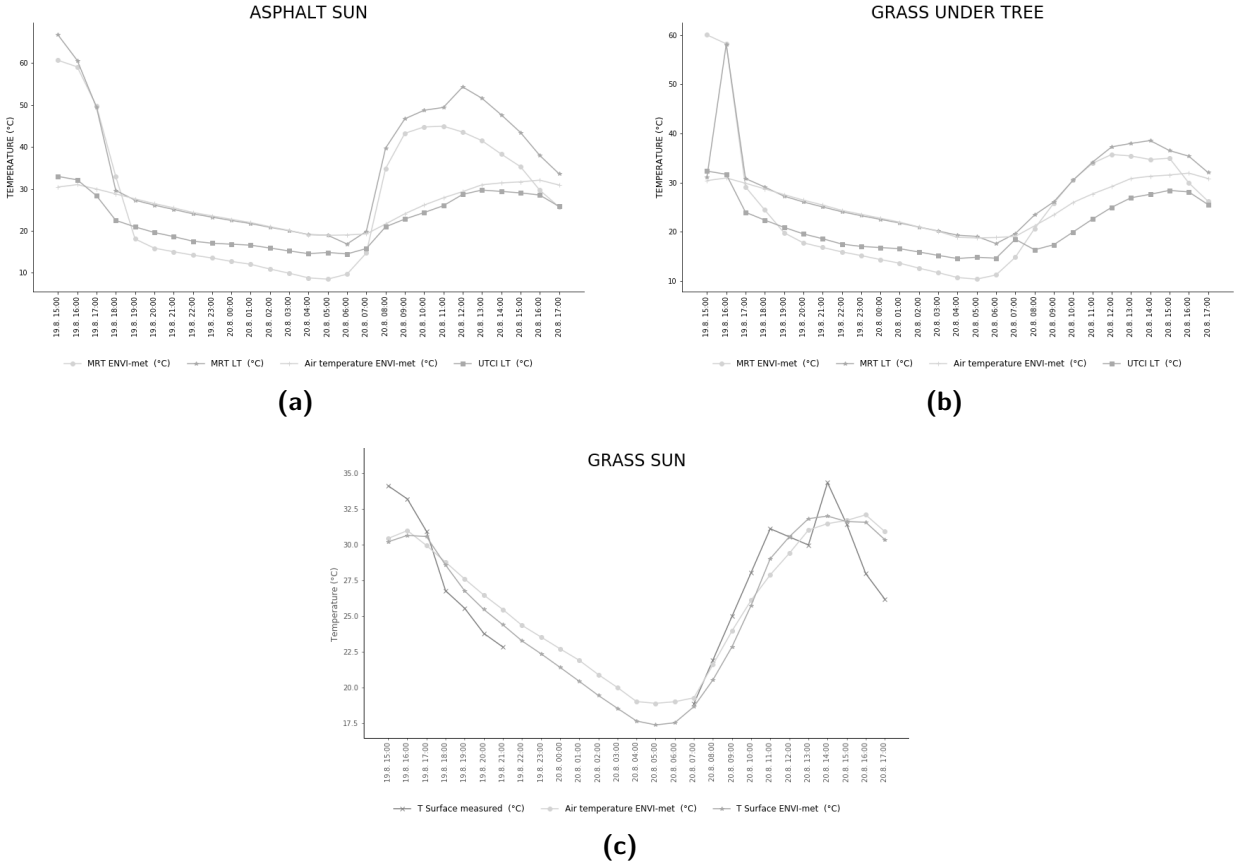

Figure 7.35. Comparison of the ENVI-met and the Ladybug Tools mean radiant and air temperature (°C) of the different locations

When discussing the simulated results and the results of the IR measurements, it is important to keep in mind that, among other things, there may be some uncertainty because the receptor (measurement) points from the microclimate simulation tools do not correspond exactly to the measured ones. Although an attempt has been made to orient the receptor (measuring) points from the simulation software as closely as possible to the measured ones, there are still differences.
Also, the simulated values have, at some locations, very different surface temperatures than the measured ones but similar trends. One reason could be that thermal camera images are only a snapshot and the simulations in ENVI-met and the Ladybug Tools are hourly average values.

7.2.5. EPW vs. Actual Weather Data simulated in ENVI-met

According to the study by Tsoka, Tolika, et al. (2018), the typical weather year (TMY) is mainly derived from several years of meteorological recordings outside urban centres. Due to their location, the complex interaction of meteorological parameters, which lead to the creation of the urban heat island effect and to higher air temperatures, cannot be taken into account. The results of the study showed a 1°C higher air temperature inside the urban canyon compared to the TMY (Tsoka, Tolika, et al., 2018). EPW data, which are usually collected outside the city center, do not necessarily represent the urban microclimate of the city.
For this reason, a further approach was to use not only the EPW file but also a simulation with current weather data prevailing on that day as input for the simulation in ENVI-met.

Surface Temperature

It can be generally seen that the actual weather data have consistently higher values than those from the EPW file. Since ENVI-met is cooler than the measured surface temperature at some measurement locations, the current data is partly more similar to the measured data. This can be seen very well e.g. at facade south (Figure 7.36 (a)). Sometimes it can be seen, like in asphalt shadow or grass shadow (Figure 7.36 (b) and (c)), that the progressions from the current weather data become similar to the Ladybug Tools. However, in the case of grass shadow it can be seen that Ladybug Tools results and both variants of ENVI-met data are significantly higher than the measured ones (Figure 7.36 (c)).

Mean Radiant Temperature

The MRT data from the actual weather data are, like the surface temperature, higher than when the EPW file serves as input and therefore during the day usually higher than the Ladybug Tools results (Figure 7.36 (d) and (e)).

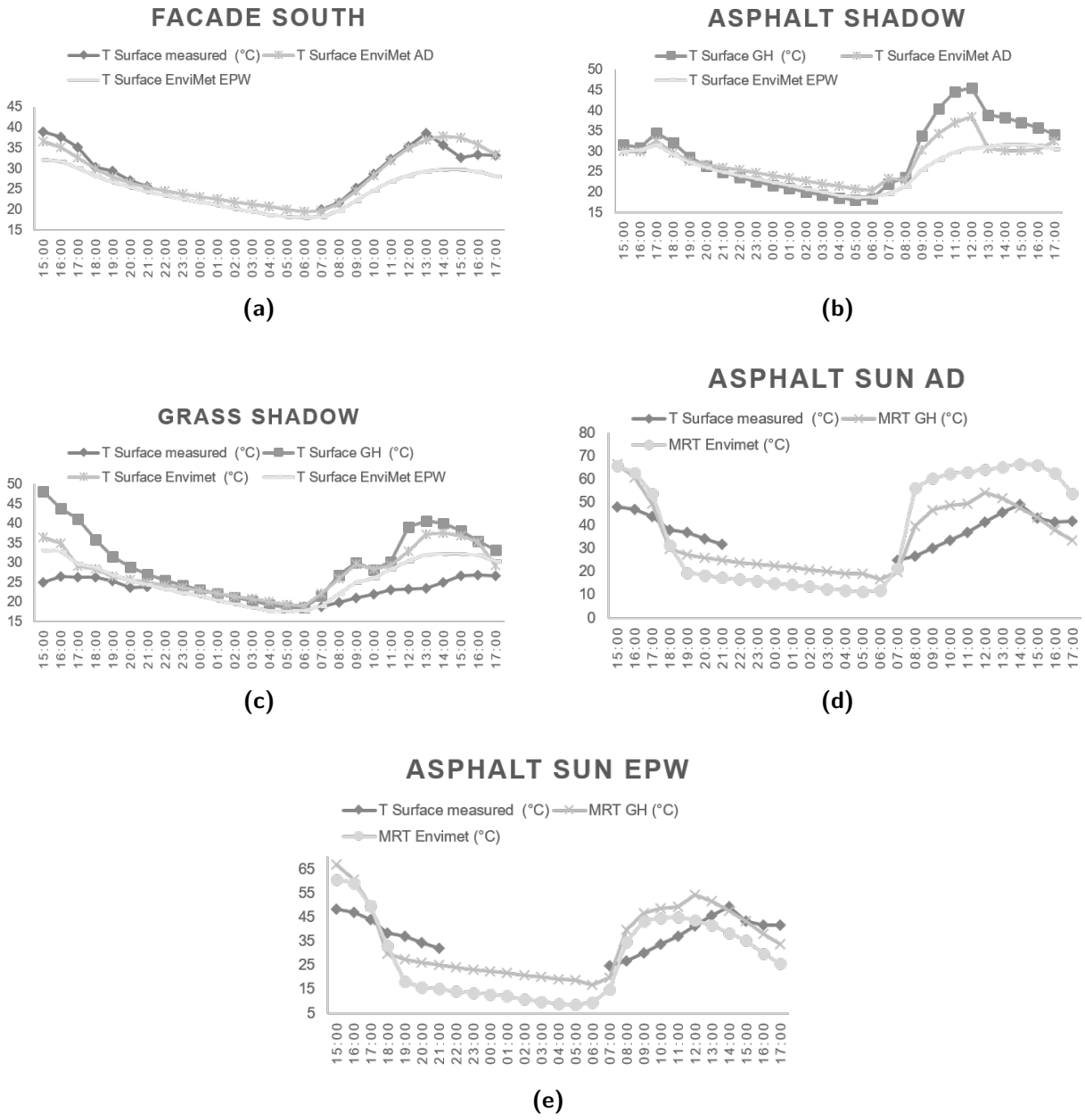

Figure 7.36. Comparison of the actual weather data and the EPW data

8. Conclusion

This concluding chapter summarizes the most important findings of the thesis and answers the research questions raised at the beginning.
The aim of the thesis was to compare and evaluate two microclimate simulation models in order to apply the knowledge gained and to obtain correct results according to measurements and literature. With this knowledge and the application of the tools, the effects of climate change and the increasing density of cities and their growing impact on the microclimate can be shown. Suitable measures against UHIs and for climate-friendly cities can also be identified.
For this purpose the practical work was divided into two parts. First, a sensitivity analysis was created, which compares the two simulation programs (ENVI-met and Ladybug Tools) each in itself. The basic model was left unchanged and only different wall materials were applied and simulated for different seasons. The effects of vegetation and different greening scenarios have also been tested. Secondly, a case study was created in which the results of the simulations were compared with real measured data.

In the following part the research questions are answered in detail:

- *Which are the most appropriate models to show the impact of urban densification on microclimate conditions on different scales?*

  It depends above all on what the user wants to represent. Basically, both tools are suitable for showing the effects on the microclimate. Depending on the resources available, but also on the choice of parameters used, one or the other tool is more suitable. As can be seen in table 5.1, ENVI-met covers a wider range of output parameters and elements to be investigated. The Ladybug Tools on the other hand require less computing time, are open source and very well compatible with other software.

- *What limitations do ENVI-met and the Ladybug Tools have simulating the microclimate?*

  The results show that both tools have their limitations in terms of simulation results, especially with regard to vegetation. ENVI-met does not simulate vegetation as it acts in the real world and the Ladybug Tools cannot yet calculate the evapotranspiration.

- *Can we always trust available tools?*

  The results of existing tools can never be trusted, unless the method, data or research

design behind them is also included in the interpretation. As figure 7.5 in chapter 7.1.1 shows, the handling and the defined settings of the tool has a major impact on the results, as does the correct choice of input data. Garbage in, garbage out.

- *What effect have different greening measurements (e.g. green buildings, trees) on the microclimate in the Ladybug Tools as well as in ENVI-met?*

  As shown in chapter 7.1.3, both tools act differently on the different types of greening. Since the Ladybug Tools do not take evapotranspiration into account, the respective greening is only used as a shading element. Due to the additional insulation layer, all scenarios with facade and/or roof greening have a cooling effect on the microclimate in the Ladybug Tools. Also in the Ladybug Tools trees cast a shadow and cool the area below. In the night this effect, due to the absence of the sun, does not occur anymore. Evapotranspiration is included in ENVI-met. During the day the MRT is cooler near or under a tree. However, at night the tree emits heat. This effect was also achieved when comparing the facade greening with the bare facade. The air temperature during the day is higher in a greened street canyon than in a non-greened street canyon. This effect is reversed at night.

- *What effects do different building materials have on the microclimate in the Ladybug Tools as well as in ENVI-met?*

  As can be seen in chapter 7.1.1, both tools create a dissimilar microclimate due to the use of different wall materials. Depending on the chosen material, the ambient temperature will increase or decrease. Depending on the season, the materials also act differently. The different wall materials in ENVI-met and in the Ladybug Tools perform very similar to each other. ENVI-met also shows that trees present in the model emit more or less heat depending on the material, which seems to be correct, as the MRT includes all radiation fluxes.

- *How does the input (weather) data effect the simulation result?*

  The input weather data has a major impact on the data. As described in chapter 7.2.5, the different input weather data lead to a big difference in the output data. The results with the current prevailing weather data at this location are much more consistent with the measured values.
  Especially, for projects that take place in the city center, it is important to use suitable weather data. Many TMY weather data sets are from meteorological measuring stations outside the densely built-up area and can therefore falsify the results significantly.

This last part summarizes the main findings and results of this thesis. It shows the main limitations of the two simulation programs (ENVI-met and the Ladybug Tools), both in terms of usability, functionality and accuracy. It also shows the most important results from the comparison with the measured data.

Important findings and features regarding ENVI-met:

- Performance wall material mostly good, but ratio with vegetation radiation doesn't fit
- MRT of trees at night higher than no vegetation
- Air temperature of trees during day higher than no vegetation
- Green facade MRT hotter than BC and air temperature cooler than BC
- High computing time
- Low compatibility
- Includes evapotranspiration

Important findings and features while working with the Ladybug Tools:

- Different performance of glass wall material than in ENVI-met (summer)
- Trees only as shading element
- Accurate simulation of green buildings (mainly through insulation of the additional layer)
- Low computing time
- High compatibility
- No evapotranspiration

Results and findings regarding the case study:

- ENVI-met simulates lower values in MRT and surface temperature than Ladybug Tools
- Ladybug Tools results have more variation in the temperature curve than ENVI-met results
- Grass locations lower temperature as simulated and closer to ENVI-met surface temperature
- Asphalt locations temperature closer to Ladybug Tools surface temperature
- Roof concrete and roof green higher values as simulated
- Actual weather data simulate results closer to measured data than EPW file

9. Outlook

There are many possibilities to continue research on this topic. It would make sense to continue further attempts to increase the spin-up time. As the results in this thesis, but also the studies of Skelhorn et al. (2014) and Jänicke et al. (2015) show, spin-up time has an enormous influence on the results. In Srivanit and Hokao (2013) experiments were conducted with increasing the number of nesting grids. In this study nesting grids of 195 m leads to 0.103°C difference between field measured and in ENVI-met simulated data (Srivanit & Hokao, 2013). Unfortunately, this approach could not be included in the present thesis, but should definitely be considered in future experiments.

The experiments in this thesis already show what effect the input (weather) data has on the result. In future tests and applications of the tools, more attention should be paid to the quality and characteristics of the input data.

The ENVI-met plug-in for Grasshopper, which was unfortunately not tested in this thesis, was developed by Antonello Di Nunzio. In further studies a closer look at this plug-in would be interesting. The plug-in allows you to create the whole process around the simulation in the Grasshopper visual scripting environment. The simulation takes place in ENVI-met but without directly opening the ENVI-met software. The input of the geometry data can be done like in the Ladybug Tools via SHP file, because the tool allows to convert Rhino 3D designs to an INX formatted ENVI-met model area (DiNunzio, 2018). The plug-in thus combines a simpler handling with the comprehensive parameters that can be examined in ENVI-met.

A very important point is the integration of evapotranspiration in the Ladybug Tools (or Grasshopper). It was tried to find possibilities and integrate them into the simulation process, but unfortunately this would go beyond the scope of the master thesis. Nevertheless, two approaches could be found. Kongsgaard (2018) dealt with this issue in his master thesis and developed Livestock which is using CMF - Catchment Modeling Framework as the base for hydrological modeling. At the end of May 2020 a paper named, PANDO: Parametric Tool for Simulating Soil-Plant Atmosphere of Tree Canopies in Grasshopper, was released by a research group among others of the TU Munich, in which a new plug-in for Grasshopper was presented (Chokhachian & Hiller, 2020). No tests with PANDO could be performed yet, but after a first evaluation it looks very promising. Since the lack of evapotranspiration is the biggest limitation in the Ladybug Tools, the integration of this plug-in could take the usability of the Ladybug Tools to a whole new level.

Bibliography

Albdour, M. S., & Baranyai, B. (2019). An overview of microclimate tools for predicting the thermal comfort, meteorological parameters and design strategies in outdoor spaces. *Pollack Periodica*.

Alliance-for-Sustainable-Energy-LLC. (n.d.). OpenStudio [Accessed: 2020-06-20]. https://www.openstudio.net/

Aniello, C., Morgan, K., Busbey, A., & Newland, L. (1995). Mapping micro-urban heat islands using Landsat TM and a GIS. *Computers & Geosciences*, *21*(8), 965–969.

ANSYS. (n.d.). About Ansys [Accessed: 2020-06-20]. https://www.ansys.com/en-in/about-ansys

Avio. (n.d.). HandyThermoTVS-200EX [Accessed: 2020-06-20]. http://www.infrared.avio.co.jp/en/products/ir-thermo/lineup/tvs-200ex/index.html

Awino, H. R. A. (2019). *Design-Integrated Urban Heat Island Analysis Tool and Workflow: Development and Application*.

Bai, X., Dawson, R. J., Ürge-Vorsatz, D., Delgado, G. C., Barau, A. S., Dhakal, S., Dodman, D., Leonardsen, L., Masson-Delmotte, V., & Roberts, D. C. (2018). Six research priorities for cities and climate change.

Balzert, H. (2008). *Wissenschaftliches Arbeiten: Wissenschaft, Quellen, Artefakte, Organisation, Präsentation*. W3l GmbH.

Berardi, U. (2016). The outdoor microclimate benefits and energy saving resulting from green roofs retrofits. *Energy and Buildings*, *121*, 217–229.

Besir, A. B., & Cuce, E. (2018). Green roofs and facades: A comprehensive review. *Renewable and Sustainable Energy Reviews*, *82*, 915–939. https://doi.org/10.1016/j.rser.2017.09.106

Betsill, M., & Bulkeley, H. (2003). *Cities and climate change* (Vol. 4). Routledge.

Bigladder Software [Accessed: 2020-06-20]. (n.d.). https://bigladdersoftware.com/epx/docs/8-0/input-output-reference/

Bölcskey, E., & Bruckner, H. (2014). *Baustofflehre Werkstofftechnologie und Brandsicherheit - Naturwissenschaftliche Grundlagen zur Baustofflehre* (2nd ed.). TU Wien - Institut für Hochbau und Technologie.

Bornstein, R. D. (1968). Observation of the Urban Heat Island Effect in New York City. *Journal of applied Meteorology*, *7*, 575–582.

Bruse, M. (2000). Anwendung von mikroskaligen Simulationsmodellen in der Stadtplanung. *Simulation raumbezogener Prozesse: Methoden und Anwendung [Application of microscale simulation models in urban planning]. Münster*.

Bruse, M. (2003). Stadtgrün und Stadtklima.

Bruse, M., & Fleer, H. (1998). Simulating surface–plant–air interactions inside urban environments with a three dimensional numerical model. *Environmental modelling & software*, *13*(3-4), 373–384.

Chokhachian, A., & Hiller, M. (2020). PANDO: Parametric and Tool for Simulating and Soil-Plant Atmosphere and of Tree and Canopies.

Chokhachian, A., Perini, K., Dong, S., & Auer, T. (2017). How material performance of building façade affect urban microclimate. *Powerskin 2017*.

Chris, M., Keith, A., Matthew, D., & Mostapha Sadeghipour, R. (2015). Hydra [Accessed: 2020-06-20]. http://hydrashare.github.io/hydra/

Crawley, D. B. (1998). Which weather data should you use for energy simulations of commercial buildings? *Transactions-American society of heating refrigerating and air conditioning engineers*, *104*, 498–515.

Crawley, D. B., Pedersen, C. O., Lawrie, L. K., & Winkelmann, F. C. (2000). EnergyPlus: Energy Simulation Program. *ASHRAE Journal*, *42*, 49–56.

Davidson, S. (n.d.). Grasshopper [Accessed: 2020-06-20]. http://www.grasshopper3d.com/

DiNunzio, A. (2018). Dragonfly legacy envimet components [Accessed: 2020-06-20]. https://discourse.ladybug.tools/t/dragonfly-legacy-envimet-components/4626

Dynamo [Accessed: 2020-06-20]. (n.d.). http://www.dynamobim.org

Elwy, I., Ibrahim, Y., Fahmy, M., & Mahdy, M. (2018a). Outdoor microclimatic validation for hybrid simulation workflow in hot arid climates against ENVI-met and field measurements. *Energy Procedia*, *153*, 29–34. https://doi.org/10.1016/j.egypro.2018.10.009

Elwy, I., Ibrahim, Y., Fahmy, M., & Mahdy, M. (2018b). VALIDATION OF OUTDOOR MICROCLIMATE SIMULATION FOR HOT ARID REGIONS USING A PARAMETRIC WORKFLOW. *The International Conference on Civil and Architecture Engineering*, *12*(12th International Conference on Civil and Architecture Engineering), 1–11.

ENVI-met [Accessed: 2020-06-20]. (n.d.). https://www.envi-met.com/

ENVI-met. (n.d.-a). Albero [Accessed: 2020-06-20]. https://www.envi-met.com/learning-support/albero/

ENVI-met. (n.d.-b). Basic Layout of ENVI-met [Accessed: 2020-06-20]. http://www.envi-met.info/documents/onlinehelpv3/hs800.htm/

ENVI-met. (n.d.-c). Company Journal [Accessed: 2020-06-20]. https://www.envi-met.com/brochures/

ENVI-met. (n.d.-d). EnviMet Dokumentation [Accessed: 2020-06-20]. http://www.envi-met.info/doku.php?id=root:start

ENVI-met. (n.d.-e). Expertenunterricht [Accessed: 2020-06-20]. https://www.envi-met.com/de/lernen-support/expertenunterricht/

ENVI-met. (n.d.-f). Getting Started [Accessed: 2020-06-20]. https://www.envi-met.com/learning-support/getting-started/

ENVI-met. (n.d.-g). Spaces [Accessed: 2020-06-20]. https://www.envi-met.com/learning-support/spaces/

Esri. (n.d.-a). About [Accessed: 2020-06-20]. https://www.esri.com/

Esri. (n.d.-b). ArcGIS [Accessed: 2020-06-20]. https://www.esri.com/

Feng, H., & Hewage, K. (2014). Energy saving performance of green vegetation on LEED certified buildings. *Energy and Buildings*, *75*, 281–289. https://doi.org/10.1016/j.enbuild.2013.10.039

Filho, W. L., Icaza, L. E., Emanche, V., & Al-Amin, A. Q. (2017). An Evidence-Based Review of Impacts, Strategies and Tools to Mitigate Urban Heat Islands. *International Journal of Environmental Research and Public Health*, *14*(12), 1600. https://doi.org/10.3390/ijerph14121600

Glen, S. (n.d.). RMSE: Root Mean Square Error [Accessed: 2020-06-20]. https://www.statisticshowto.com/probability-and-statistics/regression-analysis/rmse-root-mean-square-error/

Godbole, S. (2018). Investigating the Relationship Between Mean Radiant Temperature (MRT) and Predicted Mean Vote (PMV): A Case Study in a University building.

Hong, W., Guo, R., & Tang, H. (2019). Potential assessment and implementation strategy for roof greening in highly urbanized areas: A case study in Shenzhen, China. *Cities*, *95*, 102468. https://doi.org/10.1016/j.cities.2019.102468

Howard, L. (1883). The Climate of London, Deduced from Meteorological Observations, Made at Different Places in the Neighbourhood of the Metropolis. 2 vols. London: W. Philips 1818–1820. *Rev. Ed.*

Jänicke, B., Meier, F., Hoelscher, M.-T., & Scherer, D. (2015). Evaluating the effects of façade greening on human bioclimate in a complex urban environment. *Advances in Meteorology, 2015*.

Kongsgaard, C. (2018). *Hygrotermic Control of the Microclimate Around Buildings*.

Kraus, F., Fritthum, R., Robausch, E., Scharf, B., Preiss, J., Enzi, V., Steinbauer, G., Oberbichler, C., Lichtblau, A., Haas, S., Dyk, G., Korjenic, A., Tudiwer, D., & Jesner, L. (2019). Leitfaden Fassadenbegrünung.

Ladybug Tools [Accessed: 2020-06-20]. (n.d.). www.ladybug.tools

Lazzarin, R. M., Castellotti, F., & Busato, F. (2005). Experimental measurements and numerical modelling of a green roof. *Energy and Buildings*, *37*(12), 1260–1267. https://doi.org/10.1016/j.enbuild.2005.02.001

Li, H. (2016). Impacts of Pavement Strategies on Human Thermal Comfort. *Pavement Materials for Heat Island Mitigation* (pp. 281–306). Elsevier. https://doi.org/10.1016/b978-0-12-803476-7.00013-1

Lindberg, F., Holmer, B., & Thorsson, S. (2008). SOLWEIG 1.0–Modelling spatial variations of 3D radiant fluxes and mean radiant temperature in complex urban settings. *International journal of biometeorology*, *52*(7), 697–713.

Loibl, W., Etminan, G., Österreicher, D., Ratheiser, M., Stollnberger, R., Tschannett, S., Tötzer, T., Vuckovic, M., & Walal, K. (2019). Urban Densification and Urban Climate Change–Assessing Interaction through Densification Scenarios and Climate Simulations. *Proceedings of the REAL CORP*.

Mackey, C., & Roudsari, M. S. (2017). The Tool(s) Versus The Toolkit. *Humanizing Digital Reality* (pp. 93–101). Springer Singapore. https://doi.org/10.1007/978-981-10-6611-5_9

Matzarakis, A., Rutz, F., & Mayer, H. (2000). Modellierung der mittleren Strahlungstemperatur in urbanen Strukturen.

McNeel-and-Associates. (n.d.). Rhinoceros [Accessed: 2020-06-20]. https://www.rhino3d.com/.

Meteodyn. (n.d.). Software, Studies and Consulting [Accessed: 2020-06-20]. https://meteodyn.com/

Mohammad, A., & Balint, B. (2019). An overview of microclimate tools for predicting the thermal comfort, meteorological parameters and design strategies in outdoor spaces. *Pollack Periodica*.

Naboni, E., Coccolo, S., Meloni, M., & Scartezzini, J.-L. (2018). Outdoor comfort simulation of complex architectural designs: a review of simulation tools from the designer per-

spective. *2018 Building Performance Analysis Conference and SimBuild co-organized by ASHRAE and IBPSA-USA*, (CONF).

Naboni, E., Meloni, M., Coccolo, S., Kaempf, J., & Scartezzini, J.-L. (2017). An overview of simulation tools for predicting the mean radiant temperature in an outdoor space. *Energy Procedia*, *122*, 1111–1116.

Nakata-Osaki, C. M., Souza, L. C. L., & Rodrigues, D. S. (2018). THIS–Tool for Heat Island Simulation: A GIS extension model to calculate urban heat island intensity based on urban geometry. *Computers, Environment and Urban Systems*, *67*, 157–168.

Nichol, J. (2005). Remote sensing of urban heat islands by day and night. *Photogrammetric Engineering & Remote Sensing*, *71*(5), 613–621.

Oke, T. (1995). The heat island of the urban boundary layer: characteristics, causes and effects. *Wind climate in cities* (pp. 81–107). Springer.

Oke, T., Johnson, G., Steyn, D., & Watson, I. (1991). Simulation of surface urban heat islands under 'ideal'conditions at night part 2: Diagnosis of causation. *Boundary-Layer Meteorology*, *56*(4), 339–358.

OpenCFD-Limited. (n.d.). OpenFoam [Accessed: 2020-06-20]. https://www.openfoam.com/

Perini, K., Chokhachian, A., & Auer, T. (2018). Green streets to enhance outdoor comfort. *Nature based strategies for urban and building sustainability* (pp. 119–129). Elsevier.

Perini, K., Chokhachian, A., Dong, S., & Auer, T. (2017). Modeling and simulating urban outdoor comfort: Coupling ENVI-Met and TRNSYS by grasshopper. *Energy and Buildings*, *152*, 373–384. https://doi.org/10.1016/j.enbuild.2017.07.061

Perini, K., Ottelé, M., Fraaij, A., Haas, E., & Raiteri, R. (2011). Vertical greening systems and the effect on air flow and temperature on the building envelope. *Building and Environment*, *46*(11), 2287–2294. https://doi.org/10.1016/j.buildenv.2011.05.009

Peronato, G., Kämpf, J. H., Rey, E., & Andersen, M. (2017). *Integrating urban energy simulation in a parametric environment: a Grasshopper interface for CitySim* (tech. rep.).

Pflieger, V. (2014). Bestimmtheitsmaß R^2 - Teil 2: Was ist das eigentlich, ein $R^{2?}$ [Accessed: 2020-06-20]. https://www.statisticshowto.com/probability-and-statistics/coefficient-of-determination-r-squared/.

Priyadarsini, R., Hien, W. N., & David, C. K. W. (2008). Microclimatic modeling of the urban thermal environment of Singapore to mitigate urban heat island. *Solar energy*, *82*(8), 727–745.

PythonSoftwareFoundation. (n.d.). Python [Accessed: 2020-06-20]. https://www.python.org/

Rakha, T., Zhand, P., & Reinhart, C. (2005). A Framework for Outdoor Mean Radiant Temperature Simulation: Towards Spatially Resolved Thermal Comfort Mapping in Urban Spaces.

Robitu, M., Musy, M., Inard, C., & Groleau, D. (2006). Modeling the influence of vegetation and water pond on urban microclimate. *Solar energy*, *80*(4), 435–447.

Roth, M., Oke, T., & Emery, W. (1989). Satellite-derived urban heat islands from three coastal cities and the utilization of such data in urban climatology. *International Journal of Remote Sensing*, *10*(11), 1699–1720.

Roth, M., & Lim, V. H. (2017). Evaluation of canopy-layer air and mean radiant temperature simulations by a microclimate model over a tropical residential neighbourhood. *Building and Environment*, *112*, 177–189.

Roudsari, M. S., Pak, M., Smith, A., et al. (2013). Ladybug: a parametric environmental plugin for grasshopper to help designers create an environmentally-conscious design. *Proceedings of the 13th international IBPSA conference held in Lyon, France Aug*, 3128–3135.

Salata, F., Golasi, I., de Lieto Vollaro, A., & de Lieto Vollaro, R. (2015). How high albedo and traditional buildings' materials and vegetation affect the quality of urban microclimate. A case study. *Energy and Buildings*, *99*, 32–49.

Salata, F., Golasi, I., de Lieto Vollaro, R., & de Lieto Vollaro, A. (2016). Urban microclimate and outdoor thermal comfort. A proper procedure to fit ENVI-met simulation outputs to experimental data. *Sustainable Cities and Society*, *26*, 318–343.

Shashua-Bar, L., Pearlmutter, D., & Erell, E. (2011). The influence of trees and grass on outdoor thermal comfort in a hot-arid environment. *International journal of climatology*, *31*(10), 1498–1506.

Shashua-Bar, L., Tsiros, I. X., & Hoffman, M. E. (2010). A modeling study for evaluating passive cooling scenarios in urban streets with trees. Case study: Athens, Greece. *Building and Environment*, *45*(12), 2798–2807.

Skelhorn, C., Lindley, S., & Levermore, G. (2014). The impact of vegetation types on air and surface temperatures in a temperate city: A fine scale assessment in Manchester, UK. *Landscape and Urban Planning*, *121*, 129–140.

Solcerova, A., van de Ven, F., Wang, M., & van de Giesen, N. (2016). Effect of green roofs on air temperature; measurement study of well-watered and dry conditions. *EGUGA*, EPSC2016–10999.

Srivanit, M., & Hokao, K. (2013). Evaluating the cooling effects of greening for improving the outdoor thermal environment at an institutional campus in the summer. *Building and environment*, *66*, 158–172.

Tan, C. L., Wong, N. H., & Jusuf, S. K. (2013). Outdoor mean radiant temperature estimation in the tropical urban environment. *Building and Environment*, *64*, 118–129.

TAS Engineering [Accessed: 2020-06-20]. (n.d.). https://www.edsl.net/tas-engineering/

Toparlar, Y., Blocken, B., Maiheu, B., & Van Heijst, G. (2017). A review on the CFD analysis of urban microclimate. *Renewable and Sustainable Energy Reviews*, *80*, 1613–1640.

Tsoka, S., Tolika, K., Theodosiou, T., Tsikaloudaki, K., & Bikas, D. (2018). A method to account for the urban microclimate on the creation of 'typical weather year' datasets for building energy simulation, using stochastically generated data. *Energy and Buildings*, *165*, 270–283. https://doi.org/10.1016/j.enbuild.2018.01.016

Tsoka, S., Tsikaloudaki, A., & Theodosiou, T. (2018). Analyzing the ENVI-met microclimate model's performance and assessing cool materials and urban vegetation applications–A review. *Sustainable cities and society*, *43*, 55–76.

Ubakus [Accessed: 2020-06-20]. (n.d.). https://www.ubakus.de/

U.S.DepartmentofEnergy. (2019). Auxiliary Programs.

Vardasca, R., Plassmann, P., Gabriel, J., & Ring, E. (2014). Towards a Medical Imaging Standard Capture and Analysis Software. *Proceedings of the 2014 International Conference on Quantitative InfraRed Thermography*. https://doi.org/10.21611/qirt.2014.168

Vysoudil, M. (2015). Urban space and climate: Introduction to the Special Issue. *Moravian Geographical Reports*, *23*(3), 2–7. https://doi.org/10.1515/mgr-2015-0012

Waldmann, T. (2019). Python [Accessed: 2020-06-20]. https://wiki.python.org/

Wang, Y., Bakker, F., de Groot, R., Wortche, H., & Leemans, R. (2015). Effects of urban trees on local outdoor microclimate: synthesizing field measurements by numerical modelling. *Urban Ecosystems*, *18*(4), 1305–1331.

Wintour, P. (2016). Ladybug & Honeybee [Accessed: 2020-06-20]. https://parametricmonkey.com/2016/03/13/ladybug-honeybee/

Yin, H., Kong, F., Middel, A., Dronova, I., Xu, H., & James, P. (2017). Cooling effect of direct green façades during hot summer days: An observational study in Nanjing, China using TIR and 3DPC data. *Building and Environment*, *116*, 195–206. https://doi.org/10.1016/j.buildenv.2017.02.020

Appendices

A. Diagrams

A.1 Diagrams of the Simulated MRT and the IR-measurements

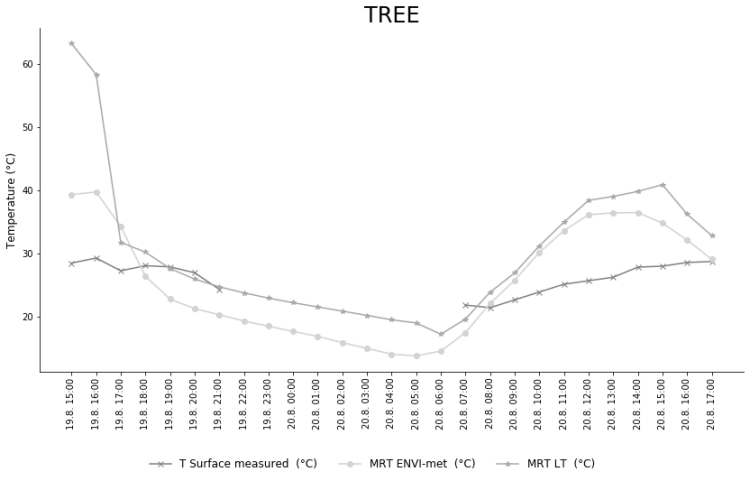

(a)

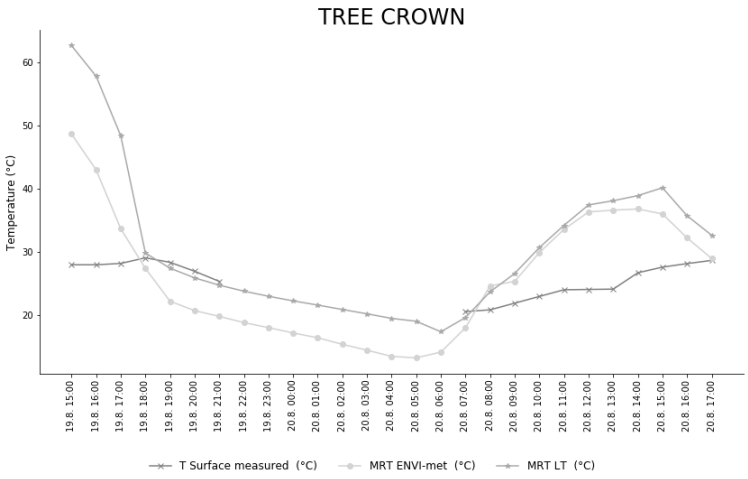

(b)

Figure A.1. Comparison of ENVI-met and the Ladybug Tools (LT) mean radiant temperature (°C) and the IR - measurements (measured), of the different locations

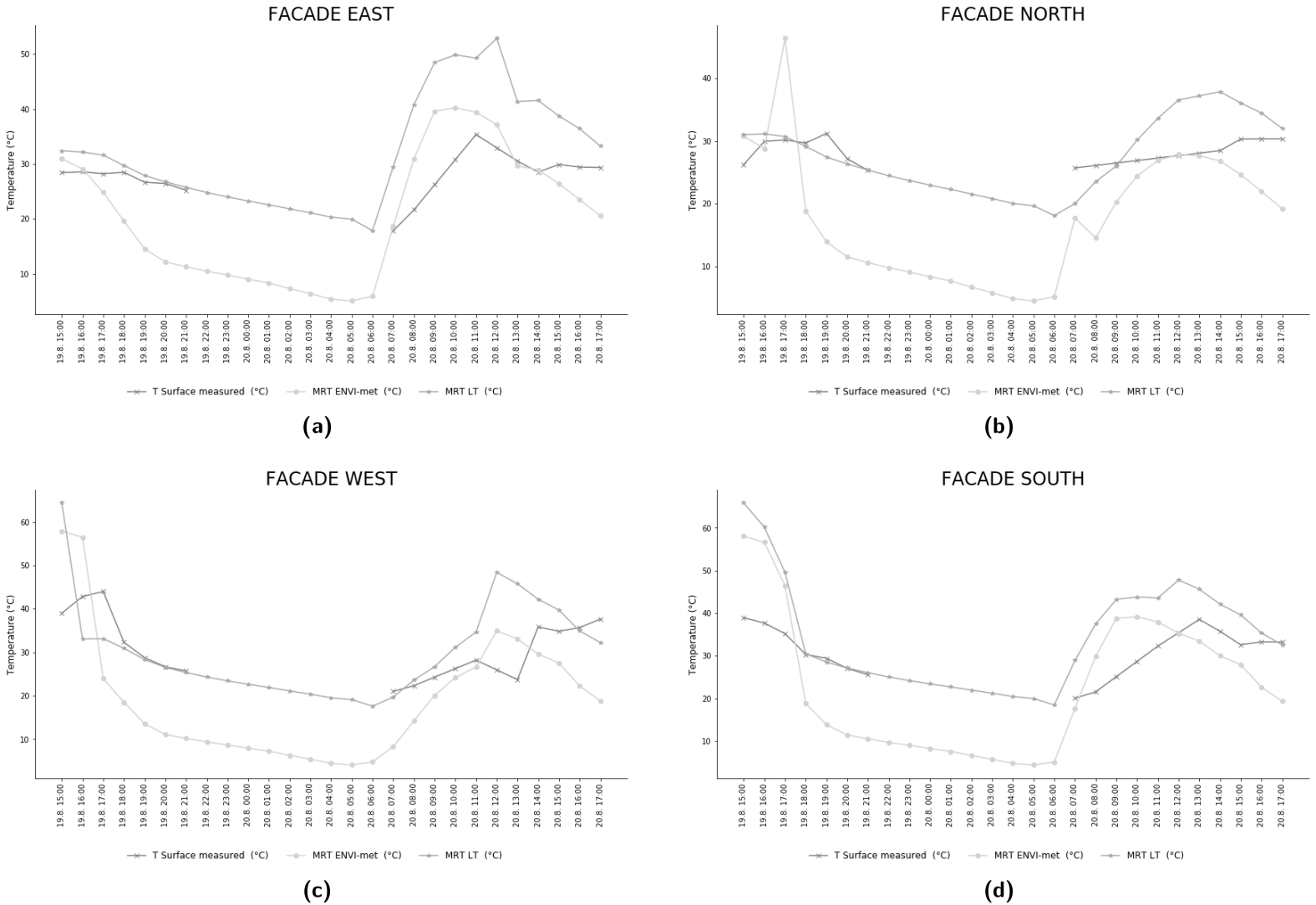

Figure A.2. Comparison of ENVI-met and the Ladybug Tools (LT) mean radiant temperature (°C) and the IR - measurements (measured), of the different locations

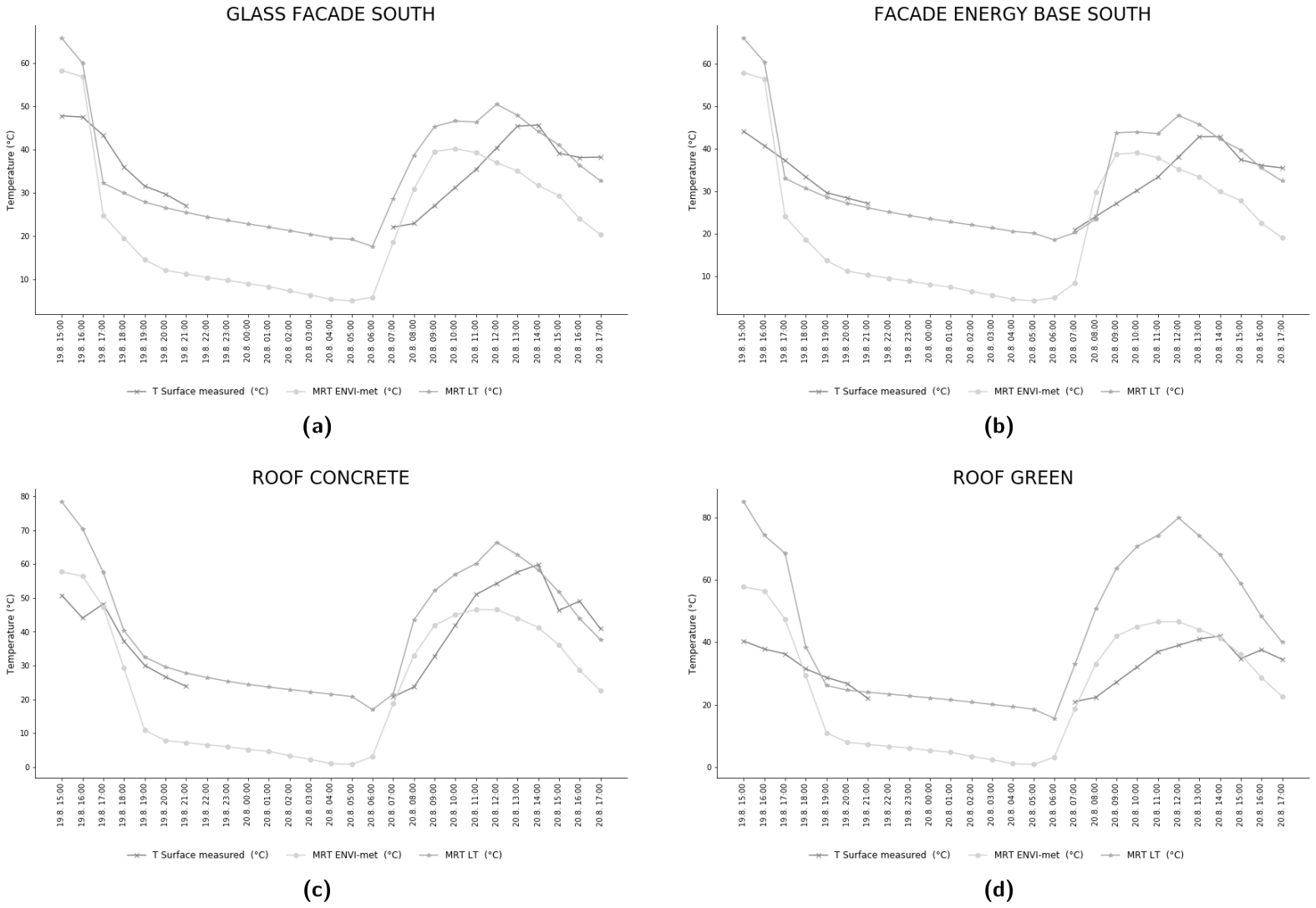

Figure A.3. Comparison of ENVI-met and the Ladybug Tools (LT) mean radiant temperature (°C) and the IR - measurements (measured), of the different locations

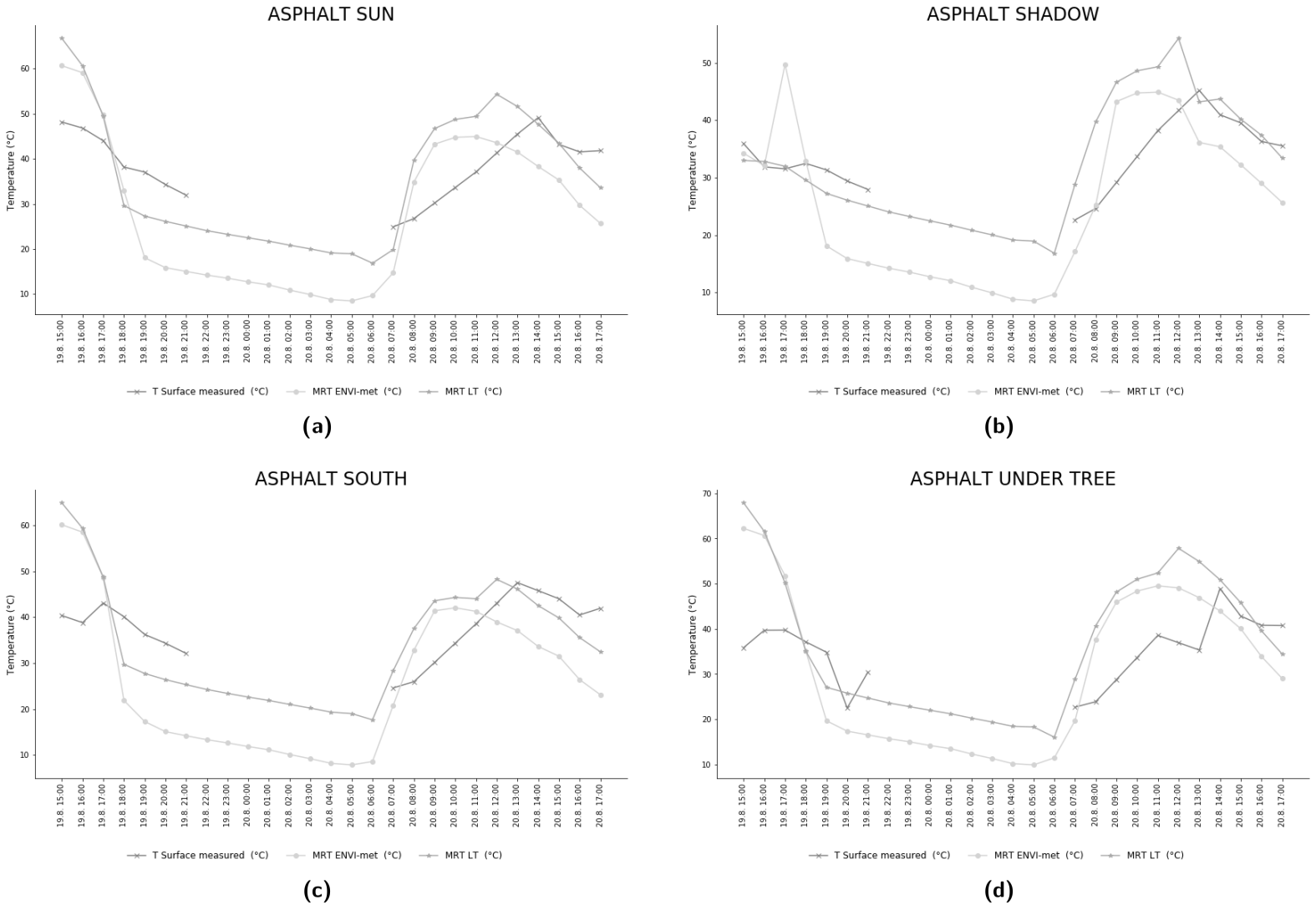

Figure A.4. Comparison of ENVI-met and the Ladybug Tools (LT) mean radiant temperature (°C) and the IR - measurements (measured), of the different locations

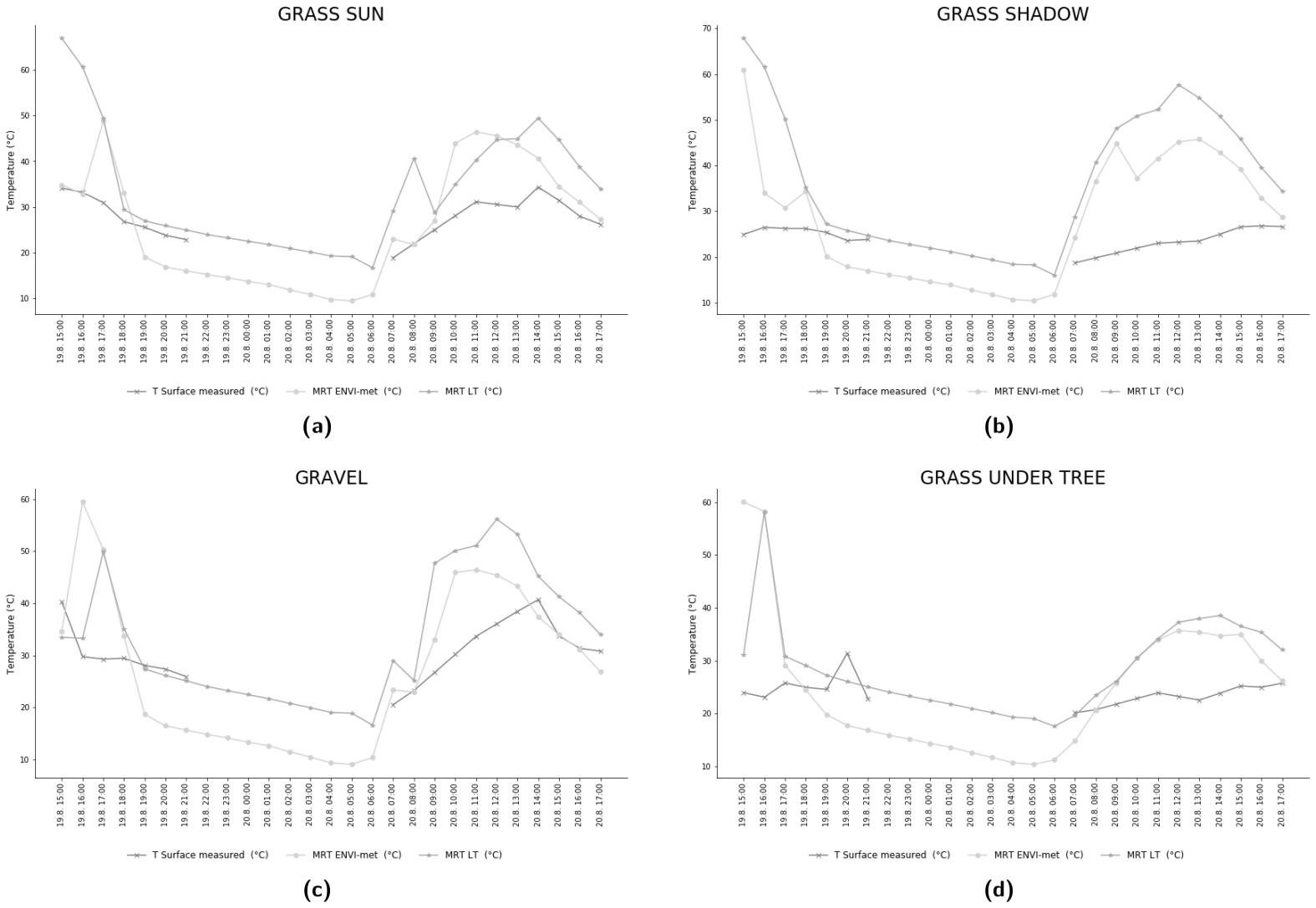

Figure A.5. Comparison of ENVI-met and the Ladybug Tools (LT) mean radiant temperature (°C) and the IR - measurements (measured), of the different locations

A.2 Diagrams of the MRT, UTCI and Air Temperature Simulated in ENVI-met and the Ladybug Tools

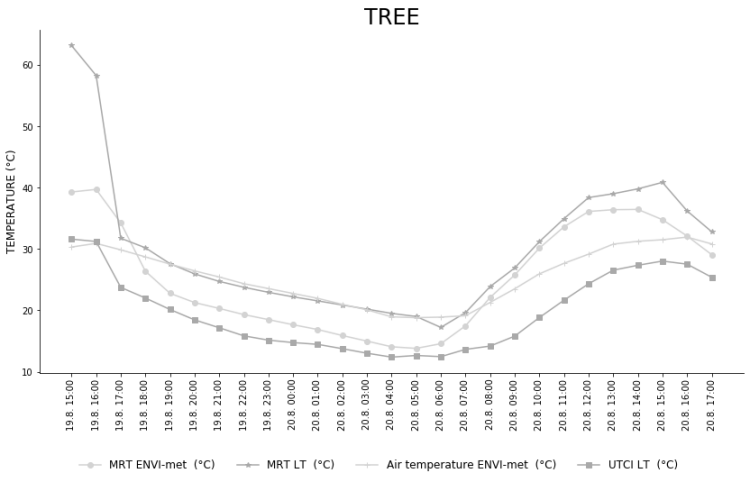

(a)

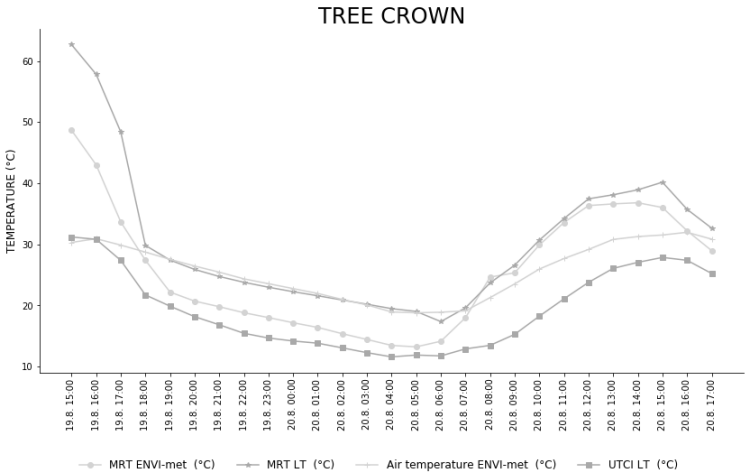

(b)

Figure A.6. Comparison of the MRT, UTCI and Air Temperature simulated in ENVI-met and the Ladybug Tools (LT) of the different locations

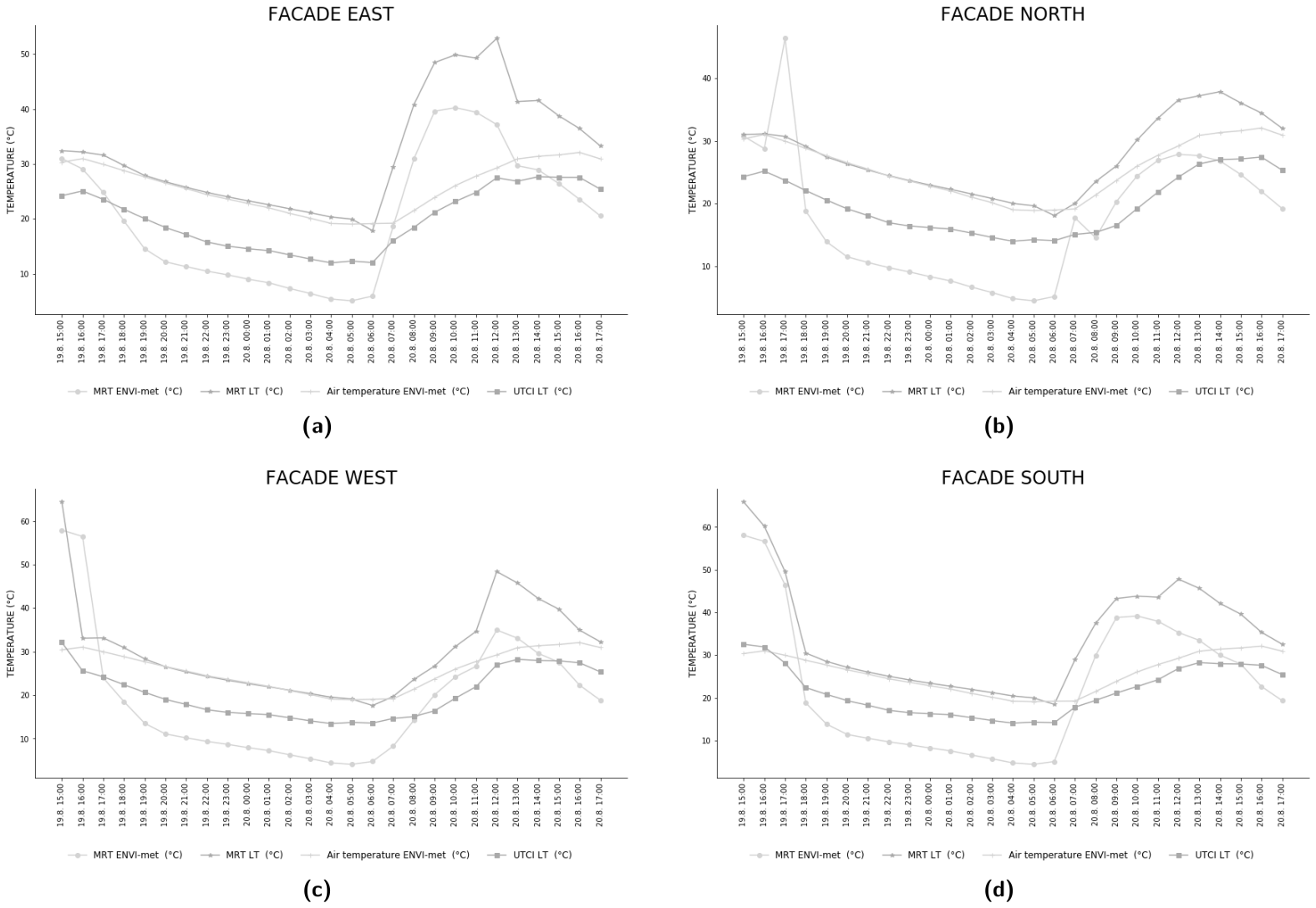

Figure A.7. Comparison of the MRT, UTCI and Air Temperature simulated in ENVI-met and the Ladybug Tools (LT) of the different locations

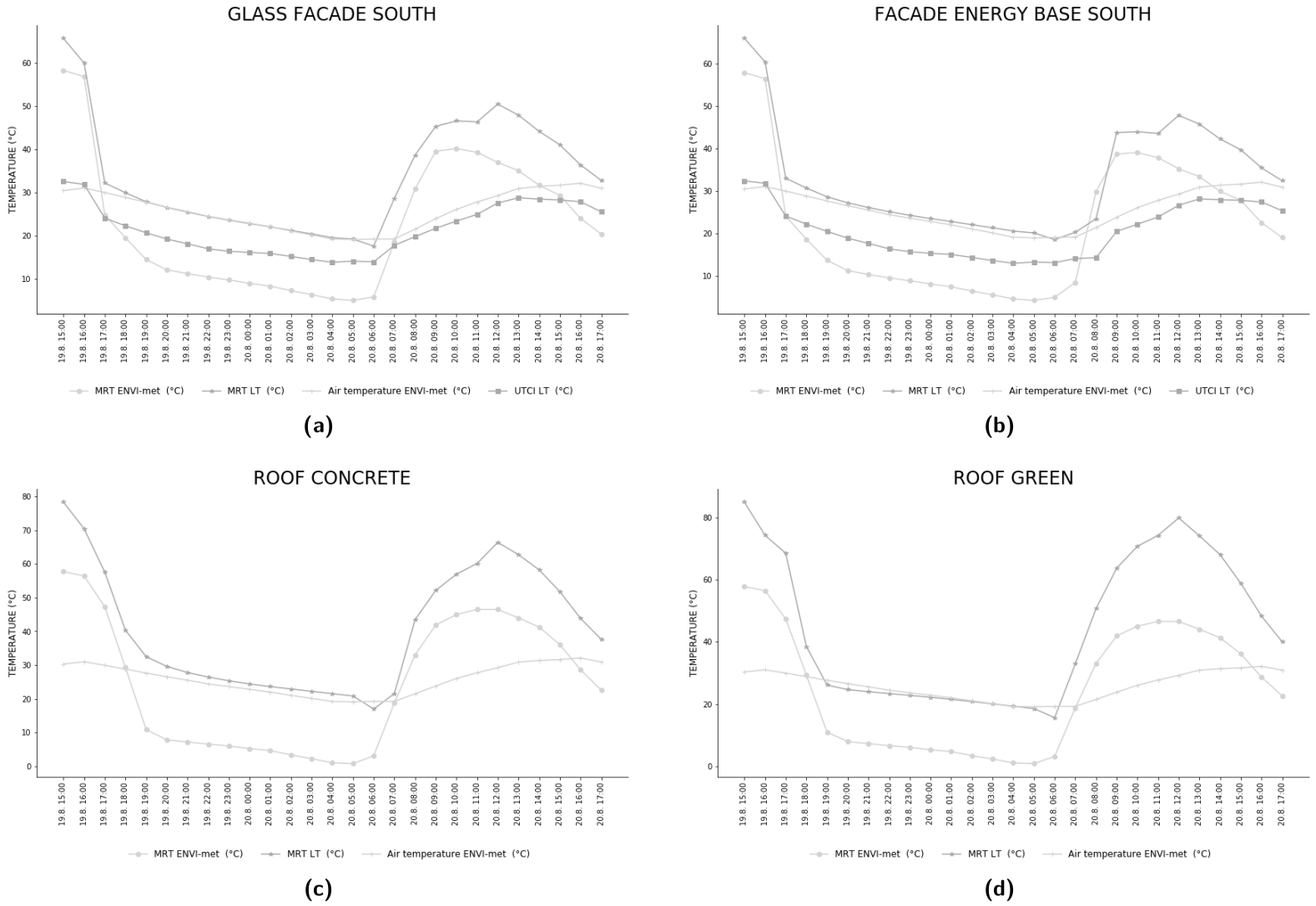

Figure A.8. Comparison of the MRT, UTCI and Air Temperature simulated in ENVI-met and the Ladybug Tools (LT) of the different locations

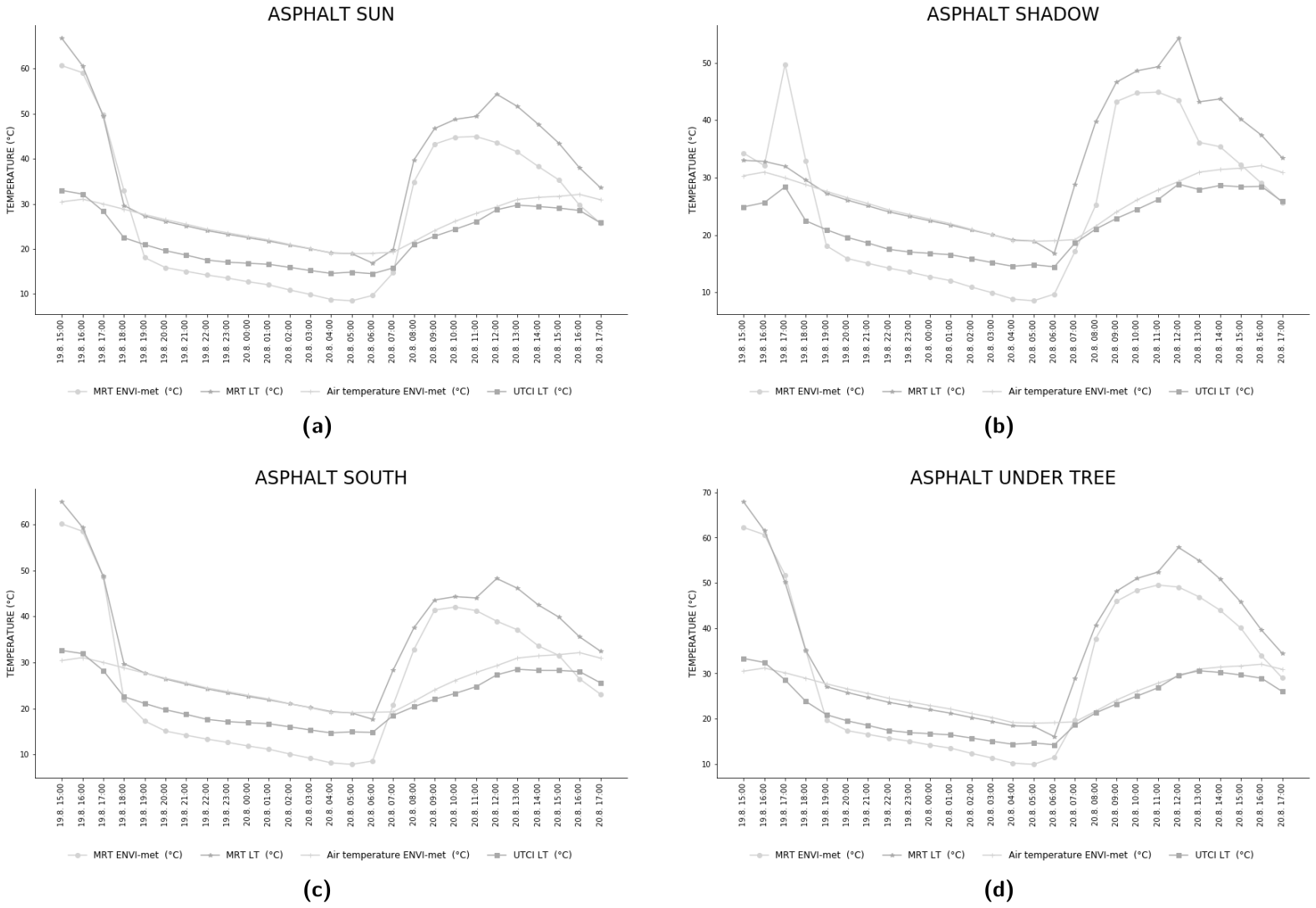

Figure A.9. Comparison of the MRT, UTCI and Air Temperature simulated in ENVI-met and the Ladybug Tools (LT) of the different locations

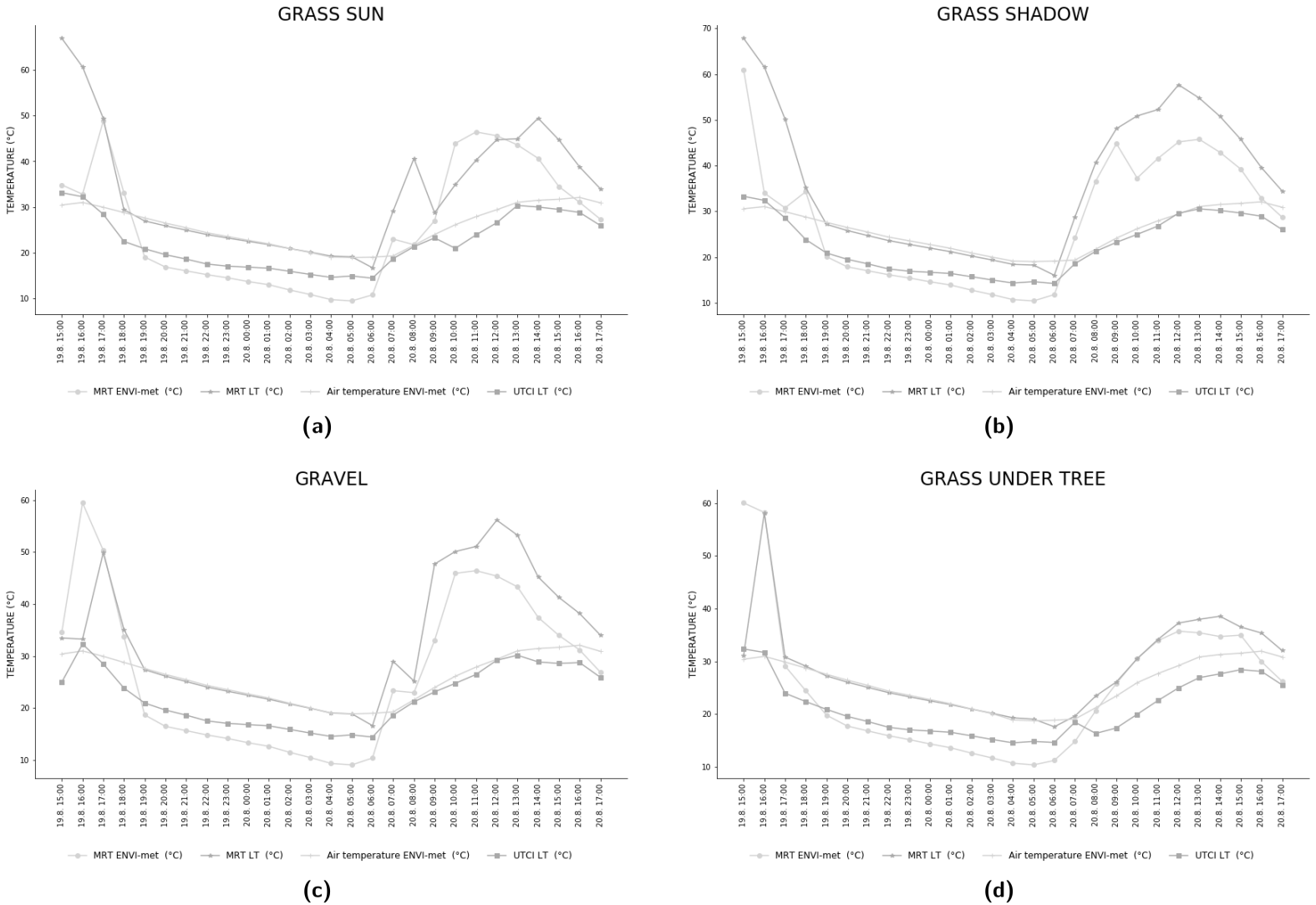

Figure A.10. Comparison of the MRT, UTCI and Air Temperature simulated in ENVI-met and the Ladybug Tools (LT) of the different locations

B. Grasshopper Scripts

Pictures of the grasshopper scripts can be found in the following appendix.

The following scripts are listed:

- General script for sensitivity analysis (1)
- Script for the case study (2)
- Script for the difference maps (3)

For the sake of clarity, only one Grasshopper script for the sensitivity analysis, in which the simulation steps are explained in general terms, has been included in the appendix. The experiments in the sensitivity analysis were always created with the same geometry and the same weather file. The different wall materials, simulation days or the different types of green buildings were integrated in this file.

The script for creating the difference maps was kindly provided by DI Dr. techn Milena Vuckovic.

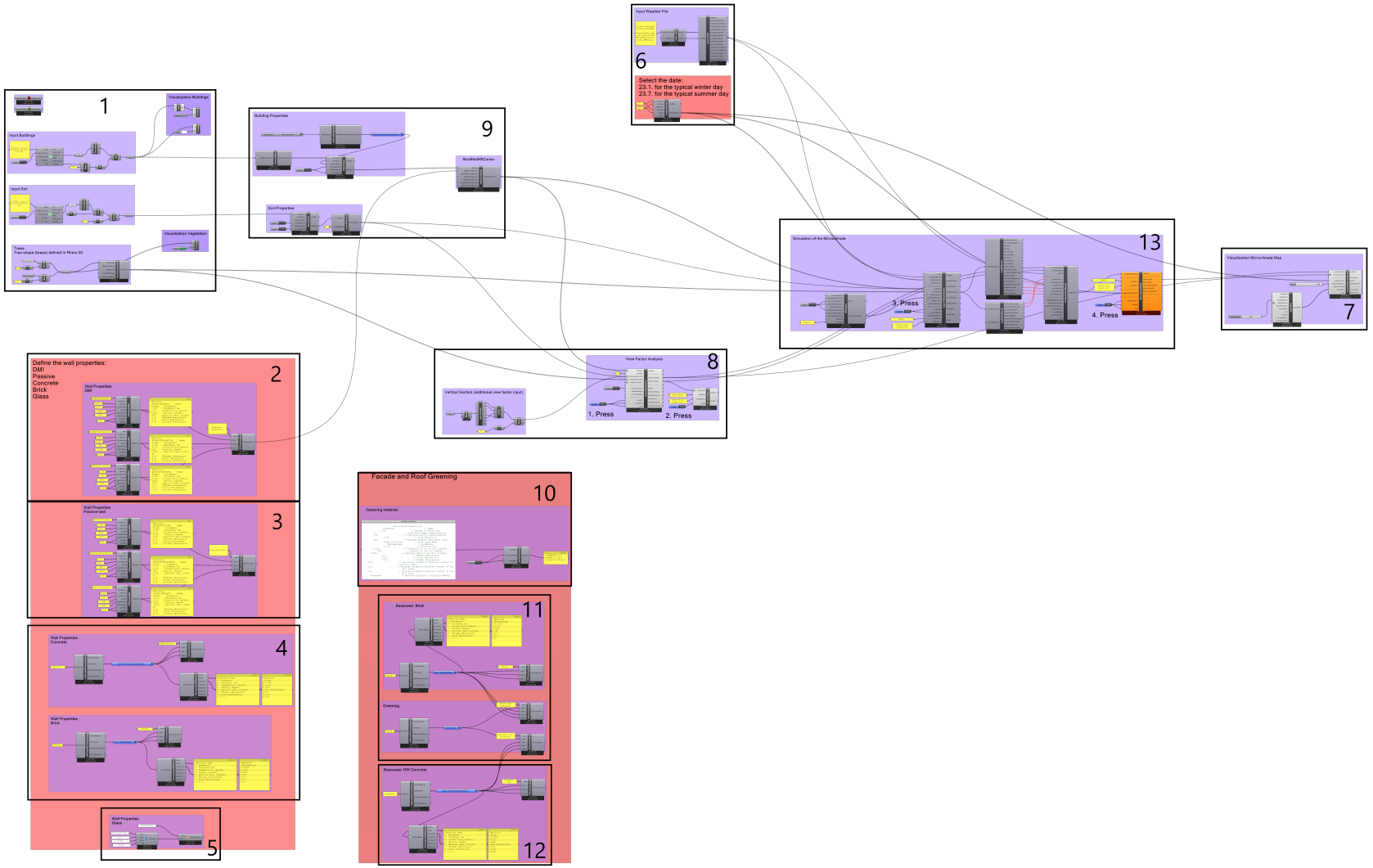

Figure B.1. Grasshopper script for sensitivity analysis

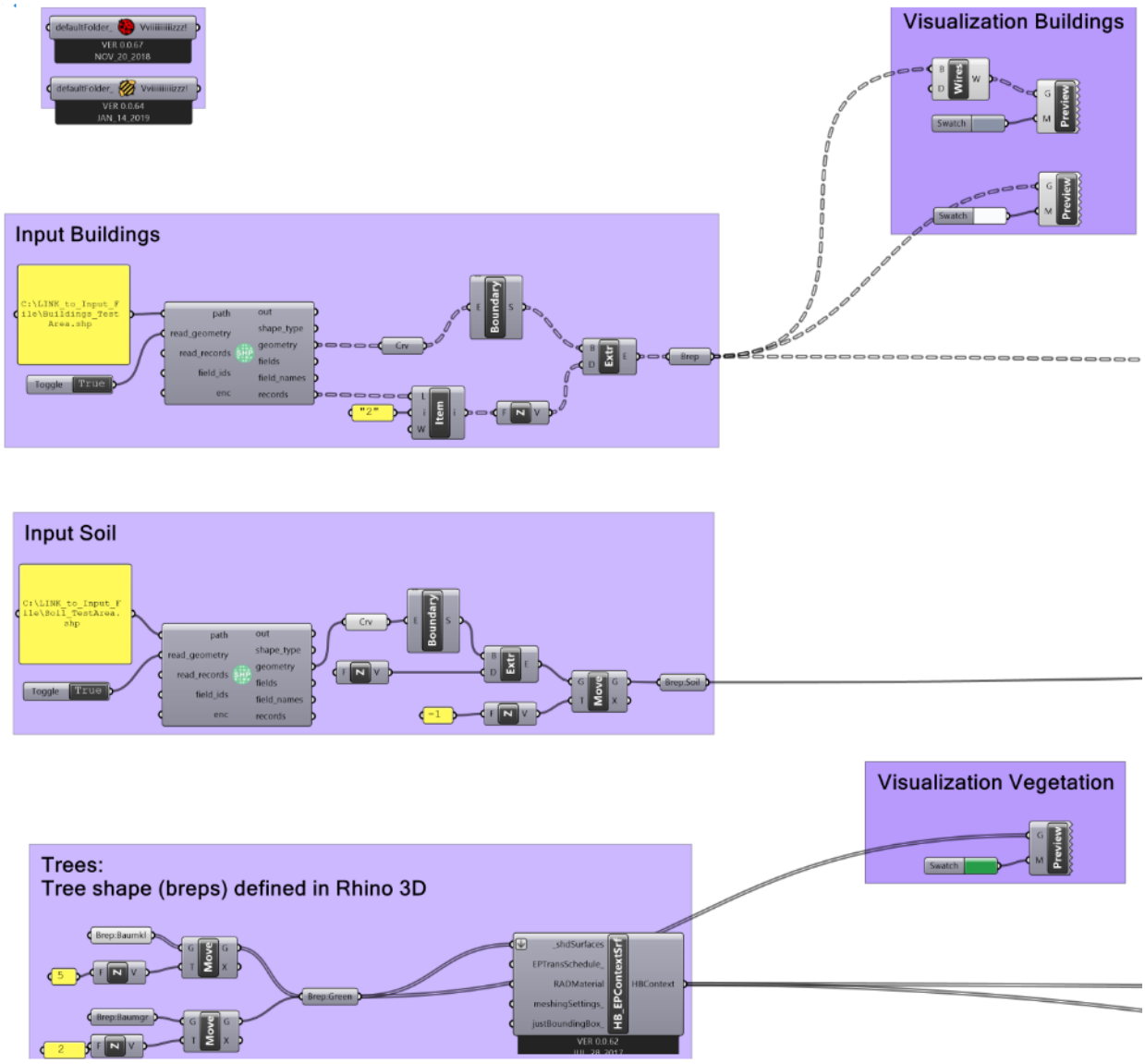

Figure B.2. Grasshopper script for sensitivity analysis - 1

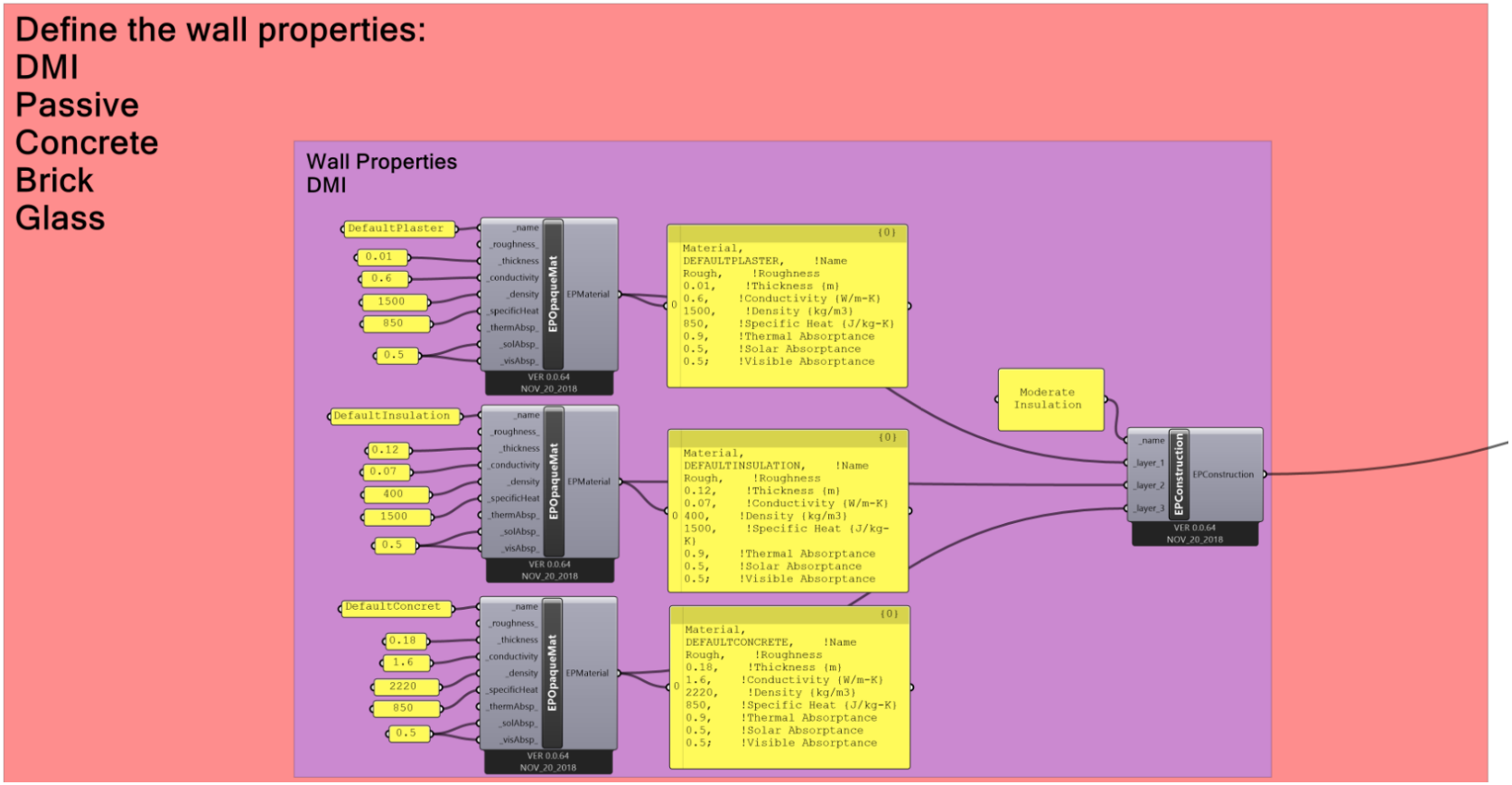

Figure B.3. Grasshopper script for sensitivity analysis - 2

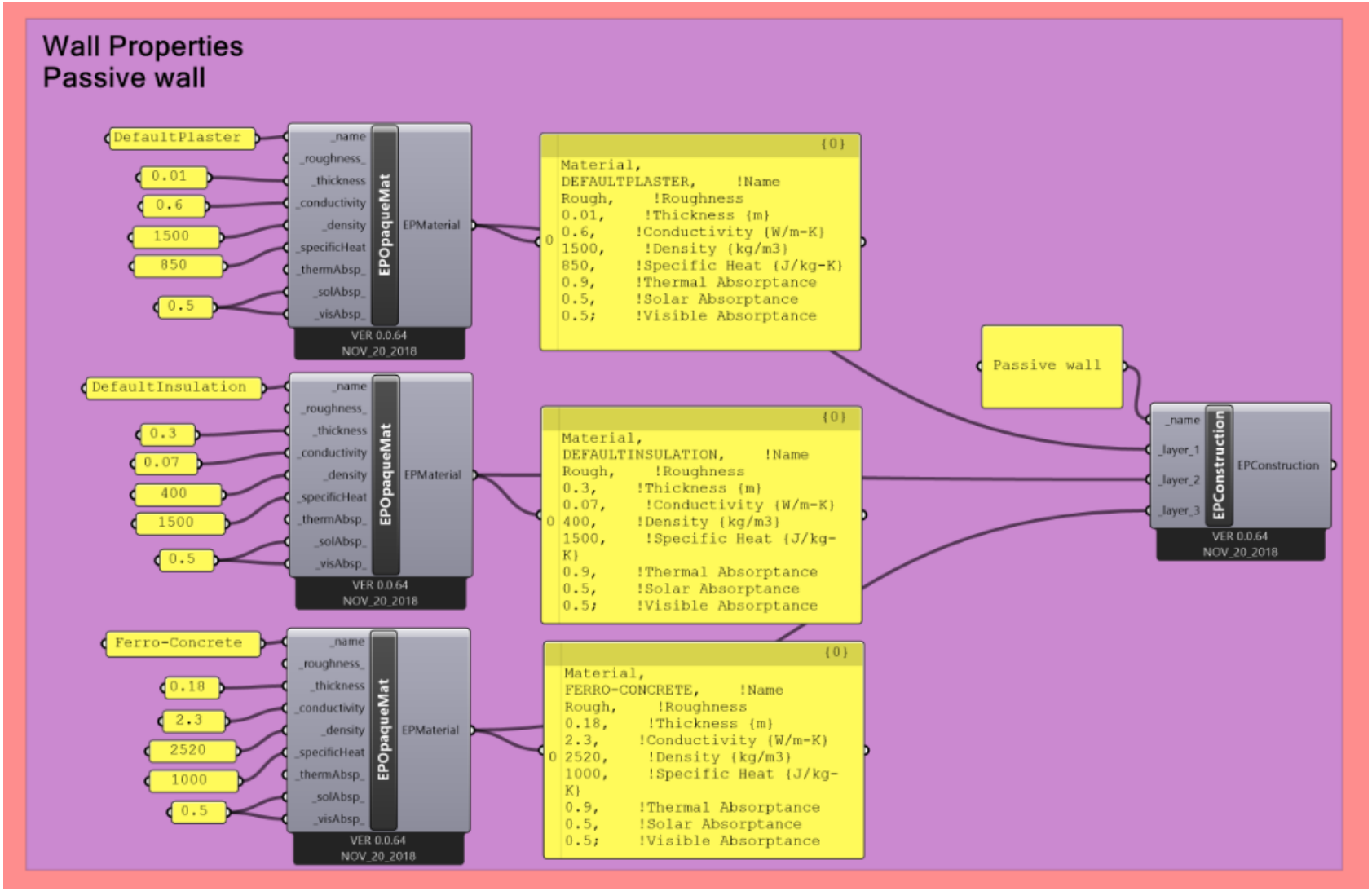

Figure B.4. Grasshopper script for sensitivity analysis - 3

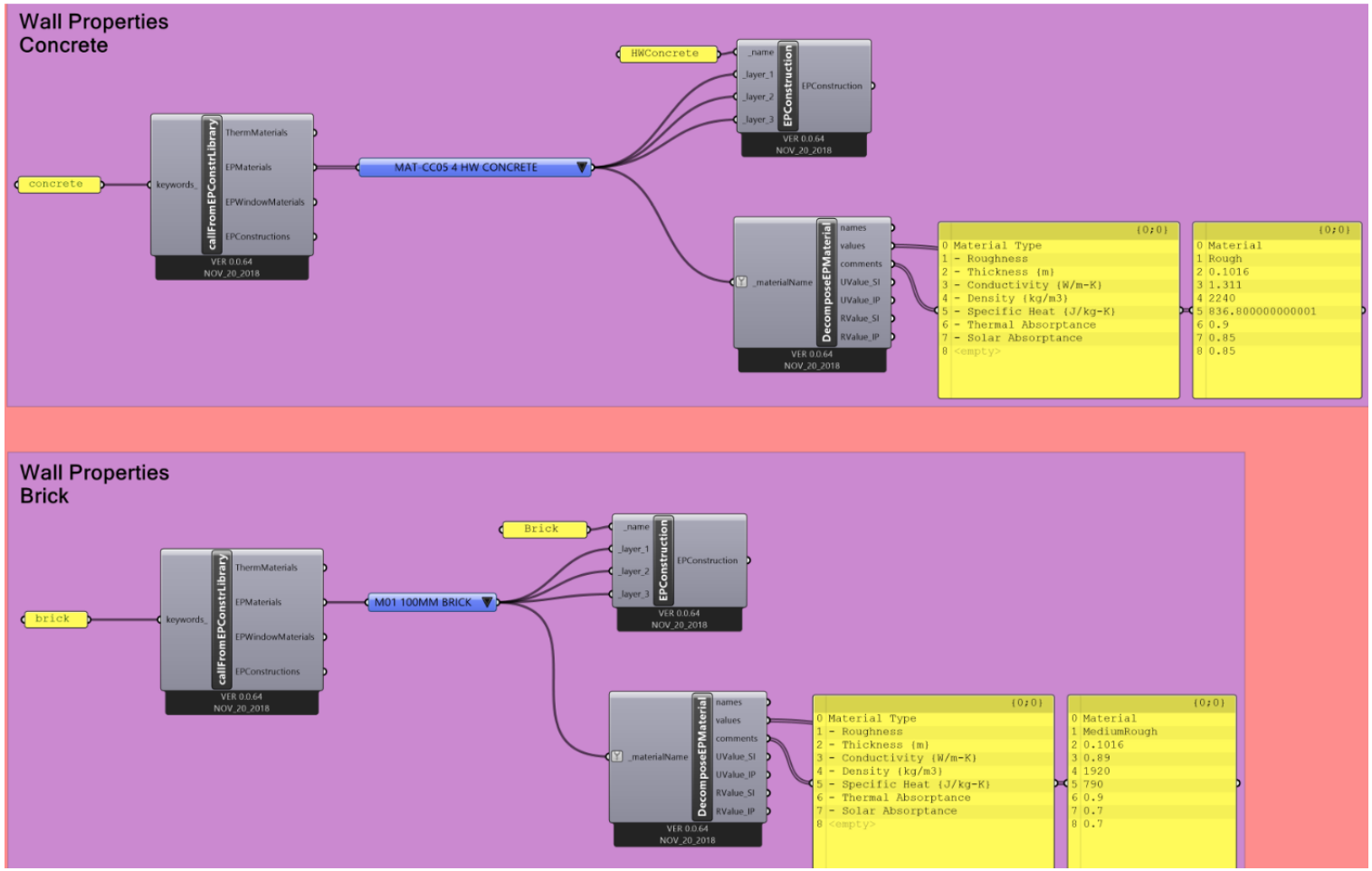

Figure B.5. Grasshopper script for sensitivity analysis - 4

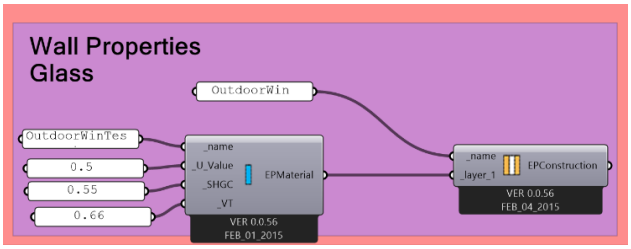

(a)

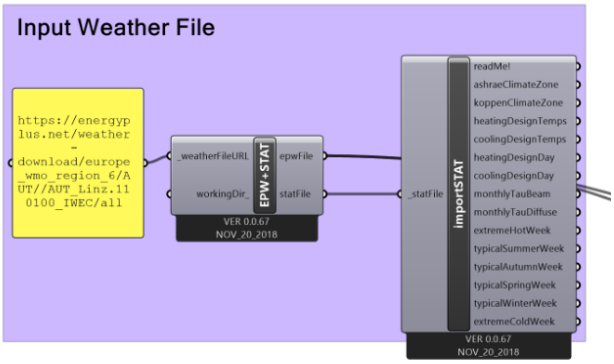

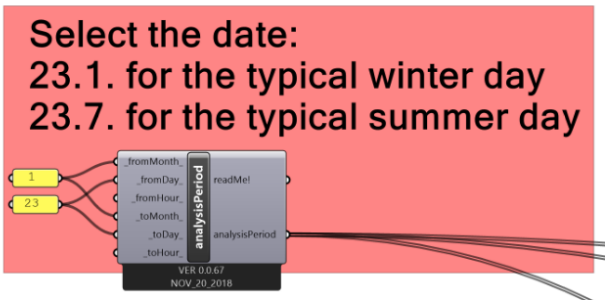

(b)

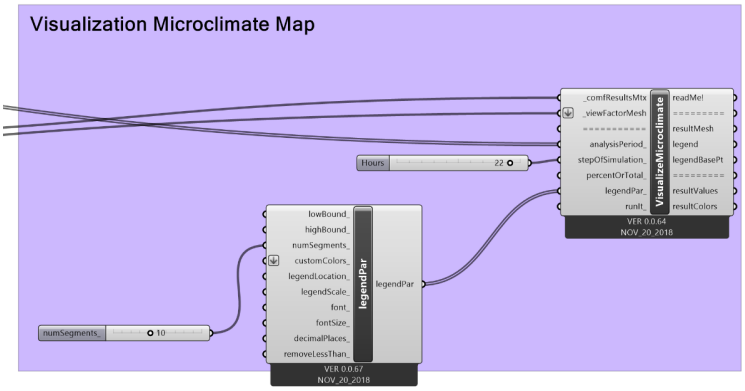

(c)

Figure B.6. Grasshopper script for sensitivity analysis - 5 (a), 6 (b), 7 (c)

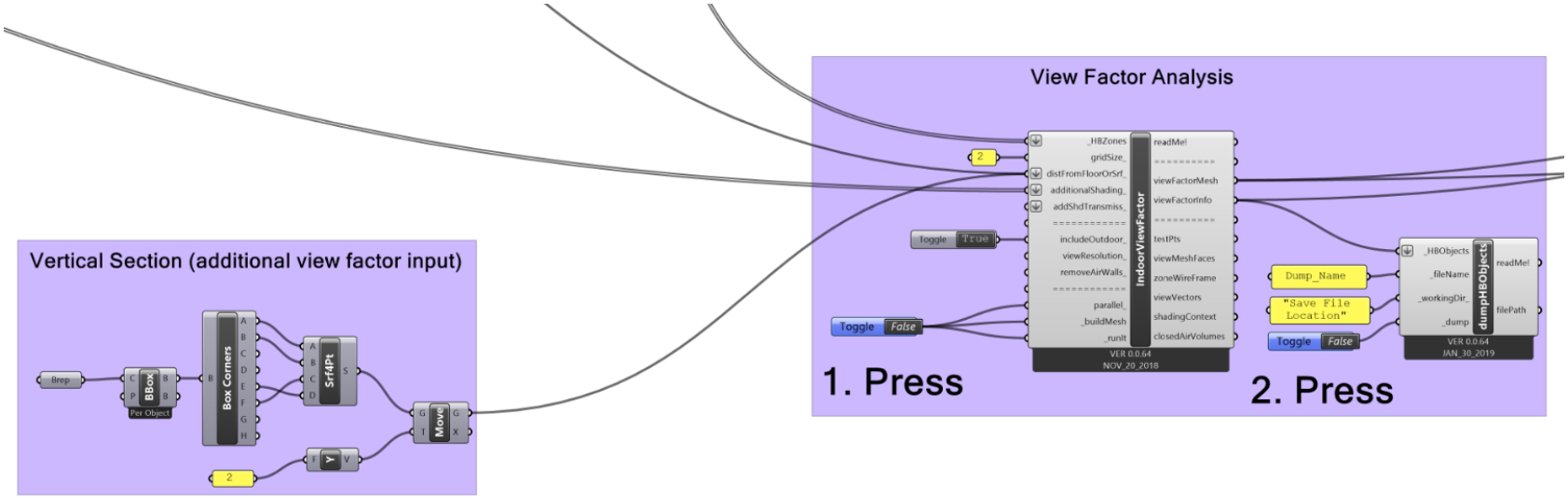

Figure B.7. Grasshopper script for sensitivity analysis - 8

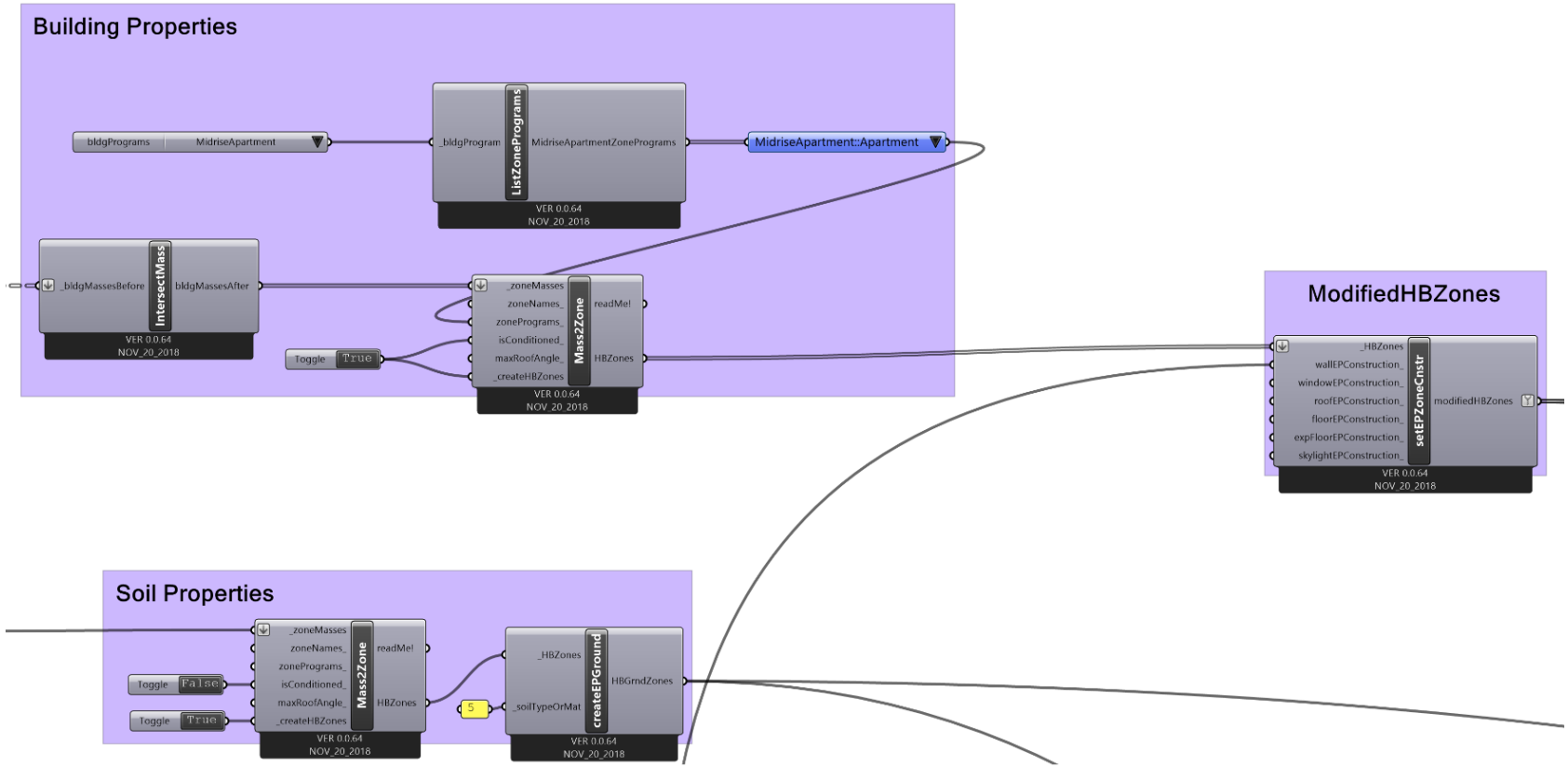

Figure B.8. Grasshopper script for sensitivity analysis - 9

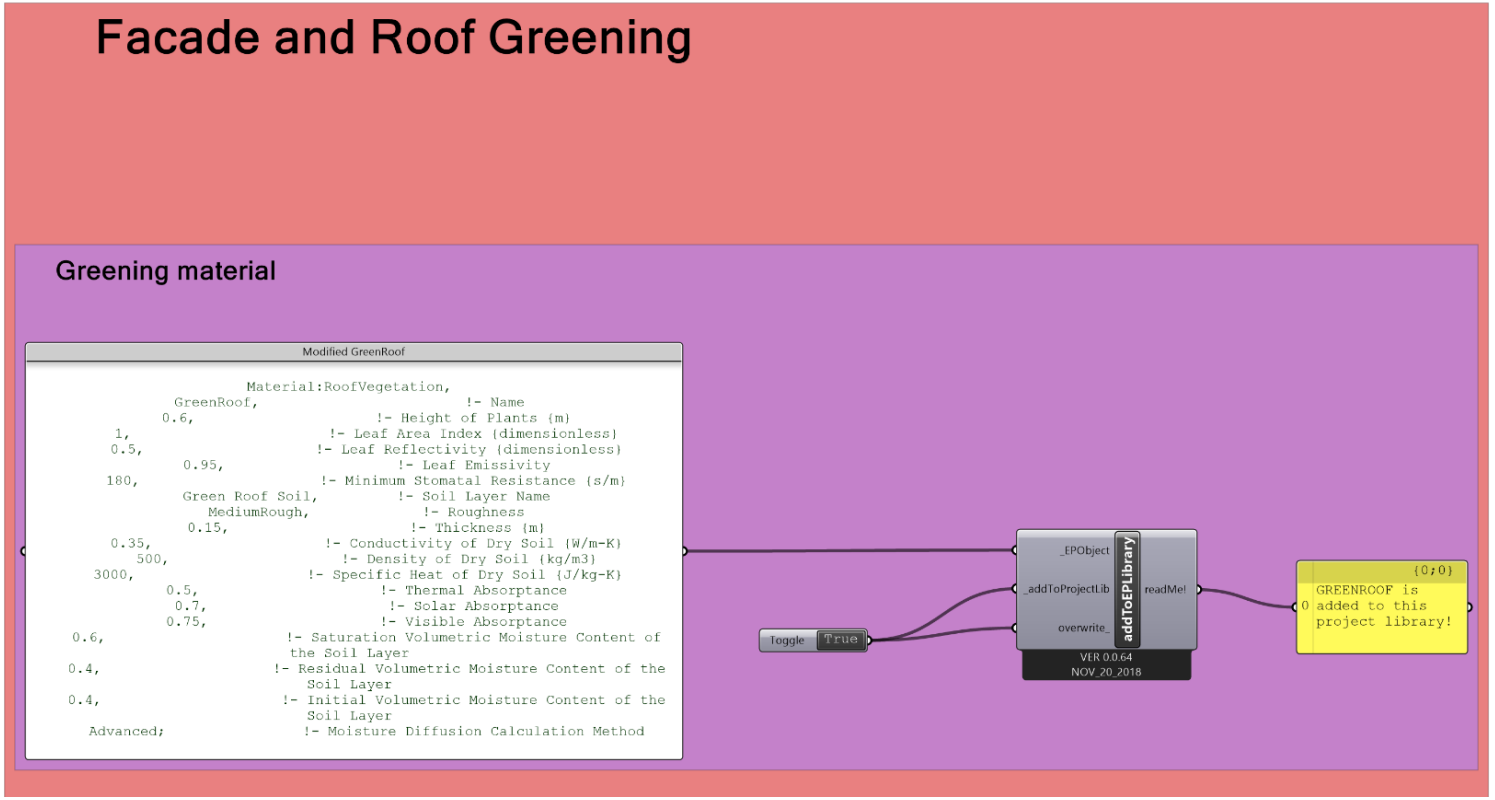

Figure B.9. Grasshopper script for sensitivity analysis - 10

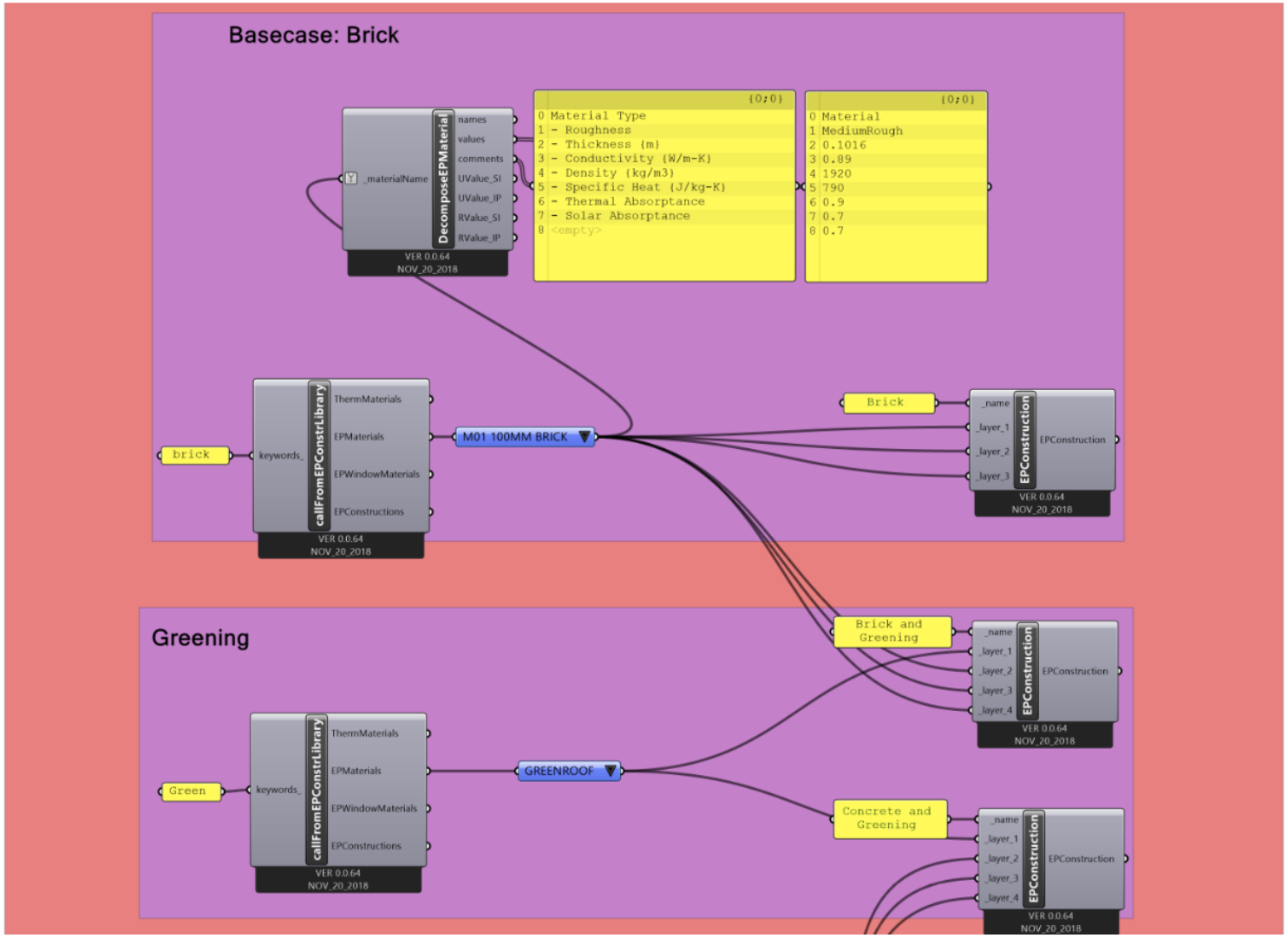

Figure B.10. Grasshopper script for sensitivity analysis - 11

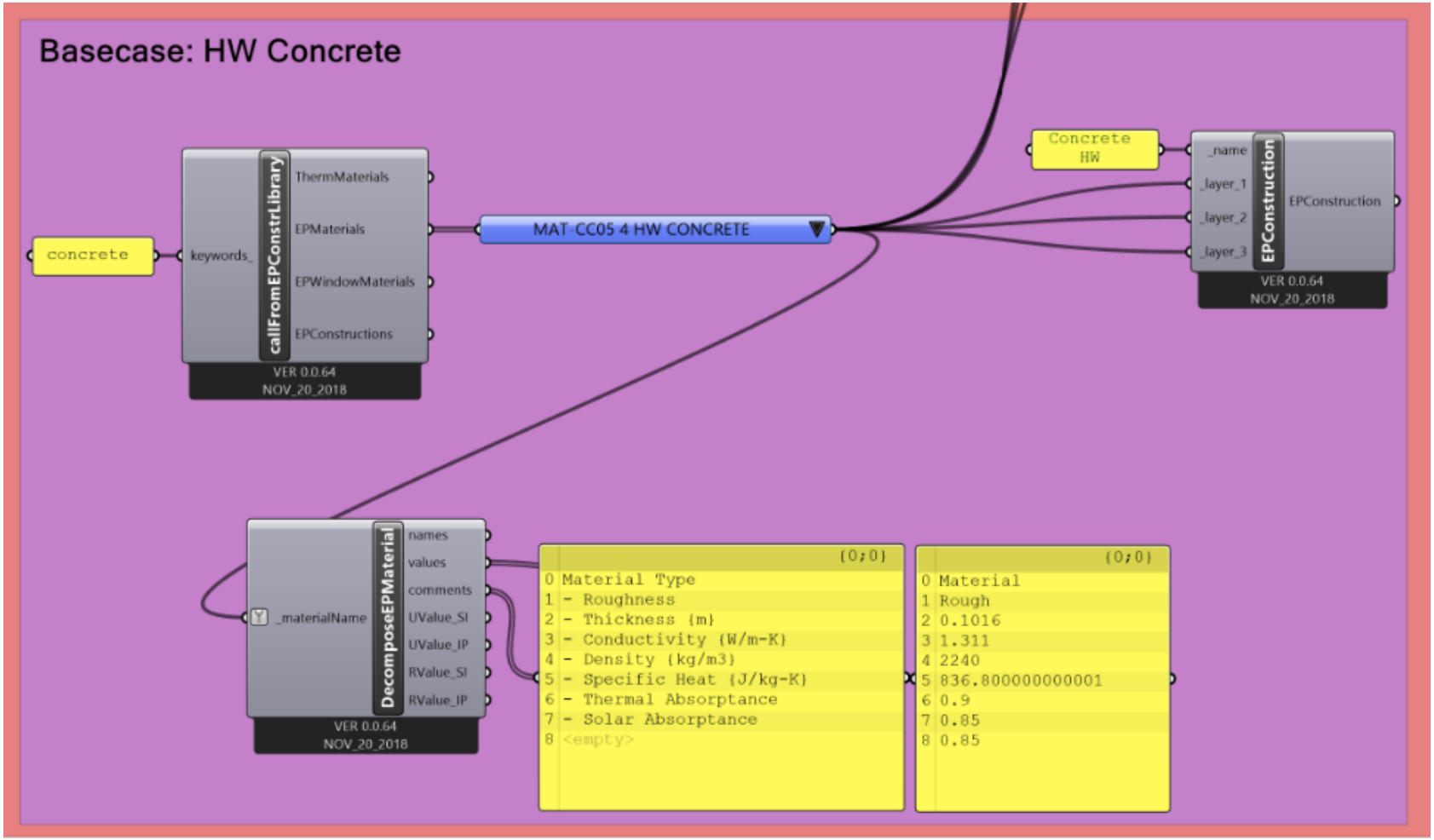

Figure B.11. Grasshopper script for sensitivity analysis - 12

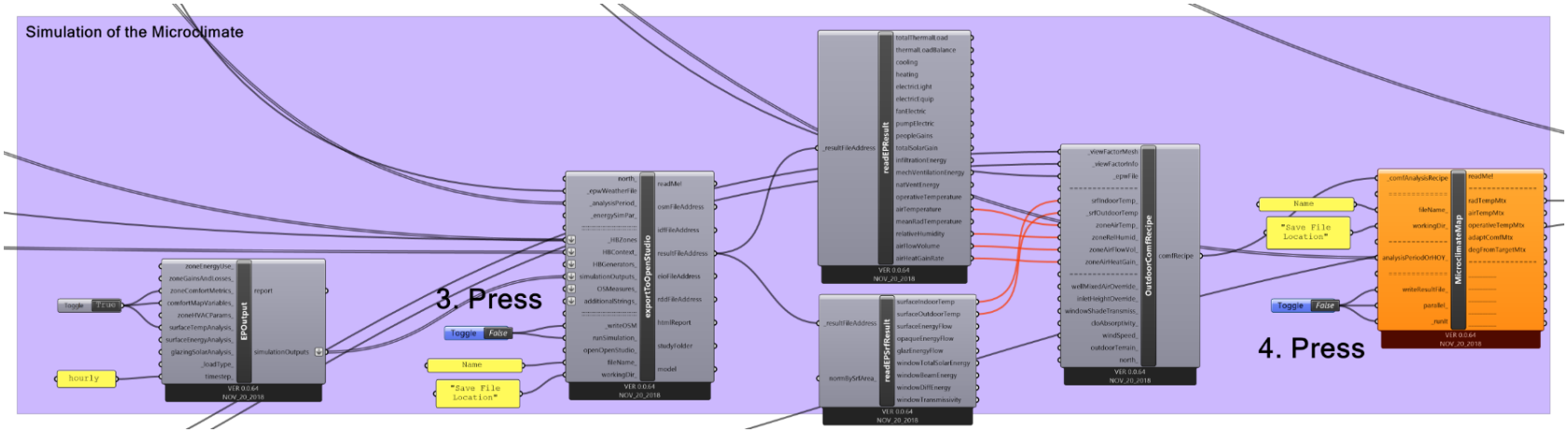

Figure B.12. Grasshopper script for sensitivity analysis - 13

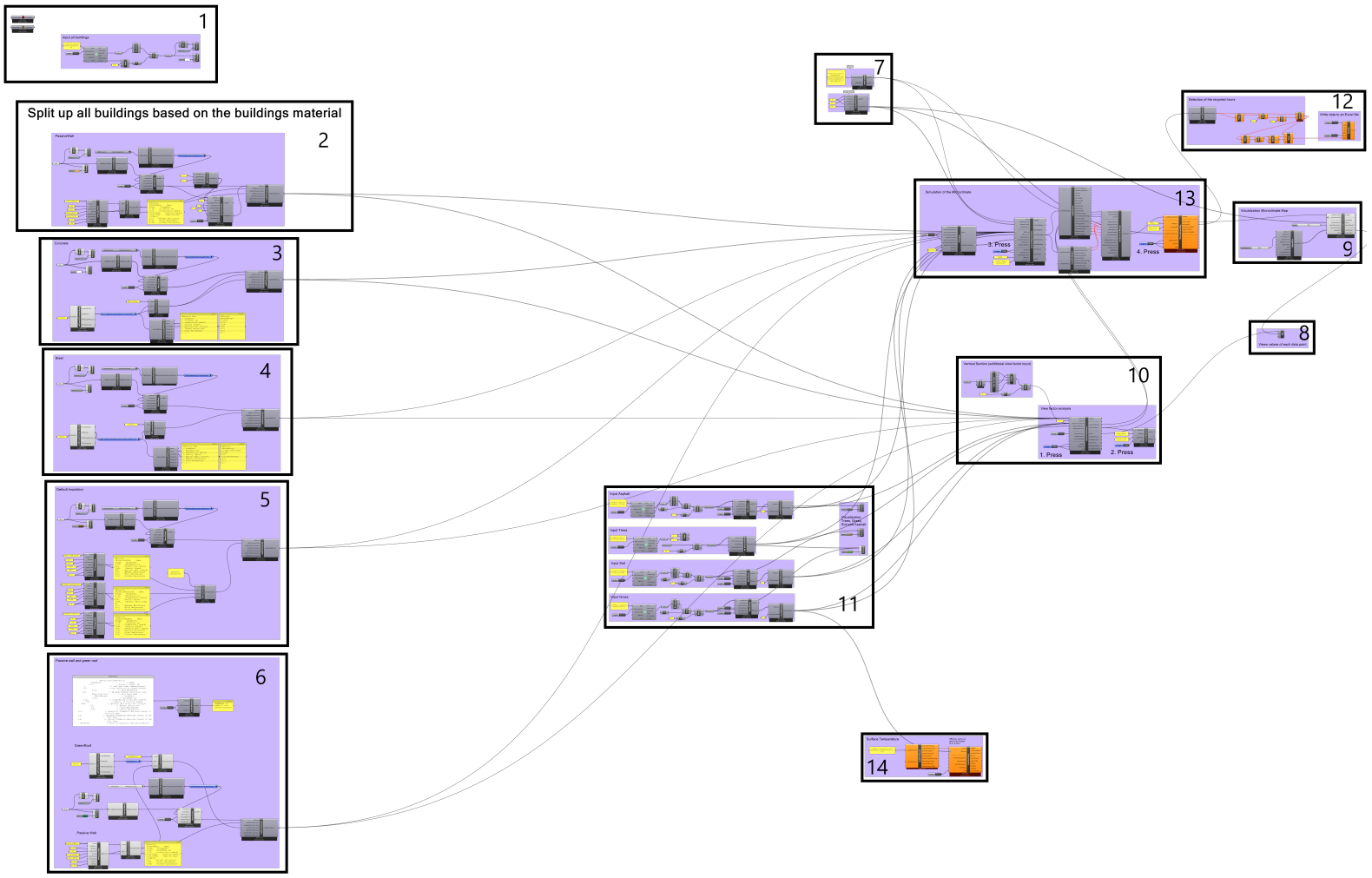

Figure B.13. Grasshopper script for the case study

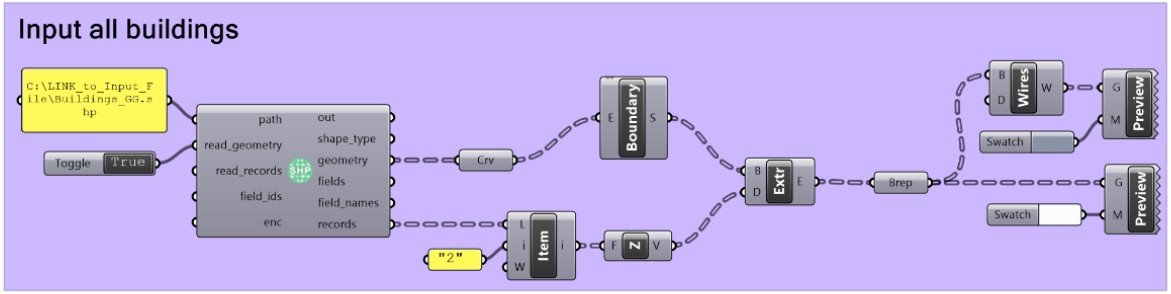

Figure B.14. Grasshopper script for the case study - 1

Split up all buildings based on the buildings material

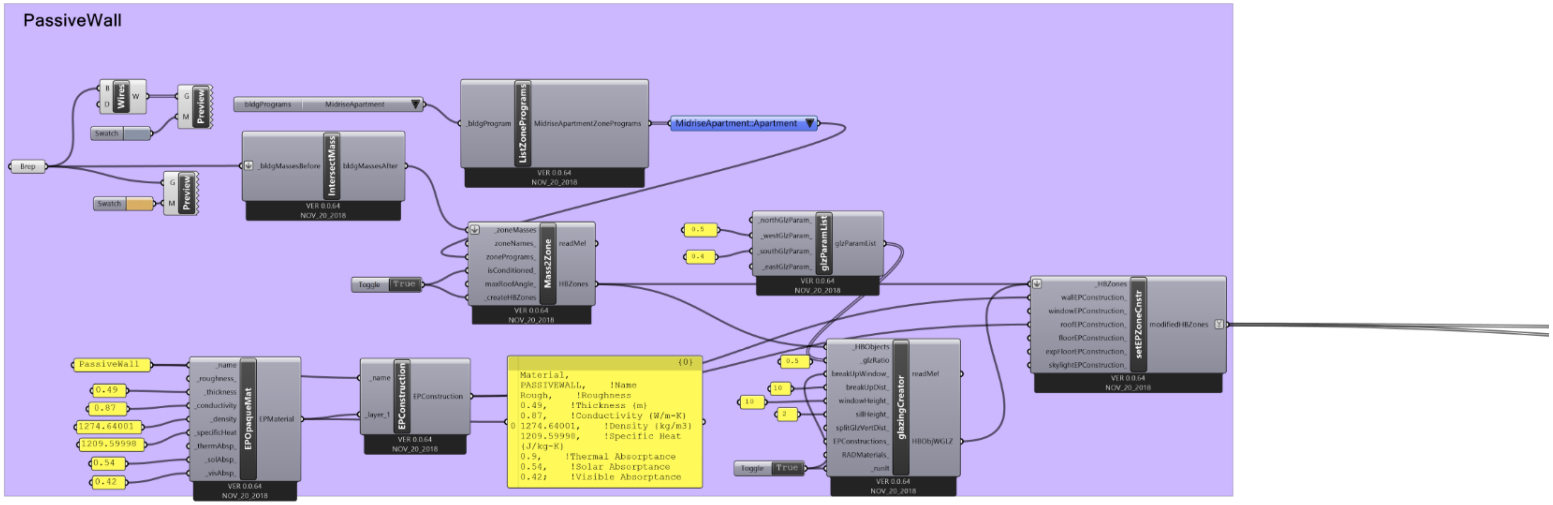

Figure B.15. Grasshopper script for the case study - 2

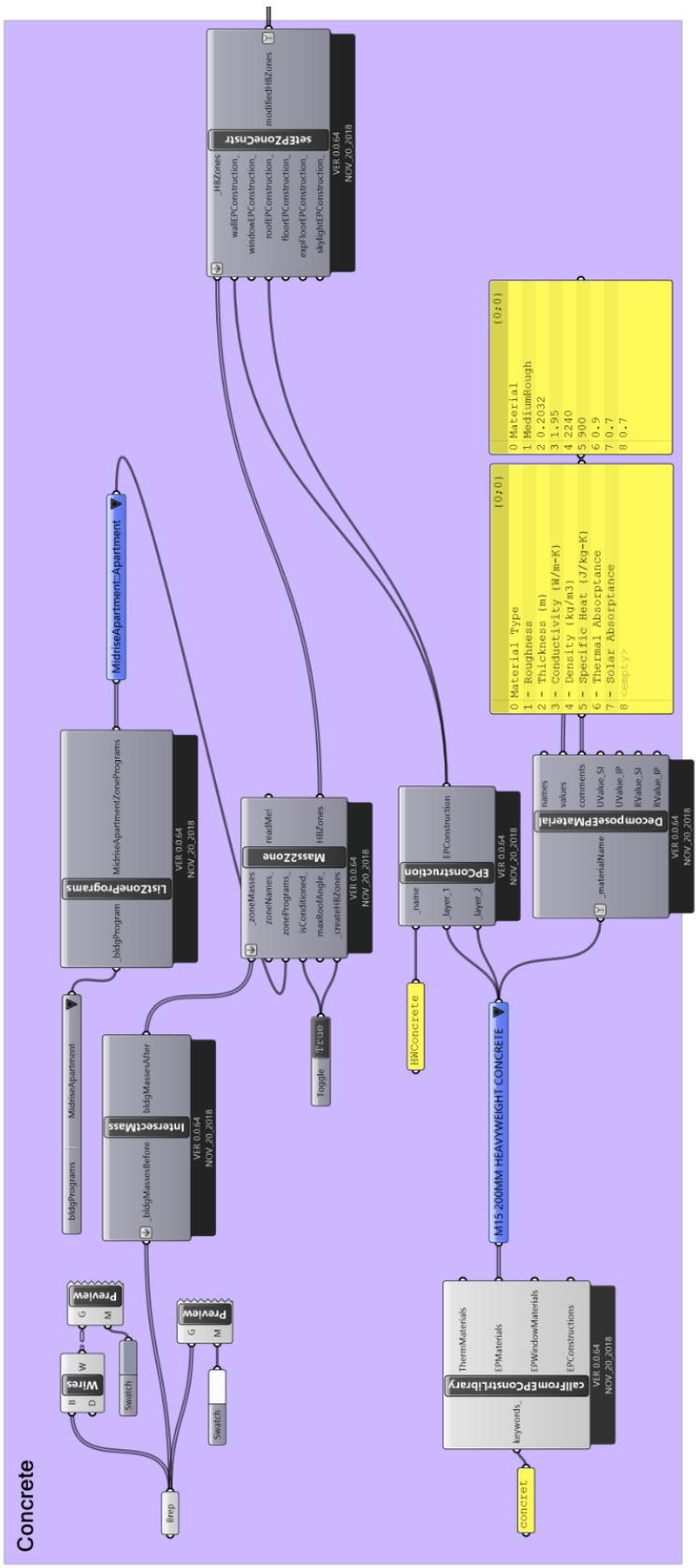

Figure B.16. Grasshopper script for the case study - 3

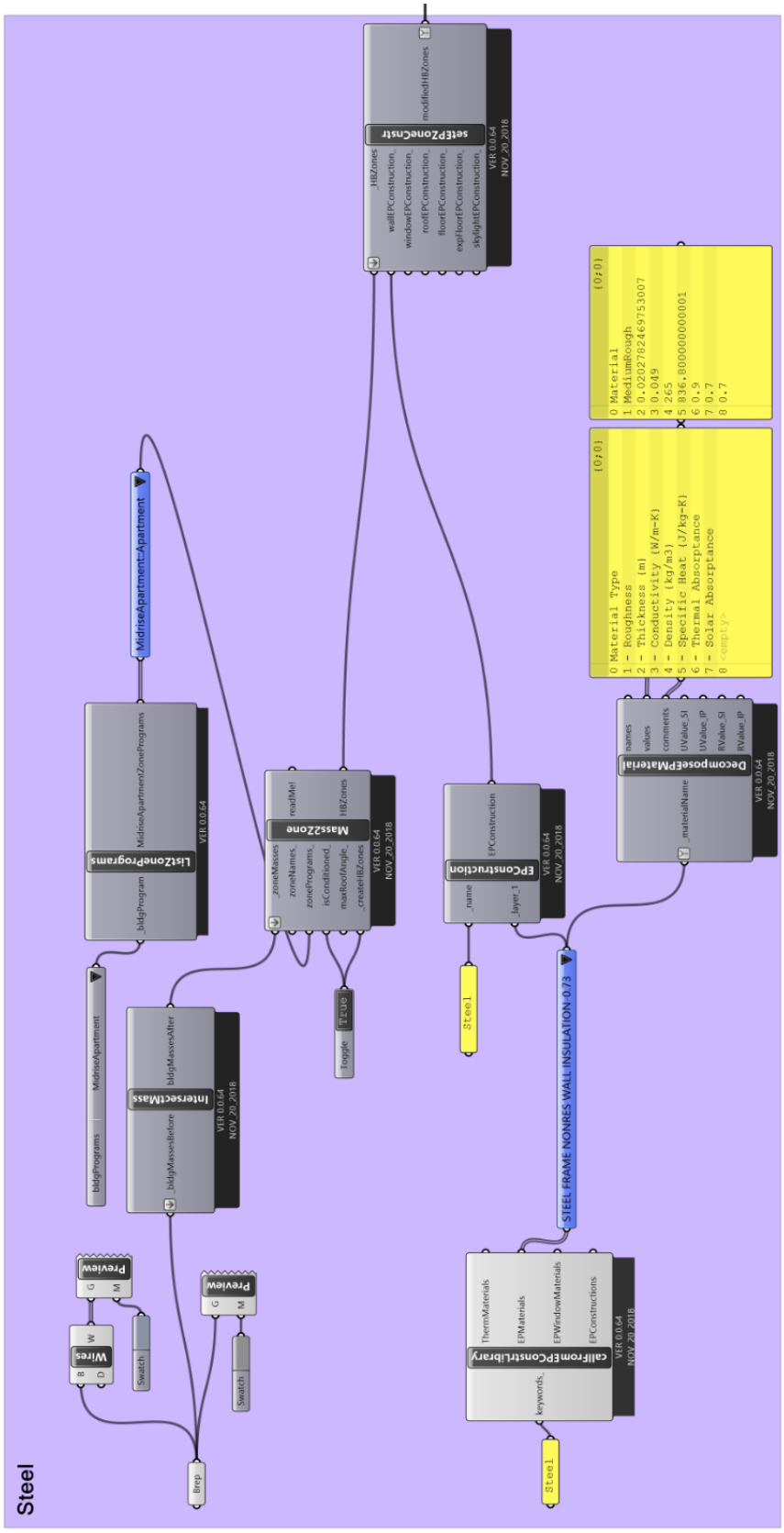

Figure B.17. Grasshopper script for the case study - 4

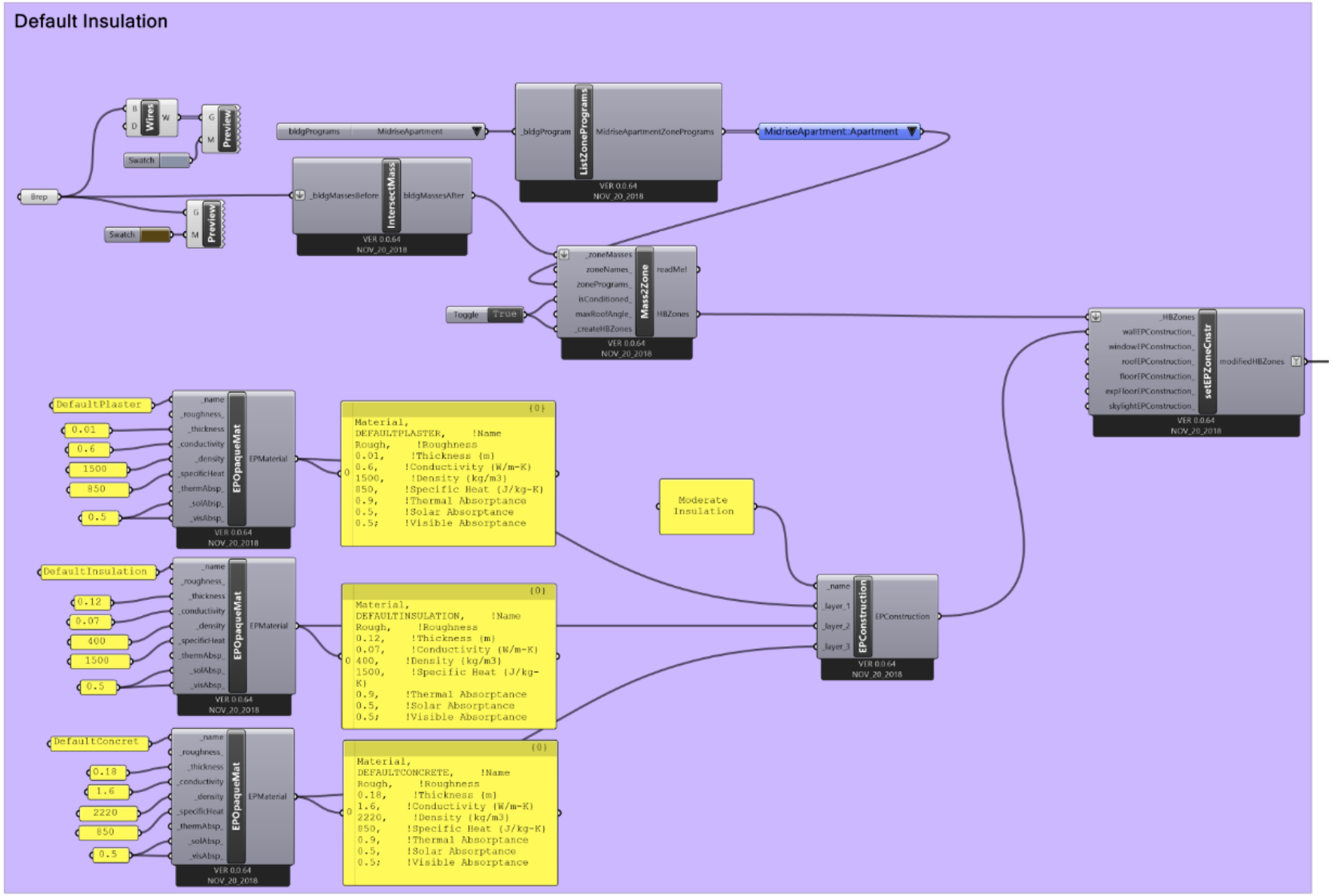

Figure B.18. Grasshopper script for the case study - 5

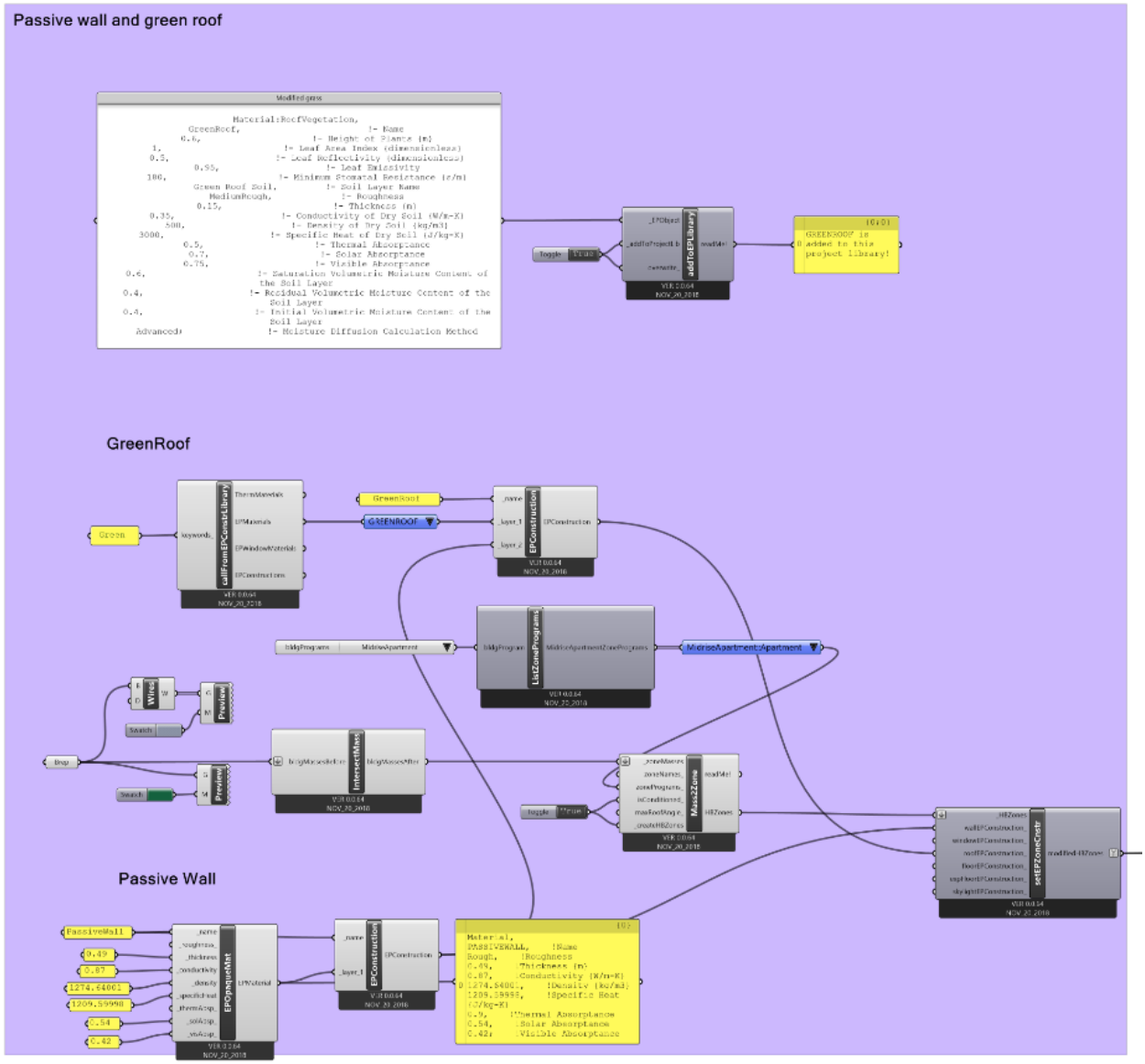

Figure B.19. Grasshopper script for the case study - 6

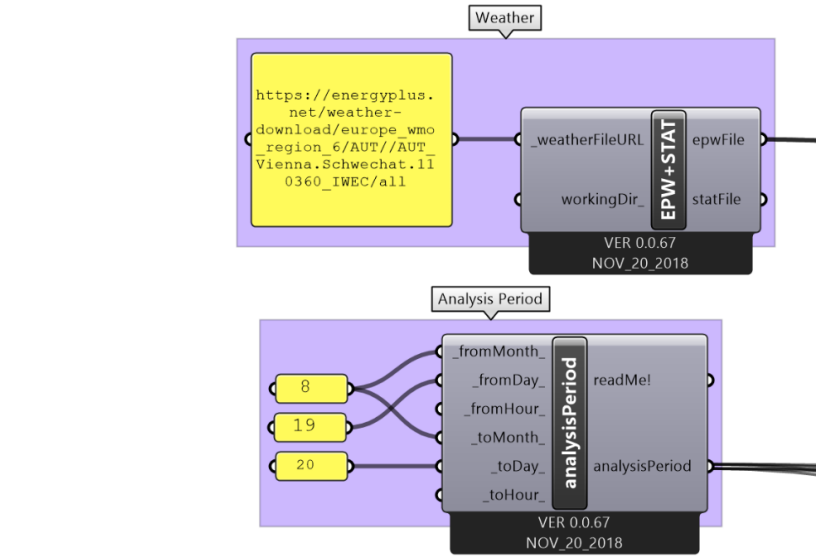

(a)

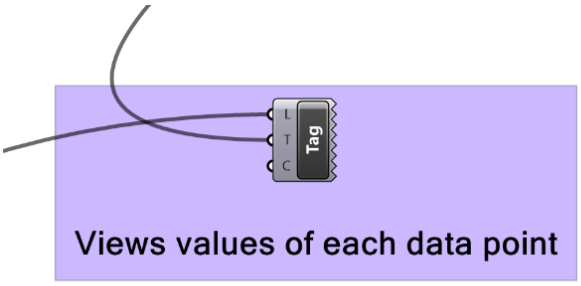

(b)

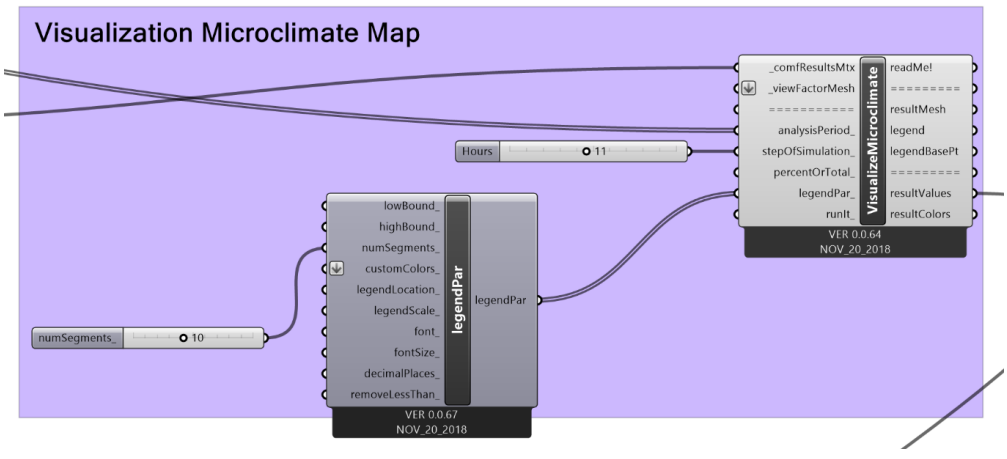

(c)

Figure B.20. Grasshopper script for the case study - 7 (a), 8 (b), 9 (c)

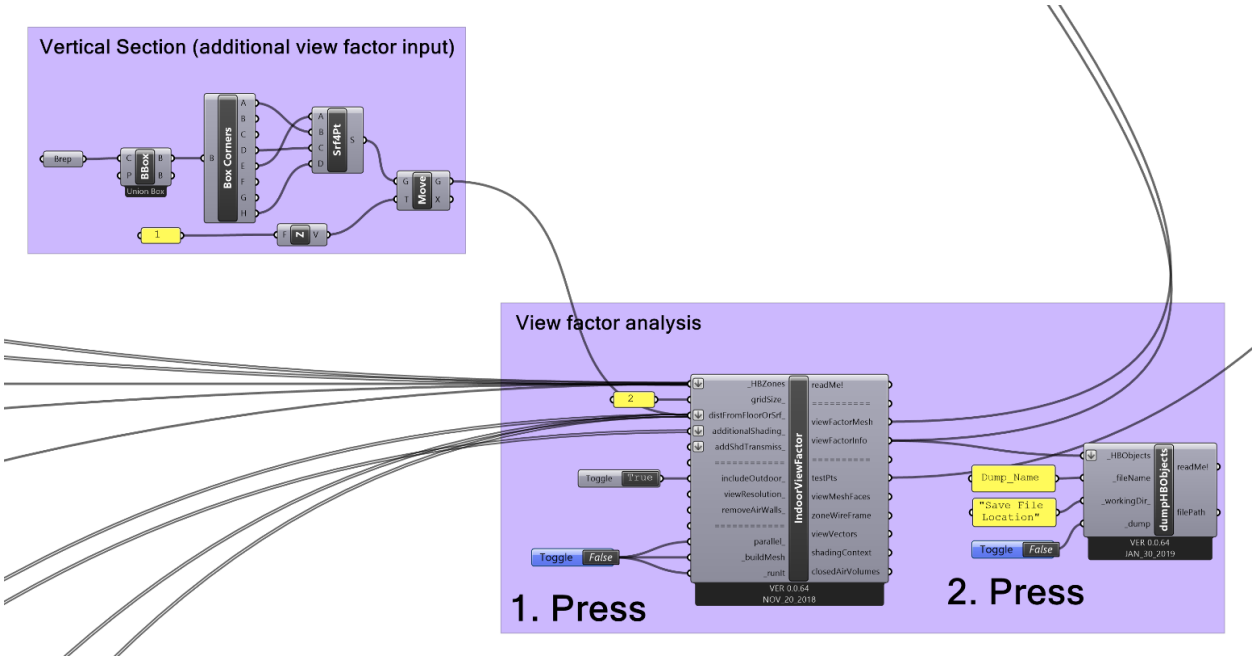

(a)

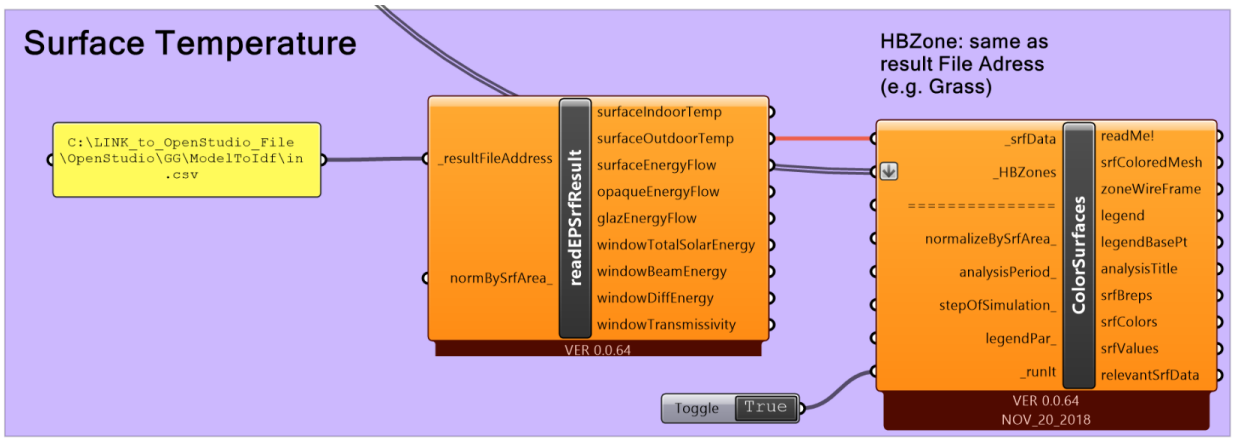

(b)

Figure B.21. Grasshopper script for the case study - 10 (a), 14 (b)

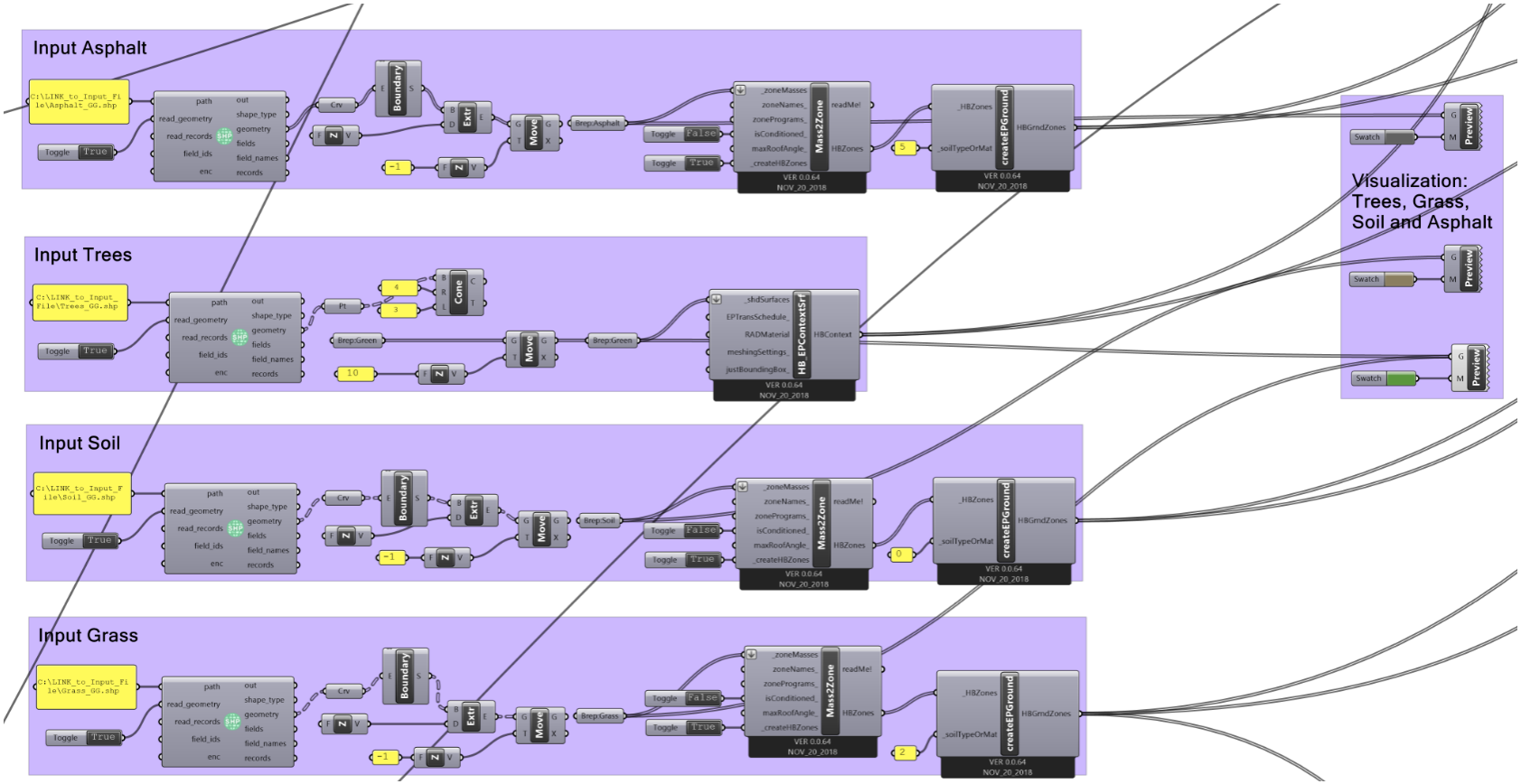

Figure B.22. Grasshopper script for the case study - 11

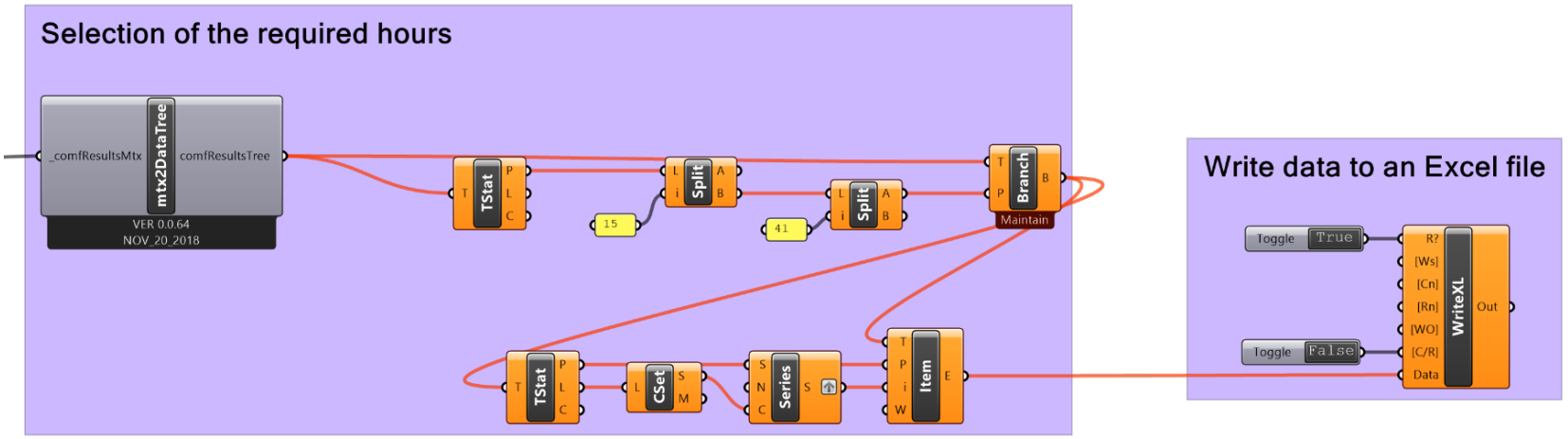

Figure B.23. Grasshopper script for the case study - 12

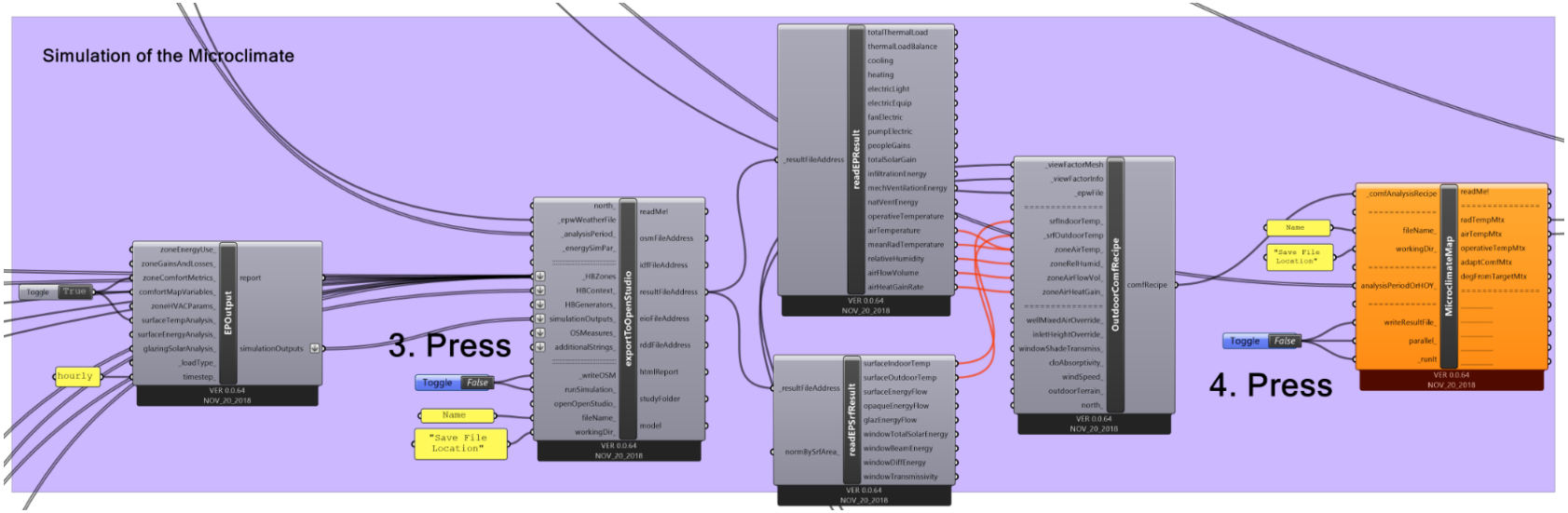

Figure B.24. Grasshopper script for the case study - 13

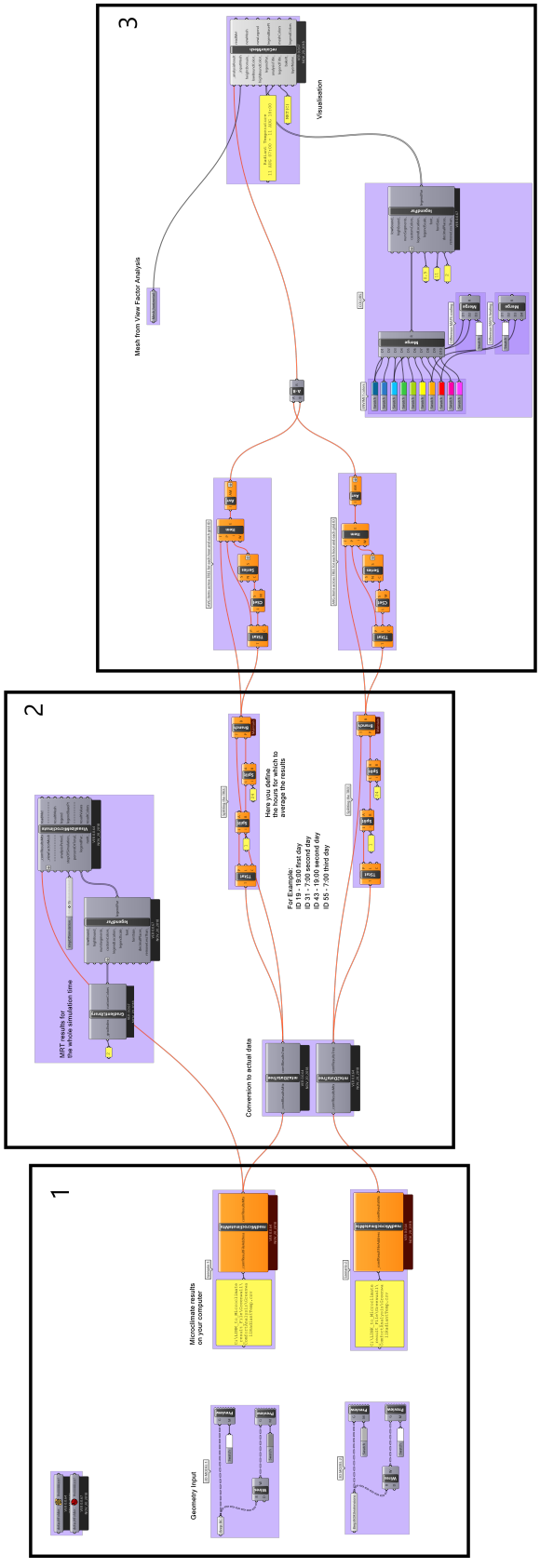

Figure B.25. Grasshopper script for the difference maps

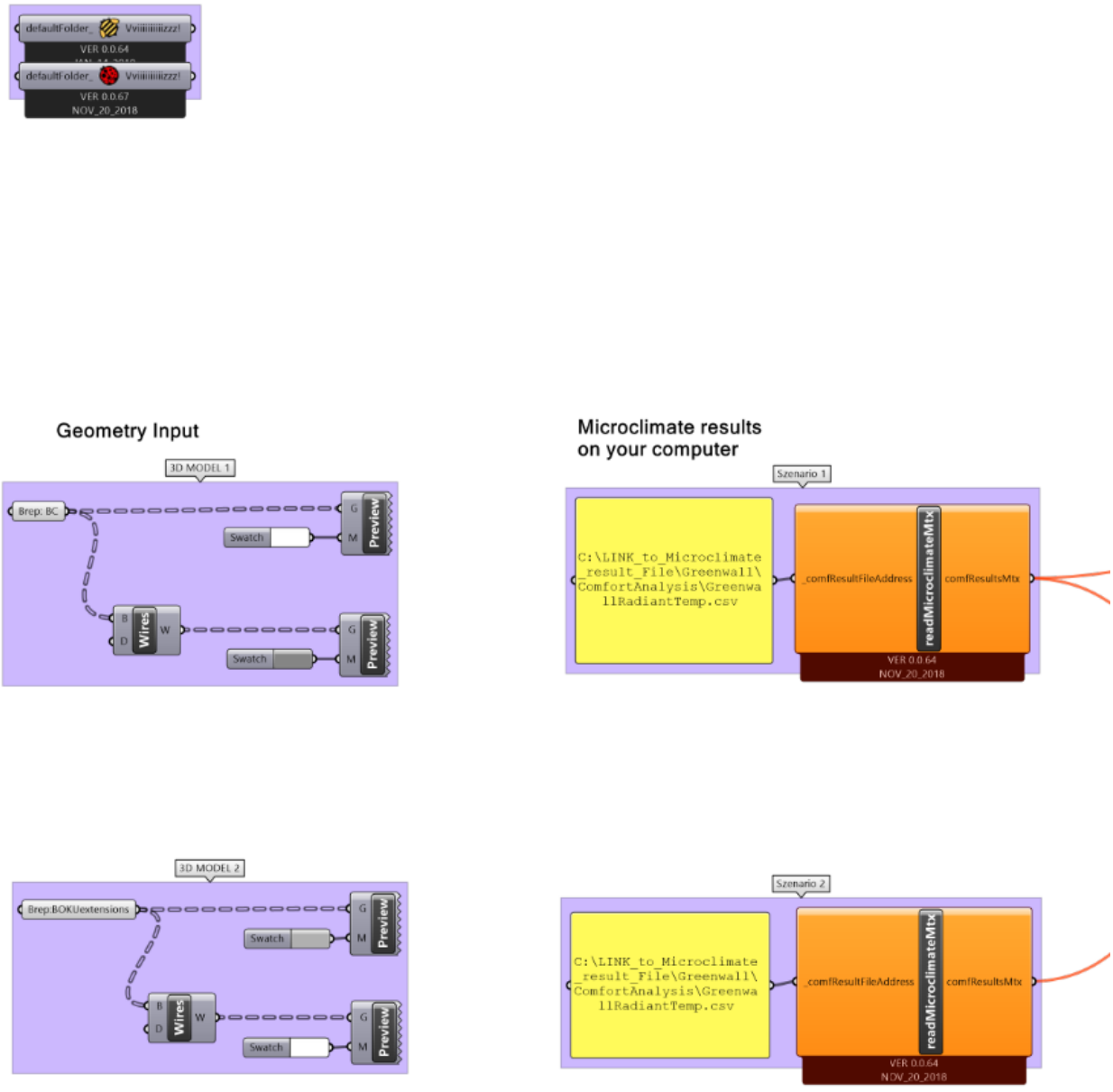

Figure B.26. Grasshopper script for the difference maps - 1

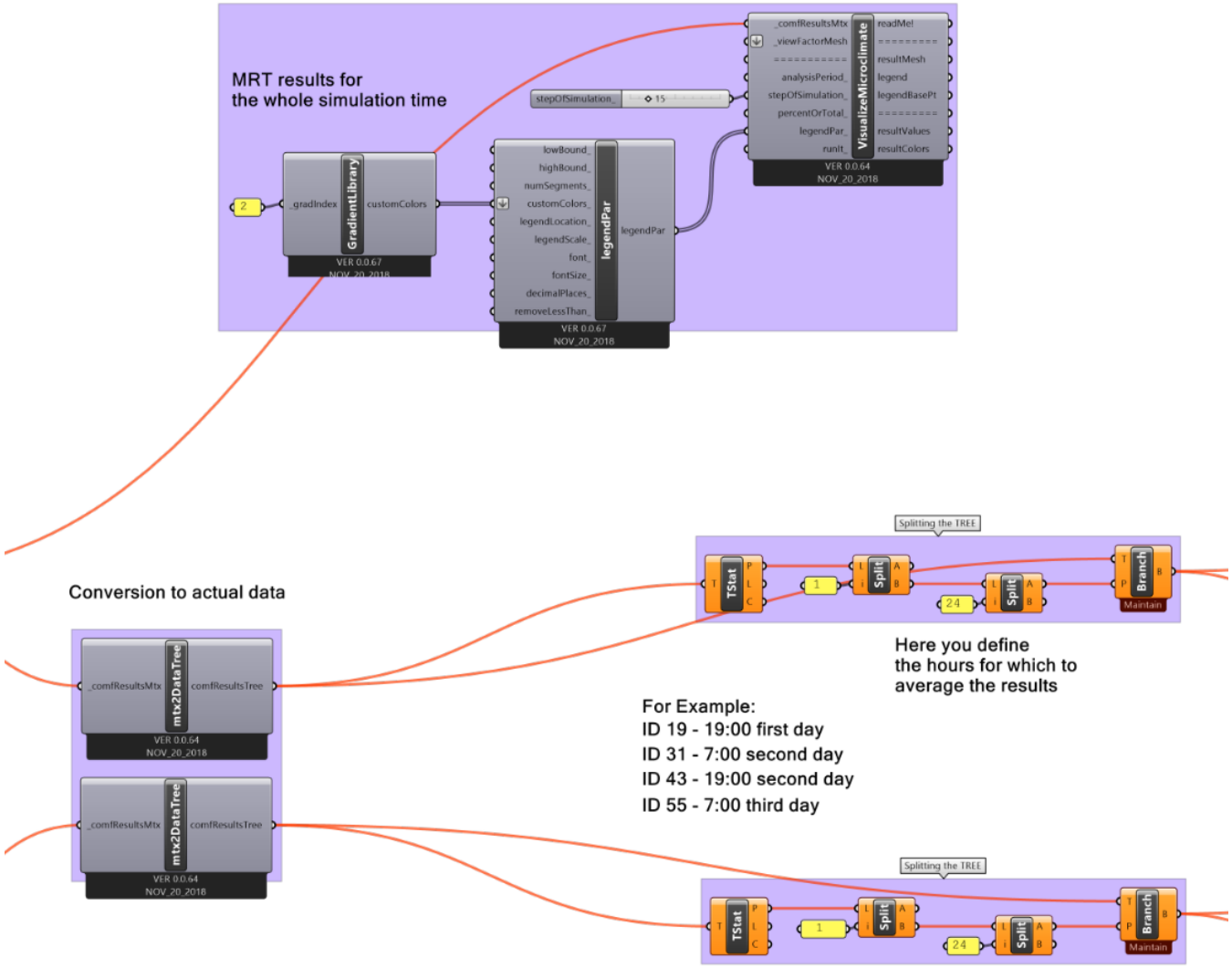

Figure B.27. Grasshopper script for the difference maps - 2

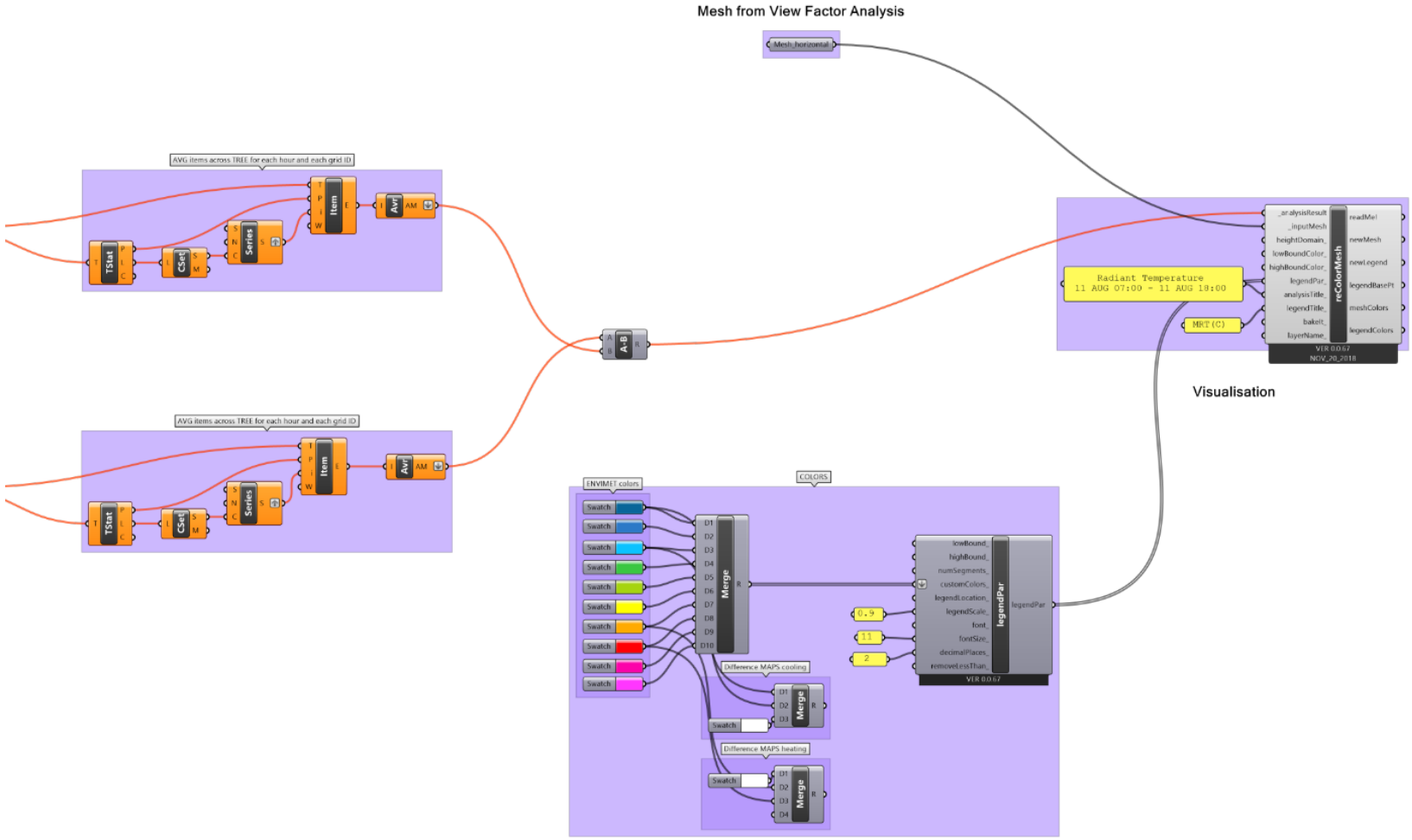

Figure B.28. Grasshopper script for the difference maps - 3

C. NetCDF

MRT (°C) comparison of the EDX files in Leonardo and after conversion to NetCDF in ArcGIS

Time	Min Leonardo	Max Leonardo	Min ArcGIS	Max ArcGIS	Error
08:00	33.86	66.64	19.56	25.03	
09:00	39.18	70.96	33.86	66.64	
10:00	45	72.85	50.75	81.67	
11:00	50.07	74.88	35.76	62.68	
12:00	53.75	77.1	16.51	57.22	
13:00	55.7	80	55.7	80	
14:00	55.93	82.22	21.93	26.69	
15:00	54.38	83.13	17.85	23.63	
16:00	50.75	81.67	55.93	82.22	
17:00	44.84	75.64	19.85	19.85	
18:00	35.76	62.68	23.61	27.78	
19:00	27.06	35.34	50.07	74.88	
20:00	23.61	27.78	27.06	35.34	
21:00	21.93	26.69	19.85	19.85	
22:00	20.61	25.79	53.75	77.1	
23:00	19.56	25.03	19.36	24.79	
00:00	19.36	24.79	54.38	83.13	
01:00	18.23	24.07	39.18	70.96	
02:00	17.85	23.63	20.61	25.79	

Red/Green indicates a missmatch/match of the values in Leonardo and in ArcGIS

Time in Leonardo which corresponds to Time in ArcGIS

Time Leonardo	Time ArcGIS	Min Leonardo	Max Leonardo	Min ArcGIS	Max ArcGIS	Error
08:00	09:00	33.86	66.64	33.86	66.64	
09:00	01:00	39.18	70.96	39.18	70.96	
10:00		45	72.85			
11:00	19:00	50.07	74.88	50.07	74.88	
12:00	22:00	53.75	77.1	53.75	77.1	
13:00	13:00	55.7	80	55.7	80	
14:00	16:00	55.93	82.22	55.93	82.22	
15:00	00:00	54.38	83.13	54.38	83.13	
16:00	10:00	50.75	81.67	50.75	81.67	
17:00		44.84	75.64			
18:00	11:00	35.76	62.68	35.76	62.68	
19:00	20:00	27.06	35.34	27.06	35.34	
20:00	18:00	23.61	27.78	23.61	27.78	
21:00	14:00	21.93	26.69	21.93	26.69	
22:00	02:00	20.61	25.79	20.61	25.79	
23:00	08:00	19.56	25.03	19.56	25.03	
00:00	23:00	19.36	24.79	19.36	24.79	
01:00		18.23	24.07			
02:00	15:00	17.85	23.63	17.85	23.63	

Red/Green indicates a missmatch/match of the values in Leonardo and in ArcGIS

Remaining errors after assignment

Time ArcGIS	Min ArcGIS	Max ArcGIS	Comment
17:00	19.85	19.85	incorrect
21:00	19.85	19.85	incorrect
12:00	16.51	57.22	unassignable

D. Python Scripts

E.1 Post-processing IR-measurements

```
# Read, calculate and write multiple csv
# For each location every hourly csv file will be first read, than mean, max,
# min and median will be calculated and each result will be written to a
# seperate csv file

import glob
import os
import numpy as np
import pandas as pd
import csv


#Path to the folder
path = 'C:/Users/shyam/MasterThesis/ThermalC/Locations/*'


# Multiple reading and calculation
for filename in glob.glob(os.path.join(path,'*.csv')):
    df = pd.read_csv(filename,sep=';',decimal=',')
    print ('Current File Being Processed is:  ')
    print (filename)
    print (df)

    Mean = np.nanmean(df)
    print ('Mean')
    print (Mean)
    Min = np.nanmin (df)
    print ('Min')
    print (Min)
    Max = np.nanmax(df)
    print ('Max')
    print (Max)
    Median = np.nanmedian(df)
    print ('Median')
    print (Median)



# write results to new csv file with the same name but add 'edited' to the
#filename and DTime (works as an index), Time and Date as a new column
```

```
    print ('Current File Being Processed is:  ')
    print (filename)

    with open(filename + '_edited.csv','w', newline = '') as f:
        wr = csv.writer(f, delimiter=',')
        wr.writerow(['DTime','Date','Time','Mean','Min','Max','Median'])
        for i in range (1,2):
            DTime = filename [55:66]
            Time = filename [64:66]
            Date = filename [55:63]
            wr.writerow([DTime, Date, Time, Mean, Min, Max, Median])


################################################################################
# Merge all new hourly csv files into one for each location

########Change Location number
out_filename = 'C:/Users/shyam/MasterThesis/ThermalC/Locations/Location_01.csv'
path1 = 'C:/Users/shyam/MasterThesis/ThermalC/Locations/Location_01'
########
if os.path.exists(out_filename):
    os.remove(out_filename)

# only read files with edited in filename, header only once in combined csv
read_files = glob.glob(os.path.join(path1,'*_edited.csv'))
header_saved = False
with open(out_filename, 'w') as outfile:
    for filename in read_files:
        with open(filename) as infile:
            header = next(infile)
            if not header_saved:
                outfile.write(header)
                header_saved = True
            for line in infile:
                outfile.write('{}\n'.format(line.strip()))
```

E.2 Interpolation IR-measurements

```
# For each loaction duplicate hours will be deleted and missing hours will be
# interpolated (except night hours)
# each result will be written to a seperate csv file

import glob
import os
import pandas as pd



#filepath where files for each location are stored
path = 'C:/Users/shyam/MasterThesis/ThermalC/Locations'


# opens all files in the folder with 'Location_' in the file name
for filename in glob.glob(os.path.join(path, 'Location_*.csv')):
    df = pd.read_csv(filename,sep=',',decimal='.', dtype=None)
    print ('Current File Being Processed is:  ')
    print (filename)
    print (df)


# Append empty and Location_*, delete duplicates, sort values
    doublefile = 'C:/Users/shyam/MasterThesis/ThermalC/Locations/Empty.csv'
    empty = pd.read_csv(doublefile,sep=';',decimal=',', dtype=None)
    print (empty)
    both = df.append(empty)
    print (both)
    df2 = both.drop_duplicates(subset = 'DTime')
    print (df2)
    df3 = df2.sort_values(by = ['DTime'], ascending=True)
    print (df3)

# linear Interpolation
    interp = df3.interpolate(methode = 'time')
    print (interp)

#Write new CSV file and add '_Interpolation.csv' to the filename
    interp.to_csv(os.path.join(path, filename + '_Interpolation.csv'))
```

E.3 Statistics

```
import numpy as np
import csv
import glob
import os
import pandas as pd


#Statistic

#MSE and RMSE

#filepath where files for each location are stored
path = 'C:/Users/shyam/MasterThesis/LocationsStat/'


# opens all files in the folder with "Location_" in the file name
for filename in glob.glob(os.path.join(path, 'Location_*.csv')):
    read_files = pd.read_csv(filename, delimiter=';', dtype=None)
    print ('Current File Being Processed is:  ')
    print (filename)
    print (read_files)

# define the variables
    meas = read_files ['Mean']
    surf = read_files ['T Surface  (°C)']
    mrt_e = read_files ['Mean Radiant Temp.  (°C)']
    at_e= read_files ['Air Temperature  (°C)']
    surfgh = read_files ['Surface_GH']
    mrt_gh = read_files ['MRT_GH']
    utci= read_files ['UTCI_GH']


# Calculation of MSE and RMSE

#Measured and Surface Envi
    mse = np.square(np.subtract(meas,surf)).mean()
    rmse = np.sqrt (mse)
    print(rmse)

#Measured and Envi MRT
    mse1 = np.square(np.subtract(meas,mrt_e)).mean()
    rmse1 = np.sqrt (mse1)
    print (rmse1)

#Measured and AirT Envi
    mse2 = np.square(np.subtract(meas,at_e)).mean()
    rmse2 = np.sqrt (mse2)
    print (rmse2)

#Measured and Surface GH
    mse3 = np.square(np.subtract(meas,surfgh)).mean()
```

```
    rmse3 = np.sqrt (mse3)
    print(rmse3)

#Measured and GH MRT
    mse4 = np.square(np.subtract(meas,mrt_gh)).mean()
    rmse4 = np.sqrt (mse4)
    print (rmse4)

#Measured and UTCI
    mse5 = np.square(np.subtract(meas,utci)).mean()
    rmse5 = np.sqrt (mse5)
    print (rmse5)

#MRT Envi and MRT GH
    mse6 = np.square(np.subtract(mrt_e,mrt_gh)).mean()
    rmse6 = np.sqrt (mse6)
    print (rmse6)

#Surface Envi and Surface GH
    mse7 = np.square(np.subtract(surf,surfgh)).mean()
    rmse7 = np.sqrt (mse7)
    print (rmse7)

##############################################################################

#R2

    from statistics import mean

# Define variables for R²

    xs = read_files ['Mean']
    ys = read_files ['T Surface  (°C)']
    ys1 = read_files ['Mean Radiant Temp.  (°C)']
    ys2 = read_files ['Air Temperature  (°C)']
    ys3 = read_files ['Surface_GH']
    ys4 = read_files ['MRT_GH']
    ys5= read_files ['UTCI_GH']


#Calculation of R²

#Mean and Surface Envi
    def best_fit_slope_and_intercept(xs,ys):
        m = (((mean(xs)*mean(ys)) - mean(xs*ys)) /
             ((mean(xs)*mean(xs)) - mean(xs*xs)))
        b = mean(ys) - m*mean(xs)
        return m, b

    def squared_error(ys_orig,ys_line):
        return sum((ys_line - ys_orig) * (ys_line - ys_orig))

    def coefficient_of_determination(ys_orig,ys_line):
```

```
        y_mean_line = [mean(ys_orig) for y in ys_orig]
        squared_error_regr = squared_error(ys_orig, ys_line)
        squared_error_y_mean = squared_error(ys_orig, y_mean_line)
        return 1 - (squared_error_regr/squared_error_y_mean)

    m, b = best_fit_slope_and_intercept(xs,ys)
    regression_line = [(m*x)+b for x in xs]

    r_squared = coefficient_of_determination(ys,regression_line)
    print(r_squared)



#Measured and Envi MRT

    def best_fit_slope_and_intercept(xs,ys1):
        m = (((mean(xs)*mean(ys1)) - mean(xs*ys1)) /
             ((mean(xs)*mean(xs)) - mean(xs*xs)))
        b = mean(ys1) - m*mean(xs)
        return m, b

    def squared_error(ys1_orig,ys1_line):
        return sum((ys1_line - ys1_orig) * (ys1_line - ys1_orig))

    def coefficient_of_determination(ys1_orig,ys1_line):
        y_mean_line = [mean(ys1_orig) for y in ys1_orig]
        squared_error_regr = squared_error(ys1_orig, ys1_line)
        squared_error_y_mean = squared_error(ys1_orig, y_mean_line)
        return 1 - (squared_error_regr/squared_error_y_mean)

    m, b = best_fit_slope_and_intercept(xs,ys1)
    regression_line = [(m*x)+b for x in xs]

    r_squared1 = coefficient_of_determination(ys1,regression_line)
    print(r_squared1)

#Measured and AirT Envi

    def best_fit_slope_and_intercept(xs,ys2):
        m = (((mean(egr = squared_error(ys2_orig, ys2_line)
        squared_error_y_mexs)*mean(ys2)) - mean(xs*ys2)) /
             ((mean(xs)*mean(xs)) - mean(xs*xs)))
        b = mean(ys2) - m*mean(xs)
        return m, b

    def squared_error(ys2_orig,ys2_line):
        return sum((ys2_line - ys2_orig) * (ys2_line - ys2_orig))

    def coefficient_of_determination(ys2_orig,ys2_line):
        y_mean_line = [mean(ys2_orig) for y in ys2_orig]
        squared_error_ran = squared_error(ys2_orig, y_mean_line)
        return 1 - (squared_error_regr/squared_error_y_mean)
```

```
    m, b = best_fit_slope_and_intercept(xs,ys2)
    regression_line = [(m*x)+b for x in xs]

    r_squared2 = coefficient_of_determination(ys2,regression_line)
    print(r_squared2)


#Mean and Surface GH
    def best_fit_slope_and_intercept(xs,ys3):
        m = (((mean(xs)*mean(ys3)) - mean(xs*ys3)) /
             ((mean(xs)*mean(xs)) - mean(xs*xs)))
        b = mean(ys3) - m*mean(xs)
        return m, b

    def squared_error(ys3_orig,ys3_line):
        return sum((ys3_line - ys3_orig) * (ys3_line - ys3_orig))

    def coefficient_of_determination(ys3_orig,ys3_line):
        y_mean_line = [mean(ys3_orig) for y in ys3_orig]
        squared_error_regr = squared_error(ys3_orig, ys3_line)
        squared_error_y_mean = squared_error(ys3_orig, y_mean_line)
        return 1 - (squared_error_regr/squared_error_y_mean)

    m, b = best_fit_slope_and_intercept(xs,ys3)
    regression_line = [(m*x)+b for x in xs]

    r_squared3 = coefficient_of_determination(ys3,regression_line)
    print(r_squared3)


#Mean and MRT GH
    def best_fit_slope_and_intercept(xs,ys4):
        m = (((mean(xs)*mean(ys4)) - mean(xs*ys4)) /
             ((mean(xs)*mean(xs)) - mean(xs*xs)))
        b = mean(ys4) - m*mean(xs)
        return m, b

    def squared_error(ys4_orig,ys4_line):
        return sum((ys4_line - ys4_orig) * (ys4_line - ys4_orig))

    def coefficient_of_determination(ys4_orig,ys4_line):
        y_mean_line = [mean(ys4_orig) for y in ys4_orig]
        squared_error_regr = squared_error(ys4_orig, ys4_line)
        squared_error_y_mean = squared_error(ys4_orig, y_mean_line)
        return 1 - (squared_error_regr/squared_error_y_mean)

    m, b = best_fit_slope_and_intercept(xs,ys4)
    regression_line = [(m*x)+b for x in xs]

    r_squared4 = coefficient_of_determination(ys4,regression_line)
    print(r_squared4)
```

```
#Mean and UTCI GH
    def best_fit_slope_and_intercept(xs,ys5):
        m = (((mean(xs)*mean(ys5)) - mean(xs*ys5)) /
             ((mean(xs)*mean(xs)) - mean(xs*xs)))
        b = mean(ys5) - m*mean(xs)
        return m, b

    def squared_error(ys5_orig,ys5_line):
        return sum((ys5_line - ys5_orig) * (ys5_line - ys5_orig))

    def coefficient_of_determination(ys5_orig,ys5_line):
        y_mean_line = [mean(ys5_orig) for y in ys5_orig]
        squared_error_regr = squared_error(ys5_orig, ys5_line)
        squared_error_y_mean = squared_error(ys5_orig, y_mean_line)
        return 1 - (squared_error_regr/squared_error_y_mean)

    m, b = best_fit_slope_and_intercept(xs,ys5)
    regression_line = [(m*x)+b for x in xs]

    r_squared5 = coefficient_of_determination(ys5,regression_line)
    print(r_squared5)


#MRT Envi and MRT GH
    def best_fit_slope_and_intercept(ys1,ys4):
        m = (((mean(ys1)*mean(ys4)) - mean(ys1*ys4)) /
             ((mean(ys1)*mean(ys1)) - mean(ys1*ys1)))
        b = mean(ys4) - m*mean(ys1)
        return m, b

    def squared_error(ys4_orig,ys4_line):
        return sum((ys4_line - ys4_orig) * (ys4_line - ys4_orig))

    def coefficient_of_determination(ys4_orig,ys4_line):
        y_mean_line = [mean(ys4_orig) for y in ys4_orig]
        squared_error_regr = squared_error(ys4_orig, ys4_line)
        squared_error_y_mean = squared_error(ys4_orig, y_mean_line)
        return 1 - (squared_error_regr/squared_error_y_mean)

    m, b = best_fit_slope_and_intercept(ys1,ys4)
    regression_line = [(m*x)+b for x in ys1]

    r_squared6 = coefficient_of_determination(ys4,regression_line)
    print(r_squared6)


#Surface Envi and Surface GH
    def best_fit_slope_and_intercept(ys,ys3):
        m = (((mean(ys)*mean(ys3)) - mean(ys*ys3)) /
             ((mean(ys)*mean(ys)) - mean(ys*ys)))
        b = mean(ys3) - m*mean(ys)
        return m, b
```

```
    def squared_error(ys3_orig,ys3_line):
        return sum((ys3_line - ys3_orig) * (ys3_line - ys3_orig))

    def coefficient_of_determination(ys3_orig,ys3_line):
        y_mean_line = [mean(ys3_orig) for y in ys3_orig]
        squared_error_regr = squared_error(ys3_orig, ys3_line)
        squared_error_y_mean = squared_error(ys3_orig, y_mean_line)
        return 1 - (squared_error_regr/squared_error_y_mean)

    m, b = best_fit_slope_and_intercept(ys,ys3)
    regression_line = [(m*x)+b for x in ys]

    r_squared7 = coefficient_of_determination(ys3,regression_line)
    print(r_squared7)


#Create Table

    mydata = pd.DataFrame([('Surface/Building T',rmse, r_squared,rmse3,
                            r_squared3, rmse7, r_squared7), ('MRT',rmse1,
                            r_squared1, rmse4, r_squared4, rmse6, r_squared6),
                           ('Air T/UTCI', rmse2, r_squared2, rmse5, r_squared5)])
    headers = ['Parameter','RMSE','R²','RMSE','R²','RMSE','R²']


#Write new CSV file and add "_Statistics.csv" to the filename
    mydata.to_csv(os.path.join(path, filename + '_Statistic.csv'))


#Merge all statistic files for each location into one file and add a column
#   with the location name from the file name

#define file name and location for merged file
out_filename = 'C:/Users/shyam/MasterThesis/LocationsStat/All_Locations_Stat.csv'
if os.path.exists(out_filename):
    os.remove(out_filename)

read_files = glob.glob(path +'*Statistic.csv')
with open(out_filename, "w") as outfile:
    for filename in read_files:
        with open(filename) as infile:
           for line in infile:
                outfile.write('{},{}\n'.format(line.strip(), filename[42:53]))
```

E.4 NetCDF Difference Maps for ENVI-met

```
import sys
import os
import glob
import numpy as np
from netCDF4 import Dataset
import matplotlib.pyplot as plt
from tkinter import filedialog
from tkinter import *

# Filedialog


root = Tk()
root.filename =  filedialog.askdirectory(title = 'Select Basecase Folder')
path = root.filename
root.destroy()


filelistdatetimeb=[]
filelistdtb=[]
filelistb=[]
for filename in sorted(glob.glob(os.path.join(path,'*.nc'))):

   #filelist.append(filename.replace('\\','/')) #Activate for Windows
   filelistb.append(filename)
   #Attention Filepath lenght
   filelistdatetimeb.append(filename[-25:len(filename)].replace(' ','_'))


for i in filelistdatetimeb:
    filelistdtb.append(i.replace('.','_'))

#Baseline

print('Number of Basecase Files loaded:', len(filelistdtb))

numoffiles= len(filelistdtb)-1


dataforbaseline=[]

for x,y in zip(filelistb[0:numoffiles],filelistdtb[0:numoffiles]):
    ncdata = Dataset(x, 'r', format='NETCDF4')
    print(y)
    print(ncdata.variables['MeanRadiantTemp'][1,0,0])
    dataforbaseline.append(ncdata.variables['MeanRadiantTemp'][0,:,:])
    ncdata.close()

bslnum =len(dataforbaseline)-1
```

```
#Berechung Baseline

baseline= sum(dataforbaseline[0:bslnum])

meandatabaseline = np.true_divide(baseline, len(filelistdtb))

# Filedialog

root = Tk()
root.filename =  filedialog.askdirectory(title = 'Select Szenario Folder')
path = root.filename
root.destroy()



filelistdatetime=[]
filelistdt=[]
filelist=[]
for filename in sorted(glob.glob(os.path.join(path,'*.nc'))):

   #filelist.append(filename.replace('\\','/')) #Activate for Windows
   filelist.append(filename)
   #Attention Filepath lenght
   filelistdatetime.append(filename[-25:len(filename)].replace(' ','_'))


for i in filelistdatetime:
    filelistdt.append(i.replace('.','_'))

#Check Number of Files

print('Number of Szenario Files loaded:', len(filelistdt))
numoffiles2= len(filelistdt)-1

if len(filelistdtb) != len(filelistdt):
 print('You have selected a different number of Input files','Basecase:',
       len(filelistdtb),'Files','Szenario:',len(filelistdt),'Files')
 com=str(input('Do you want to continue?y(y or n)'))

 if com == 'n':
  sys.exit()
 if com == 'y':
  pass


#Szenario

dataforszenario=[]

for x,y in zip(filelist[0:numoffiles2],filelistdt[0:numoffiles2]):
    ncdata = Dataset(x, 'r', format='NETCDF4')
    print(y)
```

```
    dataforszenario.append(ncdata.variables['MeanRadiantTemp'][0,:,:])
    ncdata.close()

sznum=len(dataforszenario)-1



#Berechung Szenario

szenario= sum(dataforszenario[0:sznum])

meandataszenario = np.true_divide(szenario,len(filelistdt))



#Substract Baseline Szenario

differenz = np.subtract(meandataszenario, meandatabaseline)



#Visualisierung

wo999=np.ma.masked_greater_equal(differenz,0)  # Werte gleich 0 maskiert
#wo999=np.ma.masked_less(differenz1,-2.5)  # Werte kleiner -10 maskiert

plt.ylim (0, 321)

#wo999_8_23_7=np.ma.masked_less(datafornight[0],0) # Werte kleiner 0 maskiert

minv= (np.amin(differenz)) #kleinster Wert im Array
print('minv')
print (minv)
maxv= (np.amax(differenz)) #größter Wert
print('maxv')
print (maxv)
#differenzrp= np.where(differenz==minv,50,differenz) # kleinster Wert im Array
                                                     #ersetzt durch 50

#minv= (np.amin(dataformean[0])) # kleinster Wert im Array ersetzt durch 50
#data_08_00_01_23_07_2017rp= numpy.where(differenz[0]==minv,80,differenz0])
#kleinster Wert im Array ersetzt durch 80

fig, ax = plt.subplots()
fig.set_size_inches(14.0,7.0)
plt.imshow(wo999,cmap='Blues_r', interpolation='none')
plt.colorbar()
plt.show()


#np.savetxt('differenz19.csv',differenz1,delimiter =';',fmt='%1.2f')
```

Eidesstattliche Erklärung

Hiermit versichere ich,

- dass ich die vorliegende Masterarbeit selbstständig verfasst, andere als die angegebenen Quellen und Hilfsmittel nicht benutzt und mich auch sonst keiner unerlaubter Hilfe bedient habe,
- dass ich dieses Masterarbeitsthema bisher weder im In- noch im Ausland in irgendeiner Form als Prüfungsarbeit vorgelegt habe
- und dass diese Arbeit mit der vom Begutachter beurteilten Arbeit vollständig übereinstimmt.

Wien, August 2020 Unterschrift

(Shyama Asen)